# Molecular Characterization of the Type 2 Corticotropin-releasing Hormone Receptor

by

**Kurt A. Heldwein**

## A DISSERTATION

*Presented to the Department of Molecular Microbiology and Immunology*
*and the Oregon Health Sciences University*
*School of Medicine*
*in partial fulfillment of*
*the requirements for the degree of*
*Doctor of Philosophy*
*May 2000*

School of Medicine
Oregon Health Sciences University

# CERTIFICATE OF APPROVAL

This is to certify that the Ph.D. thesis of

**Kurt A. Heldwein**

has been approved

[redacted]
Thesis Advisor, Mary P. Stenzel-Poore, Ph.D.

[redacted]
Marvin B. Rittenberg, Ph.D.

[redacted]
Scott M. Landfear, Ph.D.

[redacted]
Kent L. Thornburg, Ph.D.

# Table of Contents

# Acknowledgements

I first want to thank my friend and thesis advisor, Dr. Mary P. Stenzel-Poore, because my development as a scientist began when we met in Wylie Vale's laboratory at the Salk Institute. I am fortunate beyond description to have been trained by Mary. She is an excellent, well-rounded scientist who has never given up in her efforts to push me to higher levels of thinking and conduct in research. It was a bumpy ride, but it was worth it. I look forward to leaving the nest to testify that her efforts were not wasted, and to be able to continue our friendship unencumbered by idiosyncrasies of the student-mentor relationship. Thank you for everything, Mary.

I would like to express my appreciation for Dr. Marvin B. Rittenberg and his interest in my own personal research and development. All of his suggestions that I took to heart yielded very informative results. If I had not been such a bozo, I would have taken all of his other suggestions. Who knows what could have been? Greatness, man...greatness!

I would also like to thank all my collaborators and people who have been instrumental in bringing these studies to fruition. Specifically, I would like to thank Dr. Peter Stenzel, Dr. Kent Thornburg, Dr. Scott Landfear, Dr. William Claycomb, Dr. Roger Hohimer, Dr. Michael Silberbach, Dr. Sarah Coste, Dr. Greg Wiens, Janet Duncan, Jennifer Hill, Susan Stevens, Susan Murray, Amy Heard, and Dr. Dana Redick for their intellectual guidance and generous donation of their valuable time. I would like to acknowledge all past and present members of the Stenzel-Poore and Rittenberg labs for the informative discussions, helpful advice and tolerance of my untidiness. I would specifically like to thank Jennifer Hill for being an excellent bench mate and Susan Stevens for keeping me in line.

I would like to thank Jason McDermott, Johnan Kaleeba and Ando van der Velden for the comradeship, the support, the enthusiasm, the stress relief, the virtual

carnage and the bachelor party that I don't remember very well. A soul could not ask for better friends amongst the toils and tribulations of the graduate school. May the honorariums be fat when we invite each other to give seminars in our respective departments.

I would like to thank my parents, Carl and Sharon, for supporting me 100% no matter how badly I screwed up. Their unquestioning love and faith in me has been a constant and much needed source of strength. I would like to thank my sister Diane and brother Rick for their love, and I hope that my brother Eric will continue to watch over me.

Lastly yet mostly I would like to thank my lovely wife, Ekaterina. She is my best friend, my smarter half and my own personal comedian. I'm sticking to my story that there is not a luckier boy in the world than myself, simply because Katya is with me.

# Contributions to Thesis

Chapter 2: I conceived the idea to examine the expression of CRH-R2 in cardiac myocytes as a representative cell type within the heart. I designed the experiments and the analyses. Dr. William Claycomb generously provided AT-1 cells, and Dr. Ray Hershberger taught me how to isolate neonatal rat ventricular cardiac myocytes.

Chapter 3: I used $Crhr2^{-/-}$ mice to study the contribution of CRH-R2 to the cardiac effects of Ucn. I collaborated with Drs. Sarah Coste, George Pantely, and Roger Hohimer to design and execute echocardiographic analysis of heart function. In addition, I confirmed the critical involvement of CRH-R2 in the cAMP response of cardiac myocytes Ucn and CRH. The CRH-R2 knockout mice were generated by Drs. Peter Stenzel and Bob Kesterson. Dr. Sarah Coste studied the behavioral and cardiovascular phenotype of conscious mice.

Chapter 4: Janet Duncan and I worked together on the design of experiments to examine the regulation of CRH-R2 in mice, and we carried out the procedures together. We also both contributed equally in writing the manuscript

Chapter 5: Dr. Sarah Coste and I shared an interest in the role of CRH-R2 in the cardiovascular system. Together, we designed experiments to study the regulation of CRH-R2 *in vivo* and *in vitro* by inflammatory mediators. This work was a collaborative effort, and accordingly we have both contributed to the text of this chapter.

# Abstract

Corticotropin-releasing hormone (CRH) in the mammalian central nervous system (CNS) is a primary mediator of adaptive neuroendocrine, autonomic, and behavioral responses to adverse stimuli. However, CRH has direct effects on and is present in many peripheral tissues, suggesting that CRH in the periphery may act in conjunction with CRH in the brain to regulate the function of peripheral organs during stress. The recent identification of a novel CRH receptor, CRH-R2, expressed in the periphery provides a molecular basis for the effects of CRH outside of the CNS.

CRH-R2 is one of two known receptors that bind the neuropeptides corticotropin-releasing hormone (CRH) and urocortin (Ucn). While a highly related receptor (CRH-R1) has similar affinities for these hormones, CRH-R2 binds Ucn with ~40-fold higher affinity than CRH. CRH-related peptides, including Ucn, have long been known to be more potent than CRH in modulating the cardiovascular system. The discovery of CRH-R2 in the brain and peripheral tissues, such as the heart and skeletal muscle, provides a basis for the greater potency of Ucn versus CRH. Moreover, the presence of CRH-R2 in the heart is conserved across many species, from amphibians to humans, and suggests that Ucn or CRH, released peripherally, may directly regulate heart function. Thus, we hypothesize that CRH-R2 mediates CRH and Ucn-stimulated increases in heart function. The studies described here investigate the function and regulation of cardiac CRH-R2 at the molecular, cellular and physiological levels.

We find that CRH-R2 is expressed by cardiac myocytes and mediates Ucn- and CRH-stimulated increases in intracellular cAMP *in vitro*. In addition, CRH-R2 in the mouse mediates the hypotension and increased contractile function caused by systemically administered Ucn. Furthermore, we find that inflammation and hypertension, two forms of cardiovascular stress, downregulate CRH-R2 mRNA in the

heart. However, glucocorticoids and restraint stress do not downregulate expression of CRH-R2 in the heart, suggesting that HPA axis activation is not involved in the regulation of cardiac CRH-R2 by inflammation. We tested whether pro-inflammatory cytokines regulate CRH-R2 expression in isolated adult mouse ventricular cardiac myocytes *in vitro*, and found they had no effect on CRH-R2 mRNA levels. However, we found that Ucn decreases CRH-R2 mRNA levels in ventricular cardiomyocytes, suggesting that CRH-R2 is sensitive to ligand-induced downregulation.

Collectively, these data indicate that CRH-R2 expressed on cardiac myocytes mediates the direct stimulatory effect of Ucn on the contractile function of the heart. Moreover, cardiovascular stressors, such as inflammation and hypertension, decrease CRH-R2 mRNA in the heart. This may be the result of prolonged increases in the release of Ucn or CRH in the heart, which eventually cause ligand-induced downregulation of CRH-R2 on cardiomyocytes. Thus, we propose that CRH-R2 mediates stress-induced direct stimulation of cardiac function by CRH peptides. Given this proposed role of CRH-R2 and the observation that inflammation markedly impairs cardiac function, it is possible that decreased function of cardiac CRH-R2 contributes to the failure of the heart to adapt to the adverse condition of sepsis.

# Chapter 1

# Introduction

# Introduction

Ultimately, we want to understand how CRH-R2 regulates cardiac function. This dissertation investigates the function and regulation of cardiac CRH-R2 at the molecular, cellular and physiological levels. We will show that CRH-R2 is a neurohormone receptor expressed by cardiac myocytes and regulated during inflammation. Inflammation depresses cardiovascular performance. Therefore, CRH-R2 may provide a means of integrating adaptive responses of the cardiac and nervous system to inflammatory stimuli. Such responses to immune activation can be viewed as part of the larger syndrome of stress. Accordingly, this introduction will present relevant concepts and information on these three systems.

## 1. CRH Peptides and Receptors

### 1.1. Corticotropin-releasing hormone (CRH) family of peptides

Corticotropin releasing hormone, CRH, is a major mediator of neuroendocrine responses to stress (1). It's best characterized role is that of the primary activator of the hypothalamic-pituitary-adrenal (HPA) axis during stress. Adverse stimuli induce CRH release from the hypothalamus, and CRH stimulates the release of adrenocorticotropin hormone (ACTH) from pituitary corticotrophs into the systemic circulation. In turn, ACTH stimulates the release of glucocorticoids from the adrenal cortex. Glucocorticoids prepare the host's metabolism to support a "fight-or-flight" response. Importantly, glucocorticoids also negatively regulate the HPA axis at the levels of ACTH production by the pituitary and CRH production by the hypothalamus (2). However, glucocorticoids have also been shown to upregulate CRH expression in other parts of the brain, including the central amygdala and bed nucleus of the stria terminalis (2).

This HPA axis-activating function of CRH was the basis for its molecular identification. In 1981, Wylie Vale and colleagues reported the isolation and the amino acid sequence of ovine CRH and showed that it was a potent stimulator of ACTH and β-endorphin release from dispersed rat anterior pituitary cells (1). CRH was found to be distinct from other known mammalian peptides yet similar to two previously identified non-mammalian peptides (see below). CRH has since been identified in several mammalian and lower vertebrate species, including fish and frogs (3, 4). The importance of CRH in mediating HPA axis activation was demonstrated by blocking its effects during stress. Prior intravenous injection of anti-CRH neutralizing antibodies (serum) caused a marked (75%) inhibition of plasma ACTH elevations in rats treated with ether or CRH (5). Furthermore, a CRH antagonist, α-helCRH (9-41), which consists of amino acids 9-41 of CRH, similarly blocked ether- or CRH-induced elevation of plasma ACTH (6). Thus, CRH constitutes the dominant hypothalamic corticotropin-releasing activity in rats *in vivo*.

Recent genetic studies have confirmed these observations. Mice that lack CRH have normal basal levels of plasma ACTH but lack the diurnal increase in ACTH release that peaks in mice during the dark phase (evening) (7). Furthermore, stressor-induced elevations of ACTH are markedly impaired in CRH-null mice. Mice that lack the pituitary CRH receptor, CRH-R1 (see 1.4), also display impaired ACTH release in response to stressors (8, 9).

Several CRH-like peptides (**Fig. 1.1**) are more potent vasodilators than CRH when administered systemically to mammals (see 1.11). Prior to the discovery of CRH, urotensin I from the teleost fish *Catostomus commersoni* and sauvagine from the frog *Phylomedusa sauvagai* were found to cause hypotension in mammals (10-12). Following the identification of CRH, all three peptides were found to have similar ACTH-releasing activity on rat pituitary cells. However, urotensin I and sauvagine were far more potent than CRH at inducing mesenteric artery vasodilation and hypotension in dogs (13). These

**Figure 1.1.** Amino acid sequence CRH and CRH-like peptides from vertebrates. A) Alignment is structured according to the sequence of human CRH (top). B) Alignment is structured according to the sequence of human Ucn (top). C) Alignment of human CRH and astressin, a potent CRH receptor antagonist. n=norleucine (Nle). DF=D-phenylalanine. Solid lines represent a covalent, α-helix stabilizing link between $Glu^{30}$ and $Lys^{33}$. In all panels, sequence identity is indicated with a dash (-).

A.

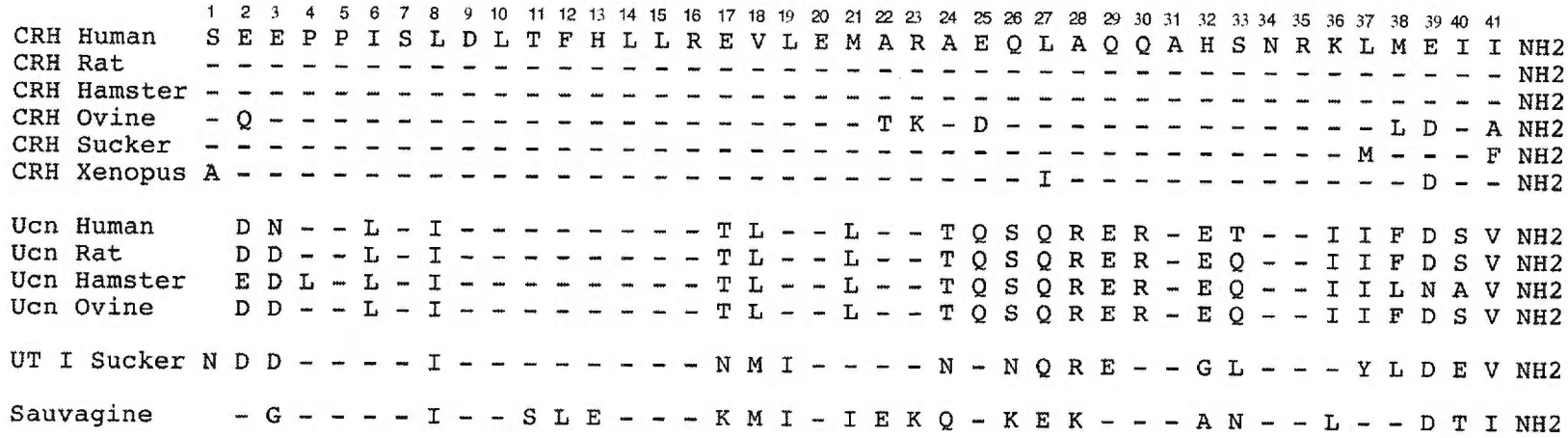

| | 1 | 2 | 3 | 4 | 5 | 6 | 7 | 8 | 9 | 10 | 11 | 12 | 13 | 14 | 15 | 16 | 17 | 18 | 19 | 20 | 21 | 22 | 23 | 24 | 25 | 26 | 27 | 28 | 29 | 30 | 31 | 32 | 33 | 34 | 35 | 36 | 37 | 38 | 39 | 40 | 41 | |
|---|---|---|---|---|---|---|---|---|---|---|---|---|---|---|---|---|---|---|---|---|---|---|---|---|---|---|---|---|---|---|---|---|---|---|---|---|---|---|---|---|---|---|
| CRH Human | S | E | E | P | P | I | S | L | D | L | T | F | H | L | L | R | E | V | L | E | M | A | R | A | E | Q | L | A | Q | Q | A | H | S | N | R | K | L | M | E | I | I | NH2 |
| CRH Rat | - | - | - | - | - | - | - | - | - | - | - | - | - | - | - | - | - | - | - | - | - | - | - | - | - | - | - | - | - | - | - | - | - | - | - | - | - | - | - | - | - | NH2 |
| CRH Hamster | - | - | - | - | - | - | - | - | - | - | - | - | - | - | - | - | - | - | - | - | - | - | - | - | - | - | - | - | - | - | - | - | - | - | - | - | - | - | - | - | - | NH2 |
| CRH Ovine | - | Q | - | - | - | - | - | - | - | - | - | - | - | - | - | - | - | - | - | - | - | T | K | - | D | - | - | - | - | - | - | - | - | - | - | - | - | L | D | - | A | NH2 |
| CRH Sucker | - | - | - | - | - | - | - | - | - | - | - | - | - | - | - | - | - | - | - | - | - | - | - | - | - | - | - | - | - | - | - | - | - | - | - | - | M | - | - | - | F | NH2 |
| CRH Xenopus | A | - | - | - | - | - | - | - | - | - | - | - | - | - | - | - | - | - | - | - | - | - | - | - | - | - | I | - | - | - | - | - | - | - | - | - | - | - | D | - | - | NH2 |
| Ucn Human | | D | N | - | - | L | - | I | - | - | - | - | - | - | - | - | T | L | - | - | L | - | - | T | Q | S | Q | R | E | R | - | E | T | - | - | I | I | F | D | S | V | NH2 |
| Ucn Rat | | D | D | - | - | L | - | I | - | - | - | - | - | - | - | - | T | L | - | - | L | - | - | T | Q | S | Q | R | E | R | - | E | Q | - | - | I | I | F | D | S | V | NH2 |
| Ucn Hamster | | E | D | L | - | L | - | I | - | - | - | - | - | - | - | - | T | L | - | - | L | - | - | T | Q | S | Q | R | E | R | - | E | Q | - | - | I | I | L | N | A | V | NH2 |
| Ucn Ovine | | D | D | - | - | L | - | I | - | - | - | - | - | - | - | - | T | L | - | - | L | - | - | T | Q | S | Q | R | E | R | - | E | Q | - | - | I | I | F | D | S | V | NH2 |
| UT I Sucker | N | D | D | - | - | - | - | I | - | - | - | - | - | - | - | - | N | M | I | - | - | - | - | N | - | N | Q | R | E | - | - | G | L | - | - | - | Y | L | D | E | V | NH2 |
| Sauvagine | | - | G | - | - | - | - | I | - | - | S | L | E | - | - | - | K | M | I | - | I | E | K | Q | - | K | E | K | - | - | - | A | N | - | - | L | - | - | D | T | I | NH2 |

B.

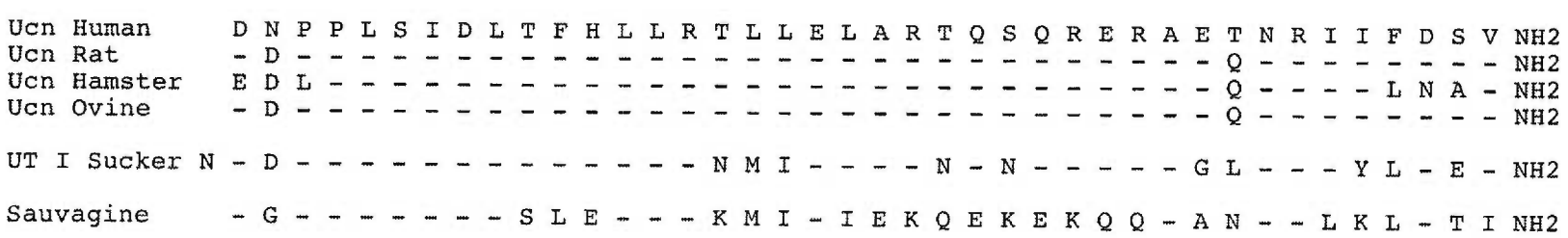

| | | | | | | | | | | | | | | | | | | | | | | | | | | | | | | | | | | | | | | | | | | |
|---|---|---|---|---|---|---|---|---|---|---|---|---|---|---|---|---|---|---|---|---|---|---|---|---|---|---|---|---|---|---|---|---|---|---|---|---|---|---|---|---|---|---|
| Ucn Human | | D | N | P | P | L | S | I | D | L | T | F | H | L | L | R | T | L | L | E | L | A | R | T | Q | S | Q | R | E | R | A | E | T | N | R | I | I | F | D | S | V | NH2 |
| Ucn Rat | | - | D | - | - | - | - | - | - | - | - | - | - | - | - | - | - | - | - | - | - | - | - | - | - | - | - | - | - | - | - | - | Q | - | - | - | - | - | - | - | - | - | NH2 |
| Ucn Hamster | | E | D | L | - | - | - | - | - | - | - | - | - | - | - | - | - | - | - | - | - | - | - | - | - | - | - | - | - | - | - | - | Q | - | - | - | - | L | N | A | - | NH2 |
| Ucn Ovine | | - | D | - | - | - | - | - | - | - | - | - | - | - | - | - | - | - | - | - | - | - | - | - | - | - | - | - | - | - | - | - | Q | - | - | - | - | - | - | - | - | - | NH2 |
| UT I Sucker | N | - | D | - | - | - | - | - | - | - | - | - | - | - | - | - | N | M | I | - | - | - | - | N | - | N | - | - | - | - | - | G | L | - | - | - | Y | L | - | E | - | NH2 |
| Sauvagine | | - | G | - | - | - | - | - | - | - | S | L | E | - | - | - | K | M | I | - | I | E | K | Q | E | K | E | K | Q | Q | - | A | N | - | - | L | K | L | - | T | I | NH2 |

C.

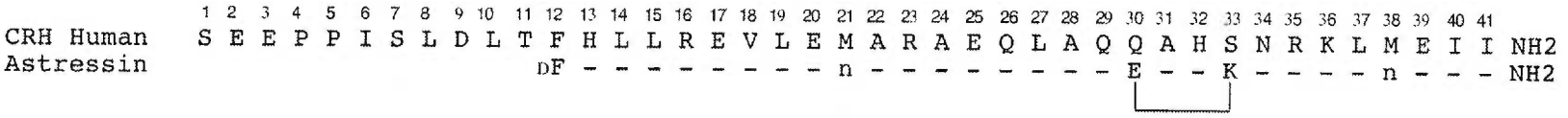

| | 1 | 2 | 3 | 4 | 5 | 6 | 7 | 8 | 9 | 10 | 11 | 12 | 13 | 14 | 15 | 16 | 17 | 18 | 19 | 20 | 21 | 22 | 23 | 24 | 25 | 26 | 27 | 28 | 29 | 30 | 31 | 32 | 33 | 34 | 35 | 36 | 37 | 38 | 39 | 40 | 41 | |
|---|---|---|---|---|---|---|---|---|---|---|---|---|---|---|---|---|---|---|---|---|---|---|---|---|---|---|---|---|---|---|---|---|---|---|---|---|---|---|---|---|---|---|
| CRH Human | S | E | E | P | P | I | S | L | D | L | T | F | H | L | L | R | E | V | L | E | M | A | R | A | E | Q | L | A | Q | Q | A | H | S | N | R | K | L | M | E | I | I | NH2 |
| Astressin | | | | | | | | | | | | DF | - | - | - | - | - | - | - | - | n | - | - | - | - | - | - | - | E | - | - | K | - | - | - | - | n | - | - | - | NH2 |

early findings indicated the presence of multiple forms of CRH receptors in mammals. Moreover, they suggested the presence of additional CRH-like peptides in mammals.

The latter was confirmed by the identification of urocortin (Ucn) in rats and humans (14, 15). Antiserum specific for urotensin I identified regions of the rat brain containing a urotensin I-like substance but lacking CRH mRNA or peptide. A cDNA library made from one such region, the Edinger-Westphal nucleus (EW), yielded an open-reading frame for a novel peptide with homology to urotensin I and, to a lesser extent, CRH. This novel neuropeptide hormone was named urocortin (Ucn) based on its homology to both peptides. Although Ucn was found to be equipotent with CRH at inducing ACTH release from rat pituitaries, this newly discovered peptide was considerably more potent than CRH at inducing hypotension when administered to rats systemically (15). Thus, an endogenous peptide had been identified in rats with greater direct vascular effects than mammalian CRH.

At the genetic level, the organization of the Ucn gene is similar to that of CRH; both genes contain a single intron between the promoter and the coding region (16, 17). CRH and likely Ucn are produced as larger precursors (i.e., preproCRH) and processed to yield mature bioactive peptides (**Fig. 1.2**). Prohormone convertases (PCs) are thought to cleave preproCRH at a dibasic site (Lys-Arg) that precedes the mature peptide coding region. A mouse neuroblastoma cell line, Neuro 2 A, expressing PC-2 (prohormone convertase-2) and transfected with the cDNA for human CRH, can secrete large amounts of mature CRH (1-41) (18). In contrast, when CHO cells, which express another protease involved in protein maturation, furin, are transfected with the CRH cDNA, they only secrete unprocessed preproCRH. Multiple prohormone convertases (PC-1, 2, and 5) are expressed in the paraventricular and supraoptic nuclei, which express large amounts of CRH and Ucn, respectively (see below) (19). A second processing event necessary to produce bioactive CRH involves cleavage and amidation of the carboxyl terminus. Carboxypeptidase H cleaves a Lys from the C-

**Figure 1.2.** Processing of CRH and Ucn precursors. PreproCRH, and likely preproUcn, undergo two major post-translational processing events to yield mature, bioactive peptides. First, prohormone convertases cleave the precursor at a dibasic moiety (Lys-Arg in CRH) that precedes the beginning of the mature peptides. Second, a C-terminal amino acid (Lys in CRH) is cleaved by a carboxy peptidase, and the exposed Gly residue is modified by a peptidylglycine alpha-amidating monooxygenase resulting in a C-terminal carboxamide group on CRH and Ucn.

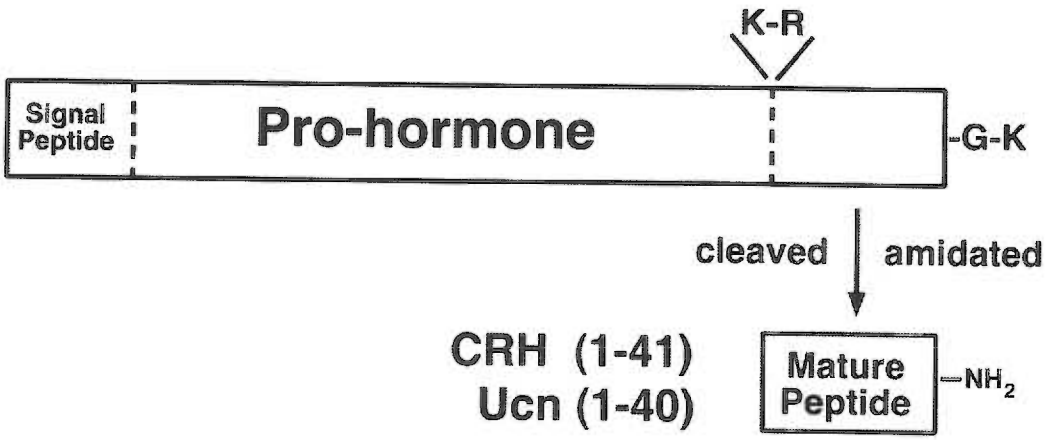
K-R
Signal Peptide
Pro-hormone
-G-K
cleaved
amidated
CRH (1-41)
Ucn (1-40)
Mature Peptide
—NH2

terminus of CRH (20), and the exposed C-terminal Gly is converted into an amide group by peptidylglycine alpha-amidating monooxygenase (21, 22).

## 1.2. Central and peripheral distribution of CRH

Early studies on the distribution of CRH peptide in rodents are confounded by the potential cross-reactivity of the anti-CRH antibodies used in these studies with the undiscovered Ucn. For example, the lateral hypothalamic area was previously reported to contain a substantial number of CRH-immunoreactive cells but has recently been shown to contain not CRH but rather large amounts of Ucn (23, 24). Thus, reference will be made primarily to a recent comparative study of Ucn- and CRH-specific immunoreactivity in the brain (24). Co-localization of CRH, Ucn and CRH receptors in the brain is discussed in section 1.7.

CRH-positive neurons have been detected throughout the cortex, cerebellum (molecular, granule, and Purkinje layers), bed nucleus of the stria terminalis, parvicellular region of the paraventricular nucleus (PVN), dorsal medial hypothalamus, the anteroventral preoptic nucleus, dorsal peduncular cortex, hippocampus, supraoptic nucleus, lateral reticular nucleus, and lateral parabrachial nucleus (24). CRH-containing fibers have also been demonstrated in the lateral septum, the medial vestibular nucleus, the central nucleus of the amygdala, area postrema, median eminence, posterior pituitary, and locus coeruleus (24). A comparative study of Ucn and CRH peptide distribution in peripheral tissues using specific antibodies has not been done. However, using reverse transcriptase PCR (RT-PCR), a very sensitive technique, CRH mRNA is readily detectable in several peripheral tissues of the mouse, including the adrenal gland, testis, ovary, gut, heart, lung and to a lesser degree in spleen (25). CRH mRNA has also been detected in the spleen, thymus (26), and inflamed arthritic joints of rats (27).

## 1.3. Central and peripheral distribution of urocortin (Ucn)

Ucn has a more limited distribution in the brain than CRH. A small number of Ucn-containing neurons are scattered through the cortex, the hippocampus, and paraventricular nucleus. However, many Ucn-positive neurons are present in the supraoptic nucleus (SON), lateral hypothalamus, Edinger-Westphal nucleus (periaqueductal gray), interpeduncular nucleus, medial vestibular nucleus, lateral superior olive, inferior olive, dorsal raphe, several premotor nuclei in the brainstem, and the nucleus of the solitary tract (24, 28). Ucn-containing fibers have been localized to the median eminence, sphenoid nucleus, lateral septal nucleus, posterior pituitary, and medial vestibular nuclei (24).

With regard to the hypothalamus, Ucn immunoreactivity is weak in the region of the PVN where there are CRH-containing neurons that project to the median eminence (ME) (28). Instead, Ucn is expressed in regions of the PVN known to send projections to autonomic cell groups in the brainstem and spinal cord (28). Ucn is also present in several autonomic and motor nuclei of the brainstem (28). These results suggest that Ucn may be important for control of the autonomic nervous system, and, unlike CRH, may not function as a hypothalamic mediator of pituitary ACTH release during stress. The latter conclusion is supported by the finding that specific neutralizing anti-Ucn antibodies, administered systemically, do not affect the elevation of circulating ACTH in foot shocked rats (29). However, Ucn *is* present in SON projections to the median eminence (24). Thus, Ucn may be released into the hypophyseal portal vessels in response to changes in blood volume, pressure, and osmolality, all of which activate neurons in the SON (30-32). In addition, the presence of Ucn and CRH in nerve fibers in the rat posterior pituitary (24) may enable their release into the systemic circulation. However, the cellular origin of Ucn and CRH in the posterior pituitary is unknown. Of note is the recent finding that a few regions of the brain (intermediate lateral septal, hypothalamic ventromedial and amygdaloid medial nuclei) containing urotensin I-immunoreactivity do not contain Ucn- or CRH-

immunoreactivity (28). Thus, additional uncharacterized urotensin I-like peptides may be present in mammals.

Ucn is more widely expressed in peripheral tissues than CRH. Ucn mRNA is highly expressed in the rat thymus, spleen, stomach, gut, kidney, testes, liver, and heart, as measured by RNase protection (33). In the mouse, Northern blot analysis only detects Ucn mRNA in the midbrain (34). This could be due to species differences or, most likely, the higher sensitivity of RNase protection as compared to Northern blots.

The physiological roles of CRH and Ucn remain unclear. In the immune system, CRH and Ucn have been shown to stimulate or inhibit immune cell activity and proliferation (35-42). Interpretations are further confounded by lack of information on cellular distribution (33) and species differences in the cellular distribution of CRH and Ucn in secondary lymphoid organs. Moreover, antisera used to localize CRH before the discovery of Ucn may cross-react with this highly related peptide. Furthermore, CRH and Ucn have also been shown to have opposing effects on inflammation. Neutralizing antibodies to CRH decrease exudate volume and cellularity at sites of aseptic inflammation (43), yet exogenous Ucn inhibits injury-associated edema due to its effects on blood pressure (44). To clarify the roles of peripheral CRH and Ucn, it will be necessary to co-localize CRH and/or Ucn mRNA and peptide, investigate the regulation of their expression, and utilize CRH receptor knockouts, receptor-specific antagonists, or peptide-specific neutralizing antisera.

## 1.4. Identification, tissue distribution and pharmacology of CRH receptors

Two types of receptors for CRH and Ucn have been cloned and characterized (45-49). Both of these receptors, CRH-R1 and CRH-R2, were identified before Ucn, thus they were named corticotropin-releasing hormone receptors for their only known mammalian ligand. These receptors belong to the Class II, secretin/glucagon subfamily of

putative seven-transmembrane G-protein coupled receptors. This subfamily of GPCRs is characterized by the presence of Cys residues in a long extracellular N-terminal tail and by the absence of an Asp-Arg-Tyr (DRY) motif found in the third transmembrane region of Class I receptors, which is important for regulated activation (50). Also, Class II receptors have numerous introns whose positions are roughly conserved and enable the expression of multiple splice variants of any one receptor (51). Class II comprises receptors for other neuropeptides such as secretin, glucagon, calcitonin, parathyroid hormone (PTH), pituitary adenylyl cyclase-activating peptide (PACAP), vasoactive intestinal peptide (VIP), and calcitonin gene-related peptide (CGRP) (52, 53). Thus, there may be similar structural constraints that dictate the interaction of most neuropeptides, including Ucn and CRH, with their cognate receptors (e.g. extracellular regions involved in ligand binding, conformational changes in the receptor upon ligand binding).

The first CRH receptor identified, CRH-R1, is the more prevalent receptor in the brain and pituitary and mediates activation of the HPA axis by CRH (8, 9). CRH-R1 has high affinity for CRH, Ucn, and sauvagine, and COS cells transfected with the cDNA for the human CRH-R1 receptor respond to these three peptides with similar increases in intracellular levels of cAMP (15). Thus, high-level expression of CRH-R1 in pituitary corticotrophs provides a basis for the equivalent potency of CRH and related peptides at inducing ACTH release in mammals.

As stated earlier, studies on the vascular effects of CRH suggested that a second class of CRH receptors with higher affinity for sauvagine and urotensin I than for CRH exists in the periphery of rats (13). This second class of CRH receptors, CRH-R2, was cloned based on sequence homology to CRH-R1 (45, 47, 48). Indeed, CRH-R2 is 69% identical to CRH-R1 in amino acid sequence. However, CRH-R2 differs from CRH-R1 in four fundamental ways: 1) ligand specificity, 2) distribution in the central nervous system, 3) expression in peripheral tissues, and 4) prevalence of different functional isoforms.

First, CRH-R2 was initially found to have higher affinity for the non-mammalian CRH-like peptides, sauvagine and urotensin I, than for CRH. The discovery of Ucn in mammals (14, 15) identified an endogenous, high affinity ligand for CRH-R2. The relative binding of Ucn and CRH to CRH-R1 and CRH-R2 is shown in **Table 1.1**. These values have been determined using cell lines transfected with the cDNAs for the CRH receptors and thus represent non-native systems. In mouse, rat, and human, CRH-R2 has higher affinity for Ucn than for CRH. Moreover, this ligand selectivity is characteristic of all examined isoforms of CRH-R2. The higher affinity of CRH-R2 for Ucn than CRH has led to speculation that CRH-R2 is the endogenous receptor for Ucn. Further support for this conclusion lies in the fact that numerous Ucn-containing fibers terminate in regions of the gut (54) and in the brain (see 1.7) (28) that express CRH-R2. However, it is important to bear in mind that CRH has only modest affinity for CRH-R2, and that both CRH and Ucn are high-affinity agonists for CRH-R1. Co-localization of Ucn peptide, CRH peptide, and CRH receptors is discussed below.

Second, CRH-R1 and -R2 patterns of expression in the brain differ significantly and suggest that they serve different functions. In situ hybridization analysis of CRH-R1 and -R2 mRNA distribution in the rat brain (55) indicates that localization of CRH-R1 and CRH-R2 does not overlap. Nevertheless, some regions such as the hippocampus (CA1, dentate gyrus, entorhinal cortex) express equivalent amounts of mRNA for both CRH receptors (55). Based on the known functions of the different brain regions alone, it has been proposed that CRH-R1 mediates the pituitary, cortical, cerebellar, and sensory effects of CRH or Ucn, while CRH-R2 mediates hypothalamic, autonomic, and behavioral actions of CRH or Ucn in the brain (55). However, during stress there is rapid induction of CRH-R1 expression on CRH-expressing cells in the PVN (56, 57), suggesting that CRH-R1 may be an important mediator of hypothalamic activation and, at the very least, is stress-responsive. Furthermore, the CRH-R1 specific, non-peptide antagonist, antalarmin,

**Table 1.1.** Ki† of mammalian CRH receptors for mouse, rat and human CRH and Ucn

| Species | Receptor | CRH | Ucn |
|---|---|---|---|
| mouse | CRH-R1 | 4.5 nM[5] | n.r. |
| rat | CRH-R1 | 0.95 nM[4] | 0.12 nM[4] |
| human | CRH-R1 | 0.95 nM[1] | 0.41 nM[1] |
| rat | CRH-R2α | 13 nM[1] | 0.58 nM[1] |
| human | CRH-R2α | 57 nM[3] | 8.9 nM[3] |
| mouse | CRH-R2β | 17 nM[4] | 0.41 nM[4] |
| rat | CRH-R2β | 65 nM[6] | 0.21 nM[6] |
| human | CRH-R2β | 54 nM[3] | 8.8 nM[3] |
| human | CRH-R2γ | 25 nM[2] | 1.4 nM[2] |

† Ki were determined by displacement of different iodine-labeled CRH receptor ligands.

* determined for urotensin I prior to discovery of Ucn

n.r. = not reported

1 ref (14)

2 ref (58)

3 ref (59)

4 ref (15)

5 ref (60)

6 ref (61)

blocks anxiety induced by intermittent foot shocks (62), and mice genetically lacking CRH-R1 show reduced anxiety during stress compared to normal mice (8, 9, 63).

CRH-R2 knockout (*Crh2*$^{-/-}$) mice tend to show slightly enhanced anxiety, though this phenotype is difficult to determine accurately because it varies among the different lineages of CRH-R2 knockout mice (64-66) In addition, *Crh2*$^{-/-}$ mice display stress-induced ACTH secretion that is greater in magnitude but shorter in duration compared to wild-type mice (64, 65). Moreover, *Crh2* prolongs the Ucn-induced hypophagia mediated initially by CRH-R1 (64). Thus, CRH-R2 appears to modulate stressor-induced endocrine and behavioral responses initially mediated by CRH-R1.

Third, CRH-R2 is most highly expressed in peripheral tissues, namely the gut, skeletal muscle, and heart (45, 47, 48, 67). The expression of CRH-R2 in the heart was somewhat surprising because cardiac effects of intravenously administered urotensin I had not been observed previously (11). However, the discovery of CRH-R2 expression in the heart provided a molecular basis for three reports of direct effects of CRH on myocardial tissue or hearts *ex vivo* (see 1.12) (68-70). The presence of CRH receptors in the heart raises the intriguing possibility that in some mammals, CRH and CRH-like peptides could control heart function directly.

Fourth, CRH-R1 is predominantly expressed as one isoform, although truncated variants or forms with an insertion in the first intracellular loop have been cloned (49, 71-73). CRH-R2 exists in mammals in three functional isoforms that differ in sequence only at their N-terminal domain (45, 58, 67, 74, 75). Initially, two isoforms of CRH-R2 were identified in the mouse (**Fig 1.3**) (45, 74) and rat (47). CRH-R2α is the principal isoform expressed in the rat brain and is predominantly neuronal, while CRH-R2β is highly expressed in peripheral tissues (e.g. heart, gut, and skeletal muscle), central and peripheral arterioles, and in the chorioid plexus (55). Humans express CRH-R2α, -R2β and a novel isoform, CRH-R2γ found only in humans so far (58, 67, 76). The multiple isoforms of human as well as rodent CRH-R2 result from alternative splicing of exons

**Figure 1.3.** Model of mouse CRH-R2β. Extracellular and intracellular domains are noted as EC and IC, respectively. Putative transmembrane domains are boxed and numbered. For comparison, the shorter N-terminus of the CRH-R2α variant with sequence from rat is shown, however this splice variant also is expressed in mice. Arrow denotes splice site for the α- and β- N-terminal domains. (**) denotes a putative PKC phosphorylation site. (Y) denotes putative glycosylation sites in the EC1 domain.

Extracellular
Trans-
Membrane
Intracellular
Rat
CRH-R2α
MOUSE
CRH-R2β
EC1
EC2
EC3
EC4
IC1
IC2
IC3
IC4
I
II
III
IV
V
VI
VII
COOH-
430

from a single gene. All three isoforms are present in the brain (58), but unlike rodents, CRH-R2α is the dominant isoform present in human heart and skeletal muscle (58, 67). Despite the species-specific expression of CRH-R2 isoforms in the heart, all isoforms of CRH-R2 have higher affinity for Ucn than for CRH (**Table 1.1**) (59, 77). Thus, while the presence of CRH-R2 in the heart is conserved, the functional relevance of multiple N-terminal isoforms of the cardiac CRH-R2 among mammals remains to be determined.

## 1.5. Determinants of function in CRH peptides

All identified CRH peptides in vertebrates posses two distinct regions of high amino acid homology (**Fig. 1.1**). The region of greatest homology among all peptides lies between amino acids 4 and 16 (numbered according to CRH). In the C-terminal half of the peptides, $Glu^{20}$, $Ala^{31}$, $Asn^{34}$, and $Arg^{35}$ are strictly conserved among all vertebrate CRH peptides. Interestingly, ovine CRH is significantly different from its rat and human homologues. Substitutions in ovine CRH render it less potent than rat CRH in binding to rat CRH-R1 (see 1.4) (48) although ovine CRH is a significantly higher affinity agonist for ovine CRH-R1 than rat CRH (78). Ovine Ucn is identical to its rat homologue and also strikingly similar to human Ucn. Ucn is more homologous to urotensin I (63%) than to CRH (45%), suggesting that mammalian Ucn is derived from fish urotensin I. Notably, sauvagine has higher homology to CRH (48%) and urotensin I (50%) than to Ucn (35%). CRH- and sauvagine-like immunoreactivities were found to coexist in the central nervous system of the bullfrog, *Rana catesbeiana* while urotensin I-like immunoreactivity was undetectable (79). It is not clear whether frogs lack the gene for urotensin I and instead utilize CRH-derived sauvagine, or whether sauvagine is a highly mutated derivative of urotensin I in frogs.

Both the N- and C-terminal regions of CRH peptides contain determinants of receptor activation. Most studies of critical elements of receptor binding and activation have focused on mammalian CRH, utilizing primary or transfected cells expressing CRH-

R1. Fewer studies have been done on Ucn, urotensin I, and sauvagine. Thus, the following discussion of peptide structure-function studies will focus on CRH with reference to other CRH-like peptides when possible.

The majority of studies of the N-terminal region of CRH peptides have concentrated on the first 12-13 amino acids. Ovine CRH (4-41) and full-length ovine CRH are equipotent at stimulating ACTH release from pituitary cells, indicating that the first 2-3 amino acids of CRH peptides, which diverge considerably, do not participate in receptor binding or activation. In contrast, ovine CRH (10-41) and rat/human CRH (9-41) behave as CRH receptor antagonists (1, 6). Ucn and sauvagine lacking their first 7 and 8 amino acids, respectively, are also CRH receptor antagonists (80). Specifically, $Ser^7$ and $Leu^8$ play a critical role in the bioactivity of CRH (80). Alanine (Ala) mutations of ovine CRH residues 5-19 dramatically reduce its ACTH-releasing activity (81). This indicates that amino acids 4-8 of the N-terminal region of CRH peptides may be part of an activation domain. Alternatively, amino acids 4-8 may be important for the stability of an activation domain(s) elsewhere in these peptides (see below). Truncation of amino acids 1-10 converts sauvagine from a high affinity agonist for both mammalian CRH receptors to a selective (110-fold) antagonist (antisauvagine-30) for CRH-R2β, while Ucn(11-40) is a far less (7-fold) selective antagonist (82). This is interesting because amino acids 1-10 of Ucn and sauvagine are very homologous except for one non-conservative ($Asp\text{-}Gly^2$) substitution and two conservative ($Leu\text{-}Ile^4$, $Thr\text{-}Ser^{10}$) substitutions. It is possible that the $Gly^2$ of sauvagine is involved in the interaction of this peptide with CRH-R1 but not CRH-R2.

As described earlier, processing of CRH peptides into their mature bioactive form entails amidation of the C-terminal carboxy group. Ovine CRH that lacks a C-terminal carboxamide group or has an Ala instead of the conserved $Arg^{35}$ has practically no ACTH-releasing activity (1, 83). However, ovine CRH mutants containing Ala at many other positions from 25-40 have similar or improved potency compared to native ovine CRH

(81). Thus, the sequence of the C-terminal half of CRH may be more constrained by structural requirements instead of the chemical identity of the amino acid side chains. This may explain why CRH, Ucn and sauvagine all have high affinity for CRH receptors despite the considerable divergence of their C-terminal sequences.

CRH, Ucn, urotensin I, and sauvagine have been shown to possess a prominent α-helical secondary structure (6, 84, 85). Circular dichroism studies strongly predict α-helices in the region from $Ile^{8/9}$/$Leu^{8}$ to $Asn^{33/34}$ of CRH, urotensin I and sauvagine (85). Specifically, $Leu^{8}$, $Asp^{9}$, $Phe^{12}$, $His^{13}$, $Leu^{15}$, $Arg^{16}$, $Leu^{19}$, $Glu^{20}$, and $Arg^{23}$ of CRH are thought to be critical for its amphipathic helical structure. Only sauvagine has a single non-conservative substitution at any of these amino acid positions ($Phe^{12}$-Ser), highlighting the central importance of these residues to the α-helical structure of CRH, Ucn, urotensin I and sauvagine. In addition, the C-terminal 2-3 amino acids of CRH and urotensin I have an α-helical nature, while the equivalent region of sauvagine forms a putative β-strand. Cleavage of the first 8-11 amino acids of these peptides greatly decreases their bioactivity. However, the affinity of CRH (9-41) and CRH (12-41) for CRH-R1 is also decreased (86). At high concentrations necessary to antagonize the activity of native CRH, these two analogs display residual intrinsic agonist activities (86). Modifications that stabilize the α-helical secondary structure of truncated forms of CRH, Ucn, and sauvagine (e.g. substitution of oxidizable methionines, stabilizing stacking interactions between phenyl rings of neighboring side chains, and an engineered salt bridge between substituted Glu and Lys residues at positions 30 and 33) greatly increase their affinity for CRH-R1 and, thus, increase their potency as antagonists (86, 87). Such studies led to the development of astressin, a potent peptide antagonist for both CRH-R1 and CRH-R2 (**Fig. 1.1**). Moreover, findings from a recent study where α-helical spacers were placed in a synthetic composite peptide of Ucn and urotensin I suggest that the rotational orientation of the N- and C-terminal domains is central to the bioactivity of CRH peptides (83).

## 1.6. Determinants of ligand binding in CRH receptors

Various determinants of ligand binding in CRH-R1 and CRH-R2 have been mapped. The following discussion of binding determinants focuses on studies involving human CRH receptors because they provide the most extensive understanding of CRH receptor/ligand interactions so far. For simplicity, the extracellular N-terminus will be referred to as EC1, and the three extracellular loops will be referred to as EC2, EC3, and EC4. Chimeric receptors have been created where the EC1 domain of human CRH-R2 was replaced with the EC1 domain of CRH-R1 (77) This chimeric protein exhibits binding characteristics indistinguishable from those of native CRH-R2. Thus, CRH-R2 must use elements outside of EC1 to discriminate between CRH and Ucn. This conclusion is supported by the finding that the three known N-terminal isoforms of CRH-R2 discriminate between CRH and Ucn (**Table 1.1**). Interestingly, mutations in the EC1 of native CRH-R1 affect the binding of CRH and Ucn equally (88). A similar mutational study of the N-termini of CRH-R2 has not been done; thus, the contribution of the EC1 of CRH-R2 to binding of Ucn and CRH is unknown. It should be noted that cysteines in the N-terminal tail of CRH-R1, a distinguishing feature of the CRH receptors and other Class II neuropeptide GPCRs, form disulfide bridges critical for mouse CRH-R1 binding to CRH (89). However, the role of these Cys in Ucn binding has not been determined.

Amino acids that confer low affinity for CRH have been identified in CRH-R2. A partial comparison of the amino acid sequence of human CRH-R1 and CRH-R2 (all isoforms) from EC2 through the 5th transmembrane domain is shown in **figure 1.4** (from (90)). Replacement of the residues $Val^{266}$, $Tyr^{267}$, and $Thr^{268}$ in CRH-R1 with Asp, Leu, and Val (non-homologous amino acids in equivalent regions of CRH-R2), respectively, reduces the affinity of CRH-R1 for CRH by 10-fold, but does not alter the affinity for Ucn. Pairing this triple mutation with a single amino acid substitution of His (from CRH-R2) for the $Arg^{189}$ found in CRH-R1 causes a further 8-fold decrease in affinity for CRH.

**Figure 1.4.** Schmatic model of the human CRH receptors (adapted from (91)). Sequence alignment of human CRH-R1 and CRH-R2α is shown between EC2 and transmembrane region 5. The conserved amino acids are shown in *solid circles* and the divergent amino acids are shown in *open symbols*. The amino acid sequence of CRH-R1 is shown on the *left* and those of CRH-R2 are shown on the *right*. The amino acids that are important for high affinity CRH binding are in squares. The amino acids that are important for binding the non-pepdide CRH-R1 antagonist, antalarmin, are in diamonds. Numbering is based on the sequence of human CRH-R1.

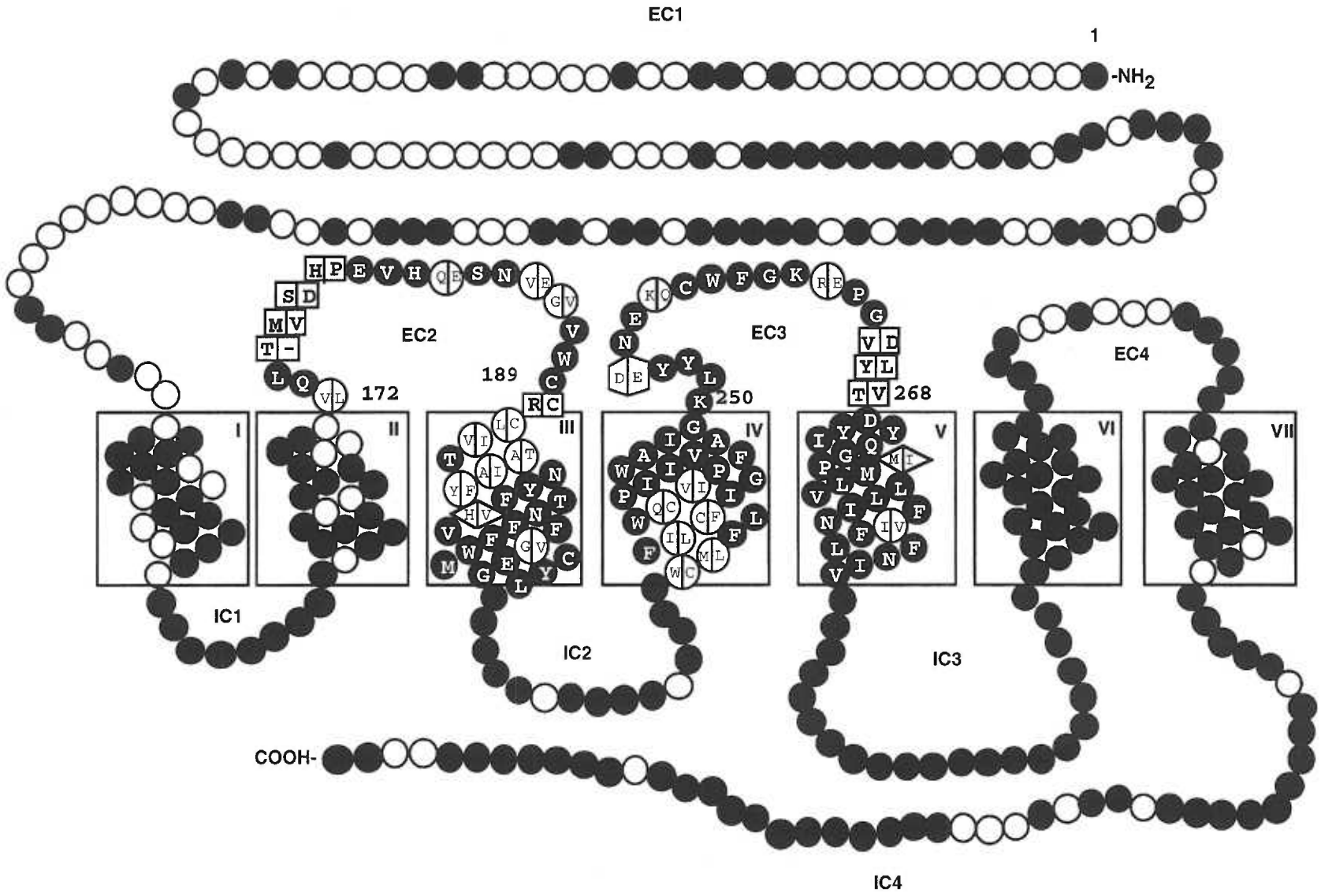
EC1
1
-NH2
EC2
EC3
EC4
172
189
250
268
I
II
III
IV
V
VI
VII
IC1
IC2
IC3
IC4
COOH-

A similar result occurs if the Asp-Leu-Val mutation is paired with a deletion of the $Thr^{175}$ and replacement of $Met^{176}$, $Ser^{177}$, and $Phe^{178}$ of CRH-R1 with Val, Asp, and His from a similar region of CRH-R2. In summary, a major determinant of the low affinity of CRH-R2 for CRH exists at the border of EC3 with the 5th transmembrane domain, and this cooperates with two determinants in EC2 to reduce affinity for CRH even further without significantly affecting affinity for Ucn.

A unique region in CRH-R1 and CRH-R2 has been shown to be important for sauvagine binding. The replacement of $Val^{266}$, $Tyr^{267}$, and $Thr^{268}$ in CRH-R1 with Asp, Leu, and Val of CRH-R2, described above, also lowers the affinity of CRH-R1 for sauvagine ~30-fold. However, high affinity binding is restored by a second mutation that changes $Asp^{254}$ of CRH-R1 to Glu, the residue in the equivalent position of CRH-R2. Thus, two regions of the EC3 domain of the CRH receptors cooperate to bind sauvagine with high affinity, but CRH-R1 and CRH-R2 utilize different amino acids at these positions to accomplish this.

## 1.7. Functional relationship of Ucn, CRH and CRH receptor expression in the brain

The distribution of Ucn-immunoreactivity, CRH-immunoreactivity and CRH receptor mRNAs in the brain do not support exclusive CRH/CRH-R1 and Ucn/CRH-R2 functional associations in the central nervous system. There is an overlap of Ucn-containing terminals and CRH-R2 expressing neurons in regions of the brain such as the paraventricular nucleus, supraoptic nucleus, ventromedial hypothalamus, dorsal and linear raphe nuclei, and lateral septum (92). However, not all CRH-R2 expressing regions of the brain, including the bed nucleus of the stria terminalis, ependyma, and posterior cortical amygdala, receive input from Ucn-containing nerve fibers (92). In contrast, there are regions (e.g. the inferior olive) that express CRH-R1 mRNA but receive input from fibers that contain large amounts of Ucn (93). Finally, intracerebroventricular (icv) injection of

CRH can cause activation of neurons in regions of the brain (e.g. ventromedial hypothalamic nucleus) that express high amounts of CRH-R2 but almost no CRH-R1 (93). Thus, it is likely that Ucn- or CRH-containing fibers in the brain innervate neurons expressing both CRH-R1 and CRH-R2, and that this functional overlap precludes exclusive Ucn/CRH-R2 and CRH/CRH-R1 relationships in the central nervous system.

## 1.8. CRH receptor signaling pathways

Both types of mammalian CRH receptors have been shown to activate multiple signaling pathways. CRH-R1 and -R2 variants can mediate the stimulation of adenylyl cyclase and cAMP production in many cell types. CRH-mediated increases in cAMP lead to phosphorylation and activation of the cAMP-response element-binding protein (CREB) by protein kinase A (PKA) (94). Additionally, both types of CRH receptors can stimulate $Ca^{2+}$ influx into cells across the plasma membrane (95-98) In some cells (e.g. AtT20 and transfected CHO cells), CRH-R1 and -R2 mediated elevations of intracellular $Ca^{2+}$ leads to activation of phospholipase-C (PLC), phosphoinositol-3 kinase (PI-3K), and MAP kinase ($MAPK^{p42}$) (94, 96). However, in CATH.a cells, which have many properties of neurons in the locus coeruleus, CRH stimulation increases intracellular cAMP production but inhibits VIP-induced increases in intracellular $Ca^{2+}$ (99). The pregnant human myometrium expresses CRH-R1 and CRH-R2β, which mediate CRH-stimulated production of cAMP but inhibit $PGE_2$ production (72, 100-102). Thus, both CRH-R1 and CRH-R2 mediate increases in intracellular cAMP and regulate intracellular $Ca^{2+}$ levels in cells, potentially activating multiple intracellular signaling pathways.

## 1.9. Desensitization and downregulation of CRH receptors

Similar to other G protein-coupled receptors (GPCRs), CRH-R1 is subject to rapid and reversible ligand-induced (homologous) desensitization, characterized by decreased signaling and removal of binding sites from the cell surface (95, 103, 104). CRH-R1 in Y-

79 cells is rapidly desensitized after stimulation by CRH, and transfection of G protein-coupled receptor kinase (GRK3) antisense cDNA into these cells inhibits CRH-induced CRH-R1 desensitization (105). Thus, GRK3 is critically involved in agonist-induced CRH-R1 desensitization and, likely, phosphorylation in Y-79 cells. CRH-R1 transfected and expressed in COS fibroblasts is also rapidly phosphorylated and internalized after exposure to CRH (105). However, CRH-R1 is not phosphorylated after treatment of the COS cells with forskolin (cAMP) or ionomycin ($Ca^{2+}$). It is possible that CRH-R1 in COS cells must be bound to ligand (Ucn or CRH) in order to be a substrate for cAMP-dependent (PKA) or $Ca^{2+}$-dependent (PKC, $Ca^{2+}$/calmodulin [CaM]) kinases. If so, then phosphorylation of CRH-R1 in COS cells following stimulation with CRH or Ucn might involve PKA, PKC, or CaM-kinase after all. However, PKA, PKC or CaM-kinase, activated by another receptor, would not mediate heterologous desensitization of CRH-R1 in COS cells. However, CRH receptors in pregnant human myometrium are subject to a form of heterologous desensitization following stimulation by oxytocin (71). Oxytocin decreases the measurable affinity of myometrial CRH receptors (CRH-R1 and CRH-R2β) for CRH, which is dependent on phosphorylation of CRH receptors by PKC.

It is currently unknown whether internalization of CRH receptors involves dynamin and clathrin-coated pits (**Fig. 1.5**), or occurs in the absence of GRK phosphorylation and subsequent arrestin binding. In addition, it is unknown whether α-helCRH(9-41), an antagonist for CRH-R2 but partial agonist for CRH-R1 (106), also causes homologous desensitization of CRH-R1, or whether it allosterically forces the receptor into a conformation that is capable of signaling but is a poor substrate for GRKs (107).

CRH receptors are also subject to downregulation, which occurs at the level of steady-state receptor mRNA levels (**Fig. 1.5**) and is delayed compared to receptor desensitization. Ligand-induced downregulation of CRH-R1 mRNA is observed in rat anterior pituitary cells stimulated with CRH for several hours (108, 109). Such ligand-induced downregulation of receptor mRNA is not uncommon among GPCRs (110-115).

**Figure 1.5.** Possible molecular mechanisms contributing to the homologous desnsitization and downregulation of G protein-coupled receptors (from (116)). Steps are as follows: (1) Receptor activation by agonist A, (2) Activation of down stream effector, phosphorylation by G protein-coupled receptor kinase(s) (GRK) and receptor uncoupling, (3) β-Arrestin binding to phosphorylated receptor, (4) Receptor endocytosis and sequestration in clathrin-coated vesicle, (5) Transport of receptor to lysosome and degradation, (6) Alternative transport of receptor to endosome, (7) Recycling of receptor to plasma membrane after dephosphorylation, (8) Synthesis of new receptors and transport to the plasma membrane, (9) Down- or upregulation of receptor at the level of mRNA stability, and (10) Down- or upregulation of receptor at the level of transcription.

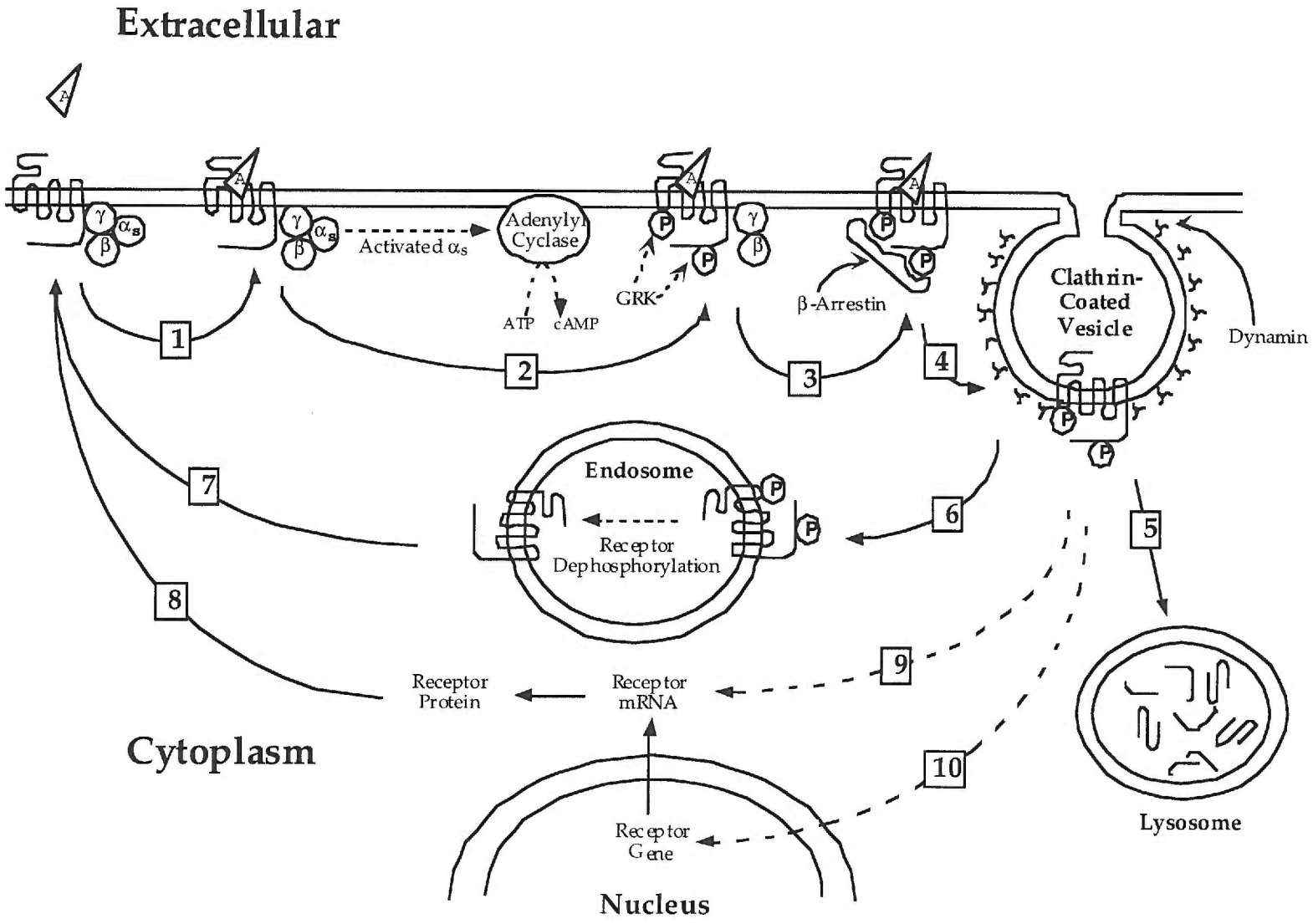
Extracellular
A
γ
β
$\alpha_s$
Activated $\alpha_s$
Adenylyl Cyclase
ATP
cAMP
GRK
P
β-Arrestin
Clathrin-Coated Vesicle
Dynamin
1
2
3
4
5
6
7
8
9
10
Endosome
Receptor Dephosphorylation
Receptor Protein
Receptor mRNA
Receptor Gene
Cytoplasm
Nucleus
Lysosome

Furthermore, decreased mRNA stability following agonist exposure has been found to be the underlying mechanism (111-115, 117). CRH-R1 is also subject to heterologous downregulation; endotoxin and IL-1β can decrease CRH-R1 mRNA levels in pituitary cells (118). However, the mechanisms of CRH-, endotoxin- and IL-1β induced CRH-R1 mRNA downregulation in the pituitary is unknown.

### 1.10. CRH and CRH receptors in the sympathetic nervous system

Several studies support the notion that the sympathetic nervous system may provide a pathway for direct actions of CRH or Ucn on peripheral tissues. Abundant Ucn- and CRH-like immunoreactivity has been detected in the spinal cord of the rat (28, 119). CRH is also present in the spinal cord of sheep, and some of these CRH-positive fibers are double-labeled after injection of a retrograde tracer, fluorogold, into the adrenal medulla (120). Taken together with the detection of CRH binding sites in the adrenal medulla (121, 122), direct control of adrenal function by CRH-like peptides may occur via sympathetic nervous system pathways. CRH or CRH binding sites have also been detected in several sympathetic chain ganglia. CRH mRNA was detectable in the celiac ganglion of the developing mouse (123), suggesting a possible role for CRH in the development of one or more abdominal organs (e.g., adrenal, pancreas, stomach, liver, and abdominal vasculature). In primates, CRH binding sites were found in the adrenal medulla and sympathetic chain ganglia, including the lumbar, thoracic, cervical, and coeliac (122). Furthermore, the CRH binding sites in the primate medulla had ~10-fold higher affinity for sauvagine than for CRH, suggesting CRH-R2 like ligand specificity. Moreover, CRH-like substances have also been detected in the stellate, or inferior cervical ganglion of the cat (124), and CRH-like immunoreactivity has been observed in nerve fibers within peripheral tissues in the rat, namely in the thymus, spleen, and in and around blood vessels (125). Thus, peripheral neurons and nerve fibers contain immunoreactive CRH-like peptides. These findings strongly implicate CRH in the autonomic regulation of several peripheral

tissues, including the cardiovascular system. Likewise, because of the high degree of homology between CRH and Ucn and the use of antibodies that may not distinguish between these peptides, the CRH-like immunoreactivity, described in postganglionic sympathetic neurons and fibers, may be Ucn instead of CRH.

### 1.11. Cardiovascular effects of CRH

Several studies have demonstrated direct hypotensive effects of CRH, Ucn, and other CRH-like peptides on the vascular system of mammals *in vivo* (13, 15, 126-129), and on isolated vessels *in vitro* (130, 131). I will discuss a particularly informative study that compared the direct (iv) and indirect (icv) effects of CRH on the iliac and mesenteric arteries of conscious, free-moving rats (132). This study emphasizes the contribution of the sympathetic nervous system to the vascular response to CRH by employing a ganglionic blocking agent, chlorisondamine. Thus, this study highlights 1) the division of central versus systemic effects of CRH on the cardiovascular system, 2) the specificity of CRH effects on different vascular beds, and 3) CRH effects in the presence or absence of sympathetic control of vascular tone and cardiac function. However, despite the use of CRH in this study, it should be noted again that Ucn is much more potent modulator of the cardiovascular system than CRH when administered systemically.

Central (icv) CRH caused a sustained (>60 min) increase in mean arterial pressure (MAP) and also increased heart rate (i.e. positive chronotropic effect). Specifically, icv CRH caused a sustained increase in resistance in the mesenteric (gut) vascular bed leading to a decrease in flow. More importantly, icv CRH caused a sustained decrease in resistance in iliac vessels leading to increased blood flow through the hind limb muscles. However, concurrent ganglionic block (chlorisondamine) abrogated the effects of icv CRH on the mesentery. Interestingly, chlorisondamine did not significantly alter the icv CRH-induced increase in blood flow in the iliac artery. This could be due to increased exploration, burrowing, and grooming caused by central administration of CRH since exercise of the

skeletal muscle alone can increase blood flow to this tissue. Nevertheless, alterations in regional hemodynamics induced by central elevations of CRH (shunting blood flow from the gut to the skeletal muscle) are mediated by the sympathetic nervous system. This could be a physiologic strategy to sustain a fight-or-flight response to stress, but it is could also be a CRH-regulated pathway for adjustment of blood flow in responses to day-to-day changes in activity and posture. Importantly, none of the effects of icv administered CRH were blocked by systemic (iv) administration of the CRH antagonist, α-helCRH (9-41), demonstrating that CRH was likely to act only in the CNS without leaking into the peripheral circulation.

In addition to central CRH stimulation of the sympathetic nervous system, there is evidence for CRH modulation of the parasympathetic nervous system (133, 134). Central administration of CRH inhibits the baroreflex to altered hemodynamics, and this effect is mediated by suppression of cardiac vagal efferent responses to baroreceptor input. It is not known what effect central CRH has on vasomotor component of the baroreceptor, if any. However, CRH in the central nervous system clearly coordinates the cardiac response to stressors by stimulating sympathetic input while inhibiting parasympathetic input.

The vascular effects of systemic (iv) administration of CRH appear to oppose those of centrally administered CRH (132). Iv CRH caused a sustained decrease in MAP and a sustained increase in heart rate. Ganglionic blockade reduced MAP even further. In contrast, the increase in heart rate caused by iv CRH was abrogated by ganglionic blockade, indicating that the increased heart rate was a sympathetic reflex to the concurrent hypotension. The effect of iv CRH on the mesentery opposed that of icv CRH in direction and duration. Iv CRH caused a marked but only transient decrease in resistance and concurrent increase in flow in the mesenteric artery. Ganglionic blockade prolonged this effect of CRH, suggesting that the effect of iv CRH alone was transient because of reflex vasoconstriction mediated by the sympathetic nervous system. The effect of iv CRH on the hind-limb muscle circulation also opposed that of icv CRH in direction and duration. Iv

CRH caused a transient increase in resistance and thus decreased flow in the iliac artery. However, instead of prolonging this effect, concurrent ganglionic blockade reversed the effect; iv co-treatment with chlorisondamine and CRH resulted in a sustained decrease in resistance and thus increased flow through the skeletal muscle. Therefore, similar to the mesentery, the sympathetic reflex to iv CRH opposes the otherwise hypotensive effect of CRH on the iliac artery, but in the skeletal muscle the reflex is so great that it results in vasoconstriction. Importantly and in contrast to central CRH, iv administration of the CRH antagonist, α-helCRH(9-41) completely blocked the cardiovascular effects of iv CRH. Thus, in the presence of sympathetic activity, the cardiovascular effects of systemic (iv) CRH on MAP, mesenteric, and iliac resistance and blood flow oppose the effects of central (icv) CRH and are mediated by CRH-specific receptors on cells of the vasculature. It is possible that systemic actions of CRH on the vascular system are intended to restore homeostasis following the adaptive response to stress.

The hypotensive effects of CRH peptides on the mesenteric vascular bed *in vivo* are paralleled by the vasodilatory effect of CRH peptides on isolated vessels *in vitro*. CRH induces relaxation of isolated vessels that have been pre-constricted with various pressor agents, e.g., vasopressin and noradrenaline (135). Vessels from mesenteric, cerebral, and femoral vascular beds are all dilated by CRH in vitro. In addition, urotensin I has been shown to antagonize the pressor activities of $\alpha_1$-adrenergic agonists (e.g. phenylephrine) but not $\alpha_2$-adrenergic agonists (130). It is not clear if this selective antagonism of different adrenergic receptor functions is the basis for the differential effects of CRH peptides on various vascular beds in vivo. However, these results indicate that vascular CRH receptors functionally interact with adrenergic signaling pathways, and may have implications for CRH receptor-mediated regulation of sympathetic effects on the heart as well.

## 1.12. Effects of CRH on the myocardium

In addition to these vascular effects, there are conflicting reports describing direct effects of CRH on the heart. Early investigation of the cardiovascular effects of urotensin I, a high affinity CRH-R2 agonist, in dogs did not show any change in cardiac function following systemic administration (11). However, CRH was shown to increase the contractile function (i.e. positive inotropic effect) of isolated guinea pig ventricular myocardial strips in vitro (136). Furthermore, CRH increased ANP release, coronary flow and cardiac output of isolated, perfused rat hearts *ex vivo* (137, 138). These results indicate that CRH might have inotropic effects and increase cardiac function in mammals *in vivo*. The discovery of CRH-R2 in hearts suggests that this receptor mediates the effects of CRH on myocardial tissue.

# 2. Inflammation and the Heart

Inflammation and inflammatory mediators are critically important for host defense against injury and infection. Relatively minor injuries elicit local inflammatory reactions. Extensive injuries (trauma, burns) and infections induce high level production of pro-inflammatory cytokines by immune and non-immune cells in the periphery where they are important for host defense. Moreover, cytokines produced systemically can modulate the central nervous system and, similar to exogenous stressors, provoke a broad range of endocrine, behavioral, and autonomic responses. Strong, presumably beneficial, systemic inflammatory responses can also produce effects that lead to peripheral organ dysfunction. These characteristics have made inflammation both an attractive model for investigating mechanisms of stress and an important physiological target of drug therapies for numerous human diseases. This section will introduce important mediators of inflammation, pathways by which they stimulate the central nervous system, and some of their detrimental effects in the periphery.

## 2.1. Mediators of inflammation

The complexity of mammalian immune processes, innate or adaptive, precludes a complete consideration here. This section will focus on key aspects of three pro-inflammatory cytokines that are of central importance to host defense, normal responses to inflammation, and inflammation-induced disease.

### 2.1.1. Tumor necrosis factor-α (TNFα)

Tumor necrosis factor-α (TNFα), originally identified by its detrimental effects on tumor cells and muscle (cachectin), is a broad-acting, pro-inflammatory cytokine produced primarily by monocytes, macrophages, mast cells, and T-lymphocytes (139-142).

However, non-immune cells such as cardiac myocytes also produce TNFα (143-145). Expression of TNFα is regulated at the levels of transcription, mRNA stability, and translation. TNFα is synthesized as a large membrane-bound precursor, and the main active form of TNFα is a soluble homotrimeric protein with a molecular weight (monomer) of 17 kDa. In addition, membrane-bound TNFα trimers are also bioactive. The effects of TNFα are largely mediated by two types of receptors, p55 (TNFα-R1) and p75 (TNFα-R2). TNFα-R1 has high affinity for TNFa and mediates most of its pro-inflammatory effects while TNFα-R2 has relatively lower affinity and functions mainly as a soluble neutralizer of TNFα (146). TNFα is an immediate-response cytokine whose plasma levels peak rapidly after induction of inflammation. TNFα stimulates the production of many other cytokines, including IL-1 and IL-6. TNFα is important for both formation of germinal centers and host defense (147, 148), but excessive or improper production of TNFα is frequently associated with diseases such as heart failure and septic shock (140, 141). To this extent, neutralization of TNFα (e.g. anti-TNFα antibodies, TNFα-R deficiency) can block or ameliorate the detrimental effects of gram-negative lipopolysaccharide (endotoxin) and inflammation in many but not all instances (146, 149-151). Thus, TNFα plays dual roles that provide beneficial (e.g. host defense against microbial pathogens, tumor clearance) but also harmful (e.g. vasodilation, myocardial depression) effects of inflammation.

### 2.1.2. Interleukin-1 (IL-1)

The term interleukin 1 (IL-1) actually describes two pro-inflammatory cytokine activities produced primarily by monocytes and macrophages during the acute phase of inflammatory responses (139, 152, 153). IL-1α and IL-1β are products of two different genes that have <20% sequence homology but strong secondary and tertiary structural homology. Furthermore, while their activities *in vivo* are very similar, they do not have overlapping roles in inflammation (154). Both are produced as larger precursors that are

cleaved into active forms. IL-1β-converting enzyme (ICE) specifically processes IL-1β in vitro, but ICE-deficient mice have impaired production of both IL-1β and IL-1α in response to endotoxin *in vivo* (155). The basis of this phenomenon is not understood; possibly, IL-1β is an important inducer of IL-1α production. Both IL-1α and IL-1β are agonists for IL-1 receptors, which consist of the signaling IL-1RI subjunit and the IL-1RAcP (accessory protein). The effects of IL-1 are regulated by a non-signaling decoy IL-1RII. This decoy receptor, which can either be membrane bound or secreted, binds IL-1 with high affinity, and thus effectively sequesters IL-1 and reduces the amount of free bioactive IL-1 available to bind IL-1RI. The activity of IL-1 is further regulated by an endogenous IL-1 receptor antagonist (IL-1RA), which inhibits IL-1 binding to IL-1RI and -RII and blocks the effects of IL-1 *in vivo* (156). IL-1 is a potent inducer of IL-6 production, and IL-1 blockade can inhibit IL-6 production in some models of inflammation (e.g., turpentine) but not in others (e.g., endotoxin) (154). Exogenous IL-1 can also cause shock similar to TNFα, and inhibition of IL-1 can protect against the lethal effects of endotoxin (155). Thus, IL-1 is also an important pro-inflammatory cytokine with actions similar to those of TNFα.

### 2.1.3. Interleukin-6 (IL-6)

Interleukin-6 (IL-6) is a pro-inflammatory cytokine produced by leukocytes, lymphocytes, and some non-immune cells primarily in response to TNFα, IL-1, and endotoxin (157, 158). IL-6 is secreted as a functional monomer and stimulates cells through a receptor complex of IL-6Rα and IL-6Rβ. The latter, also known as gp130, is the cellular signaling component of the IL-6R complex and of receptors for many other hormones and cytokines, including IL-11, leukocyte-inhibitory factor (LIF), cardiotropin-1 (CT-1), and ciliary-derived neurotrophic factor (CNTF) (159). Interestingly, the IL-6Rα chain can be cleaved into a soluble form, bind soluble IL-6, and facilitate activation of cells expressing gp130 but not membrane-bound IL-6Rα. For this reason, IL-6 has been found

to have many of the activities of IL-11, LIF, CT-1, and CNTF such as inducing the hypertrophy of cardiac myocytes. Elevated levels of circulating IL-6 correlate well with many inflammatory diseases, and IL-6 is a potent inducer of acute-phase proteins from liver (e.g., haptoglobin, $\alpha_1$ acid glycoprotein, serum amyloid A, and C-reactive protein), which are elevated during systemic inflammation. However, IL-6 administration does not induce septic shock, and blockade of IL-6 effects confers very little protection from endotoxic shock compared to blockade of TNFα and IL-1. In fact, IL-6 can suppress IL-1 production, and IL-6 deficiency exacerbates toxin-induced liver injury (160). In addition, IL-6 has been proposed to be important in inflammatory proliferative diseases, and IL-6 deficiency impairs hematopoiesis, T lymphocyte proliferation, and B lymphocyte maturation. Thus, IL-6 is a cytokine important for immune system development and acute-phase reactions; however, it does not have the lethal inflammatory effects of TNFα and IL-1.

### 2.1.4. Gram-negative bacterial lipopolysaccharide (Endotoxin)

In addition to the infectious pathogen itself, purified components of infectious organisms are capable of directly activating mammalian cells *in vitro* and eliciting systemic inflammatory responses *in vivo*. The most characterized of these is bacterial lipopolysaccharide (LPS), or endotoxin (161-163). Endotoxin is a large glycolipid present in the outer leaflet of the outer membrane of gram-negative bacteria. Naturally occurring LPS can contain polysaccharide chains of various lengths. Most of the LPS activity is localized to the lipid A portion of the molecule, but proteins often associated with LPS also stimulate mammalian cells. Genetic, cellular, and biochemical studies have shown that mammals recognize and respond to the lipid A portion of endotoxin primarily through LPS-binding protein (LBP), CD14, and Toll-like receptor 4 (TLR4). LBP is a lipid transfer protein that catalyzes the transfer of amphiphilic LPS monomers from soluble aggregates to CD14 and TLR4. LBP is critically involved in cellular responses to endotoxin *in vitro*, but

LBP-deficient mice display normal elevations in circulating TNFα in response to endotoxin administration (164). CD14 is a small LPS-binding protein most often tethered to the plasma membrane via a glycophosphoinositol (GPI) moiety yet also existing in a soluble form that lacks a GPI anchor. TLR4 is a member of a large family of mammalian proteins with strong homology to *Toll* from Drosophila, which is also involved in host responses to pathogens. TLR4 but not CD14 has cell-signaling capacity. LBP and CD14 may catalyze binding of LPS to dimers of TLR4 in complex with another protein, MD-2. TLR4 is required for cellular responses to endotoxin, while CD14 augments or amplifies the response. The cytoplasmic domain of mammalian TLR proteins is homologous to the cytoplasmic domain of IL-1RI, and stimulation of cells through TLR4 elicits responses very similar to those elicited by IL-1. Thus endotoxin acts through endogenous mammalian receptors to stimulate responses similar to IL-1, including the production of multiple cytokines such as TNFα, IL-1, and IL-6.

## 2.2. Cardiovascular effects of Inflammation (Sepsis Syndrome)

Sepsis is a clinical condition generally described as a systemic microbial infection with associated host inflammatory responses, which often cause cardiovascular dysfunction (165). This condition is prevalent in post-operative patients in hospitals and offers a poor prognosis for these patients; there is roughly 40% mortality among patients diagnosed with sepsis. A major component of the pathological sequelae associated with sepsis syndrome is the acute vascular dysfunction caused by the direct effects of cytokines and indirect effects of the nitric oxide (NO) they induce. In sepsis, the major inflammatory mediators induced by microbial agents such as endotoxin include TNFα, IL-1, IL-6, IL-8, IFNγ, prostaglandins, and complement and platelet activating factor from monocytes/macrophages and endothelial cells (166-169). Neutralization of TNFα blocks most of the lethal effects of endotoxin in animals (149). Cytokines induce NO production by endothelial and smooth muscle cells. Excessive NO production leads to vasodilation,

increased vascular permeability, and hypotension, which eventually results in organ failure (140, 170). Pharmacological blockade of NO production alleviates the vascular effects of cytokines and elevates organ perfusion pressures. However, vasoconstriction in the absence of NO can prevent adequate blood flow and oxygen delivery to organs that are hypoxic in the later stages of the sepsis syndrome when cardiac contractility is depressed.

The negative inotropic effect of inflammatory mediators, or their inhibitory influence on the contractile function of cardiomyocytes, has been demonstrated *in vitro*. TNFα, IL-1, and IL-6 decrease voltage-activated $Ca^{2+}$ influx and contractility of isolated, beating cardiomyocytes *in vitro* (140, 171-173). Furthermore, these cytokines can also inhibit the inotropic and chronotropic effects of β-adrenergic stimulation (2, 174). Endotoxin itself inhibits cardiomyocyte contractility *in vitro* (175, 176). Although results vary, cytokines increase inducible nitric oxide synthesis (iNOS) expression in cardiomyocytes, and NO appears to be an important contributor to the negative inotropic effect of cytokines (140, 171, 172, 175, 176). Intracellular cGMP production has also been shown to contribute to the depressive effects of cytokines (172, 175). Furthermore, stress hormones such as AVP and cardiac natriuretic peptides can enhance the negative inotropic influences of cytokines (177, 178). Thus, there is extensive evidence for cytokine- and endotoxin-induced depression of cardiomyocyte contractile function that may involve increased production of NO and cGMP.

Increases in circulating catecholamines and sympathetic nervous activity are observed soon after induction of experimental sepsis (91). Cardiac contractility also increases early following initiation of experimental sepsis, consistent with sympathetic activation (179). However, later during the sepsis syndrome (shock), myocardial contractility becomes depressed below baseline levels. Even during the period of increased heart function early after onset of sepsis in rats, analysis of such hearts *ex vivo*, in the absence of sympathetic inotropic support, reveals significant depression of contractile function (180, 181). Thus, inflammation has a negative inotropic effect on the heart even

early during sepsis. However, the stimulation of cardiac contractility by the sympathetic nervous system is able to maintain cardiac performance at or above control levels until later phases of the sepsis syndrome (shock).

## 2.3. Effects of inflammation on skeletal muscle

The effects of TNFα and IL-1 on skeletal muscle *in vivo* and *in vitro* vary. *In vivo*, endotoxin causes protein degradation in skeletal muscle (182), but the effects of exogenous TNFa or IL-1 on skeletal muscle protein degradation *in vivo* vary (182-184). However, neither TNFα nor IL-1 have been shown to induce protein degradation in rat skeletal muscle *in vitro* (185), indicating that their role in skeletal muscle proteolysis *in vivo* is likely indirect or requires the combined action of several inflammatory mediators. TNFα has been shown to inhibit glucose uptake by skeletal muscle *in vivo* (186) and *in vitro* (187), and inhibits insulin signaling in skeletal myocytes *in vitro* (187). IL-1 increases (188) or decreases (186) glucose uptake by skeletal muscle *in vivo* depending on the dose of IL-1 used. Moreover, even though TNFα and IL-1 activate JNK and NF-κB in most cells (189, 190) the receptors for TNFα and IL-1 differ in their sequence, structure, and activated signaling pathways (189, 190). However, it should be noted that endotoxin, acting through Toll-like receptor 4 and IL-1 receptor-associated kinase (IRAK), activates the same cellular signaling pathway as IL-1 (190).

## 2.4. Pathways of central nervous system activation by inflammation

While endotoxin and pro-inflammatory cytokines have a broad range of direct effects on peripheral immune and non-immune tissues, many of the physiological responses to inflammation are controlled by the central nervous system. Inflammatory stimuli in the periphery activate neurons within the central nervous system primarily via afferent fibers in the 10th cranial or vagus nerve (191, 192). Afferent vagal transmission of inflammatory stimuli to the brain has been shown convincingly by experiments in which

subdiaphragmatic vagotomy blocks fever and HPA axis activation normally caused by low doses of endotoxin, IL-1β and TNFα in rodents. While vagal nerves do not posses binding sites for cytokines such as IL-1β, this cytokine has been shown to bind to paraganglia that surround vagal fibers (193). The paraganglionic neurons synapse with the vagal fibers and likely transmit inflammatory signals to the vagus nerve. These cytokine-responsive paraganglia extend from the abdomen through the lung, and their presence above and below the diaphragm may explain the inability of subdiaphragmatic vagotomy to inhibit CNS activation following i.v. administration of endotoxin and cytokines. Nevertheless, the afferent vagal fibers are an important pathway of immune-CNS communication.

In addition, endotoxin and cytokines induce hypotension in mammals by stimulating NO production directly by endothelial cells (140, 170). The status of the cardiovascular system, including blood pressure, is monitored by arterial baroreceptors and atrial stretch receptors (194). This information is also transmitted along vagal afferents to the central nervous system. Thus, afferent vagal fibers are also an important pathway of cardiovascular-CNS communication.

There are additional pathways by which cytokines stimulate the central nervous system (195). There is evidence for cytokine transport into the brain (196), cytokine leakage through circumventricular organs where the blood-brain barrier is weak (191, 197), and cytokine activation of brain endothelial cells (198). However, because complete vagotomy is lethal, the contribution of these "alternative" pathways can not be qunatitated separately from vagal transmission.

## 2.5. Central nervous system responses to inflammation

Inflammation stimulates a broad range of physiological responses, including fever, HPA axis activation, altered sleep-wake cycles, anorexia, inactivity, and malaise (195). This broad range of responses reflects extensive neuronal activation in many regions of the

brain following systemic administration of endotoxin or cytokines (199). Among the regions activated are those involved in the control of thermoregulation and the autonomic nervous system. These include the hypothalamic paraventricular nucleus (PVN), barabrachial nucleus, central/periaqueductal gray (PAG), ventromedial preoptic area, (VPO) prelimbic cortices, ventrolateral medulla (VLM), and nucleus of the solitary tract (NTS). Neurons in the PAG, VPO, VLM, and NTS activated by endotoxin also make direct connections to the PVN, which is the principal site of CRH production in the hypothalamus and also mediates the endocrine response to inflammation (200-202). In turn, premotor neurons of the PVN, including those that express CRH, send projections to sympathetic preganglionic neurons in the spinal cord, including preganglia that innervate the stellate ganglion, the primary sympathetic postganglion that innervates the heart (203, 204). The distribution of endotoxin-activated, Fos-immunoreactive neurons provides an anatomical basis for the diverse physiological responses to inflammation, and implicates the PVN as being important in controlling the autonomic portion of these responses (205).

Pathways mediating the neuroendocrine responses to hypotension have also been characterized (206). Most baroreceptor afferent fibers travel up the vagus and innervate the NTS and medulla oblongata. The NTS, in turn, projects to the VLM, lateral parabrachial nucleus, locus coeruleus, PAG, lateral hypothalamus, supraoptic nucleus (SON), PVN, the central nucleus of the amygdala, and the bed nucleus of the stria terminalis. Following hypotensive hemorrhage, neuronal activation marked by cFos-immunoreactivity is observed in the NTS, VLM, lateral parabrachial nucleus, locus coeruleus, supraoptic nucleus, and PVN. Thus, inflammation and hypotension can cause neuronal activation in similar regions of the brain.

In addition, cytokines are produced by cells in the brain itself in response to systemic inflammation. Peripheral endotoxin administration can induce mRNA for TNF$\alpha$, IL-1, and IL-6 in the pituitary and in various regions of the brain, including the hypothalamus (207, 208). IL-1 injection into the brain elicits responses similar to systemic

inflammation, including fever and altered sleep-wake cycles. IL-1 is likely produced by brain astrocytes and microglia, but has also been detected in nerve fibers (209). Thus, in addition to being produced systemically, endotoxin-induced inflammation can result in cytokine production within the CNS.

Systemic inflammation is a potent regulator of CRH and its receptors in the brain and pituitary. Systemic administration of endotoxin induces transcription and accumulation of CRH mRNA in the PVN (209, 210). In addition, systemic inflammation also induces CRH-R1 expression in CRH-producing neurons in the PVN (57). Interestingly, central CRH administration induces upregulation of CRH gene expression as well as CRH-R1 in the PVN (56). However, no induction of CRH-R1 mRNA was seen in a model of adjuvant-induced arthritis (211), and CRH expression was not induced in the PVN in a model of antigen-specific immune stimulation (212). Thus, upregulation of CRH-R1 in hypothalamic CRH-producing neurons may constitute a feed-forward mechanism of HPA and autonomic activation during inflammation and suggests that CRH may upregulate its own receptor in the PVN. Furthermore, regulation of CRH and receptors in the brain are dependent on the manner and intensity of systemic immune activation. In contrast to CRH-R1 upregulation in the hypothalamus, endotoxin-induced inflammation results in CRH-R1 downregulation in the pituitary *in vivo* (118). Endotoxin and IL-1 downregulate CRH-R1 mRNA in pituitary cells *in vitro* (118), suggesting they might have a significant direct effect on CRH-R1 mRNA levels in the pituitary during inflammation *in vivo*. However, this would be in addition to the effects of CRH and dexamethasone, which are also capable of downregulating CRH-R1 mRNA on pituitary cells (109, 213).

The effects of inflammatory mediators on CRH-R2 expression and function are unknown. This is likely due, in part, to the paucity of understanding of the role of CRH-R2 in mammals *in vivo*, and the lack of an identified, model cell type in which to study CRH-R2 *in vitro*. However, some inferences can be made based on what is known about CRH-R2 and inflammation. First, CRH-R1 expression in tissues where it plays a role in

the regulation of the HPA axis (e.g. hypothalamus and pituitary) is regulated by inflammatory mediators. Because CRH-R2 is highly related to CRH-R1, the expression of CRH-R2 may also be regulated by inflammation. Second, CRH-R2 is expressed in the heart and in vessels, which are two tissues whose funcitons are pathologically altered by inflammatory mediators. If CRH-R2 plays an important role in the regulation of the cardiovascular system, then its expression or function in the heart and vessels may also be altered during inflammation. Thus, the study of CRH-R2 regulation by inflammation may provide clues as to the role of CRH-R2 in the cardiovascular system under normal and adverse (stressful) conditions.

# Chapter 2

# Manuscript #1

# Hypothesis

CRH-R2 is highly expressed in the heart, and has been shown by in situ hybridization to be localized in the walls of coronary vessels. This pattern of CRH-R2 expression in the heart provides a molecular basis for the vasodilatory effect of CRH on the coronary vasculature of perfused hearts. However, CRH also has potent, direct inotropic actions on myocardium from rats and guinea pigs. Therefore, we will test the hypothesis that cardiac myocytes express functional CRH-R2.

# Corticotropin-Releasing Hormone Receptor Expression and Functional Coupling in Neonatal Cardiac Myocytes and AT-1 Cells

**Kurt A. Heldwein, Dana L. Redick, Marvin B. Rittenberg, William C. Claycomb‡ and Mary P. Stenzel-Poore**

*Department of Molecular Microbiology and Immunology, Oregon Health Sciences University. Portland, OR 97201, ‡Department of Biochemistry and Molecular Biology, Louisiana State University Medical Center, New Orleans, LA 70112*

**Published in Endocrinology 137(9): 1361-1369 (1996)**

## Abstract

Corticotropin-releasing hormone (CRH) is the principal mediator of the stress response in mammals. In addition to pituitary and central nervous system effects, peripheral effects of CRH have been observed involving the immune and cardiovascular systems. Two CRH receptor subtypes, CRH-R1 and CRH-R2, have been cloned and show significant amino acid homology (69%) but differ in their tissue distribution. CRH-R1 is expressed predominantly in the brain and pituitary while the CRH-R2 subtype is highly expressed in heart and skeletal muscle. To investigate the role of CRH in cardiac signaling, we have analyzed the effect of CRH on freshly isolated neonatal rat cardiomyocytes and murine atrial cardiomyocyte tumor cells, AT-1, which express CRH-R2 mRNA. We show that stimulation of these cells with CRH and the CRH-related peptides, sauvagine from frog and urotensin I from fish, elicits large increases in the intracellular level of 3',5' cyclic adenosine monophosphate (cAMP). This stimulation is transient, reaching a maximum in 5-15 minutes in neonatal cardiomyocytes, and in 2-4 minutes in AT-1 cells followed by a rapid decline. We show that stimulation of AT-1 cells by these peptides is specific for CRH receptors since the CRH antagonist, α-helCRH(9-41) inhibits cAMP increases. Furthermore, we show that CRH, sauvagine and urotensin I stimulation is dose-dependent in both neonatal cardiomyocytes and AT-1 cells. Sauvagine and urotensin I are more potent than CRH at stimulating an increase in intracellular cAMP in neonatal cardiomyocytes ($EC_{50}$ = 1.74 nM, 2.61 nM, 6.42 nM, respectively) and AT-1 cells ($EC_{50}$ = 16.2 nM, 15.8 nM, and 149 nM, respectively). This rank order is consistent with that previously demonstrated in CRH-R2 transfected HEK 293 cells and parallels the *in vivo* vasodilatory activity of these peptides. In summary, this is the first evidence that CRH, sauvagine and urotensin I act directly on cardiac myocytes to stimulate increases in intracellular cAMP presumably through CRH-R2. In addition, these results indicate that

cardiac myocytes may be an informative *in vitro* model to investigate the effects of CRH and its role in the cardiovascular response to stress.

## Introduction

Corticotropin-releasing hormone (CRH) is a 41-amino acid peptide produced in the hypothalamus as well as throughout the brain where it plays a central role in the behavioral and autonomic response to stress. CRH is the major stimulator of adrenocorticotropin hormone (ACTH) and β-endorphin release from the pituitary (1), and recently, a direct role has also been suggested for CRH in the modulation of the immune and cardiovascular systems (69, 214-217). CRH is a member of a small family of peptides that includes sauvagine from frog, urotensin I from fish and a recently identified urotensin homologue discovered in mammals, urocortin (15) (**Fig 2.1**). These peptides have been shown to stimulate ACTH release from mammalian pituitary and to bind to CRH receptors (45, 218).

In addition to potent effects in the pituitary, CRH and the CRH-related peptides elicit a number of cardiovascular responses when administered systemically, most notably, marked vasodilation and hypotension in the peripheral vascular system (15, 127, 219). It is interesting that, although these related peptides are equipotent at stimulating ACTH release from mammalian pituitary, sauvagine and urotensin I are 10-fold more potent than CRH at inducing a long lasting hypotensive response (219).

Recently, a direct action of CRH in the heart has been suggested by studies performed with CRH on isolated perfused rat hearts (69, 70, 137). Following a bolus injection of CRH into the left atrium, a prolonged increase in coronary flow rate, a transient positive inotropic effect on heart muscle, and a transient rise in the rate of atrial natriuretic peptide (ANP) secretion were observed (70). Furthermore, the CRH-induced increase in ANP secretion in the heart could be attenuated by perfusion with the prostaglandin synthesis inhibitor, indomethacin, but prolonged by addition of nitro-L-arginine, an inhibitor of nitric oxide (NO) synthesis (69). Thus, CRH may stimulate production of prostaglandins from endothelial cells and/or myocytes which subsequently modulate cardiomyocyte function in an autocrine or paracrine fashion. NO may have a restraining

influence in this pathway. In addition, CRH has also been shown to have a positive inotropic effect on explanted guinea-pig ventricular myocardium which can be blocked by the $Ca^{2+}$ channel blocker, diltiazem (68). Taken together, these data indicate that the effects of CRH on cardiac function, in part, may result from direct stimulation of cardiac myocytes through a CRH-specific receptor.

Two receptor subtypes for CRH, CRH-R1 and CRH-R2, have been identified which share ~70% homology and belong to the secretin family of G-protein coupled seven-transmembrane receptors (45-47, 49, 60, 74). CRH-R1 is expressed primarily in the brain and pituitary and is believed to mediate the ACTH-releasing function of CRH (49, 220). CRH-R2 has a distinct pattern of expression characterized by high level expression in heart and skeletal muscle (45, 47, 74). In the rat, two isoforms of CRH-R2 (CRH-R2α and CRH-R2b) that differ in their N-termini have been observed that appear to be splice variants from a single gene (221). CRH-R2α is expressed primarily in the central nervous system and is barely detectable in the heart while CRH-R2β is most highly expressed in skeletal and cardiac muscle (221). The CRH-R2 cDNAs cloned from mouse heart cDNA libraries (45, 47, 74) are most homologous to the rat CRH-R2β isoform.

AT-1 cardiac myocytes were derived originally from left atrial tumors of adult transgenic mice expressing the SV40 large T-antigen (TAG) oncogene fused to the ANP promoter (222-224). Recently, several laboratories have used these cells as a model of cardiac cell function (225-227). These cells beat spontaneously in culture, contain well-developed myofibrils and a transverse tubular system, and also possess the perinuclear granules seen in atrial cardiomyocytes *in vivo* (223). Furthermore, AT-1 cells are linked to adjacent cells by intercalated discs , and when transplanted into syngeneic hosts or co-cultured with normal neonatal rat myocytes they have been observed to form junctions with normal myocytes (223, 228) indicating that AT-1 cells are structurally analogous to normal cardiac myocytes. These cells also possess biochemical characteristics of highly differentiated atrial cardiac muscle cells, including a rapidly activated delayed rectifier

current ($I_{Kr}$), mRNA expression of three additional $K^+$ channel types (229) as well as angiotensin converting enzyme, renin, and angiotensin (225), and can be induced to secrete ANP (230). In addition, b-adrenergic receptors in these cells mediate agonist-stimulated modulation of cytosolic $Ca^{2+}$ currents, increase in intracellular cAMP, and homologous desensitization of the receptor (226). Thus, these cells exhibit characteristics typical of normal adult atrial cardiac myocytes while retaining the ability to proliferate, thereby representing a model of cardiac cell function.

To better understand the role of CRH in cardiovascular regulation, we have studied CRH receptor expression and signaling properties in cardiac cells. We demonstrate that freshly isolated rat neonatal cardiomyocytes and AT-1 cells possess functional CRH-R2. The mRNA for this receptor is highly expressed in AT-1 cells as well as in the heart. Receptor signaling appears to be coupled to adenylyl cyclase; the kinetics of stimulation through this receptor reflect a rapid and transient increase in the level of intracellular cAMP which can be blocked with a CRH-receptor specific antagonist. Furthermore, CRH and the CRH-like peptides, sauvagine and urotensin I, stimulate CRH-R2 with a rank order potency of sauvagine=urotensin I>CRH. These results suggest that freshly isolated neonatal cardiac myocytes and AT-1 cells may be informative *in vitro* models for CRH and CRH-like peptide stimulation of heart muscle cells thus enabling investigation of new functions for these important stress hormones regarding cardiovascular regulation.

## Materials and Methods

**Animals and Materials.** Timed-pregnant Sprague-Dawley rats were obtained from Bantin and Kingman Laboratories (Kent, WA). Rat/human (r/h) CRH, sauvagine and urotensin I were obtained from Bachem, Inc. (Torrance, CA). The CRH antagonist, a-helCRH(9-41), was purchased from Penninsula Laboratories (Belmont, CA). Heparin, fibronectin and forskolin were obtained from Sigma Chemical Co. (St. Louis, MO). Bovine insulin was obtained from Gibco-BRL (Grand Island, NY). The cAMP RIA kit was purchased from Biomedical Technologies, Inc. (Stoughton, MA).

**AT-1 Cell Culture.** Derivation of the ANP-TAG transgenic mice and the generation of the transplantable AT-1 tumor cell lineage have been described previously (222, 224). Subcutaneous tumors were aseptically removed from anesthetized mice and subsequently minced and incubated in a sterile ice-cold solution of 0.125% trypsin in Joklik's minimal essential medium (JMEM) with gentle agitation for 14 hours at 4°C followed by digestion for 10 min. in 0.1% collagenase in JMEM at 37.5°C. Tissue culture surfaces were coated with a sterile solution of 0.02% gelatin and 20 ug/ml fibronectin for ≥2 hours at 37°C and washed in Dulbecco's modified Eagle's Medium (DMEM). AT-1 cells were plated and cultured in Excell 300 medium (JRH Biosciences) supplemented with 2 mM L-glutamine, 100 units/ml penicillin, 100 ug/ml streptomycin, 12 ug/ml bovine insulin and 10% fetal bovine serum (Bio-Whittaker). Culture medium was changed every other day up to the day of the experiment.

**Primary Myocyte Isolation.** Myocytes (atrial and ventricular) were isolated from neonatal rat hearts (Sprague-Dawley, 1-day old) as previously described (231). Hearts were dissected and placed in $Ca^{2+}$/bicarbonate-free HEPES buffered Hank's solution

(CBFHH, pH 7.5) with heparin and cut into 1-2 $mm^3$ portions. Tissue pieces were washed and cells liberated by 10-16 digestions in CBFHH containing trypsin (0.15%) and DNase (20 ug/ml) at room temperature. Cells were pelleted in 14% calf serum and washed in MEM containing 5% calf serum. Cells were pre-plated on Falcon Primaria 100 mm plates (Becton Dickinson, Lincoln Park, NJ) for 30-45 minutes to allow non-myocytes to adhere to the surface. This preplating step yields myocyte-enriched cultures that were > 93% myocytes as determined by indirect staining with the monoclonal antibody, MF20 (232), which is specific for sarcomeric myosin in striated muscle (generously provided by Dr. R. Hershberger). Non-adherent cells (enriched for myocytes) were removed, counted, and plated on Primaria 6-well plates at 4.5 x $10^5$ cells/$mm^3$ in MEM containing vitamin $B_{12}$ (20 ug/ml), 5% calf serum and 0.1 mM 5-bromo-2'-deoxyuridine (Sigma, St. Louis, MO) to inhibit proliferation of non-myocytes.

**RNase Protection.** Total RNA was isolated using RNA STAT-60 reagent (Tel-Test "B", Inc., Friendswood, TX). To detect expression of mouse CRH-R2, a probe (mCRX-55) spanning TM3 and TM4 (corresponding to amino acids 204 through 283 of the cDNA) was used. CRH-R2β was detected using a probe spanning the N-terminus (corresponding to amino acids 1 to 175 of the cDNA). CRH-R1 was detected using a probe spanning TM4 and TM5 (corresponding to amino acids 234 to 289 of the cDNA). A 216 nt Rsa I fragment of the L3 cDNA (233), which encodes a ribosomal protein, was used as a loading control. Radiolabeled antisense riboprobe was generated *in vitro* as previously described (45). Radiolabeled probes were annealed with total RNA (10-20 ug) at 42°C for ≥15 hours. Hybrids were digested with RNase A (10 ug/ml) and $T_1$ RNase (600 units/ml) at 30°C for 30 minutes and resolved on 6% acrylamide, 7 M urea gels. Digital images of dried gels were made from the autoradiographic film after exposure to the gel using a ScanJet IIc scanner and DeskScan II software (Hewlett-Packard, Palo Alto, CA).

**Northern Blot**. To detect expression of mouse CRH-R2 mRNA, a 1.2 kbp restriction fragment (Pst I and Hind III) of the mouse heart cDNA spanning amino acids 1 through 366 was used. Total RNA (15 ug) was separated on a 1% agarose formaldehyde gel and transferred onto Nytran (Schleicher and Scheull, Keene, NH). Prehybridization was performed in 50% formamide, 6X SSC, 5X Denhardt's, 0.5% SDS, 10 mM EDTA, 100 ug/ml single-stranded salmon sperm DNA and 50 ug/ml tRNA at 42ϒC. The membrane was hybridized with a $^{32}$P-dATP labeled probe (3 x $10^6$ dpm/ml) in the same solution without the addition of single-stranded salmon sperm DNA or tRNA. Final washes were done in 0.1% SDS, 0.1X SSC at 55°C.

**cAMP Assays .** AT-1 cells were cultured in 24-well tissue culture plates (Costar, Cambridge, MA) for >4 days and were ~ 90% confluent at the time of the assay. Freshly isolated, beating rat neonatal cardiomyocytes were cultured overnight in 100 mm dishes. On the day of the experiment, cells were washed in plain DMEM and pre-incubated for 90 minutes in DMEM (AT-1 cells) or MEM (with vitamin $B_{12}$, neonatal rat myocytes) supplemented with 100 units/ml penicillin, 100 ug/ml streptomycin, and 0.1% fetal bovine serum. Cells were then pre-incubated in the above media supplemented with 1 mM 3-isobutyl-1-methylxanthine (IBMX) (Sigma, St. Louis, MO) to inhibit cAMP phosphodiesterase activity (234). After 30 minutes, pre-incubation medium was removed and stimulation medium was added (0.1% FBS, 1 mM IBMX containing appropriate concentrations of CRH, sauvagine, urotensin I, and/or a-helCRH(9-41)). $N_4$-D-$Phe_7$-α-melanocyte stimulating hormone (NDP-α-MSH), a melanocyte-stimulating hormone-receptor agonist, was used as a negative control in stimulation assays (generous gift of Dr. Roger Cone, Portland, OR). Rat neonatal cardiac myocytes and AT-1 cells were incubated at 37°C for the indicated lengths of time, after which the stimulation medium was removed. The cells were immediately lysed and incubated overnight at -20°C in extraction medium (95% ethanol/20 mM HCl). Samples were dried under vacuum and cAMP was measured

using a commercial radioimmunoassay kit (Biomedical Technologies, Inc., Stoughton, MA). Dose response assays were performed two to three times and time course experiments were performed twice, with duplicate wells being assayed in each experiment.

**Statistics.** All data are presented as the mean ± SEM. Statistical significance of the neonatal cardiomyocyte and AT-1 cell cAMP response to peptides over time was determined by two-way ANOVA. The means of individual points for the cAMP time courses and α-helCRH(9-41) inhibition of the sauvagine and urotensin I stimulated increase in cAMP in AT-1 cells were compared and least significant difference calculated using unpaired Student's t-test. All calculations were made using the MultiStat software (Biosoft, Cambridge, UK). The $EC_{50}$ values of the dose-dependent increases in intracellular cAMP in response to CRH, sauvagine and urotensin I were determined by non-linear regression using the GraphPad Prism software (GraphPad, Inc., San Diego, CA).

## Results

**Expression of CRH-R2 in AT-1 cells.** Preliminary studies using Northern blot analysis of total RNA from AT-1 cells indicated that they expressed CRH-R2 (data not shown). To determine whether AT-1 cells express the CRH-R2 isoform, CRH-R2β, and test for the presence of CRH-R1, RNase protection analysis was performed using probes specific for mouse CRH-R2, CRH-R2β or CRH-R1 (**Fig. 2.2A**). $^{32}$P-UTP-labeled probes were hybridized to total RNA from AT-1 cells and mouse heart, cerebellum and hypothalamus (**Fig. 2.2B**). The same amount of RNA was annealed and loaded within each tissue comparison as seen by similar intensities of L3. A band corresponding to protected riboprobe specific for CRH-R2 mRNA is easily detectable in AT-1 cells whereas no protected fragment representing CRH-R1 is present (**Fig. 2.2B**).

The probe used to detect CRH-R2β spans the N-terminus covering a region of sequence divergence between the α and β isoforms as well as a region of sequence identity preceding the first membrane spanning region (**Fig. 2.2A**); this probe protects a fragment of 385 nucleotides (nt) for CRH-R2β mRNA. The presence of CRH-R2α would be indicated by a shorter protected fragment (220 nt) if the gene organization in the mouse is the same as in the rat. CRH-R2β appears to be the dominant isoform expressed in whole heart and AT-1 cells as indicated by the presence of a strong 385 nt protected fragment (**Fig. 2.2B**) whereas a band of 220 nt length (representing CRH-R2a) is only weakly detectable. In contrast, CRH-R2α appears to be the major isoform expressed in mouse hypothalamus as evidenced by the presence of a 220 nt fragment and absence of a 385 nt CRH-R2β protected fragment. As discussed above, based on the CRH-R2 splice pattern in the rat, the presence of a 220 nt fragment in mouse hypothalamus is consistent with the expression

of CRH-R2α, although direct evaluation of CRH-R2 splicing awaits the availability of probes specific for each isoform in the mouse.

**Dose dependent stimulation of cAMP production in cardiomyocyte cultures by CRH, sauvagine and urotensin I.** To determine whether CRH-R2 was functionally expressed in AT-1 cells and cardiomyocytes isolated from neonatal rat hearts, the effect of CRH and related peptides on cAMP production was examined (**Fig 2.3**). AT-1 cells in culture were stimulated with CRH, sauvagine, urotensin I, and NDP-α-MSH in the presence of 1mM IBMX for 2 minutes (**Fig. 2.3A**). Stimulation with NDP-α-MSH was used as an irrelevant peptide negative control since it consistently failed to stimulate an increase in intracellular cAMP in this system. An increase in cAMP accumulation to similar maximum levels was seen with CRH, sauvagine, and urotensin I in these experiments (15.5 ± 2.3, 14.4 ± 1.6, 16.2 ± 0.8-fold increase over basal, respectively) whereas the level of cAMP in response to the irrelevant peptide NDP-α-MSH remained at basal level. Interestingly, the half-maximal stimulatory ($EC_{50}$) concentrations of sauvagine, and urotensin I were similar (16.2 ± 1.2 nM and 15.8 ± 2.8 nM, respectively) whereas that of CRH was 10-fold higher (149 ± 20 nM). These data demonstrate that CRH and related peptides stimulate cAMP production in a dose dependent manner and suggest that sauvagine and urotensin are more potent than CRH in stimulating cAMP accumulation in AT-1 cells.

To determine whether freshly isolated cardiomyocytes respond to CRH and related peptides, myocyte-enriched cultures from neonatal rat hearts were stimulated with various concentrations of these peptides in the presence of 1 mM IBMX for 5 minutes (**Fig. 2.3B**). The level of cAMP in the myocytes increased in a dose-dependent fashion to CRH, sauvagine and urotensin I, with the maximum level of stimulation ranging from 7.9-9.5 fold above basal. As observed in AT-1 cells, both sauvagine and urotensin I were more potent than CRH at inducing cAMP production in cardiomyocytes ($EC_{50}$ = 1.74 ±

0.26 nM, 2.61 ± 0.39 nM, 6.42 ± 0.42 nM, respectively), and NDP-α-MSH failed to stimulate cAMP production above basal levels. These results demonstrate that freshly isolated neonatal myocytes and AT-1 cells respond to CRH, sauvagine and urotensin I stimulation with increased intracellular cAMP levels.

**Kinetics of cAMP production in cardiomyocyte cultures by CRH and CRH-related peptides.** To investigate the kinetics of receptor stimulation by these peptides, cells in culture were stimulated with 100 nM CRH, sauvagine, urotensin I or NDP-α-MSH for times ranging from 0.5 to 30 minutes, lysed, and the amount of cAMP was measured in each sample. Stimulation with peptide was performed in the presence of 1mM IBMX. The intracellular level of cAMP in AT-1 cells reached a maximum within 2-4 minutes in response to CRH, sauvagine, and urotensin I, and steadily decreased over time but remained elevated at 5 to 10-fold over basal at 20 minutes (**Fig 2.4A**). Direct stimulation of adenylyl cyclase by forskolin (12 uM) displayed a different trend: levels of intracellular cAMP increased to 200-fold over basal levels by 12 minutes and then remained elevated (data not shown). The maximum level of intracellular cAMP generated in response to CRH (15.8 ± 0.5-fold over basal) was consistently lower than levels seen after stimulation of AT-1 cells with sauvagine or urotensin I (25.8 ± 2.2-fold, and 26.2 ± 4.7-fold over basal, respectively). Only a slight increase above basal levels of intracellular cAMP (2.5-3.5 fold) after stimulation with any of the three peptides was observed in AT-1 cells that were not treated with IBMX (data not shown). The irrelevant peptide control, NDP-α-MSH, did not stimulate intracellular cAMP accumulation above basal levels. The rapid decrease in cAMP levels in the AT-1 cells after 2-4 minutes of stimulation with peptides, but not with forskolin, suggests that the signaling process may be rapidly desensitized at some point(s) preceding and/or including activation of the catalytic subunit of adenylyl cyclase.

Primary cardiomyocytes from neonatal rat hearts stimulated with 100 nM CRH, sauvagine, and urotensin I in the presence of 1 mM IBMX also showed a rapid increase in

intracellular cAMP which reached a maximum within 5-15 minutes and decreased only slightly after 30 minutes (**Fig 2.4B**). CRH, sauvagine and urotensin I induced a time-dependent increase in intracellular cAMP ranging from 4-6 fold above basal level. The levels of intracellular cAMP in cardiomyocytes stimulated with irrelevant peptide control, NDP-α-MSH, remained near basal.

**Inhibition of cardiomyocyte stimulation with a CRH-specific antagonist.** The CRH receptor peptide antagonist α-helCRH(9-41) was used to test whether the effects of CRH, sauvagine and urotensin I on AT-1 cells and neonatal rat cardiomyocytes are specifically mediated by CRH receptors (**Fig. 2.5**). Increased cAMP levels in AT-1 cells caused by sauvagine and urotensin I were significantly inhibited ($P<0.01$) in the presence of α-helCRH(9-41) (**Fig. 2.5A**). The same concentration of each peptide (10 nM) was used to stimulate increases in cAMP in the presence and absence of α-helCRH(9-41). In the case of urotensin I and sauvagine, cAMP increases were readily inhibited by α-helCRH(9-41) (10 uM) demonstrating that the effect of these peptides is likely to occur through CRH receptors. Stimulation by CRH using 10 nM peptide concentration is clearly not maximal (based on our dose-response studies described above) and thus very little inhibition by α-helCRH(9-41) is detected. The rationale for selecting this lower dose in stimulating with all three peptides was to take advantage of the greater sensitivity of CRH-R2 for sauvagine and urotensin I compared to CRH. A slight rise in intracellular cAMP occurs in cells stimulated with antagonist alone, consistent with the previous observation that a-helCRH(9-41) is not a pure antagonist and has weak intrinsic agonist activity (235). These results, together with the RNAse protection data, demonstrate that stimulation of intracellular cAMP accumulation in AT-1 cells by low concentrations of sauvagine and urotensin I occurs primarily through CRH-R2β.

Similar to AT-1 cells, stimulation of cAMP accumulation by 10 nM sauvagine and urotensin I was significantly inhibited ($P<0.05$) in the presence of α-helCRH(9-41) (10

mM) in neonatal cardiac myocyte cultures (**Fig. 2.5B**). Stimulation of intracellular cAMP by a higher dose of CRH (100 nM) was markedly reduced in the presence of α-helCRH(9-41) in these cultures. The fact that a lower dose of CRH (10 nM) elicited only a small increase in cAMP that was not blocked by the CRH antagonist demonstrates the lower potency of this agonist compared with sauvagine and urotensin I on neonatal cardiomyocytes.

## Discussion

We have identified a model cardiac cell type (AT-1) that expresses CRH-R2β mRNA and responds to CRH stimulation. Furthermore, we show that freshly isolated cardiomyocytes are responsive to CRH, sauvagine and urotensin I in a similar fashion. The results reported here are the first to demonstrate CRH-stimulated increases in intracellular cAMP in cells with a cardiac muscle phenotype and suggest a direct role for CRH in modulation of the myocardial response to stress.

In the rat, two isoforms of CRH-R2 have been identified (221). CRH-R2a is expressed primarily in the central nervous system and is barely detectable in the heart while CRH-R2β is most highly expressed in skeletal and cardiac muscle (221). Consistent with this finding, we show that in mouse heart and AT-1 cells, CRH-R2β is the dominant isoform expressed from the CRH-R2 gene while in the hypothalamus a shorter fragment (220 nt) is seen indicating the expression of CRH-R2α. Our findings regarding CRH-R2 isoform expression in the mouse heart and hypothalamus parallel those in the rat and further strengthen the observation that CRH-R2β is the dominant isoform of CRH receptor in peripheral tissues.

Experiments performed previously in our laboratory (45) and others (47, 74) have demonstrated that HEK 293 and COS-M6 cells transfected with mouse CRH-R2 (now known to be CRH-R2b) suggest positive coupling to adenylyl cyclase following CRH stimulation. To determine whether this CRH receptor may be coupled to adenylyl cyclase in a homologous cell culture system where CRH-R2β is expressed endogenously, we examined cAMP accumulation in neonatal rat cardiac myocytes and AT-1 cells. In these cells, the response to CRH, sauvagine, and urotensin I stimulation is rapid. The peak cAMP response in neonatal cardiomyocytes occurs within 5-15 minutes, while AT-1 cells

reached maximum intracellular cAMP levels within 4 minutes. The effect of these peptides on AT-1 cells was potentiated by incubation with IBMX (1 mM) indicating that the increase in intracellular cAMP mediated by CRH-R2β is not likely to occur by inhibition of cAMP phosphodiesterase but rather via activation of adenylyl cyclase although direct measurements of cyclase activity have not yet been done in this system. In addition, our finding that the CRH-receptor specific antagonist, α-helCRH(9-41) reduced sauvagine and urotensin I-stimulated increases in cAMP in AT-1 cells and neonatal cardiomyocytes indicates that peptide stimulation occurs through a CRH-receptor specific mechanism.

The rapid fall in cAMP accumulation in AT-1 cells despite incubation of the cells with IBMX for 30 minutes prior to stimulation with peptides may indicate that CRH-R2β is quickly desensitized following exposure to the ligand. It is interesting that in a similar ligand-receptor system that exists in cardiac myocytes, stimulation with calcitonin gene related peptide (CGRP) results in rapid desensitization of CGRP receptors (236). In that study, CGRP (100 nM) elicited an increase in intracellular cAMP (5-fold) in myocytes treated with 0.1 mM IBMX; the maximum increase was reached within 1 minute of hormone stimulation and cAMP levels declined to near basal levels within 5 minutes (236). The intracellular cAMP levels in AT-1 cells stimulated with CRH, sauvagine and urotensin I reached a peak within 5 minutes and then declined 2-3 fold during the remaining stimulation period (20 min.) although these levels did not reach basal levels. Neonatal cardiomyocytes cAMP levels remained near the maximum up to 30 minutes after stimulation. Maintenance of elevated intracellular cAMP levels over time may be due to the use of a higher concentration of IBMX (1.0 mM) in our studies compared with those of Fisher, et. al. (236). Thus while receptor signaling may become uncoupled from adenylyl cyclase activation, efficient inhibition of intracellular phosphodiesterase activity by IBMX could prevent the return of cAMP levels to near basal during this time. Our studies presented here do not address the mechanisms of CRH-R2β regulation in cardiac

myocytes; however, it is possible that agonist-induced changes alter the sensitivity or availability of this receptor as has been recently reported for CRH-R1 (108), CRH-receptors in the central nervous system and pituitary (237-239) and other G-protein coupled receptors (240, 241).

The difference in kinetics of CRH, sauvagine and urotensin I-stimulated intracellular cAMP accumulation between AT-1 cells and neonatal cardiomyocytes treated with 1 mM IBMX could be due to differences in the differentiation state of the muscle cells. It is known that signal transduction systems are not always equivalent in neonatal and adult cardiomyocytes such as been reported with $b_2$-adrenergic receptors, protein kinase C isoform expression and turnover of phosphotidylinositol molecules (242-244). In addition, receptor density on adult cardiomyocytes may differ from neonatal cardiomyocytes by as much as 4-fold (243). We are in the process of examining freshly isolated adult cardiac myocytes as well as neonatal cells to compare their responses to CRH and related peptides and determining receptor density.

Stimulation of cAMP production in neonatal rat cardiomyocytes parallels our studies and those of others (74) using HEK 293 cells transfected with mouse CRH-R2b. Sauvagine has been shown to bind to mouse CRH-R2β with 50-fold higher affinity than CRH (45) and both sauvagine and urotensin I have been shown to be 30-fold and 10-fold, respectively, more potent than CRH at stimulating a rise in the intracellular cAMP level in these cells (74). In the present study, sauvagine and urotensin I were more effective than CRH at stimulating cAMP production in neonatal rat cardiomyocytes. Vascular responses to CRH, sauvagine and urotensin I in mammals have revealed similar trends in potency between these peptides. Peripheral administration (i.v.) and application of these peptides *in vitro* have shown that sauvagine and urotensin I are more potent than CRH at inducing vasodilation in mammals (15, 127, 219, 245). In addition, the newly described CRH-

related peptide, urocortin is more potent than CRH in decreasing mean arterial pressure in rats and stimulating intracellular cAMP accumulation in CHO cells transfected with CRH-R2β (15). Our results suggest that the same receptor type, CRH-R2β, is present in neonatal cardiac cells and could thus mediate similar vascular effects.

The finding that myocytes are responsive to CRH *in vitro* is intriguing in light of the observation that CRH increases the rate of ANP secretion in the isolated working heart model perhaps indicating that CRH, acting through CRH-R2b, may directly mediate stimulation of ANP production. Elevations in intracellular cAMP levels have been reported to increase ANP release from cardiomyocytes under certain conditions (246, 247), however, this effect appears to depend on whether the experimental system involves intact atria or isolated cells (248). While it is generally believed that isolated atrial myocytes do not show increases in ANP release in response to cAMP (249), isolated ventricular myocytes may exhibit increased ANP secretion following stimulation of cAMP levels (246). In the latter case, however, effects of cAMP on ANP secretion were seen in the context of phorbol-12-myristate 13-acetate (PMA) which activates PKC; thus, increased cAMP levels alone may not significantly alter ANP secretion in isolated cardiomyocytes. It is conceivable that CRH-R2 may be positively coupled to both cAMP production and PKC activation, particularly in light of the recent finding that CRH-R1 mediates increases in cAMP and $IP_3$ turnover in COS-7 cells (250). Similar dual signaling properties of CRH-R2β in cardiac tissue may mediate CRH-dependent stimulation of ANP release from cardiomyocytes.

CRH induces a transient positive inotropic effect (68, 70, 137) which may result from increased intracellular cAMP levels. Activation of cAMP-dependent protein kinase A (PKA) has been shown to be an important component in the regulation of contractility (251). Known substrates for PKA in cardiomyocytes include L-type calcium channels

(252) and ryanodine-sensitive calcium release channels (253, 254). In addition, blockade of PKA activity has been shown to suppress the inotropic response of rat cardiomyocytes to isoprenaline, secretin and vasoactive intestinal peptide, all of which are known to stimulate cAMP production (255). Thus, the finding that CRH-R2β mediates an increase in intracellular cAMP in neonatal cardiomyocytes and AT-1 cells in response to CRH and related peptides provides a potential mechanism by which these peptides may directly influence cardiomyocyte contractility.

Current and previous findings demonstrating an effect of CRH on cardiac function raises the interesting question of a possible source of bioactive CRH within the heart. Detection of mRNA for CRH in whole heart tissue (25) suggests that any of the cells of the heart, such as neurons within the heart, cardiomyocytes, fibroblasts and/or endothelial cells, may be the primary source of CRH in cardiac tissue. Immunoreactivity for another neuropeptide, CGRP, has been found in sensory neurons and it has been suggested that release of CGRP from these fibers may influence heart contractility (236). Similarly, it is possible that CRH may be released into the heart from post-ganglionic sympathetic nerves, representing a direct route by which the central response to stress could modulate cardiac function. It is also possible that CRH is co-released within the heart with adrenergic receptor agonists. In view of the contrasting effects of CRH and a-adrenergic receptor agonists on vascular tone (245) this would strengthen the idea proposed by others (43, 256) that peripheral CRH may function in opposition to the actions of central CRH. Interestingly, urocortin, a recently identified CRH-like peptide, has been shown to be more potent than CRH on CRH-R2β, which raises the possibility that urocortin may be the endogenous ligand for this receptor (15). It is not known yet whether urocortin expression in the CNS could affect ganglia that regulate heart function or if urocortin is expressed in the heart. Thus, identification of a source of CRH-R2β agonist production that acts in the heart would aid our current understanding of the cardiovascular response to stress.

In conclusion, we have found that neonatal rat cardiac myocytes and atrial cardiomyocytes, AT-1, express functional CRH-R2β. The CRH receptor expressed by these cells responds to CRH and the CRH-related peptides, sauvagine and urotensin I with a strong and transient increase in intracellular cAMP accumulation; the rank order potency of these peptides is sauvagine=urotensin >CRH . In addition, since AT-1 cells possess many characteristics of mature, highly differentiated cardiac myocytes, these cells may serve as a useful *in vitro* model to investigate the cardiac effects of CRH in the cardiovascular response to stress.

**Figure 2.1.** Aligned amino acid sequences of the mature peptide for rat/human (r/h) CRH (257), urocortin (15), sauvagine from *Phyllomedusa sauvagei*, (258) and urotensin I from *Catostomus commersoni* (245). Regions of homology are noted within boxed frames.


r/h CRH S E E P P I S L D L T F H L L R E V L E M A R A E Q L A Q Q A H S N R K L M E I I
sauvagine - G - - - - - - - - S L E - - - K M I - I E K Q - K E K - - - A N - - L - L D T -
urotensin I N D D - - - - - - - - - - - - - - - N M I - - - - I - N E R E - - G L - - - Y L D E V
urocortin D D - - - - - - - - - - - - - - - T L - - L - - T Q S Q R E R - E Q - - I I F D S V

**Figure 2.2.** Expression of CRH-R2 by AT-1 cells. (A) Map of probes used to detect expression of mouse CRH-R1, CRH-R2, and CRH-R2β. (B) RNAse protection analysis of total RNA (10-20 ug) from AT-1 cells and mouse heart, cerebellum and hypothalamus using $^{32}$P-UTP labeled probes. The L3 probe is a control for quantity of RNA and protects a 110 nt band. CRH-R1 protects a 169 nt band and the CRH-R2 probe protects a 239 nt band. The CRH-R2β probe will protect a 385 nt CRH-R2β fragment and a smaller 220 nt CRH-R2a fragment (*), lying within the CRH-R2β segment, which can be seen in the hypothalamus but not in the heart or AT-1 cells.

A.

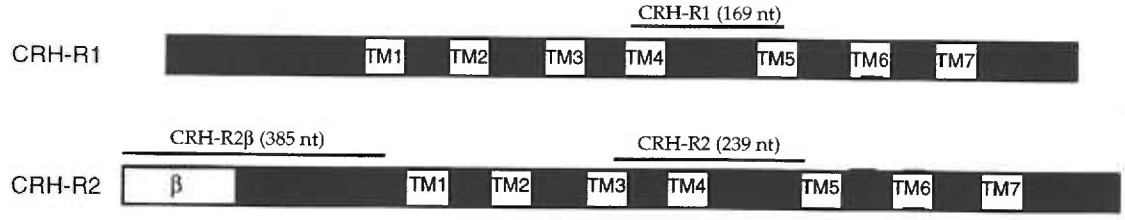
CRH-R1 (169 nt)
CRH-R1
TM1
TM2
TM3
TM4
TM5
TM6
TM7
CRH-R2β (385 nt)
CRH-R2 (239 nt)
CRH-R2
β
TM1
TM2
TM3
TM4
TM5
TM6
TM7

B.

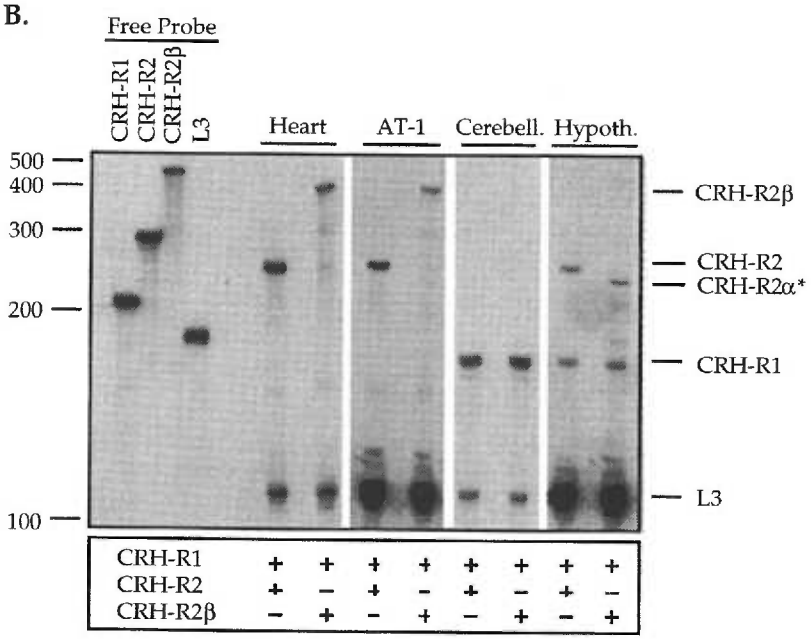
Free Probe
CRH-R1
CRH-R2
CRH-R2β
L3
Heart
AT-1
Cerebell.
Hypoth.
500
400
300
200
100
CRH-R2β
CRH-R2
CRH-R2α*
CRH-R1
L3
CRH-R1 + + + + + + + +
CRH-R2 + − + − + − + −
CRH-R2β − + − + − + − +

**Figure 2.3.** Dose dependent stimulation of cAMP accumulation in AT-1 cells and neonatal rat cardiomyocytes by CRH, sauvagine, and urotensin I. (A) Dose response of AT-1 cells to increasing concentrations of indicated peptides following 2 minute stimulation with peptide. Points are the average (± SD) of duplicate wells from 2-3 experiments. (B) Dose response of freshly isolated myocytes to increasing concentrations of indicated peptides following 5 minute stimulation with peptide. Points represent the average (± SD) of duplicate wells from a representative experiment.

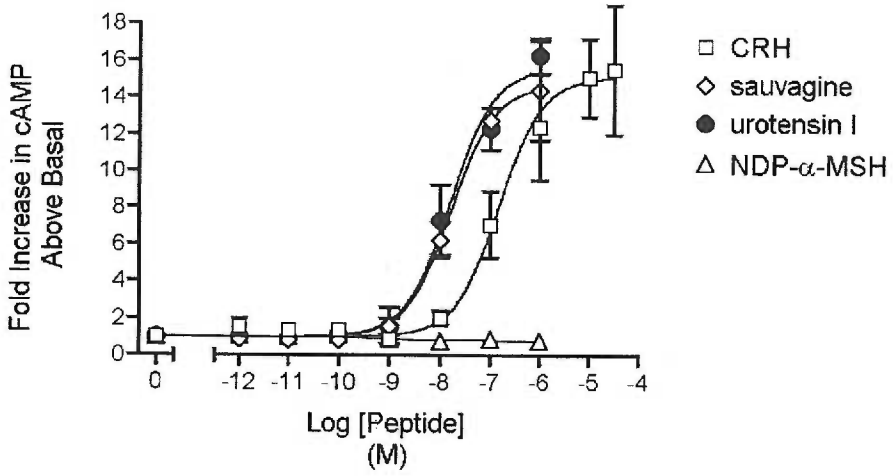
Fold Increase in cAMP Above Basal
18
16
14
12
10
8
6
4
2
0
0
-12 -11 -10 -9 -8 -7 -6 -5 -4
Log [Peptide] (M)
CRH
sauvagine
urotensin I
NDP-α-MSH

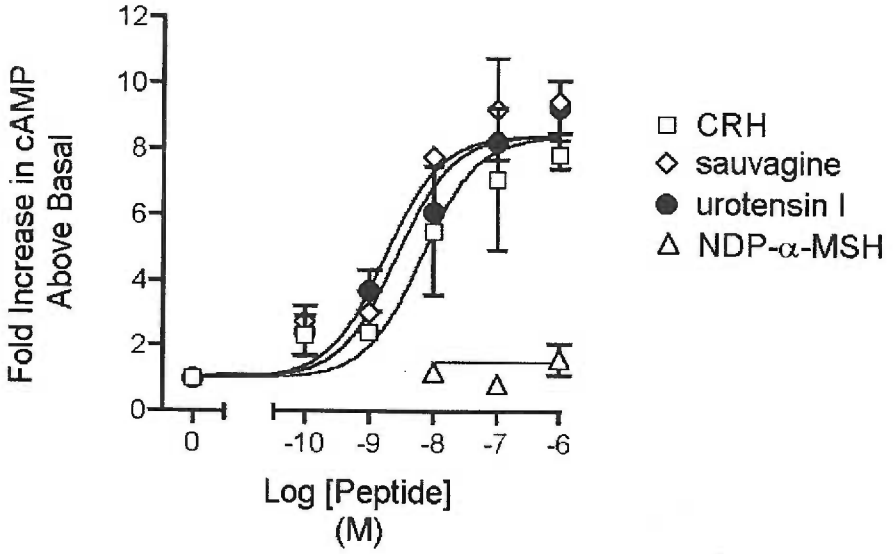
Fold Increase in cAMP Above Basal
12
10
8
6
4
2
0
0
-10 -9 -8 -7 -6
Log [Peptide] (M)
CRH
sauvagine
urotensin I
NDP-α-MSH

**Figure 2.4.** Time dependent elevation of cAMP in AT-1 cells and neonatal rat cardiomyocytes by CRH, sauvagine, and urotensin I. (A) AT-1 cells were stimulated with each peptide (100 nM) for the indicated times. Intracellular cAMP responses to CRH, sauvagine ($P<0.001$) and urotensin I ($P<0.01$) were significantly higher than the response to NDP-α-MSH. The mean increase in cAMP stimulated by CRH, sauvagine and urotensin I was significantly different ($P<0.05$) than NDP-α-MSH-stimulated levels at all time points. (B) Freshly isolated myocytes were stimulated with each peptide (100 nM) for the times indicated. Intracellular cAMP responses to CRH, sauvagine and urotensin I ($P<0.001$) were significantly higher than the response to NDP-α-MSH. The mean increase in cAMP stimulated by sauvagine and urotensin I was significantly different ($P<0.05$) than NDP-α-MSH-stimulated levels at all time points, with the response to CRH being significant after 2 min. ($P<0.05$). Points represent the average (± SD) of duplicate wells from a representative experiment.

A.

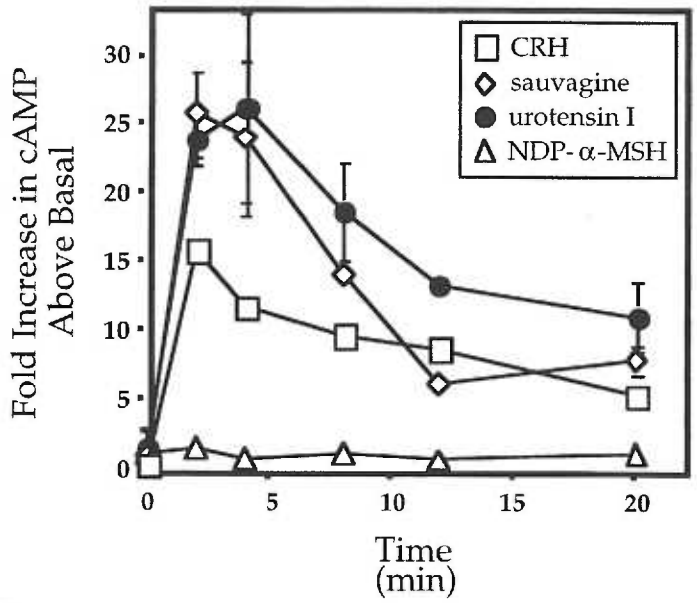
CRH
sauvagine
urotensin I
NDP-α-MSH
Fold Increase in cAMP Above Basal
30
25
20
15
10
5
0
0
5
10
15
20
Time (min)

B.

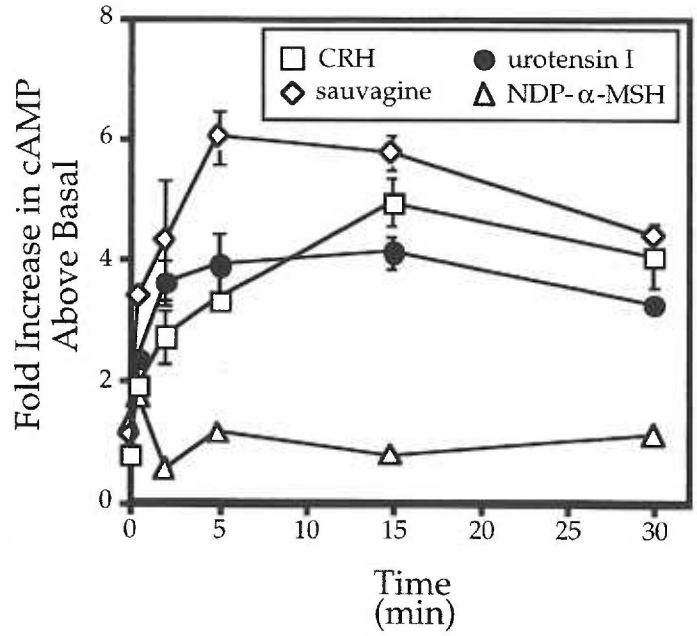
CRH
sauvagine
urotensin I
NDP-α-MSH
Fold Increase in cAMP Above Basal
8
6
4
2
0
0
5
10
15
20
25
30
Time (min)

**Figure 2.5.** Inhibition of stimulation of AT-1 cells and neonatal rat cardiomyocytes with the CRH antagonist, α-helCRH(9-41). A) Stimulation of AT-1 cells with indicated peptides (10 nM) in the presence or absence of the CRH-receptor antagonist (10 mM). *P<0.01 compared to the same peptide stimulation without α-helCRH(9-41). B) Stimulation of neonatal rat cardiomyocytes with CRH (10 nM and 100nM), sauvagine (10 nM), urotensin I (10 nM) and NDP-α-MSH (10 nM) in the presence or absence of the CRH-receptor antagonist (10 mM). Bars are the average (± SD) of duplicate wells from a representative experiment. *P<0.05 compared to the same peptide stimulation without a-helCRH(9-41).

A.

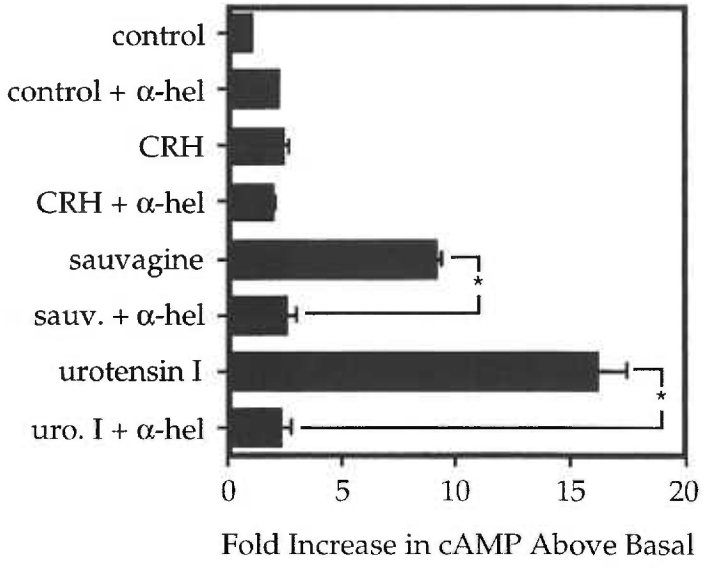
control
control + α-hel
CRH
CRH + α-hel
sauvagine
sauv. + α-hel
urotensin I
uro. I + α-hel
*
*
0
5
10
15
20
Fold Increase in cAMP Above Basal

B.

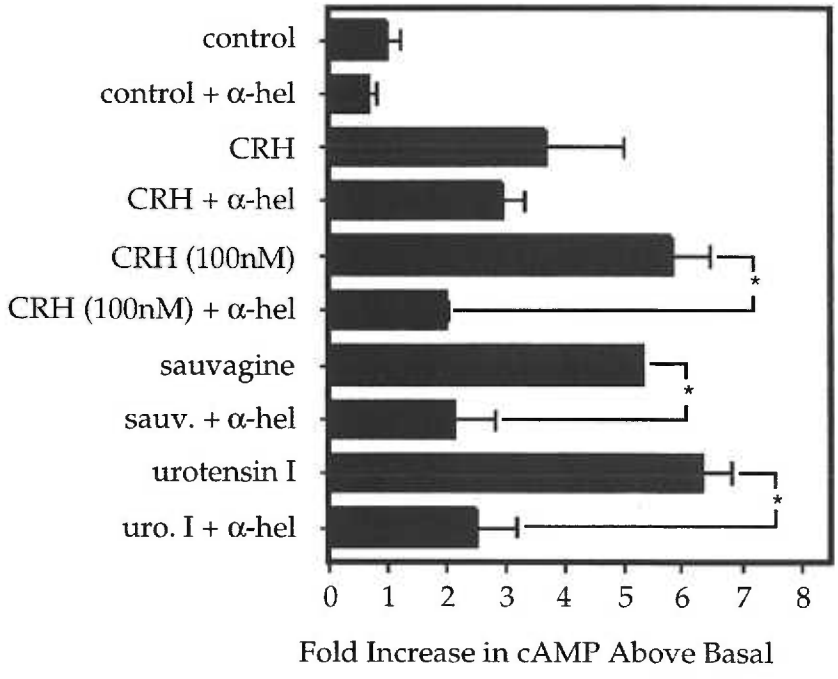
control
control + α-hel
CRH
CRH + α-hel
CRH (100nM)
CRH (100nM) + α-hel
sauvagine
sauv. + α-hel
urotensin I
uro. I + α-hel
*
*
*
*
0
1
2
3
4
5
6
7
8
Fold Increase in cAMP Above Basal

## Acknowledgements

We thank Beverly Stallworth for expert technical assistance and Dr. Ray Hershberger for providing us with expertise in culturing neonatal cardiomyocytes. We gratefully acknowledge Drs. R. Cone. and P. Stenzel for helpful discussions and T. Martin, M. Brown and Drs. S. Landfear, R. Kesterson, E. Whitcomb, G. Wiens, and L. Kenney for critical review of the manuscript. This work was supported by NIH Grants AI-14985, AI-26827 and MH-52393-02.

# Chapter 3

# Manuscript #2

# Hypothesis

Both CRH and Ucn have direct vasodilatory effects, and the greater potency of Ucn vs. CRH reflects the pharmacology of CRH-R2 but not CRH-R1. In addition, we have shown that the mouse cardiac myocyte cell line, AT-1, expresses functional CRH-R2, with no evidence for CRH-R1 mRNA. Thus, we hypothesize that CRH-R2 mediates the direct cardiovascular effects of Ucn in the mouse.

# Abnormal adaptations to stress and impaired cardiovascular function in mice lacking corticotropin-releasing hormone receptor-2.

Sarah C. Coste[1§], Robert A. Kesterson[8§], Kurt A. Heldwein[1], Susan L. Stevens[1], Amanda D. Heard[1], Jacob H. Hollis[1], Susan E. Murray[1], Jennifer K. Hill[1], George A. Pantely[2,7], Alan R. Hohimer[3,7], Daniel C. Hatton[4,7], Tamara J. Phillips[4,9], Deborah A. Finn[4], Malcolm J. Low[6], Marvin B. Rittenberg[1], Peter Stenzel[5,7] and Mary P. Stenzel-Poore[1,7]

*Departments of [1]Molecular Microbiology and Immunology, [2]Medicine, [3]Obstetrics and Physiology, [4]Behavioral Neuroscience, [5]Pathology, [6]Vollum Institute, [7]Congenital Heart Research Center, Oregon Health Sciences University, Portland, Oregon 97201, USA. [8]Department of Molecular Physiology and Biophysics, Vanderbilt University Medical Center, Nashville, Tennessee 37232, USA. [9]Department of Veterans Affairs Medical Center, Portland, Oregon 97201, USA.*

§Both authors contributed equally to this work.

**Published in Nature Genetics 24(4): 403-409 (2000)**

## Abstract

The actions of corticotropin-releasing hormone (CRH), a critical mediator of endocrine(1) and behavioral responses to stress(259), and the related hormone urocortin (Ucn)(15) are coordinated by two receptors, CRH-R1 and CRH-R2(45, 49). These receptors may exhibit distinct functions due to unique tissue distribution(55) and pharmacology(45, 49). *Crhr1* null mice have defined central functions for CRH-R1 in anxiety and neuroendocrine stress responses(8, 9); CRH-R2 functions have not been similarly defined. We created CRH-R2 null mice (*Crhr2*$^{-/-}$) to identify specific roles for CRH-R2. We show that CRH-R2 supplies important regulatory features to the hypothalamic-pituitary-adrenal axis (HPA) stress response. Although initiation of the stress response appears normal, *Crhr2*$^{-/-}$ mice show early termination of ACTH release suggesting that CRH-R2 is involved in maintaining HPA drive. CRH-R2 also appears to modify the recovery phase of the HPA response, as corticosterone levels remain elevated 90 min post stress in *Crhr2*$^{-/-}$ mice compared to wild-type mice. In addition, behavioral responses to novelty are aberrant in *Crhr2*$^{-/-}$ mice. Specifically, self-grooming, considered a stress-coping behavior associated with dearousal, is significantly reduced in *Crhr2*$^{-/-}$ mice. We also demonstrate that CRH-R2 is essential for sustained Ucn-induced feeding suppression (hypophagia). Feeding is initially suppressed in *Crhr2*$^{-/-}$ mice following Ucn; however, *Crhr2*$^{-/-}$ mice recover more rapidly and completely than wild-type mice. Hence, CRH-R2-dependent and CRH-R2-independent pathways are required for complete Ucn-induced hypophagia. In addition to central nervous system (CNS) effects, we find that, in contrast to wild-type mice, *Crhr2*$^{-/-}$ mice fail to show the enhanced cardiac performance or reduced blood pressure associated with systemic Ucn suggesting that CRH-R2 mediates these peripheral hemodynamic effects. Moreover, *Crhr2*$^{-/-}$ mice have elevated basal blood pressure demonstrating that this receptor participates in cardiovascular homeostasis. These results identify specific responses in the brain and periphery that critically involve CRH-R2.

## Results and Discussion

We created *Crhr2*$^{-/-}$ mice by homologous recombination in embryonic stem (ES) cells. The targeting construct contained *Crhr2* with a neomycin cassette (**Fig. 3.1A**). We verified correctly targeted ES cell clones and germline transmission of the mutant allele by Southern blot analyses (**Fig. 3.1B**). Homozygous offspring are viable, fertile and indistinguishable (size, body weight) from wild-type littermates. In addition, we found no significant abnormalities in organ histology or immune composition of *Crhr2*$^{-/-}$ mice.

To test whether the mutation impaired CRH-R2 signaling, we treated cultured adult cardiomyocytes, which normally express CRH-R2 (ref. (260)), with Ucn or CRH (**Fig. 3.1C**); cAMP levels did not increase in *Crhr2*$^{-/-}$ cardiomyocytes although wild-type cardiomyocytes showed robust elevations. *Crhr2*$^{-/-}$ cardiomyocytes showed a normal cAMP response to forskolin, thus, the mutation specifically impaired signaling through CRH-R2.

We assessed whether *Crhr2* deficiency leads to alterations in other genes known to be involved in HPA regulation (e.g. *Crhr1*, *Crh* and *Ucn*). RNase protection analysis of hypothalamic and midbrain mRNA showed similar levels of *Crh*, *Crhr1* and *Ucn* expression in wild-type and *Crhr2*$^{-/-}$ mice (**Fig. 3.1D**). In addition, *in situ* hybridization showed no differences in *Crh* expression in the paraventricular nucleus (PVN). However, we noted a modest *Ucn* elevation in the Edinger-Westphal nucleus in *Crhr2*$^{-/-}$ mice (**Fig. 3.1E**).

The response to stress involves initiation, maintenance and recovery processes. CRH and CRH-R1 are critical for initiation of the HPA hormone cascade(8, 9) . We postulated that CRH-R2 modifies the stress response following initial activation of the HPA. We

measured HPA hormone levels following stress. Compared to wild-type mice, *Crhr2*$^{-/-}$ mice displayed a more robust ACTH response following 2 and 5 min restraint (**Fig. 3.2D**). Furthermore, ACTH levels in *Crhr2*$^{-/-}$ mice declined sooner (by 10 min) compared to wild-type levels which continued to rise after 10 min of restraint. Not surprisingly, corticosterone levels were significantly higher at 10 min in *Crhr2*$^{-/-}$ mice reflecting earlier robust increases in ACTH. Our findings replicate those observed by Bale *et al.* in independently generated CRH-R2 deficient mice(261). More rapid termination of ACTH in *Crhr2*$^{-/-}$ mice suggests that CRH-R2 may sustain the early ACTH response possibly through CRH actions on CRH-R2 in the PVN, a site known to express CRH-R2 (ref. (55)). Existence of such a feed-forward mechanism has been suggested by previous studies showing CRH stimulation of its own expression in the PVN(262) and CRH-enhanced pituitary-adrenal activation(263). *Crhr2*$^{-/-}$ mice also exhibit abnormal recovery from HPA activation. *Crhr2*$^{-/-}$ mice had significantly elevated corticosterone levels (90 min post-stress) compared to wild-type mice (**Fig. 3.2B**). Thus, CRH-R2 may regulate the recovery phase of the stress response perhaps by influencing negative feed-back of the HPA—an effect likely to be independent of its feed-forward actions in the hypothalamus. Collectively, the data suggest that CRH-R2 shapes the HPA response to stress.

Stress and CRH induce anxiety-related behaviors(259). *Crhr1*$^{-/-}$ mice showed reduced anxiety responses(8, 9) implicating a primary role for CRH-R1 in mediating anxiety. CRH-R2 may also play a role directly or by modulating effects of CRH-R1. We examined *Crhr2*$^{-/-}$ mice for anxiety responses using the elevated plus maze and observed no differences between mutant and wild-type mice (**Fig. 3.3A**). In addition, locomotor activity measurements in a novel open-field revealed no differences in total ambulation between genotypes (Fig. 3*b*). However, compared to wild-type mice, *Crhr2*$^{-/-}$ mice did exhibit a tendency to spend less time in the center of the open-field (P=0.10) (**Fig. 3.3B**). Such aversion to the center region seen in *Crhr2*$^{-/-}$ mice may reflect subtle changes in

anxiety-like behavior or reduced ability to cope with novelty through appropriate exploratory behavior. We went on to test whether intracerebroventricular (icv) Ucn administration modulated locomotor activity and found comparable reductions in activity (**Fig. 3.3C**) in both genotypes indicating that Ucn actions on activity in an open-field do not depend exclusively on CRH-R2. Our results showing normal anxiety responses in *Crhr2*$^{-/-}$ mice differ from those of Bale *et al.* (personal communication) who report anxiety-like behavior in the elevated plus maze in independently generated CRH-R2 null mice. This discrepancy may be due to differences in genetic background that result from use of ES cells derived from different 129 mouse substrains. Furthermore, the elevated plus maze is known to be sensitive to both environmental and genetic differences.

Our data suggest that *Crhr2*$^{-/-}$ mice show abnormal adaptations in the HPA stress response and in exploration of a novel center field. Our results, coupled with recent findings by others implicating CRH-R2 in stress coping behaviors(264), led us to examine self-grooming, a behavior thought to reflect dearousal and coping following stress(265). Compared to wild-type mice, *Crhr2*$^{-/-}$ mice exhibit significantly reduced grooming behavior in a novel, open-field ($P<0.05$) (**Fig. 3.3D**). This suggests that CRH-R2 is involved in mediating allostasis—a process of achieving stability through adaptation(266).

CRH and Ucn suppress feeding(267, 268) and increase metabolism(268) thereby blunting energy storage. We posited that CRH-R2 mediates CRH/Ucn-induced hypophagia based on its selective predominance in the ventromedial hypothalamus (VMH) and PVN(55). CRH-R2 in these locations is ideally situated to interact with neural circuitry regulating feeding(269). We found that although basal food intake is similar in wild-type and *Crhr2*$^{-/-}$ mice (not shown), the feeding response to Ucn differed between genotypes. Ucn (icv) decreased food intake ($P<0.001$) in *Crhr2*$^{-/-}$ and wild-type mice beginning 1 h after infusion (**Fig. 3.4**). Feeding was reduced in *Crhr2*$^{-/-}$ mice in the initial phase but

reached control rates by 6 h post-injection (**Fig. 3.4**, inset). In contrast, wild-type mice remained suppressed for >10 h. Thus, the early phase of Ucn-induced hypophagia occurs via a CRH-R2-independent pathway, likely CRH-R1, but late-phase suppression critically depends on CRH-R2. In comparison, Ucn-treated *Crhr1*$^{-/-}$ mice are the mirror image—hypophagic during the late but not early phase(270) further supporting a role for CRH-R1 in the initial phase of feeding suppression.

CRH is a potent modulator of cardiovascular function, exhibiting divergent effects when delivered into the brain (icv) versus intravenously (iv)(271). CRH delivered icv increases arterial blood pressure and heart rate similar to effects of stress. In contrast, Ucn or CRH delivered systemically induces a marked decrease in blood pressure(15) due to vasodilation in specific vascular beds(271). We examined the role of CRH-R2 in regulation of basal blood pressure and iv Ucn-induced hypotension in cannulated, free-moving animals (**Table 3.1**). *Crhr2*$^{-/-}$ mice showed significantly elevated mean arterial pressure (MAP) and diastolic pressure compared with wild-type mice. Tailcuff measurements also demonstrated that *Crhr2*$^{-/-}$ mice had elevated blood pressure (systolic; 133.0 versus 110.5 mm Hg, P=0.02). Furthermore, elevated MAP in *Crhr2*$^{-/-}$ mice was not due to increased resting heart rate. These findings indicate a role for CRH-R2 in maintenance of basal MAP. Ucn, known to exist in both the CNS(15) (e.g. Edinger-Westphal nucleus, lateral septum, hypothalamus) and periphery(15, 272) (e.g. duodenum, heart) may influence MAP via actions in the vasculature, the CNS or both. In addition, we found that systemic Ucn administration failed to decrease MAP in *Crhr2*$^{-/-}$ mice, whereas wild-type mice showed a marked decrease (-35.4 mm Hg) demonstrating that CRH-R2 mediates the hypotensive effect of systemically administered Ucn.

CRH and Ucn increase cardiac contractility *in vitro*(70) and *in vivo* following systemic administration(273). In view of CRH-R2 expression in cardiomyocytes(260), we

investigated the cardiac response to Ucn in *Crhr2*$^{-/-}$ mice using transthoracic echocardiography(274). Basal left ventricular function, represented as the heart rate-corrected velocity of fiber shortening ($Vcf_c$), was similar in wild-type and *Crhr2*$^{-/-}$ mice (2.33 ± 0.30 circ/s versus 1.87 ± 0.28 circ/s). However, Ucn (iv) steadily increased cardiac function in wild-type mice to ~2-fold above baseline but had no effect on *Crhr2*$^{-/-}$ mice (**Fig. 3.5A,B**). Also, Ucn decreased MAP only in wild-type mice (**Fig. 3.5C**) and had little influence on heart rate (**Fig. 3.5D**) in either genotype. In contrast to our measurements in conscious animals, baseline MAP values do not differ between wild-type and *Crhr2*$^{-/-}$ mice under isoflurane anesthesia. Isoflurane has direct vasodilatory and cardiodepressant properties(275) which may mask MAP differences seen in awake animals. Increased cardiac function in wild-type mice is likely due to direct actions of Ucn on cardiomyocytes since CRH-R2 activation in these cells increases cAMP(260), a stimulant of cardiac contractility(276). However, decreased blood pressure following Ucn injection may contribute to the increase in $Vcf_c$. Although additional studies are needed to dissect the precise mechanism(s) involved in Ucn actions on the heart, our findings clearly show that changes in cardiac function and blood pressure critically depend on CRH-R2. Interestingly, stress-induced effects and those induced by CRH icv lead to similar cardiovascular changes: elevation in arterial pressure and heart rate and a marked change in regional blood flow resulting in shunting from mesentery to skeletal muscle(271) which are favorable during the "fight or flight" response. Systemic or paracrine actions of Ucn may oppose these CNS effects by re-directing local blood flow thereby bringing regional hemodynamics closer to a basal state while maintaining increased cardiac function.

Our results in *Crhr2*$^{-/-}$ mice suggest that CRH-R2 is involved in physiological adaptations to stress. CRH-R2, as the dominant CRH receptor in the PVN and VMH(55), is well-poised to co-ordinate effects of CRH/Ucn in neuroendocrine, cardiovascular and feeding responses to stress. Finding that the effects of Ucn on feeding are CRH-R2-

dependent only during the late-phase suggests that early anorectic effects of Ucn are likely CRH-R1-dependent. In addition, changes in the maintainence and recovery phases of the HPA stress response in mutant mice demonstrate a role for CRH-R2 in shaping responses initiated by CRH-R1. Finally, that *Crhr2*$^{-/-}$ mice have reduced stress-coping behaviors supports the view that CRH-R2 may aid in recovery from stress following CRH-R1 activation. Taken together, these findings suggest that responses originating through CRH-R1 may be governed by adaptations mediated through CRH-R2.

## Materials and Methods

**Targeting vector.** We constructed the targeting vector using a 10.4 kb segment of *Crhr2* that had been subcloned originally from a λ phage clone bearing a 19.2 kb insert of a 129/Sv strain mouse genomic library (Stratagene). We cloned a 1.4 kb *XbaI*/*Hind*III segment of *Crhr2* into pBluescript containing a PGK-thymidine kinase cassette. The segment contained a neomycin resistance cassette (linked to a phosphoglycerate kinase (PGK) promoter) in place of transmembrane regions 3 and 4 including the second intracellular loop and portions of the first and second extracellular loops.

**Generation of *Crhr2*$^{-/-}$ mice.** We electroporated RW-4 ES cells (Genome Systems, Inc.) derived from a 129/SvJ embryo with 20 μg of linearized targeting vector. We screened the G418/ganciclovir resistant clones using Southern blot analysis of *Eco*RI digested DNA to identify ES cell homologous recombinants. A 5' probe located upstream of the targeting vector that flanks the 5'-homology region was used to detect 13.5 kb and 12.1 kb *Eco*RI fragments expected in wild-type and mutant alleles, respectively (Fig. 1). A 3' probe detected the expected *Sph*I fragments of 10.5 and 7.1 kb in the wild-type and mutated alleles, respectively. The targeting frequency was ~20%. We injected heterozygous ES cell clones into C57BL/6J blastocysts which produced three chimeric founder animals from one clone. Chimeras were bred to C57BL/6J mice to generate offspring harboring the mutant allele. Southern blot analyses were performed using tail DNA digested with *Eco*R1 or *Sph*I to determine germline transmission of the mutant allele (see Fig. 1). In all experiments, we used homozygous and wild-type F2 hybrid mice generated by F1 intercrosses except in locomotor activity and elevated plus maze experiments wherein we used mice backcrossed three generations onto C57BL/6J. Genotyping of mice was performed by PCR using CRH-R2 specific primers

(5'-CATTCCCTGCCCTATCATCATCGCC-3' and
5'-CCACCTACCGAGGCAGCCTTCCAC-3') and neomycin cassette primers
(5'-CTGTGCTCGACGTTGTCACTG-3' and
5'-GATCCCCTCAGAAGAAGAACTCGT-3').

**Animals.** Mice were given food and water *ad libitum* unless otherwise noted. All procedures met NIH guidelines with the approval of the Oregon Health Sciences University Institutional Animal Care and Use Committee.

**Histology.** We embedded tissues from adult mice (male and female, 16 wk) in paraffin or methylmethacrylate and stained with hematoxylin/eosin or toluidine blue. We examined histologic sections of heart, aorta, skeletal muscle, kidney, pituitary, adrenal, pancreas, gut, spleen, thymus and liver by light microscopy.

**Brain RNA isolation and RNase protection analysis.** We used a C57BL/6 mouse brain atlas(277) to guide our dissection of specific brain regions for RNA isolation. Brains were removed and and placed in ice-cold saline for 30 seconds. Olfactory bulbs were removed from frontal cortex and frozen separately. We removed the hypothalamus as a tissue block 1.5 mm wide across the midline and 1.5 mm thick with the anterior margin at the optic chiasm and the posterior margin at the mammillary bodies. For isolation of a region designated as midbrain containing the Edinger-Westphal nucleus, the remaining brain tissue was placed in a mouse brain block (Zivic-Miller Laboratories) on ice. We isolated a 2 mm thick coronal section extending 1.0 mm anterior and 1.0 mm posterior of the interaural line (designated as midbrain containing the Edinger-Westphal nucleus) and discarded brain tissue extending 2 mm beyond the midline. Cerebellar tissue was frozen separately following removal of the brain stem. We performed RNase protection analyses essentially as described(260). Pools of total RNA from hypothalami (13-30 μg) and

midbrain regions (50-100 μg) were hybridized to $^{32}$P-labeled probes. The *Crhr2* probe, spanning transmembrane regions three and four (corresponding to amino acids 204-283), protected a 239 nt fragment. The *Crhr1* probe, spanning transmembrane regions four and five (corresponding to amino acids 234-289) protected a 168 nt fragment. The *Crh* probe spanned amino acids 138-186 and protected a 145 nt fragment. The *Ucn* probe spanned amino acids 33-122 and protected a 269 nt fragment. We generated the *L3* probe from the *L3* cDNA digested with *Dde*I which protects a major 110 nt fragment and several minor smaller fragments. The rat *Gapd* probe digested with *Sty*I yields a major protected fragment of 133 nt. Gels were subjected to phosphorimage analysis and bands quantitated by densitometry. We normalized the intensity of the *Crh*, *Ucn*, *Crhr1* and *Crhr2* bands to the intensity of the *L3* or *Gapd* bands of the same sample.

***In situ* hybridization.** Anesthetized group-housed, female mice (n=3/genotype, 12 months) were perfused with ice-cold fixative (4% paraformaldehyde in 0.1M borate buffer, pH 9.5). After perfusion, we placed whole brains in ice-cold post-fixative solution (20% sucrose in above fixative) overnight at 4°C and subsequently stored fixed brains at -80°C until sectioning. Brains were sectioned on a cryostat (16μm) and immediately placed in anti-freeze buffer (30% ethylene glycol (v/v), 20% glycerol (v/v), 0.01% $NaN_3$ in 0.05M $NaPO_4$ buffer, pH 7.4) before mounting on poly L-lysine, gelatin-coated slides. We performed *in situ* hybridizations as previously described(278). Briefly, we treated slides with proteinase K (10 μg/ml) for 30 min at 37°C followed by acetylation in 0.1M triethanolamine with 0.0025% acetic anhydride. We dehydrated sections in ascending ethanol concentrations and dried overnight under vacuum. All riboprobes were synthesized with T7 or SP6 (Life Technologies) using 25 μCi $^{33}$P-UTP. The mouse *Crh* probe spans a 450 nt fragment including segments of the precursor and mature peptide coding region. The mouse *Ucn* probe covers 272 nt of the pre-pro-urocortin open reading frame. We incubated slides with labeled riboprobe ($5x10^6$ dpm/ml of hybridization buffer) overnight at 55°C,

then washed in 4X SSC and treated with RNase A (20 μg/ml; 37°C for 30 min). The final wash consisted of 0.1XSSC and 1 mM DTT at 65°C for 30 min. Sections were quickly dehydrated in ethanol and exposed to X-ray film for 3 days before dipping in photographic emulsion (Amersham).

**Primary myocyte isolation.** We isolated and cultured primary mouse ventricular cardiac myocytes from adult (6-12 wk) wild-type and *Crhr2*$^{-/-}$ mice as described(279) with modifications. Myocytes were allowed to pellet under gravity, washed, filtered through 70 μm mesh and then plated overnight on laminin-coated 24-well tissue culture clusters in DMEM containing sodium pyruvate, non-essential amino acids, 2X MEM vitamins, 10 mg/ml bovine insulin, penicillin/streptomycin (Gibco-BRL), 5 μg/ml holo-transferrin (Sigma), and 10% FBS (Bio-Whittaker). We stimulated cells for 20 min with rat Ucn (Bachem), rat CRH (Bachem) or forskolin (Sigma) and assayed for cAMP by RIA (Biomed Tech, Inc) as previously described(260). We performed 2 separate experiments and assayed triplicate wells in each experiment.

**Hormone measurements.** We measured plasma ACTH and corticosterone using commercial IRMA and RIA kits (Nichols Institute and ICN, respectively). Morning and evening samples were taken at 8:00 am and 6:00 pm, respectively. We obtained blood samples for basal hormone measurements from individually-housed male mice (n=8-9/genotype; 12-16 weeks) within one minute of disturbing the cage. The following morning, we obtained stressed levels immediately following 5 minute restraint stress in one group of mice (n=5) and 90 min post-restraint stress in another group of mice (n=4-5). Data were analyzed using three-factor ANOVA with time treated as a repeated measure (one group basal and 5 min values; the other group basal and 90 min values). We repeated this study in four independent experiments using male or female mice (total n= 50-60/genotype) yielding similar results. To assess the initial phase of the stress response, we bled female

mice (n=5-8/genotype at each timepoint, 28-32 weeks) immediately following 2, 5, or 10 min restraint stress, starting at 7:00 am. Data were analyzed by two factor ANOVA. Restraint stress consisted of placing mice in 50 ml conical tubes with the tip removed. We collected all blood samples (retro-orbital) without anesthesia, placed samples in ice-cold EDTA-coated tubes and froze plasma at –20°C until hormone assay.

**Behavioral measurements.** *Elevated plus maze.* The elevated plus maze consisted of two open and two enclosed horizontal perpendicular arms extending from a central platform (5 x 5 cm), 50 cm above the floor. Testing occurred in the light phase of the light/dark cycle under moderate light (175 lux) conditions. Male mice (8-12/genotype; 16 weeks) were individually placed on the central platform facing the open arm and allowed to explore freely for 5 min; the number of entries and amount of time spent in the open and closed arms were measured. We defined arm entries as entry of all four paws into the arm. The number of entries and time spent in the open arms were expressed as a percentage of the total number of arm entries and total test duration, respectively. Data were analyzed using one factor ANOVA grouped on genotype. We performed five independent experiments using male or female mice (total n=50/genotype) yielding similar results. We tested mice that were backcrossed three generations onto C57BL/6J in two independent experiments (one experiment shown here in Fig. 3) and in three other experiments, we examined F2 hybrid mice (129/SvJ x C57BL/6J). Similar genotype effects were found in both genetic backgrounds. *Locomotor activity.* We used activity monitors (Accusan), interfaced with an IBM compatible computer to measure activity. We individually placed male mice (9-12/genotype; 12-16 weeks) in the center of a clear acrylic plastic test box (40 cm x 40 cm x 30 cm) set inside an activity monitor that had 8 photocell beams and detectors evenly spaced along each of its 4 sides, 2 cm above the floor. The center of the open-field apparatus was approximately 25 square cm, measured by the inner 4 photocell beams. We recorded activity under bright light (260 lux) for 30 min in 5 min time samples as the

mouse moved about and interrupted the photocell beams. Photocell beam interruptions were used to calculate distance traveled (cm). Locomotor activity measurements were assessed using a one factor ANOVA for the total distance across the 30 min test period and a repeated measures ANOVA using 5 min time epochs. We performed three independent experiments in male or female mice (total n=40/genotype) with similar findings. In one experiment, we assessed mice that were backcrossed three generations onto C57BL/6J (Fig. 3) and in two experiments, we examined F2 hybrid mice (129/SvJ x C57BL/6J). Similar genotype effects were found in both genetic backgrounds. *Locomotor activity in response to Ucn.* We lightly anesthetized male mice (n=10/genotype, 16-20 weeks) with isoflurane for 2 min and administered icv rat Ucn (220 pmoles) or saline (0.9%) in a volume of 2 μl over 25 s. Fifteen min later, we tested the mice in the apparatus as described above. Mice were exposed to the apparatus for 30 min the day before testing. Data were analyzed by two factor ANOVA. *Grooming.* We placed male mice (n=7-8/genotype; 20-24 weeks) in a novel, open-field for 15 min. The open-field consisted of an elevated platform (26 cm x 16 cm, 15 cm above the floor) set inside a plexiglass box with approximately 4 cm open space between the edge of the platform and the walls of the box. Mirrors at the back of the box allowed for unobstructed views of the animal. Each test session was videotaped and behavior was scored by two individuals who were blind to mouse genotype. We defined grooming as self licking or washing of the body, face, tail or paws. Grooming was scored as number of bouts occurring during the 15 min test and analyzed using one factor ANOVA. We performed three independent experiments using male or female mice (total n=30/genotype) and obtained similar results in each experiment.

**Feeding studies.** *Basal feeding.* We measured 24 h food consumption for 3 consecutive days in male mice (n=14/genotype, 24 weeks). Mice were individually housed for 2 months prior to daily measurements. *Feeding response to Ucn.* Male mice (n= 7/genotype, 24 weeks) were individually housed and food deprived but given access to water for 16 h

beginning 1 h prior to the dark phase of the light/dark cycle. Following food deprivation, we icv administered rat Ucn (220 pmoles) or saline (0.9%) in a volume of 2 μl over 25 s after which we provided food (Purina PMI picolab rodent chow). Cumulative food consumption was measured each hour for 10 h. Data were analyzed using three factor ANOVA (grouped on genotype, drug treatment and time) with time treated as a repeated measure. We performed three independent experiments using male or female mice (total n=20/genotype) yielding similar results.

**Blood pressure measurement.** We made direct blood pressure measurements in conscious, free-moving female mice (n=4-5/genotype; 32-36 weeks) that we had previously implanted with a femoral artery catheter (micro-renathane tubing, .040 in OD x .025 in ID; Braintree Scientific, Inc.) advanced to the abdominal aorta. The free end of the catheter was tunneled subcutaneously to exit at the nape of the neck and catheters were filled with heparinized saline. We housed each animal individually and allowed 24-48 h recovery before measurement of blood pressure. We measured blood pressure using pressure transducers in line with a PC-based data acquisition system and custom software (Kent Scientific). After analog-to-digital conversion, the program samples data at 100 Hz and stores the data as 5 s interval averages. Following attachment of the pressure transducer, mice were left undisturbed for 60 min prior to baseline measurements, which spanned a 15 min interval. Following baseline measurements, we injected rat Ucn (7.5 μg $kg^{-1}$, 0.01 ml; Bachem) via the femoral catheter and determined MAP for 30 min. We measured indirect systolic pressure by a programmable sphygmomanometer (BP-2000; Visitech) using the tail-cuff method as previously described(280). Male mice (n=8/genotype, 32-36 weeks) were habituated to the measurement procedure for 4 days; measurements (10 recordings/mouse) collected on the fifth day were averaged to generate a group mean for analysis. Statistical analysis was performed using one-factor ANOVA. Results are expressed as mean values.

**Cardiac measurements.** We lightly anesthetized (isoflurane, 1-2% in $O_2$) and cannulated female mice (n=5-7/genotype; 24-28 weeks) through the femoral artery as described above. We performed echocardiography as described(274) with an Acuson Sequoia ultrasound system (Acuson) using a 15 MHz phased arrayed transducer. We derived left ventricular (LV) diameters along the short axis from 2-dimensional targeted M-mode echocardiographic recordings. LV chamber diameters (LVD) at end-diastole (ed) and end-systole (es) were measured as described(274). We calculated LV fractional shortening as $[(LVD_{ed} - LVD_{es})/LVD_{ed}]$ and derived ejection times (ET) from continuous wave Doppler recordings of aortic outflow corrected for heart rate ($ET_c$). We calculated heart rate-corrected velocity of LV circumferential fiber shortening ($Vcf_c$), a measure of cardiac contractility, as $FS/ET_c$. For all indices, we determined average dimensions from three successive beats and used these averages to calculate the mean. MAP was measured through the femoral artery catheter. We recorded baseline cardiac function and blood pressure for 10-40 min prior to intravenous injection of 7.5 μg $kg^{-1}$ rat Ucn (Bachem) in 100 μl of pyrogen-free saline. Cardiac function and blood pressure was measured every 5 min for 30 min following injection of peptide.

**Intracerebroventricular (icv) cannulation.** We anesthetized mice with isoflurane (1-2% in $O_2$) and implanted a single cannula into the right lateral ventricle. The guide cannulae (2.5 mm length, 26-gauge, Plastics One) was positioned 1.0 mm above the lateral ventricle (coordinates: 0.6 mm posterior to bregma, 1.5 mm lateral to midline, 1.4 mm below the surface of the skull) and fixed to the skull using two stainless steel screws and dental cement. We allowed animals to recover from surgery for a minimum of 7 days before testing, during which time we placed a 30-gauge dummy cannulae inside the guide cannulae. We performed icv infusions using a 30-gauge infusion cannulae cut to extend 1.0

mm beyond the guide cannulae. Infusion cannulae were fitted to PE-50 tubing and connected to a 50 µl Hamilton syringe.

**Statistics**. We analyzed data using analysis of variance (ANOVA) grouped on genotype and performed follow-up analyses using simple main effect analysis. We used repeated measures ANOVA where appropriate. Differences were considered statistically significant when P was $< 0.05$.

**Table 3.1.** *Crhr2*$^{-/-}$ mice exhibit elevated basal blood pressure but not Ucn-induced hypotension.

| | Arterial pressure (mmHg) | | | Heart rate |
|---|---|---|---|---|
| Basal | Mean | Diastolic | Systolic | (beats/min) |
| Wild-type (n=5) | 88.2 ± 2.1 | 71.1 ± 2.2 | 109.9 ± 3.9 | 589 ± 17 |
| *Crhr2*$^{-/-}$ (n=5) | 98.1 ± 3.1[a] | 81.2 ± 2.6[b] | 117.5 ± 5.0 | 578 ± 14 |
| Urocortin (iv) | Δ Mean | Δ Diastolic | Δ Systolic | |
| Wild-type (n=4) | -32.7 ± 4.0 | -23.5 ± 1.9 | -44.5 ± 8.6 | 619 ± 10 |
| *Crhr2*$^{-/-}$ (n=4) | -1.3 ± 1.7[c] | -0.9 ± 1.3[c] | -2.3 ± 3.3[b] | 611 ± 15 |

Values are mean ± SEM. We performed statistical analysis using one-factor ANOVA. Δ indicates change from baseline blood pressure measured 30 min after urocortin injection. Significant difference from corresponding wild-type value: [a]$P<0.05$; [b]$P<0.02$; [c]$P<0.002$.

relative abundance. Bars represent the mean + STDEV. +/+, wild type; +/—, *Crhr2*$^{+/-}$ ; —/—,*Crhr2*$^{-/-}$. E) Dark field photomicrographs showing *Crh* expression in the PVN and *Ucn* expression in the Edinger-Westphal nucleus in *Crhr2*$^{-/-}$ mice compared to wild-type mice. Coronal brain sections were hybridized with $^{33}$P-UTP-riboprobes for *Crh* or *Ucn*. Magnification, x10.

**Figure 3.1.** Generation of *Crhr2*$^{-/-}$ mice. A) Restriction maps: wild-type allele, a 19.2 kb clone that includes exons encoding transmembrane domains 3-5 and contiguous sequence; targeting construct that contains a thymidine kinase cassette and a neomycin resistance cassette in place of coding sequences for transmembrane regions 3 through 4; mutated allele indicating the predicted product of homologous recombination. E, *Eco*RI; S, *Sph*I; Tm, transmembrane domain; neo, neomycin transferase gene linked to phosphoglycerate kinase (PGK) promoter; tk, thymidine kinase gene of herpes simplex linked to PGK promoter. B) Southern blot analysis of mouse tail DNA digested with *Eco*R1 and probed with a 5' probe indicated in (A), which distinguishes the mutated allele (12.1 kb) from the wild-type allele (13.5 kb). The 3' probe indicated in (A) detected the expected *Sph*I fragments of 10.5 and 7.1 kb in the wild-type and mutated alleles, respectively (data not shown). Thus, we confirmed homologous recombination of both arms of the targeting vector. C) Ucn and CRH stimulation of adult cardiomyocytes from wild-type and *Crhr2*$^{-/-}$ mice. We measured intracellular cAMP accumulation for 20 min following addition of Ucn, CRH or forskolin at the indicated concentrations. Cardiomyocytes from *Crhr2*$^{-/-}$ mice failed to respond to Ucn and CRH. **P<0.05 significant difference between *Crhr2*$^{-/-}$ cardiomyocytes versus wild-type and *Crhr2*$^{+/-}$ cardiomyocytes; * P<0.05 significant difference between wild-type versus *Crhr2*$^{+/-}$ cardiomyoctyes. D) Ribonuclease protection analysis of total RNA from hypothalamic and midbrain regions (which includes the Edinger-Westphal nucleus) of wild-type (n=9) and *Crhr2*$^{-/-}$ (n=12) mice. RNA from 3-4 hypothalami or 3 midbrain regions was pooled and hybridized to $^{32}$P-labeled cRNA probes. Each lane represents a pool of RNA from 3-4 animals. The probes and corresponding protected fragments are as follows: *Crhr2*/239 nt; *Crhr1*/168 nt, *Crh* /145 nt; *Ucn* /269 nt; *L3*/110 nt (and several minor smaller fragments); *Gapd* /133 nt. Gels were subjected to phosphorimage analysis and bands quantitated by densitometry. The intensity of the *Crh*, *Ucn*, *Crhr1* and *Crhr2* bands were normalized to the intensity of the *L3* or *Gapd* bands of the same sample and the ratios presented as

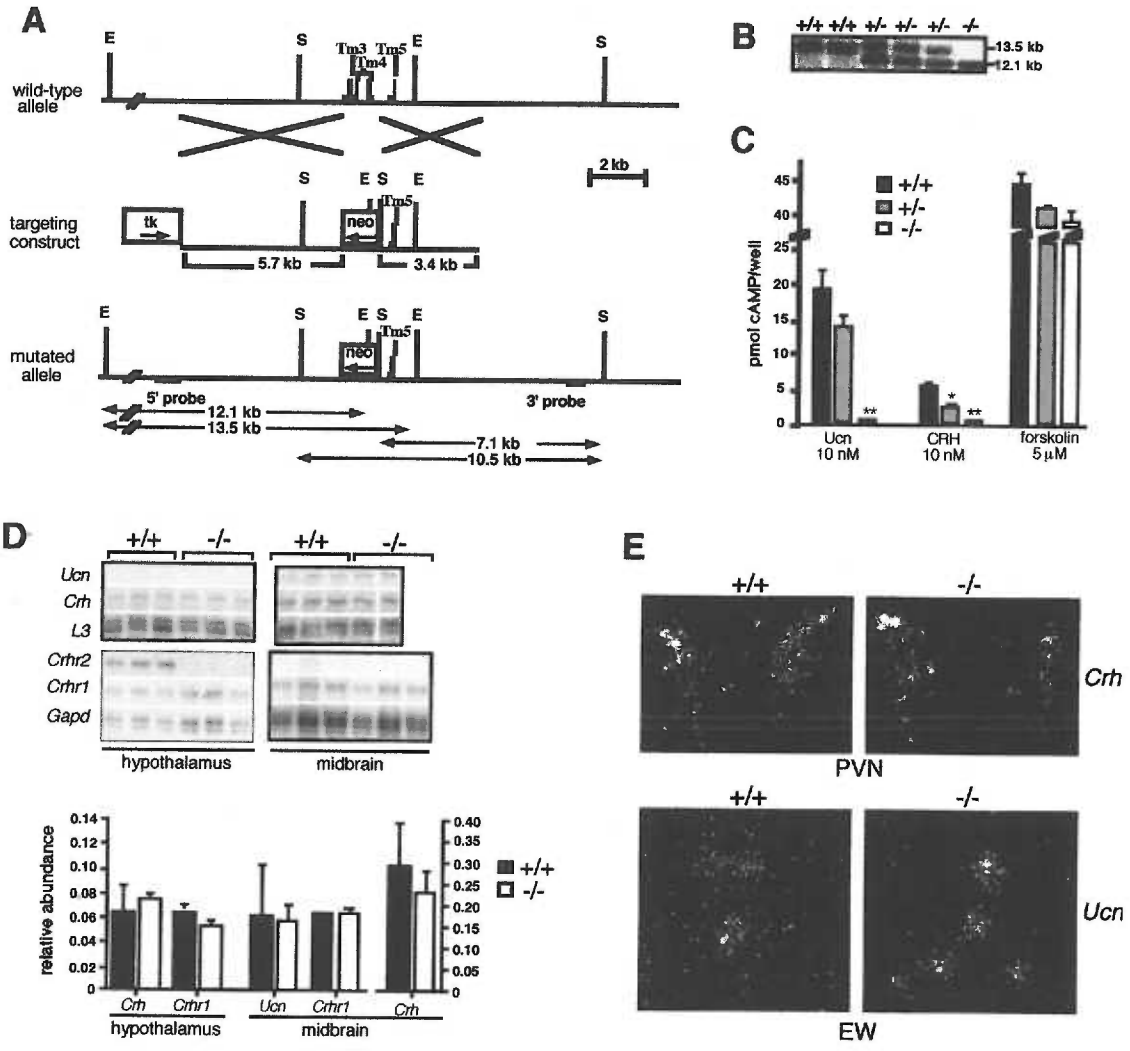
A
wild-type allele
targeting construct
mutated allele
E
S
Tm3
Tm4
Tm5
tk
neo
2 kb
5.7 kb
3.4 kb
5' probe
3' probe
12.1 kb
13.5 kb
7.1 kb
10.5 kb
B
+/+ +/+ +/- +/- +/- -/-
13.5 kb
12.1 kb
C
pmol cAMP/well
+/+
+/-
-/-
Ucn 10 nM
CRH 10 nM
forskolin 5 μM
D
+/+
-/-
Ucn
Crh
L3
Crhr2
Crhr1
Gapd
hypothalamus
midbrain
relative abundance
Crh
Crhr1
Ucn
E
PVN
EW
Crh
Ucn

**Figure 3.2.** *Crhr2*$^{-/-}$ mice have altered HPA responses to stress. A) Plasma ACTH and corticosterone levels were determined in *Crhr2*$^{-/-}$ (n=7-8/timepoint, open squares) and wild-type (n=7-8/timepoint, filled squares) female mice (28-32 weeks) immediately following 2, 5, or 10 min restraint stress. ACTH response curves were significantly different between genotypes (genotype by time interaction P=0.02). ACTH levels rose more rapidly in *Crhr2*$^{-/-}$ mice at 2 and 5 min and were declining by 10 min of restraint. *Crhr2*$^{-/-}$ mice show significantly higher corticosterone levels following 10 min restraint reflecting more robust increases in ACTH at early timepoints. Both genotypes showed similar basal levels of ACTH and corticosterone. B) *Crhr2*$^{-/-}$ mice have significantly elevated corticosterone levels 90 min post-stress compared to wildtypes. Mice (n=5/genotype) were restrained for 5 min and bled immediately or 90 min later. We performed 4 independent experiments using male or female mice (total n=50-60/genotype) with similar findings. Data are mean values ± SEM from a representative experiment. Statistical evaluation was performed by two-factor ANOVA in (A) and by three-factor ANOVA with time treated as a repeated measure (one group basal and 5 min values; the other group basal and 90 min values) in (B). **P<0.01, *P<0.05. We observed no marked abnormalities in the diurnal pattern of plasma corticosterone in *Crhr2*$^{-/-}$ mice (morning values: wild-type 19.1 ± 5.8 vs *Crhr2*$^{-/-}$ 14.7 ± 3.9 evening values: wild-type 124.4 ± 18.1 vs *Crhr2*$^{-/-}$ 124.4 ± 8.9).

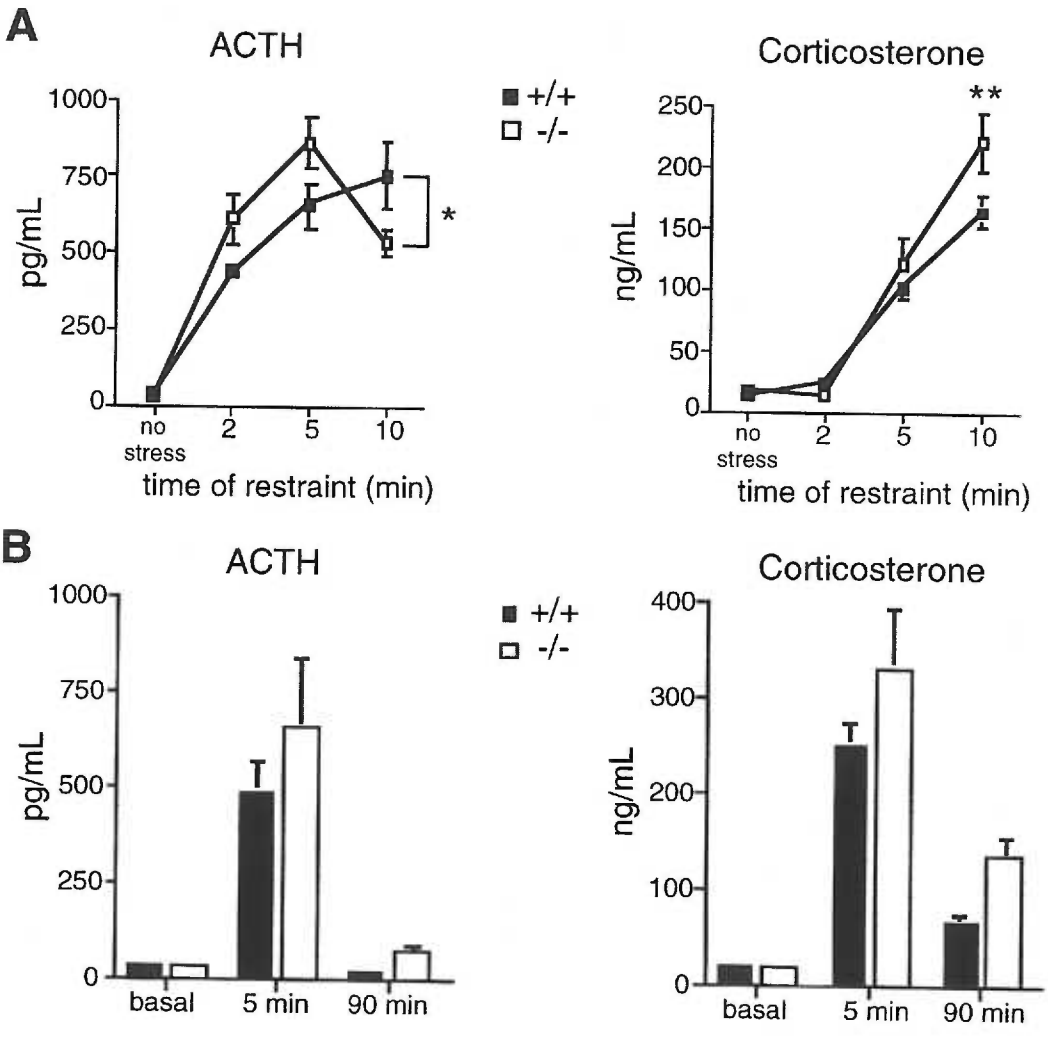
A
ACTH
1000
750
500
250
0
pg/mL
no stress
2
5
10
time of restraint (min)
*
+/+
-/-
Corticosterone
250
200
150
100
50
0
ng/mL
**
no stress
2
5
10
time of restraint (min)
B
ACTH
1000
750
500
250
0
pg/mL
basal
5 min
90 min
+/+
-/-
Corticosterone
400
300
200
100
0
ng/mL
basal
5 min
90 min

**Figure 3.3.** *Crhr2*$^{-/-}$ mice show aberrant coping behavior without concomitant alterations in anxiety or activity. A) *Crhr2*$^{-/-}$ mice show no differences in anxiety as measured by the elevated plus maze. We assessed performance in male mice (n=8-12/genotype, 16 weeks) for 5 min following placement of individual mice on the maze. Number of open arm entries and time spent on the open arms are expressed as percentage of total arm entries and total test duration, respectively. Data shown are representative of five independent experiments performed in male or female mice (total n=50/genotype). B) *Crhr2*$^{-/-}$ and wild-type mice show similar basal locomotor activity in an open-field. Mutant and wild-type mice (n=9-12/genotype, 12-16 weeks) exhibited similar patterns of waning activity over time (not shown). *Crhr2*$^{-/-}$ mice tended to spend less time in the center of the field (P=0.10). Data are presented as total horizontal distance traveled (cm) and time spent in center (sec) during the 30 min test. Data are representative of three independent experiments performed in male or female mice (total n=40/genotype). C) *Crhr2*$^{-/-}$ and wild-type mice show a similar decrease in locomotor activity in response to Ucn. Male mice (n=10/genotype/group,16-20 weeks) were lightly anesthetized and injected icv with Ucn (220 pmoles in 2 µl) or vehicle (saline in 2 µl). We assessed locomotor activity15 min later. D)*Crhr2*$^{-/-}$ mice show reduced grooming behavior. We observed self-grooming in *Crhr2*$^{-/-}$ and wild-type mice (n=7-8/genotype, 20-24 weeks) in a novel, open-field during a 15 min test session. Data are presented as number of bouts, mean values ± SEM, and are representative of three independent experiments performed in male or female mice (total n=30/genotype). Significant differences were determined by one-factor ANOVA in all behavioral studies except in panel (C) for which we performed a two-factor ANOVA. *P<0.05

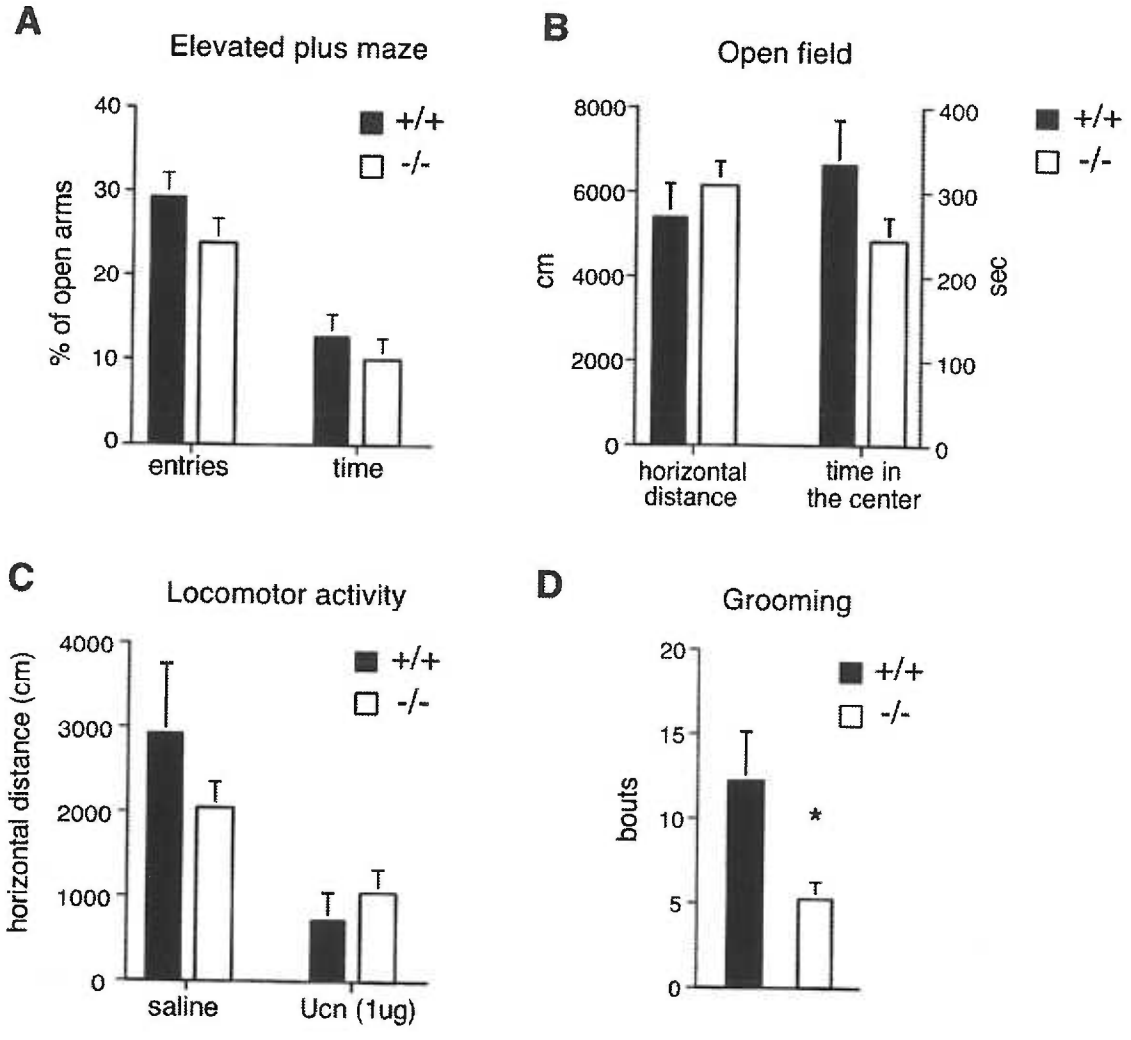
A
Elevated plus maze
% of open arms
40
30
20
10
0
+/+
-/-
entries
time
B
Open field
cm
8000
6000
4000
2000
0
sec
400
300
200
100
0
+/+
-/-
horizontal distance
time in the center
C
Locomotor activity
horizontal distance (cm)
4000
3000
2000
1000
0
+/+
-/-
saline
Ucn (1ug)
D
Grooming
bouts
20
15
10
5
0
+/+
-/-
*

**Figure 3.4.** *Crhr2*$^{-/-}$ mice show altered feeding responses to Ucn. *Crhr2*$^{-/-}$ and wild-type mice (males, n=6-7/group) were fasted for 16 h before icv injection of Ucn (220 pmoles in 2 µl) or vehicle (saline in 2 µl) and fed mice 5 min later. Food intake was initially suppressed in both Ucn-treated *Crhr2*$^{-/-}$ and wild-type mice. However, while food intake remained suppressed in Ucn-treated wild-type mice throughout the 10 h test period, *Crhr2*$^{-/-}$ mice recovered from Ucn-induced suppression by 6 h, and fed at the same rate as control (vehicle-treated) *Crhr2*$^{-/-}$ mice unlike wild-type mice (see inset). At 10 h, cumulative food intake by Ucn-treated *Crhr2*$^{-/-}$ mice did not differ significantly from *Crhr2*$^{-/-}$ controls. Data are presented as cumulative food intake (mean ± SEM) and as hourly rate ratios of Ucn-treated to vehicle-treated values (inset). In experiments not shown, low dose Ucn (22 pmoles) produced a similar temporal pattern of hypophagia with *Crhr2*$^{-/-}$ mice showing significant suppression only in the first hour and recovering to control levels thereafter whereas wild-type mice remained suppressed for the first five hours. $^{###}P<0.001$, $^{##}P<0.01$, $^{#}P<0.05$ significant difference between Ucn-treated *Crhr2*$^{-/-}$ versus vehicle-treated *Crhr2*$^{-/-}$ control mice; $\dagger\dagger\dagger P<0.001$, significant difference between Ucn-treated wild-type versus vehicle-treated wild-type control mice; $^{***}P<0.001$, $^{**}P<0.01$, $^{*}P<0.05$ significant difference between Ucn-treated *Crhr2*$^{-/-}$ versus Ucn-treated wild-type mice. Significance was determined by three-factor ANOVA with time treated as a repeated measure. Error bars at some time points are too small to be visible on the graph.

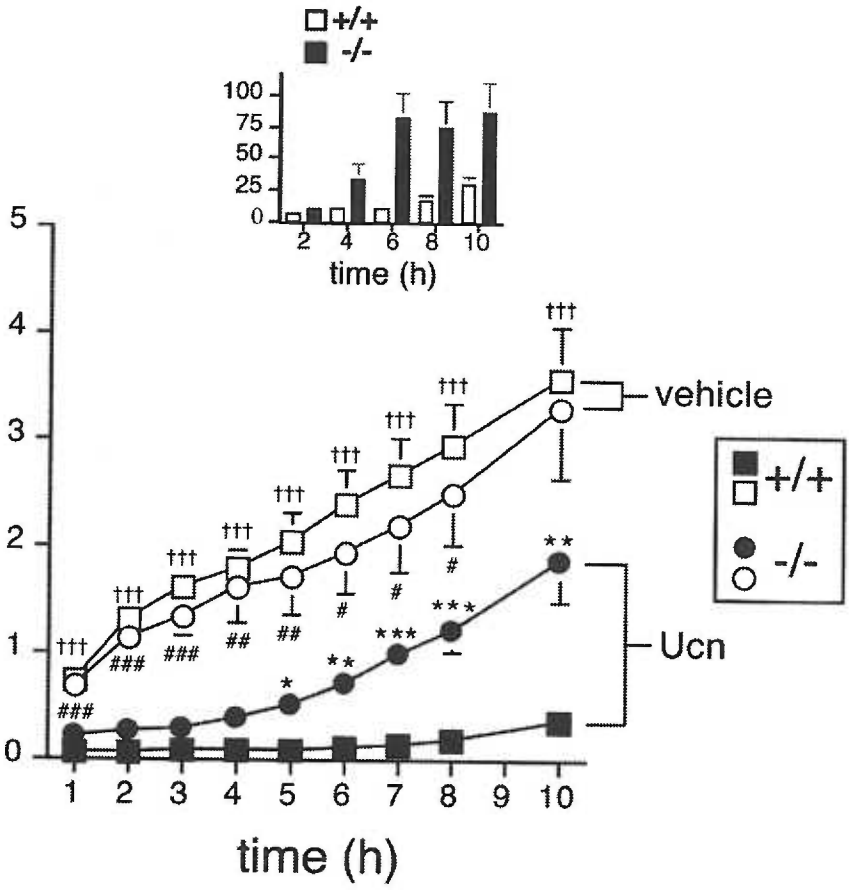
+/+
-/-
100
75
50
25
0
2 4 6 8 10
time (h)
5
4
3
2
1
0
vehicle
Ucn
+/+
-/-
1 2 3 4 5 6 7 8 9 10
time (h)

**Figure 3.5.** Ucn increases cardiac function in wild-type but not *Crhr2*$^{-/-}$ mice. We used transthoracic echocardiography to analyze cardiac function in anesthetized wild-type (n=5, filled squares) and *Crhr2*$^{-/-}$ mice (n=7, open circles) at baseline and following injection with Ucn (iv., 7.5 μg kg$^{-1}$). A) M-mode display of left ventricular function in wild-type and *Crhr2*$^{-/-}$ mice at baseline and 15 min post-injection. The largest dimension is diastole (D) and the smallest is systole (S). Ucn increases fractional shortening in wild-type mice but not *Crhr2*$^{-/-}$ mice. B) Quantification of Ucn effects on heart rate-corrected velocity of circumferential fiber shortening ($Vcf_c$) (*see methods*). C) Effect of Ucn on mean arterial blood pressure measured via the femoral artery during echocardiography. D) Effect of Ucn on heart rate during echocardiography. *P<0.01, **P<0.05 significant difference between wild-type and *Crhr2*$^{-/-}$ mice. Points represent mean ± SEM. Significance was determined by two-factor ANOVA with time treated as a repeated measure. Error bars at some time points are too small to be visible on the graph.

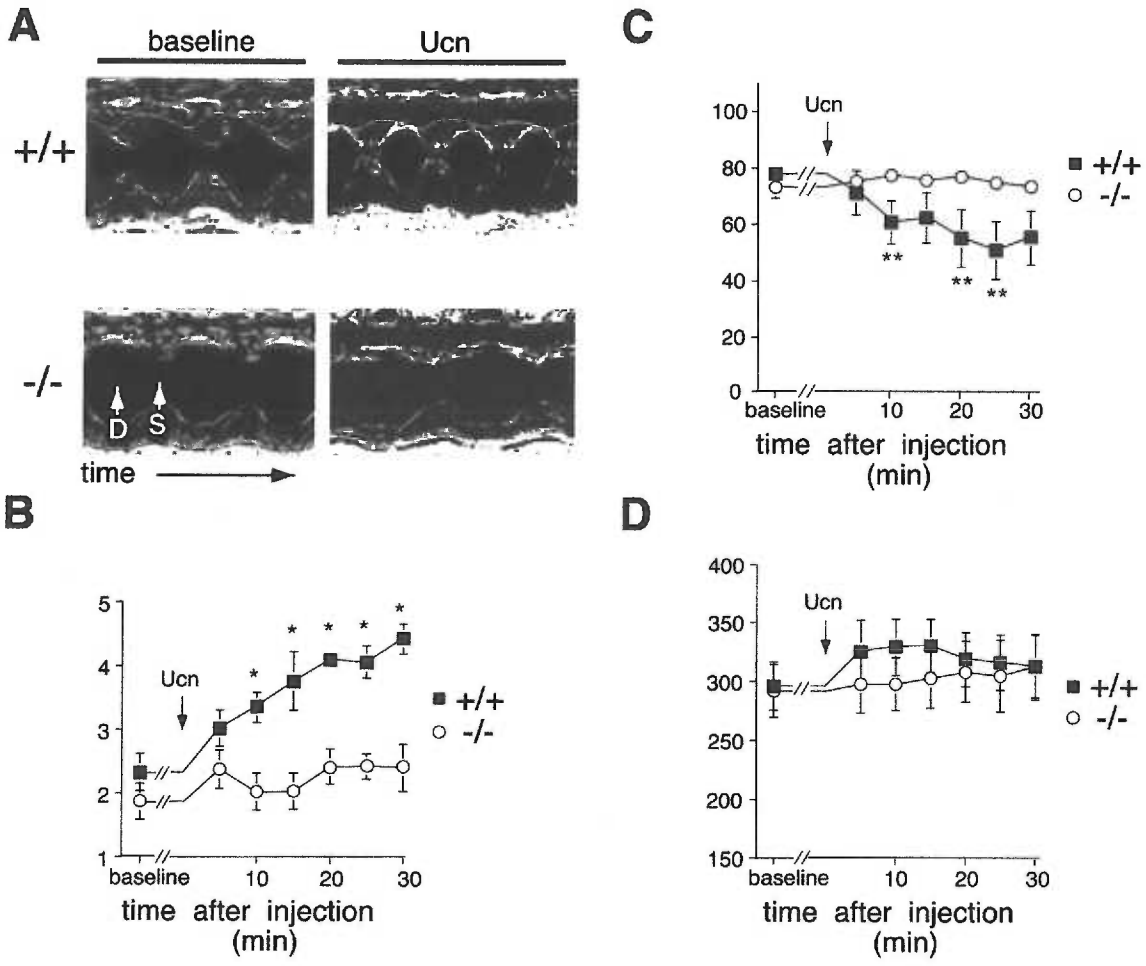
A
baseline
Ucn
+/+
-/-
D
S
time
B
Ucn
+/+
-/-
baseline
10
20
30
time after injection
(min)
C
Ucn
+/+
-/-
baseline
10
20
30
time after injection
(min)
D
Ucn
+/+
-/-
baseline
10
20
30
time after injection
(min)

## Acknowledgments

We thank K. Lee and A. Contarino for generously discussing relevant and unpublished data. We also gratefully acknowledge the valuable assistance of J. Auld, W. Yeung and Q. Yue. This work was supported by National Institute of Health grants HL55512 (M.S-P), HL45043 (A.R.H.), HD30236 (M.L.), 2T32EY07123 (K.A.H.), AI14985 (M.B.R.) and an American Heart Association Fellowship (S.C.).

# Chapter 4

# Manuscript #3

# Hypothesis

Inflammation is a potent stressor that regulates CRH and CRH-R1 expression in the hypothalamus and CRH-R1 expression in the pituitary. Inflammation is also a potent stressor of the cardiovascular system, inducing vasodilation and depressing the contractile function of the heart. Because CRH-R2 is highly related to the stress-responsive CRH-R1, we will test the hypothesis that inflammation regulates the expression of CRH-R2 in the heart.

# Endotoxin Regulates Corticotropin-Releasing Hormone Receptor 2 (CRH-R2) in Heart and Skeletal Muscle

**Kurt A. Heldwein‡, Janet E. Duncan‡, Peter Stenzel, Marvin B. Rittenberg and Mary P. Stenzel-Poore**

*Department of Molecular Microbiology and Immunology, Oregon Health Sciences University, Portland, OR 97201*

‡ Authors contributed equally to this work.

**Published in Molecular and Cellular Endocrinology 131(2):167-172 (1997)**

## Abstract

We tested the effect of endotoxin on the peripheral CRH receptor, CRH-R2, which is highly expressed in the heart. Systemic injection of LPS markedly downregulated CRH-R2 mRNA levels in the heart in a dose and time dependent manner. In contrast, CRH-R2 levels in skeletal muscle increased following exposure to endotoxin. These results suggest that CRH-R2 may be differentially regulated in cardiac tissue and skeletal muscle. Finding that CRH-R2 expression in the heart is modulated by endotoxin, a potent inducer of cardiovascular dysregulation, suggests a possible link between CRH and the cardiovascular response to stress.

*Keywords*: corticotropin-releasing hormone; heart; skeletal muscle; endotoxin; receptor; regulation

## Introduction

Corticotropin-releasing hormone (CRH) is the primary mediator of the hypothalamic-pituitary-adrenal (HPA) axis response to stress (1), acting through a specific receptor, CRH-R1 (49). In addition to its expression in the hypothalamus and fundamental role in pituitary activation, CRH is distributed throughout the brain where it plays an integral role in regulating behavioral and autonomic responses.

Peripheral administration of CRH induces a potent vascular response when given systemically or administered directly into the heart (70, 127, 281), suggesting the presence of specific CRH receptors in vascular tissue. We and others recently verified the existence of such receptors (45, 47, 48, 74) with the cloning and identification of a novel peripheral form of CRH receptor, CRH-R2. This receptor bears 69% identity with CRH-R1 (45, 49, 60, 73) and is the product of a distinct gene. Although CRH-R1 and CRH-R2 have similar binding and signaling properties, they differ in their sensitivities to certain CRH-related ligands (45, 74). Furthermore, their tissue distribution differs: CRH-R1 is most highly expressed in the pituitary and brain (73, 220, 282), whereas CRH-R2 is highly expressed in the heart and skeletal muscle (45, 47, 48, 74). Based on our observation that CRH-R2 is highly expressed in the heart, we proposed that it may mediate the peripheral effects of CRH on the cardiovascular system (45).

Increasingly it appears that CRH acts at peripheral sites to regulate specific regions of the circulation. Intravenous administration of CRH causes decreased mean arterial blood pressure and increased blood flow (127, 281, 283). Others have recently shown CRH to have direct effects in the cardiovascular system (69, 70). Addition of CRH to isolated rat heart produced a prolonged increase in coronary blood flow, a transient positive inotropic effect and increased atrial natriuretic peptide release (69, 70).

Endotoxemia has profound effects on the heart, vasculature, and other organs (284). Much of the effect of endotoxin on the cardiovascular system appears to result from endogenous production of cytokines, particularly tumor necrosis factor-α (TNFα) and interleukin-1 (IL-1) (285-288). However, there is also evidence for direct effects of endotoxin on the heart resulting in prolonged vasodilation (289).

Endotoxin exposure also causes marked activation of the HPA axis. Induction of CRH expression and secretion in the hypothalamus, ACTH production from the pituitary, and glucocorticoid release from the adrenals follow exposure to endotoxin (290). These effects are thought to occur through cytokine mediators, particularly interleukin-6 (IL-6), IL-1 and TNFα which have been shown to stimulate the HPA axis via a CRH-dependent mechanism (290). Since glucocortcoids downregulate production of several cytokines, HPA activation may be an important inhibitory feedback mechanism in endotoxemia.

Since endotoxin has been shown to upregulate CRH and CRH-R1 in the hypothalamus (291), we hypothesized that expression of the related receptor, CRH-R2, located in the heart and skeletal muscle may also be regulated by endotoxin. In contrast to positive regulation of hypothalamic CRH-R1 by endotoxin, our studies show that exposure to endotoxin markedly downregulates CRH-R2 expression in the heart, while upregulating its expression in skeletal muscle.

## Methods and Materials

**Animals.** Female mice (C57BL/6, 9-13 wk, Jackson Laboratories, Bar Harbor, ME) were maintained under specific pathogen-free conditions on a 12-hour light/dark schedule. Experimental procedures were performed in accordance with NIH guidelines for care and use of laboratory animals.

**Systemic Endotoxin Treatment.** Each group contained 6-7 animals per time point. Mice were injected intraperitoneally (ip) with 50 ug endotoxin (lipopolysaccharide, LPS*E. coli* serotype O55:B5, Sigma L2880, St. Louis, MO) in 200 ul endotoxin-free phosphate buffered saline (PBS). Controls received vehicle (endotoxin-free PBS) only, while a single group designated $T_0$ was left unhandled. Prior to injecting the other animals, mice in the unhandled group were removed quietly to an adjacent room and sacrificed. Mice treated with LPS or vehicle were sacrificed 2, 4, 6, 9 or 24 hours after injection. To minimize stress effects, mice were housed two to a cage covered with light-transparent, opaque paper beginning 1-2 days before the experiment. Mice were killed by cervical dislocation within 90 sec of handling. Whole hearts and skeletal muscle (pectorals and quadriceps) were removed and snap frozen. Pilot experiments to determine the appropriate dose of LPS (10, 50, 250 and 500 ug) were performed as described above using a single time point (7.5 h post injection) for analysis of CRH-R2 expression.

**RNA isolation and RNase protection.** Total RNA from frozen tissue was prepared using RNA STAT-60 (Tel-Test "B", Inc., Friendswood, TX.) Mouse CRH-R2 was detected with a probe (mCRX-55) spanning TM3 and TM4 (corresponding to amino acids 204 through 283) (45). A 216 nt Rsa I fragment of L3 cDNA, encoding a mouse ribosomal protein, was used as a loading control. $^{32}$P-UTP radiolabeled antisense riboprobe was generated *in vitro* as previously described (45). Probes were annealed with total RNA (25

ug) at 42°C for ≥15 hours. Hybrids were digested with RNase A (10 ug/ml) and $T_1$ RNase (600 U/ml) at 30°C for 30 min and resolved on 6% acrylamide, 7 M urea gels. Quantitative densitometry was performed with DeskScan II (Hewlett Packard) and NIH Image software. In all samples the intensity of the CRH-R2 band was normalized to the intensity of the L3 band of the same sample and results expressed in corrected arbitrary units. Normalized values represent percent of control. Data were analyzed by one-way ANOVA, using MultiStat software (BIOSOFT, Cambridge, UK.)

## Results

We tested a single ip dose of LPS (50 ug/mouse) in a pilot experiment to determine whether endotoxin modulates cardiac CRH-R2; 50 ug is in the range previously shown to induce HPA activation and cytokine production in mice (290). CRH-R2 mRNA levels in the heart were examined 2, 4, 6 and 9 hours post-injection by RNase protection analysis. Results showed that cardiac levels of CRH-R2 mRNA were reduced nearly 5-fold by six hours after LPS injection (**Table 4.1**). Saline alone failed to induce significant alterations in CRH-R2 mRNA levels compared with unhandled control animals. We performed a second pilot experiment to determine the minimal effective dose of LPS. Since 50 ug caused a marked decrease of CRH-R2 mRNA levels between 6 and 9 hours post-injection we tested various LPS doses at 7.5 hours following endotoxin challenge (**Fig. 4.1**). Mice were injected with 10, 50, 250 or 500 ug of LPS or saline only. CRH-R2 mRNA levels in the heart were markedly reduced at each of the test doses compared with control animals given vehicle (saline); 10 ug of LPS had a modest effect on CRH-R2 (~50% reduction) whereas doses of 50, 250 and 500 ug caused 4.5-7.0 fold reductions of CRH-R2 mRNA.

Based on preliminary findings we examined the kinetics of CRH-R2 modulation by LPS using 50 ug/mouse, which was the lowest dose that had significantly modulated expression. Cardiac CRH-R2 mRNA was measured at 2, 4, 6, 9 and 24 hours after LPS or saline injection. LPS induced a significant reduction in expression (**Fig. 4.2**) which appeared to be maximal between 6 and 9 hours post-injection, consistent with pilot experiments. In addition, by 24 hours after LPS challenge, CRH-R2 mRNA levels appeared to be returning toward normal although expression was still below controls at this time. Mice given 50 ug of LPS had decreased expression of CRH-R2 mRNA even at the earliest time point, 2 hours post-injection (**Fig 4.2**). CRH-R2 mRNA levels were decreased 3-fold ($p<0.05$) at 4 hours and maximally depressed (9-fold $p<0.001$) at 9

hours. By 24 hours after injection of LPS, cardiac expression of CRH-R2 had risen to nearly 60% of the level seen in time-matched saline controls.

To determine whether LPS would have a similar effect on CRH-R2 levels in skeletal muscle, we performed RNase protection analysis on RNA obtained from quadriceps and pectoral muscles. In contrast to the marked downregulation of CRH-R2 in the heart, CRH-R2 in skeletal muscle increased following LPS injection (**Fig. 4.3**). LPS caused a modest increase (1.5-fold) in CRH-R2 mRNA within two hours and reached a maximum at 6 h (2.8-fold). CRH-R2 levels were comparable to saline-injected animals by 9 h and remained so at 24 h post-injection. Furthermore, as with the modulation of CRH-R2 in the heart, the increase in CRH-R2 levels in skeletal muscle was dose dependent. Expression levels of CRH-R2 mRNA increased 1.1, 1.3 and 2.0-fold at 7.5 hours post-treatment with 10, 50 and 250 ug of LPS, respectively (data not shown). Thus, while LPS modulation of CRH-R2 mRNA levels in skeletal muscle followed a time course similar to that in the heart, the effects were markedly opposed.

## Discussion

We report here that endotoxin differentially modulates CRH-R2 mRNA levels in the heart and skeletal muscle. We show that endotoxin causes a marked decrease in CRH-R2 levels in the heart which occurs 6-9 hours following exposure. In contrast, CRH-R2 mRNA levels in skeletal muscle had a modest but significant increase during this same time period. These findings indicate that endotoxin regulates CRH-R2 mRNA levels in both cardiac tissue and skeletal muscle.

CRH and the structurally related peptides, sauvagine and urotensin, have potent vasodilatory effects when administered systemically into mammals (127, 219). In addition, urocortin, a newly identified mammalian peptide with strong homology to fish urotensin, also induces a strong vasodilatory response following iv administration (15). Moreover, there is recent evidence that CRH can affect heart function directly; CRH has been shown to induce a long-lasting vasodilatory effect and increase ANP secretion in an isolated working heart model (69, 70). Our finding that endotoxin, in view of its well recognized, potent cardiovascular effects (284), regulates CRH-R2 mRNA levels in the heart is intriguing particularly since a specific role for CRH and CRH-R2 in cardiac function has not been defined.

As mentioned above, endotoxin has been shown to upregulate CRH and CRH-R1 in the hypothalamus (291). Recent studies have shown that systemic challenge with endotoxin causes a marked increase in mRNA levels for CRH-R1 in the paraventricular and supraoptic nuclei of the hypothalamus (291). Modulation of CRH-R1 by endotoxin reached a maximum at six hours and returned to normal levels by 12 hours. This is interesting since, in the heart, we observed a marked reduction in CRH-R2 mRNA levels rather than an increase, although the kinetics of CRH-R2 mRNA modulation by endotoxin

in the heart parallel those reported for CRH-R1 in the hypothalamus. Our results showing positive regulation of CRH-R2 mRNA in skeletal muscle by endotoxin may more closely parallel those seen with CRH-R1 mRNA in the hypothalamus (291). Taken together, the findings indicate that distinct patterns of regulation of CRH-R2 and CRH-R1 by endotoxin occur depending upon tissue location.

The mechanism of modulation of CRH-R2 expression in the heart following endotoxin exposure is unknown. Production of cytokines following exposure to endotoxin could modulate CRH-R2. Some of the cardiovascular effects of cytokines are mediated by nitric oxide (NO) (292); thus, it is possible that CRH-R2 mRNA is altered via NO. Also, there is evidence for direct effects of endotoxin on the heart resulting in prolonged vasodilation (289) which could, through some yet undescribed mechanism, alter CRH-R2 expression.

Although the physiological link between cardiac expression of CRH-R2 and exposure to endotoxin is not clear, the fact that endotoxin treatment causes activation of the HPA axis via a CRH-dependent mechanism (290) may provide a means of increasing CRH in the plasma, which could directly influence CRH-R2 in the heart. Alternatively, CRH or a CRH-like peptide may be released from peripheral sources, perhaps from the heart itself, in response to endotoxin. In either case, stimulation of CRH-R2 by ligand may ultimately regulate the mRNA levels for this receptor. Such ligand-induced changes in mRNA levels have recently been shown for CRH-R1 in the pituitary (108).

In addition, glucocorticoids are released following endotoxin challenge. High levels of glucocorticoids have been shown recently to downregulate CRH-R1 in the hypothalamus and pituitary (108, 293, 294). Thus, it is plausible that in the heart, CRH-R2 mRNA may also be negatively regulated by glucocorticoids. However, thus far we have been unable to demonstrate modulation of cardiac CRH-R2 levels by dexamethasone (2.5 to 250 ug, ip),

suggesting that regulation of this receptor by endotoxin may be independent of increased glucocorticoid levels.

In conclusion, our findings provide the first evidence of CRH-R2 mRNA regulation. Exposure to endotoxin causes marked downregulation of CRH-R2 in the heart, a response that is both dose and time dependent. Moreover, the finding that CRH-R2 expression in the heart is modulated by endotoxin, a potent inducer of cardiovascular dysregulation, suggests a possible link between CRH and the cardiovascular response to stress.

**Table 4.1.** Pilot experiment showing CRH-R2 mRNA levels in the heart following injection of endotoxin.

| Time (h) post-injection of LPS (50 ug/mouse) or saline | CRH-R2 levels as % of time-matched saline-injectedcontrols (fold reduction from control levels)[a,b] |
|---|---|
| 2 | 64.7 (1.5) |
| 4 | 39.2 (2.5) |
| 6 | 21.1 (4.7) |
| 9 | 13.0 (7.7) |

[a]CRH-R2 levels were measured by RNase protection analysis as described in Materials and Methods.

[b]The intensity of the CRH-R2 band was normalized to the intensity of the L3 band of the same sample. Normalized values are presented as percent of control values.

**Figure 4.1.** Dose response of CRH-R2 expression in the heart following endotoxin (LPS) injection. RNase protection autoradiographs were quantitated by densitometry. Mice were injected ip with the indicated dose of LPS in saline and hearts were harvested after 7.5 hours.

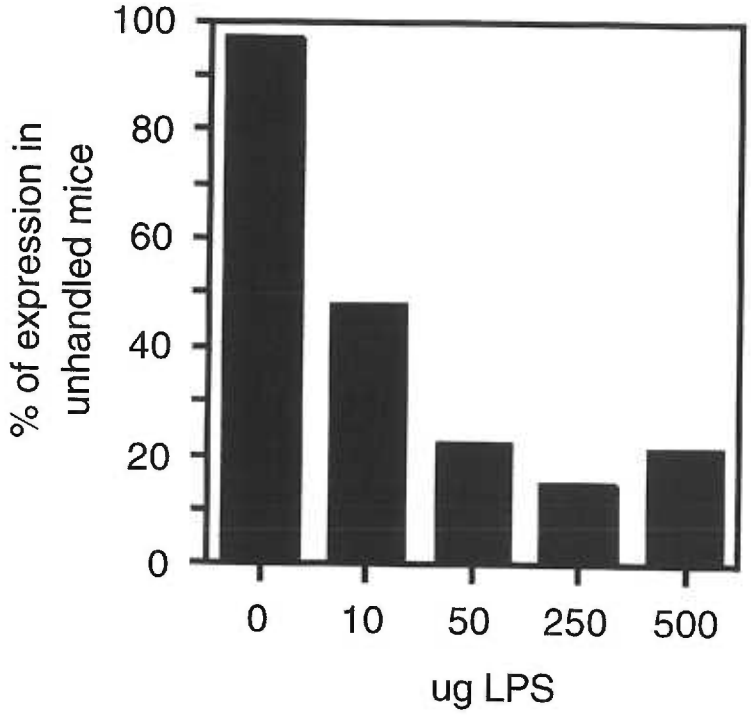
100
80
60
40
20
0
% of expression in unhandled mice
0
10
50
250
500
ug LPS

**Figure 4.2.** (A) Time course of the effect of endotoxin (LPS, 50 ug/mouse, ip) on CRH-R2 mRNA levels in the heart. Values are expressed as percent of CRH-R2 mRNA levels in mice receiving saline only, mean+SEM. Compared to saline controls, * $p<0.05$, ** $p<0.001$. Time points (2, 4, 6 and 9 hours) were calculated from two experiments, 6-7 animals/group/experiment; time point 24 hours is from a single experiment. (B)Representative RNase protection autoradiograph of heart RNA (25 ug) following ip injection of saline or endotoxin (LPS). The 0-hour lane contains RNA from unhandled animals. CRH-R2 probe protects a 239 nt fragment; L3 probe is a control for quantity of RNA and protects a 216 nt fragment.

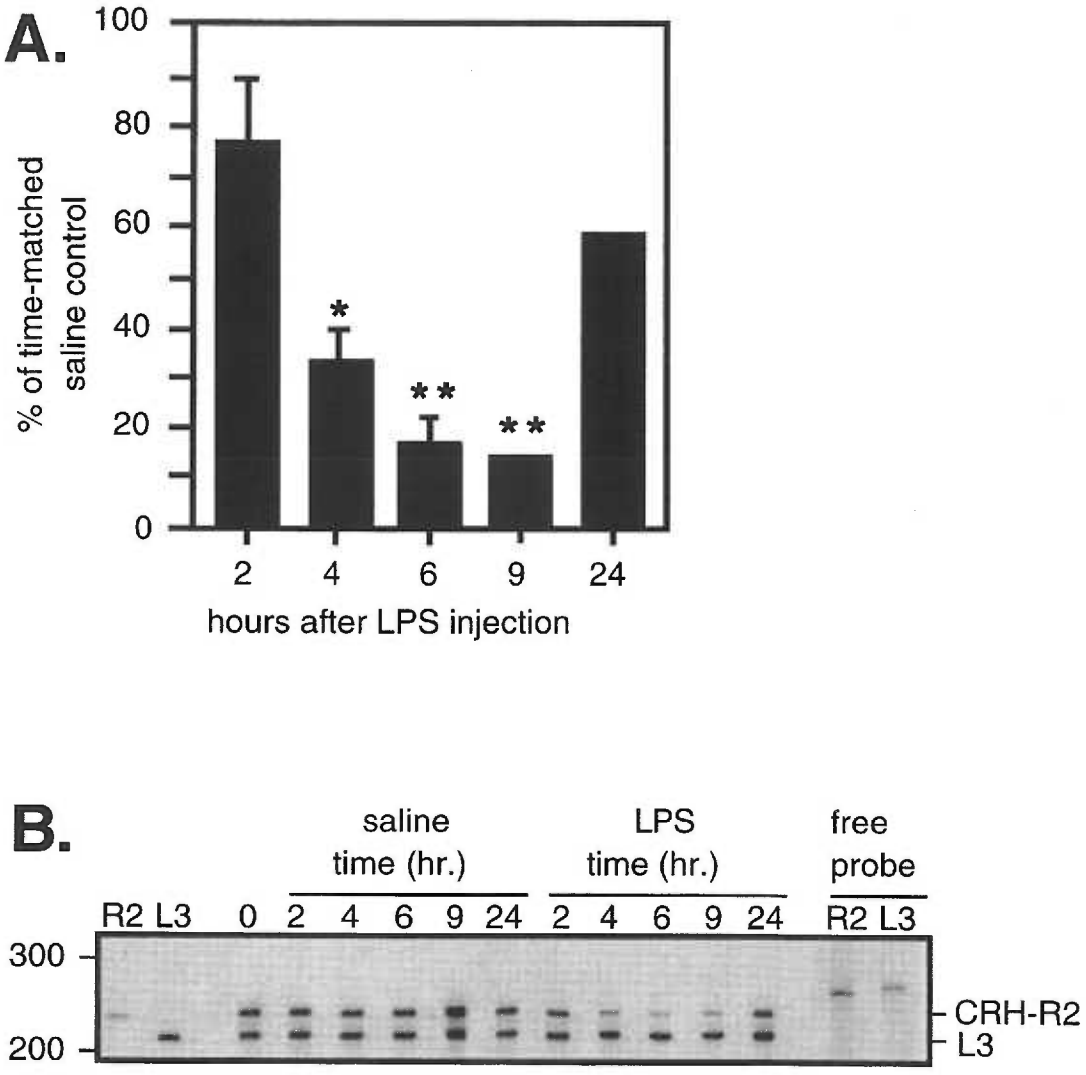
A.
100
80
60
40
20
0
% of time-matched saline control
*
**
**
2
4
6
9
24
hours after LPS injection
B.
saline time (hr.)
LPS time (hr.)
free probe
R2 L3 0 2 4 6 9 24 2 4 6 9 24 R2 L3
300
200
CRH-R2
L3

**Figure 4.3.** Time course of the effect of endotoxin (LPS, 50 ug/mouse, ip) on CRH-R2 mRNA levels in skeletal muscle. Values are expressed as percent of CRH-R2 levels in mice receiving saline only, mean + SEM. Compared to saline controls, * $p<0.01$. Time points (2, 4, 6 and 9 hours) were calculated from two experiments, 6-7 animals/group/experiment; time point 24 hours was taken from a single experiment.

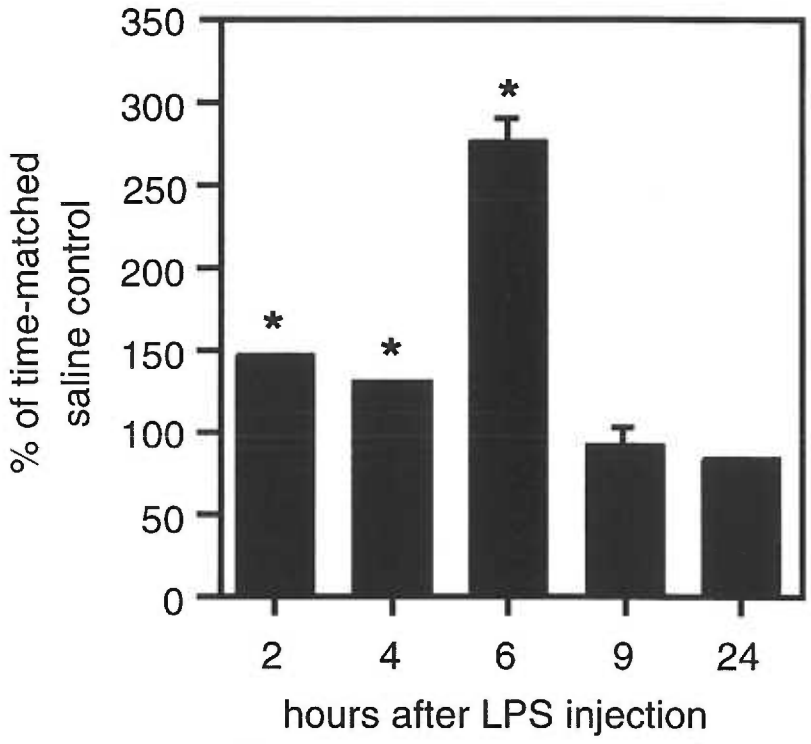
350
300
250
200
150
100
50
0
% of time-matched saline control
*
*
*
2
4
6
9
24
hours after LPS injection

## Acknowledgement

We thank Giselle Crosa and Dana Redick for technical assistance. This work was supported by NIH grants AI14985 and AI26827 (MBR) and MH52393 (MS-P), an American Heart Association Oregon Affiliate grant (MS-P) and by NIH/NEI predoctoral training grant 2T32EY07123 (KAH).

# Chapter 5

# Hypothesis

We have shown that endotoxin differentially regulates CRH-R2 mRNA levels in peripheral tissues; endotoxin downregulates CRH-R2 expression in the heart, but upregulates CRH-R2 expression in the skeletal muscle. Endotoxin can directly stimulate cells, including cardiomyocytes, via endogenous receptors. However, the principal action of endotoxin is the induction of cytokines, which mediate many of endotoxin's effects *in vivo*. Therefore, we will test the hypothesis that cytokines mediate endotoxin-induced downregulation of CRH-R2 mRNA in the heart.

# Regulation of Corticotropin-Releasing Hormone Receptor-2 in Heart and Skeletal Muscle: Differential Effects of IL-1 and TNF-α.

Kurt A. Heldwein, Sarah C. Coste, Susan L. Stevens and Mary P. Stenzel-Poore*

*Department of Molecular Microbiology and Immunology, Oregon Health Sciences University, Portland, Oregon 97201.*

*Address all correspondence and requests for reprints to:
Mary P. Stenzel-Poore, Ph.D.
Department of Molecular Microbiology and Immunology, L220
Oregon Health Sciences University
3181 SW Sam Jackson Park Rd.
Portland, OR 97201
Phone (503) 494-2423
FAX (503) 494-6862
poorem@ohsu.edu

**Abstract.**

Two receptors (CRH-R1 and -R2) have been identified for the stress-induced neuropeptide corticotropin-releasing hormone (CRH) and the related peptide, urocortin (Ucn). We previously examined CRH-R2 regulation following administration of the bacterial endotoxin, lipopolysaccharide (LPS), which is a model of systemic immune activation and inflammation. We found that LPS differentially regulates CRH-R2 expression in heart and skeletal muscle; CRH-R2 expression was dramatically down-regulated in the heart while up-regulated in skeletal muscle. We postulated that inflammatory cytokines produced following LPS exposure mediates these changes in CRH-R2 expression. Here we show that LPS does not fully depress cardiac CRH-R2 expression in TNF-α receptor deficient mice ($p55^{-/-}$, $p75^{-/-}$), suggesting that TNF-α partially mediates LPS-induced down-regulation of CRH-R2 mRNA *in vivo*. We also find that systemic TNF-α or IL-1α administration significantly down-regulates CRH-R2 mRNA in mouse heart, further indicating that these cytokines may mediate the effect of LPS on cardiac CRH-R2 expression. In skeletal muscle, TNF-α treatment decreases CRH-R2 mRNA while IL-1α does not. These data again demonstrate differential regulation of CRH-R2 in mouse heart and skeletal muscle. To test whether these cytokines directly regulate CRH-R2 expression in cardiac cells, adult mouse ventricular cardiomyocytes were cultured *in vitro* with TNF-α or IL-1α for nine hours. We find that cytokines do not reduce CRH-R2 mRNA in cultured cardiomyocytes. Furthermore, corticosterone has no effect on CRH-R2 mRNA in cardiomyocytes. However, treatment with urocortin decreases CRH-R2 mRNA in cultured ventricular cardiomyocytes. Thus, we speculate that *in vivo*, inflammatory mediators such as LPS and/or cytokines increase urocortin, which in turn down-regulates CRH-R2 expression in the heart. Given that CRH and urocortin increase cardiac contractility and coronary blood flow, impaired CRH-R2 function during systemic inflammation may ultimately diminish the adaptive response of the heart to such adverse conditions.

## Introduction

Corticotropin-releasing hormone (CRH) is well known as a primary mediator of the mammalian stress response, acting through numerous central pathways to initiate an array of neuroendocrine, behavioral and autonomic adaptive changes (295). Considerable evidence also suggests a role for CRH in regulating peripheral responses. Intravenous administration of CRH elicits a number of cardiovascular changes that include marked hypotension and vasodilation in selective vascular beds (127, 281, 283). Direct actions of CRH have been demonstrated in isolated working heart preparations where addition of CRH induces a sustained increase in coronary blood flow, a transient positive inotropic effect and a rapid rise in the release of atrial natriuretic peptide (70) Urocortin (Ucn), a recently discovered member of the CRH family which shares 45% homology to rat/human CRH and 63% homology to fish urotensin, also has pronounced effects on the cardiovascular system when given systemically that excede those elicited by CRH (15). Urocortin produces a marked, long-lasting (>30 min) reduction in mean arterial pressure in rats (15) and increases cardiac contractility and coronary blood flow in sheep (273).

CRH receptor type 2 (CRH-R2), which bears 69% sequence identity with CRH receptor type 1 (CRH-R1) (45, 49, 60, 73)is highly expressed in peripheral sites, including heart, skeletal muscle, gastrointestinal tract and arterioles, with lower levels of expression in limited brain regions (45, 47, 48, 74). This pattern of expression is in distinct contrast to CRH-R1 which is found predominantly in the pituitary and various brain regions which include cerebral cortex, cerebellum and brainstem (73, 220). We have recently shown that murine cardiovascular responses to systemic Ucn depend critically on CRH-R2, using mice that lack functional CRH-R2 ($Crhr2^{-/-}$) (64). Ucn delivered intravenously causes a pronounced decrease in mean arterial pressure in wild-type mice while $Crhr2^{-/-}$ mice do not show this hypotensive response to urocortin. In addition, we found that Ucn injection increases the velocity of left ventricular contraction in wild-type mice but again had no

effect in Crhr2$^{-/-}$ mice. Thus, Crhr2$^{-/-}$ mice do not display measurable cardiovascular responses to systemic Ucn, providing strong evidence that CRH-R2 mediates Ucn-induced effects on cardiovascular function. CRH-R2 located on cardiac myocytes may mediate CRH/Ucn actions on the myocardium *in vivo* since neonatal cardiac myocytes express CRH-R2 and respond to CRH stimulation *in vitro* with increases in intracellular cAMP (260). Interestingly, CRH-R2 has ~40-fold greater affinity for Ucn than for CRH (15). This unique sensitivity to Ucn and the greater potency of Ucn in eliciting cardiovascular responses are in keeping with the proposal that a peripheral regulatory system comprised of Ucn and CRH-R2 may exist (15).

The role of a peripheral CRH/Ucn stress-responsive system remains unclear. Previous studies from our laboratory have shown that CRH-R2 mRNA levels in the heart are markedly down-regulated (~9-fold) following administration of bacterial endotoxin (lipopolysaccharide (LPS)) (296). Furthermore, we found that LPS had the opposite effect on CRH-R2 in skeletal muscle leading to increased (~3-fold) CRH-R2 expression. Thus, endotoxin has differential effects on CRH-R2 expression in the periphery; upregulation in skeletal muscle and downregulation in the heart. Together, these studies establish an important link between CRH-R2 and inflammation and suggest that a CRH system in the periphery may be activated during immune challenge which subsequently contributes to local cardiac and skeletal muscle responses.

An important feature of endotoxemia and systemic inflammation is the marked increase in cytokine production by both immune and non-immune cells in the periphery. Increased levels of pro-inflammatory cytokines during endotoxin exposure, particularly tumor necrosis factor (TNF-α), interleukin-1 (IL-1) and interleukin-6 (IL-6), may mediate endotoxin-induced changes in cardiac CRH-R2 mRNA expression. In the cardiovascular system, TNF-α and IL-1, acting in part through nitric oxide pathways, induce vasodilation

and hypotension, effects that mimic the cardiovascular sequelae of endotoxin exposure. Accordingly, neutralization of TNF-α or IL-1 receptor anatagonism inhibits the lethal effects of endotoxin in mammals(285, 287, 288, 297). Direct effects of these cytokines have been demonstrated wherein TNF-α and IL-1 directly depress cardiomyocyte contractility in vitro (298). In skeletal muscle, TNF-α and IL-1 participate in the metabolic response to sepsis, inducing protein degradation and inhibiting protein synthesis and amino acid uptake of muscle cells ((299, 300) for review see (301)). Thus, cytokines could potentially modulate CRH pathways in these peripheral tissues. Alternatively, both endotoxin and cytokines (e.g. IL-1 and IL-6) are known to stimulate CRH gene expression in the hypothalamic paraventricular nucleus, leading to the activation of the hypothalamic-pituitary-adrenal (HPA) axis and an elevation in circulating glucocorticoids (290, 302). High levels of glucocorticoids have been shown to down-regulate CRH-R1 in the hypothalamus and the pituitary (293) and it is conceivable that CRH-R2 in the periphery is also negatively regulated by glucocorticoids, perhaps during inflammation.

To test whether cytokines regulate CRH-R2 expression in heart and skeletal muscle, we challenged mice i.p. with the inflammatory cytokines, TNF-α and IL-1α. Here we report that recombinant TNF-α and IL-1α downregulate CRH-R2 in the heart *in vivo*. Futhermore, these cytokines have different effects on CRH-R2 in skeletal muscle. However, we find that TNF-α and IL-1α do not regulate CRH-R2 mRNA in isolated mouse cardiomyocytes *in vitro*, suggesting that the suppressive effects of these cytokines, *in vivo*, occur indirectly. In testing alternative routes of modulation, we find that dexamethasone treatment and restraint stress do not appear to regulate CRH-R2 in the mouse heart. Interestingly, we find that the high affinity CRH-R2 ligand, Ucn, downregulates CRH-R2 in cardiomyocytes. Thus, we speculate that endotoxin and/or cytokines increase CRH or Ucn expression *in vivo*, which, in turn downregulates CRH-R2 expression in the heart.

## Materials and Methods.

**Animals and Reagents.** Female C57Bl/6 mice were purchased from Jackson Laboratories (Bar Harbor, MA). TNF-α receptor double knockout ($p55^{-/-}$, $p75^{-/-}$) mice were obtained from Immunex (Seattle, WA). Mice were housed under specific pathogen-free conditions on a 12 h light/dark schedule and were given free access to laboratory chow and tap water. All experimental procedures met NIH guidelines with the approval of the Oregon Health Sciences University Institutional Animal Care and Use Committee.

Rat Ucn and CRH were purchased from Bachem (Torrance, CA). For *in vivo* studies, lipopolysaccharide (LPS, Escherichia coli, serotype 055:B5) was purchased from Sigma (St. Louis, MO). Recombinant mouse TNF-α was purchased from Roche/Boehringer-Mannheim (Indianapolis, IN) and recombinant human IL-1α was a generous gift of Dr. Alvin Stern at Hoffman-LaRoche (Nutley, NJ). For *in vitro* studies, recombinant mouse TNF-α, IL-1α and IL-6 were purchased from Endogen (Woburn, MA). Dexamethasone and corticosterone were purchased from Sigma (St. Louis, MO).

***In Vivo* Regulation of CRH-R2 mRNA by IL-1α, TNF-α or Dexamethasone.** Adult female C57Bl/6 mice (8-12 weeks) were housed in pairs in shrouded cages 12 hours prior to the start of the experiment and left over night undisturbed to minimize stress, as previously described (296). In separate experiments, mice were injected i.p. with either recombinant human IL-1α (10 μg), recombinant mouse TNF-α (2.5 μg, $1x10^6$ units) or dexamethasone (2.5, 25 or 250 μg). Each experiment included time-matched groups of mice treated with vehicle (pyrogen-free saline) alone. Animals were sacrificed at the indicated times after injection (see Results section) and heart and skeletal muscle (quadriceps) were removed from individual mice and flash frozen separately in liquid nitrogen.

***In Vivo* Regulation of CRH-R2 mRNA by LPS in TNF-α-R Deficient Mice.** Mice homozygous for disruptions in the p55 and p75 forms of TNF-α-receptor (backcrossed four generations onto C57Bl/6) were intercrossed and the genotypes of offspring were confirmed by PCR of tail DNA (146). Male and female wild-type and TNF-α-R ($p55^{-/-}$, $p75^{-/-}$) mice (7-12 weeks) were housed as described above. Mice were sacrificed at 1, 3, 9 or 24 h after i.p. injection of LPS (50 μg/mouse). Heart and skeletal muscle (quadriceps) were removed from individuals and flash-frozen separately in liquid nitrogen. This experiment was performed twice.

***In Vivo* Regulation of CRH-R2 mRNA by Restraint Stress.** Adult female C57Bl/6 mice (8-12 weeks) were housed in pairs in shrouded cages as described above. Unstressed animals (n=6 mice) were sacrificed in the morning, before the initiation of the restraint stress for all other groups of mice. All other mice (n=6 mice/group) were restrained for 90 minutes in ventilated 50 ml polypropylene tubes (Falcon). Animals were sacrificed 0, 1.5, 3 or 6 h following restraint. Hearts were removed and flash frozen separately in liquid nitrogen.

**RNase Protection for CRH-R1 and CRH-R2.** Quantitation of CRH-R2 mRNA was performed as previously described (260). Briefly, total RNA was purified from mouse tissues or isolated adult mouse ventricular cardiomyocytes using RNA STAT-60 according to manufacturer's protocol (Tel-Test, Inc., Friendswood, TX). Mouse CRH-R2 was detected with a 239 nt probe (mCRX-55) spanning TM3 and TM4 (corresponding to amino acids 204 through 283) (45). Mouse CRH-R1 was detected with a 169 nt probe spanning TM3 and TM4 (corresponding to amino acids 234-289). A 216 nt Rsa I fragment or 110 nt Dde I fragment of L3 cDNA, encoding a mouse ribosomal protein (303) was used as a control for equivalent loading of RNA. 32P-UTP probes for CRH-R2, CRH-R1 and

mouse L3 were synthsized *in vitro* and hybridized to total RNA overnight. Reactions were digested with RNase A (1 μg/ml) and $T_1$ RNase (600 U/ml) and resolved on a 6% polyacrylamide gel. Gels were exposed to phosphorimage screens. Quantitation of CRH-R2 mRNA in heart, skeletal muscle and isolated ventricular cardiomyocytes was performed using the IP Lab Gel software package (Signal Analytics, Vienna, VA). All CRH-R2 band intensities were normalized to L3 band intensities from the same RNA sample.

**Isolation of adult mouse ventricular cardiac myocytes.** Cardiomyocytes were isolated from hearts of adult wild-type (C57Bl/6) or CRH-R2 KO mice as described (279, 304). Briefly, mice were injected with heparin (200 units) and anesthetized with a mixture of ketamine (8 mg/mouse) and xylazine (2 mg/mouse). Hearts were removed with the aorta intact and connective tissue was removed. Hearts were mounted onto a modified langerdorf apparatus and perfused with a 95% $O_2$/5% $CO_2$ saturated $Ca^{2+}$ free modified Tyrode's solution for ~ 1 h. Hearts were subsequently perfused with Tyrode's solution containing 2 mg/ml collagenase type II (CLS2, Worthington Biochemicals, Freehold, NJ) until the tissue was soft. Ventricles were removed, teased apart and incubated in collagenase solution. Cardiomyocytes were allowed to pellet under gravity for 20 min and the supernantant (non-myocytes) was aspirated off. Isolated cells were passed through a 70 μm mesh filter and plated onto laminin-coated Primaria (Falcon) tissue culture plates in DMEM containing 10% fetal bovine serum, sodium pyruvate, non-essential amino acids, holo-transferrin (5 μg/ml), insulin (10 μg/ml), cytosine-β-D-arabinofuranoside (3 μg/ml), 2x MEM vitamins (Gibco BRL, Rockville, MD) and penicillin/streptomycin.

***In vitro* regulation of CRH-R2 mRNA in adult mouse ventricular cardiac myocytes.** Cardiomyocytes were plated onto laminin-coated 60 mm Primaria dishes and cultured overnight at 37°C in a humidified 5% $CO_2$ incubated chamber. In separate experiments, graded doses of Ucn (0.1-100 nM), cytokines (TNF-α (5 or 25 ng/ml), IL-

1α (2 or 20 ng/ml) or IL-6 (5 or 25 ng/ml)) or corticosterone (5 uM) were added to the culture medium and cells were incubated for 9 hours. Control wells received culture medium alone. Cells were lysed in RNA-STAT60 and RNA was isolated as described above. Experiments were performed three times with duplicate wells assayed in each experiment.

**Stimulation of cAMP production in adult mouse ventricular cardiac myocytes.** Cardiomyocytes were plated into laminin coated 24-well Primaria tissue culture plates and cultured overnight at 37°C (5% $CO_2$). Cells were washed and incubated in serum-free DMEM for 90 min followed by 30 min incubation in serum-free DMEM containing 1mM IBMX (Sigma, St. Louis, MO). Myocytes were stimulated with graded concentrations of Ucn or CRH ($10^{-6}$ M to$10^{-12}$ M) for 25 minutes in DMEM (1 mM IBMX). Medium was removed and cells were immediately lysed and incubated in extraction medium (95% EtOH/20 mM HCl) overnight at -20°C. cAMP was quantitated using a commercially available cAMP RIA kit (Biomed Tech, Inc, Stoughton, MA). Experiments were performed twice with triplicate wells assayed in each experiment.

**Harvesting of individual cardiomyocytes and amplification of CRH receptor mRNAs by nested RT-PCR.** Freshly isolated adult mouse ventricular cardiomyocytes in perfusion medium were individually harvested using a small-bore (6 μm diameter) glass pipette maneuvered into position by a hydraulic micromanipulator apparatus (Narishige, Japan). Cardiac myocytes were captured by applying negative pressure to the pipette and immediately placed in 15 μl of 1X reverse transcriptase buffer (Life Technologies) with +1% NP-40 (Sigma). Cells were stored at –80°C. Samples were treated with DNase overnight at 37°C. A portion of each sample was processed without the addition of reverse transcriptase to verify the absence of contaminating DNA. Reverse transcription was carried out at 42°C using random hexamers (Pharmacia). The integrity of

the cDNA was tested using nested primers for the L3 housekeeping gene. The samples which were used in subequent PCRs showed an amplified 395 bp band in the second round of L3 of the reverse transcriptase reaction, without amplification from a parallel sample lacking reverse transcriptase. The first round of PCR amplification for CRH-R1 and CRH-R2 used specific primer pairs that resulted in the following fragment sizes: CRH-R1, 157 bp; CRH-R2, 190 bp. These reactions (1 μl) were used for the second round of amplification, which utilized nested primers for CRH-R1 and CRH-R2. The size of the products generated with internal primer pairs were 60 bp for CRH-R1 and 68 bp for CRH-R2. All PCR amplifications were allowed to progress for 45 cycles. RNA from HEK 293 cells transfected with cDNAs for mouse CRH-R1 or CRH-R2β were used as positive controls.

**Primers.** L3 housekeeping gene first round: sense (5'-GATGTCTCACAGGAAATTCTCAGC-3'), antisense (5'-TAATCTCTGTTCGGTGATGGTAGC-3'); second round sense (5'-TGTGGGAATTCTGGGATATGTTGAGACCC-3'), antisense (5'-TTGTCAAGCTTATGACATCAATCATCTCATCCTGCC-3'). CRH-R1 first round: sense (5'-ATCCTCATGACCAAACTCCG-3'), antisense (5'-TGAAGACAACCCTGGAGACC-3') second round (internal): sense (5'-TACAGGAAGGCTGTGAAGGC-3'), antisense (5'-ACATGTAGGTGATGCCCAGG-3'). CRH-R2 first round: sense (5'-CTACACCTACTGCAACACGACC-3'), antisense (5'-TTCGCAGTGTGAGTAGTTGACC-3'); second round (internal) sense (5'-ACCCGGAGCCCTAGTAGAGA-3'), antisense (5'-TTCCGGGTCGTGTTGTACTT-3').

**Statistical Analysis.** Data were analyzed using analysis of variance (ANOVA) grouped on time or dose. Follow up analyses were performed using the Newman-Keuls post-hoc test. The diffences in CRH-R2 mRNA levels between wild-type and TNF-α-R KO mice at

9 hours were analyzed by Student's unpaired t-test. For the restraint stress and dexamethasone experiments, pools of RNA from individuals in each group were used for quantitation, thus, due to the lack of variance in each group statistical analysis were not performed. Differences were considered statistically significant when $P<0.05$.

## Results.

### TNF-α partially mediates the downregulation of cardiac CRH-R2 mRNA by endotoxin.

We explored the role of TNF-α in endotoxin-induced regulation of CRH-R2 in the heart using mice that lack both TNF-α receptors, p55 and p75 (146) Homozygous knockout and wild-type mice were injected with LPS (50 μg/mouse, i.p.) or pyrogen-free saline. LPS caused a decrease in CRH-R2 mRNA levels in the hearts of wild-type and TNF-α-R ($p55^{-/-}$, $p75^{-/-}$) mice compared to time-matched controls (**Figure 5.1**). This decrease reached a maximum (34% of control) in wild-type mice by 9 hours after injection of endotoxin and had not yet returned to basal levels by 24 h. However, the decrease in CRH-R2 mRNA in the hearts of TNF-α-R ($p55^{-/-}$, $p75^{-/-}$) mice at 9 h was significantly less (65% of control) than in wild-type mice ($p<0.001$). These results indicate that TNF-α partially mediates the effect of LPS on CRH-R2 mRNA in the heart *in vivo*. Moreover, these results suggest that other cytokines, such as IL-1, may also be important mediators of the effects of endotoxin on cardiac CRH-R2 expression.

**TNF-α and IL-1 differentially regulate CRH-R2 mRNA in the heart and skeletal muscle in vivo.** We had previously shown that injection of LPS caused a time-dependent downregulation of CRH-R2 mRNA in the heart and increased CRH-R2 expression in skeletal muscle (**Figure 5.2A**, results from(296)), however, the basis for this differential regulation of CRH-R2 was unknown. Thus, we investigated whether administration of the inflammatory cytokines, IL-1α and TNF-α, which are known to be induced by LPS, modulate expression of CRH-R2 in heart and skeletal muscle.

Mice were injected with TNF-α (2.5 μg) or pyrogen-free saline (vehicle) and sacrificed at various times (3, 6, 9 h) post-injection. CRH-R2 mRNA levels in the heart and skeletal

muscle decreased significantly over time (**Figure 5.2B**). By nine hours post injection, CRH-R2 mRNA levels in the heart had dropped to 40% of control levels ($p<0.05$) and to 20% of control levels in skeletal muscle ($p<0.001$). Similar to our findings with TNF-α, administration of IL-1α (10 μg) induced a marked time-dependent decrease in CRH-R2 mRNA levels in the heart (**Figure 5.2C**) ($p<0.001$). In contrast, however, skeletal muscle expression of CRH-R2 mRNA was not modulated by IL-1α despite its marked effects in the heart. Thus, while TNF-α and IL-1α induce similar changes in CRH-R2 in the heart, they have differential effects on skeletal muscle. Moreover, both cytokines regulate CRH-R2 mRNA in skeletal muscle *in vivo* in a manner that is distinct from LPS (**Figure 5.2A**). Collectively, these findings suggest that while TNF-α and IL-1α may mediate the effect of LPS on CRH-R2 expression in the heart, regulation of CRH-R2 mRNA in skeletal muscle by LPS likely involves additional factors that lead to increased CRH-R2 mRNA levels.

**Dexamethasone and restraint stress do not downregulate cardiac CRH-R2.** Because inflammation and cytokines are potent activators of the HPA axis (290), we investigated whether glucocorticoids have an effect similar to those of LPS and cytokines on cardiac CRH-R2 levels. Mice were injected with graded doses (2.5 μg, 25 μg or 250 μg) of dexamethasone, a type I and II glucocorticoid receptor agonist (305) or vehicle alone. Analysis of heart RNA (n=3-5, pooled RNA samples) revealed only minor alterations of cardiac CRH-R2 mRNA levels across a 100-fold dose range of dexamethasone compared to saline-injected control mice (**Table 5.1**). Thus, it is unlikely that increased levels of corticosterone following endotoxin or cytokine administration lead to downregulation of CRH-R2 mRNA in the heart.

It is possible stress-responsive hormones other than adrenal glucocorticoids, produced during inflammation mediate the downregulation of CRH-R2 mRNA in the heart. To begin

to investigate this possibility, we subjected mice to a 90 minute restraint stress and compared CRH-R2 mRNA levels in the hearts of mice at 0, 1.5, 3 and 6 h following restraint to those of unstressed controls. Analysis of heart RNA (n=6, pooled RNA samples) shows that CRH-R2 mRNA levels were slightly elevated in hearts of mice immediately following the termination of the 90 min restraint period compared to unstressed controls (**Table 5.1**). However, we did not observe a decrease in cardiac CRH-R2 mRNA levels at 1.5, 3 and 6 h after the restraint period relative to that observed in unstressed mice. Thus, it appears that glucocorticoids or other hormones induced by a cognitive stressor (restraint) may not play a primary role in mediating the suppressive effects of endotoxin, TNF-α or IL-1α on expression of CRH-R2 in the heart.

**Expression and pharmacology of CRH-R2 in adult mouse ventricular cardiomyocytes**. We have shown previously that AT-1 atrial cardiomyocyte tumor cells express CRH-R2 and respond to CRH with increased cAMP production (260). However, transformed AT-1 cardiomyocyte responses may differ from those of primary adult cardiac myocytes; hence we tested the use of adult mouse cardiomyocytes as a suitable *in vitro* model system by examining the expression and pharmacology of CRH-R2. Cultures of highly enriched primary mouse ventricular cardiomyocytes express CRH-R2 mRNA at levels similar to those found in whole mouse heart (**Figure 5.3A**). Furthermore, we do not find evidence of CRH-R1 expression. The cardiomyocytes cultures are not completely devoid of non-myocyte cells (90-95% cardiomyocytes) thus we examined individually isolated cardiac myocytes for expression of CRH-R1 and CRH-R2 (**Figure 5.3B**). Using nested RT-PCR, we find that cardiac myocytes express CRH-R2, but not CRH-R1 (**Figure 5.3C**). The product amplified with CRH-R2 specific primers was sequenced and found to be identical to mouse CRH-R2. Stimulation of cultured cardiomyocytes with Ucn or CRH causes a dose-dependent increase in intracellular cAMP (**Figure 5.3D**). The EC50 values obtained for Ucn (EC50 = 3.3 ± 0.5 x $10^{-10}$ M) and CRH (EC50 = 3.4 ± 1.1

x $10^{-8}$ M) are similar to those reported previously for cells transfected with CRH-R2β (15). In addition, cAMP responses were not elevated in cardiomyocytes collected from Crhr2$^{-/-}$ mice, demonstrating that CRH/Ucn stimulation of cAMP is dependent on the presence of CRH-R2. Thus, cultured mouse cardiomyoctyes represent an appropriate *in vitro* model system to examine the regulation of CRH-R2 in the heart.

**CRH-R2 expression in isolated cardiomyocytes is not regulated by IL-1, TNF-α or IL-6.**

We tested whether cytokines that modulate cardiac CRH-R2 mRNA *in vivo* directly regulate CRH-R2 mRNA *in vitro*. Isolated cardiomyocytes were treated for nine hours with either TNF-α (5 or 25 ng/ml), IL-1α (2 or 20 ng/ml) or IL-6 (5 or 25 ng/ml) at doses previously shown to regulate cardiomyocyte function *in vitro* (173, 174, 298). We found that treatment with these cytokines failed to significantly alter CRH-R2 mRNA in these cells (**Figure 5.4**) suggesting that the *in vivo* effects of TNF-α and IL-1α on CRH-R2 levels in the heart are indirect.

To examine the possible role of glucocorticoid modulation, we treated cardiomyocytes with corticosterone (5 uM). This is a maximal dose of corticosterone that has been shown to regulate several genes in cardiac myocytes (306-308) and is higher than that shown to downregulate CRH-R1 mRNA in rat pituitary cells (108). CRH-R2 mRNA levels remained unchanged following incubation with corticosterone for nine hours (**Figure 5.4**).

**CRH-R2 expression in isolated cardiomyoctyes is downregulated by Ucn.**

We tested the effect of Ucn, which recently has been reported to be upregulated in the periphery by LPS (309). Treatment of cardiomyocytes *in vitro* with graded doses of Ucn (0.1-100 nM) for nine hours significantly decreased the level of CRH-R2 mRNA compared to controls incubated with medium alone (**Figure 5.5**). Thus, urocortin is capable of

regulating CRH-R2 expression suggesting the possibility that LPS and/or inflammatory cytokines regulate cardiac CRH-R2 mRNA indirectly by inducing and sustaining Ucn or CRH release into the heart, which subsequently leads to ligand-induced down-regulation of CRH-R2.

**Discussion.**

Inflammation is a powerful physiologic stress that affects a number of organ systems leading to marked changes in energy metabolism, immune function and cardiovascular homeostasis (310). Sepsis, a potent inducer of systemic inflammation, is characterized by vascular dysfunction, refractory hypotension and progressive depression of cardiac function and consequent diminished organ perfusion (179, 311). Depression of cardiac function in later stages of sepsis may be due, in part, to TNF-α and IL-1 which have been found to be the primary cardiodepressive factors in plasma of septic individuals (298). Although diminished cardiac function occurs following prolonged inflammation, early stages of sepsis are marked by increased cardiac function (179), which may be a compensatory response to hypotension resulting from the effects of inflammatory mediators on vascular endothelium. Increased cardiac function early in sepsis is likely to be a vital adaptation by the host that enhances survival against pathogens. Moreover, decreased cardiac function following prolonged inflammation may result from declining inotropic support due to changes such as receptor sensitivity and relative availability of inotropic mediators. Thus, mechanisms that lead to increased positive inotropic support for the heart may be particularly important during sepsis and endotoxemia. Given that Ucn increases cardiac contractility via its actions on CRH-R2 (64) it is plausible that this pathway may play a role in maintaining inotropic support for the heart. In addition, we (296) and others (309) have found that endotoxin modulates this peptide:receptor system thereby establishing an important link between CRH-R2 and inflammation.

Our findings reported here add strength to the model that CRH-R2 responses are linked to inflammatory stimuli. We show that TNF-α and IL-1α downregulate CRH-R2 mRNA in the heart. Similar reductions in CRH-R1 expression in the rat pituitary have been demonstrated following the administration of IL-1β. In addition, we demonstrate that LPS-induced modulation of CRH-R2 depends, in part, on TNF-α. LPS was not able to fully

depress CRH-R2 expression in mice lacking TNF-α receptors (p55 and p75 forms) to the degree found in wild-type controls. Thus, TNF-α plays a role in mediating the effect of endotoxin on cardiac expression of CRH-R2. However, modulation is likely complex, requiring the actions of multiple cytokines on various cell types. Furthermore, we cannot exclude the possiblity that LPS acts directly on cardiomyocytes to modulate CRH-R2 in conjunction with TNF-α, as these cells express Toll-like receptor-4, an endogenous endotoxin receptor (312).

We also show that CRH-R2 mRNA is differentially regulated in heart and skeletal muscle by cytokines and LPS. While administration of LPS, TNF-α or IL-1α decreased CRH-R2 mRNA in the heart, only TNF-α caused a similar decrease in CRH-R2 expression in skeletal muscle. IL-1α had no effect on CRH-R2 expression in skeletal muscle while endotoxin caused a 2-3 fold increase in CRH-R2 mRNA levels six hours after administration. The molecular basis for these different effects on CRH-R2 expression in skeletal muscle *in vivo* is unclear at this time. However, it is noteworthy that the observed upregulation of CRH-R2 mRNA in skeletal muscle following LPS exposure is not replicated by treatment with either TNF-α or IL-1α alone. Thus, regulation of CRH-R2 mRNA in skeletal muscle by LPS may involve direct actions of LPS or requires the synergistic effects of several inflammatory cytokines and other hormones such as glucocorticoids. Indeed, there is considerable evidence that other skeletal muscle responses to sepsis and inflammation are the result of a complex interaction between pro-inflammatory cytokines, glucocorticoids, insulin and other hormones (for review see (301, 313)). Interestingly, experiments using adrenalectomized or RU-38486-treated rats show that TNF-α exerts most of its catabolic effects through glucocorticoid release while IL-1 acts via a glucocorticoid-independent pathway (314-316). These results illustrate different pathways of cytokine modulation and suggest that TNF-α is linked to CRH pathways in skeletal muscle.

We used isolated adult mouse ventricular cardiomyocytes to examine the regulation of CRH-R2 *in vitro*. Suprisingly, low or high levels of TNF-α or IL-1α did not significantly regulate CRH-R2 mRNA in isolated cardiomyocytes. Moreover, IL-6, which is induced by TNF-α and IL-1α, also did not alter CRH-R2 mRNA expression in cardiomyocytes *in vitro*. These findings suggest that cytokines may not act directly on cardiomyocytes to modulate expression. As discussed above, it is possible that several cytokines act synergistically to influence cardiac CRH pathways. Alternatively, cytokines are potent stimulators of the HPA axis (317) and elevations in circulating glucocorticoids may regulate CRH-R2 expression in the periphery. Both CRH-R1 and CRH-R2 in the central nervous system are modulated by exogenous glucocorticoid treatment or exposure to psychological or metabolic stress. However, our studies suggest that cardiac CRH-R2 expression may not be solely regulated by HPA axis activation. We found that corticosterone did not regulate CRH-R2 mRNA in mouse cardiomyocytes *in vitro*. These findings parallel *in vivo* experiments wherein dexamethasone administration or restraint stress did not appear to alter CRH-R2 mRNA expression in heart tissue. Thus, we speculate that cytokines and glucocorticoids may not directly regulate CRH-R2 in the mouse heart *in vivo*.

We have demonstrated that Ucn, a high affinity agonist for CRH-R2, was capable of down-regulating CRH-R2 mRNA in cardiomyocytes in a dose-dependent manner. This is similar to the CRH-induced downregulation of CRH-R1 mRNA in rat anterior pituitary cells (108, 109). Moreover, ligand-induced downregulation has also been documented for a number of other G protein-coupled receptors (110-113, 115, 117, 318)and often involves decreases in mRNA stability (106, 111-113, 115, 117, 318). Downregulation of CRH-R2 mRNA in cardiomyocytes by Ucn may have important implications for the control of heart function during stress, and suggests that decreases in cardiac CRH-R2 mRNA during inflammation may be due to prolonged elevation of Ucn or CRH levels within the

myocardium. In fact, we (K. Heldwein and M. Stenzel-Poore, unpublished) and others (25) have found that Ucn and CRH mRNA are expressed in mouse heart, though currently little is known about the regulation of these cardiac transcripts. Heat shock (42°C, 3 hrs) has been shown to induce Ucn mRNA expresssion in cultured neonatal rat cardiomyocytes, however, the increase was minor (~1.8-fold over control) and seen 18 hrs after the cells were returned to 37°C (272).

Inflammation has been shown to regulate Ucn expression in rat thymus and spleen *in vivo* (309). Endotoxin increased thymic Ucn mRNA levels by 2-fold, but decreased (50% reduction) splenic Ucn mRNA levels. Interestingly, upregulation of Ucn mRNA in the thymus was adrenal-dependent, and ACTH or corticosterone also upreguated thymic Ucn mRNA. In contrast, splenic Ucn mRNA was unaltered by ACTH injection, indicating that splenic Ucn expression may be directly regulated by endotoxin or inflammatory mediators, while HPA activation is more important in regulating thymic Ucn mRNA. Because changes in Ucn peptide were not measured in this study, it is not clear how LPS or HPA activation effects the peripheral production of CRH-like peptides (125). Nevertheless, this study indicates that expression of Ucn in peripheral tissues may be stress-responsive.

Ucn expression in regions of the brain and in peripheral tissues has recently been shown to be regulated by various stimuli. Ucn mRNA in the Edinger-Westphal (EW) nucleus of the mouse is increased following restraint stress, and this was blocked by prior, chronic glucocorticoid infusion (34) indicating that glucocoticoids may desensitize or downregulate pathways that mediate stress-responsive regulation of Ucn mRNA in the EW. The number of Ucn-containing neurons in the supraoptic nucleus (SON) and fibers in the median eminence (ME) of the rat brain is increased by dehydration but decreased by food deprivation, although the number of Ucn-ir neurons in the EW is not changed by either

treatment (319). Neurons in the SON are known to be activated by several vascular stressors (e.g. changes in blood pressure, volume and osmolality) (30, 32, 320). Induction of Ucn in the SON by dehydration, which increases plasma osmolality, may lead to Ucn secretion and modulation of the vascular system.

Based on our findings, we propose a model in which systemic inflammation induces the peripheral production of Ucn or CRH, which activate CRH-R2 on cardiac myocytes in the mouse heart. Following prolonged stimulation, CRH-R2 mRNA is downregulated. Based on the stimulatory activity of Ucn and CRH on heart function, we posit that CRH-R2 may represent an inotropic pathway that contributes to an early hyperdynamic response of the heart to hypotension caused by cytokines during sepsis. We are currently studying the early cardiac response to inflammation in wild-type and Crhr2$^{-/-}$ mice. If Crhr2$^{-/-}$ mice show attenuated cardiac contracility in response to inflammation, this would lend support to our model, revealing a critical role for CRH-R2 in the regulation of heart function during stress. To date, our findings (64) and those of others (70, 273) indicate that Ucn and/or CRH are members of a family of neuropeptides (247, 321, 322) that affect heart function. Thus, CRH and Ucn may represent a mode of regulation of the cardiovascular system distinct from catecholamines, that complements or fine tunes cardiac responses during adverse conditions and threats to homeostasis.

**Table 5.1**. Effects of *in vivo* dexamethasone treatment and restraint stress on CRH-R2 mRNA expression in heart tissue.

| | Time after injection | | | |
|---|---|---|---|---|
| Dexamethasone (n=3/group) | 1h | 3 h | 6 h | 9 h |
| 2.5 µg | 96.7 | 78.6 | 112.1 | 122.7 |
| 25.0 µg | 99.8 | 78.0 | 86.4 | 106.9 |
| 250.0 µg | 103.1 | 107.0 | 80.2 | 81.9 |
| | Time after 90 min restraint stress | | | |
| Restraint Stress (n=6/group) | immediate | 1.5 h | 3 h | 6 h |
| | 149.0 | 87.0 | 77.0 | 119.0 |

Values are CRH-R2 mRNA levels expressed as a percent of saline-injected or unstressed control mice. In both experiments, RNA was pooled from individual hearts in each group.

**Figure 5.1.** Regulation of CRH-R2 mRNA in wild-type and TNF-α receptor double knockout ($p55^{-/-}$, $p75^{-/-}$) mice by endotoxin. Endotoxin (50 μg/mouse) or vehicle (saline) was injected i.p. into wild-type (C57Bl/6) and TNF-α-R ($p55^{-/-}$, $p75^{-/-}$) mice. Mice were sacrificed at indicated times. CRH-R2 mRNA was quantitated by RNase protection and normalized to L3 mRNA, a ribosomal gene used to control for RNA loading. Points represent the CRH-R2 mRNA levels in RNA pooled from wild-type (n=3) or TNF-α-R ($p55^{-/-}$, $p75^{-/-}$) mice (n=6), and are expressed as percent of time-matched saline-injected controls. B) CRH-R2 mRNA levels in individual hearts were examined at 9 hours. The error bar in wild-type mice (wt) is to small to be visible on the graph. *$p<0.001$, difference between wild-type and TNF-α-R ($p55^{-/-}$, $p75^{-/-}$) mice, determined by Student's t-test. The experiment was performed twice yielding similar results.

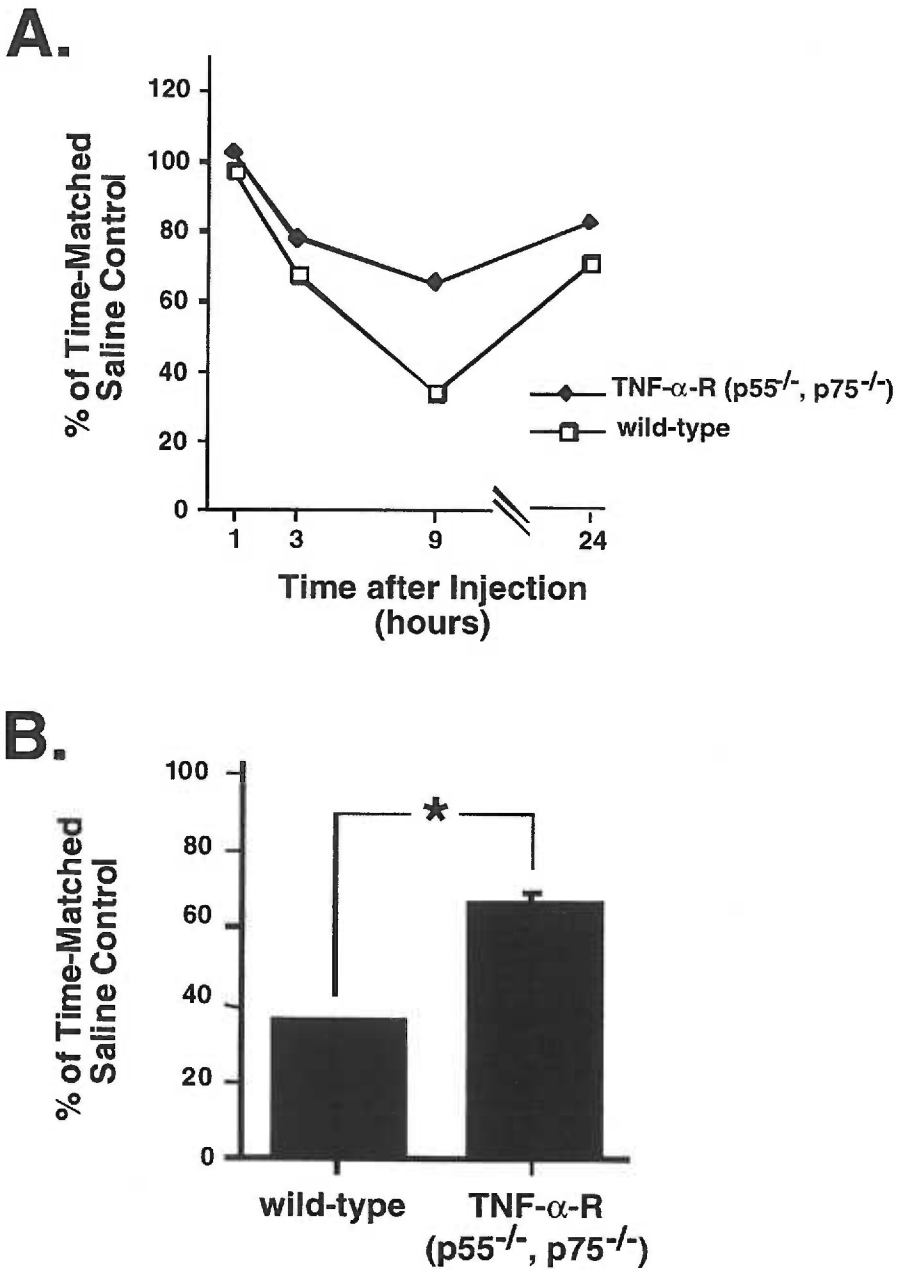
A.
% of Time-Matched Saline Control
120
100
80
60
40
20
0
1
3
9
24
Time after Injection (hours)
TNF-α-R (p55-/-, p75-/-)
wild-type
B.
% of Time-Matched Saline Control
100
80
60
40
20
0
*
wild-type
TNF-α-R (p55-/-, p75-/-)

**Figure 5.2.** Regulation of CRH-R2 mRNA in mouse heart and skeletal muscle in vivo. A) Injection (i.p.) of 50 μg of gram-negative bacterial endotoxin (LPS) (data taken from (296)). B) TNF-α (2.5 μg) or vehicle (saline) was injected i.p. into C57Bl/6 mice (n=4). C) IL-1α (10 μg) or vehicle (saline) was injected i.p. into C57Bl/6 mice (n=6). CRH-R2 mRNA was quantitated by RNase protection and normalized to L3 mRNA, a ribosomal gene used to control for RNA loading. Points represent mean CRH-R2 mRNA levels expressed as percent of time-matched, saline-injected controls ±SEM. *$p<0.05$, **$p<0.001$ using one-way ANOVA with Newman-Keuls post-hoc analysis (panels B and C) in time-matched, vehicle vs. treatment groups.

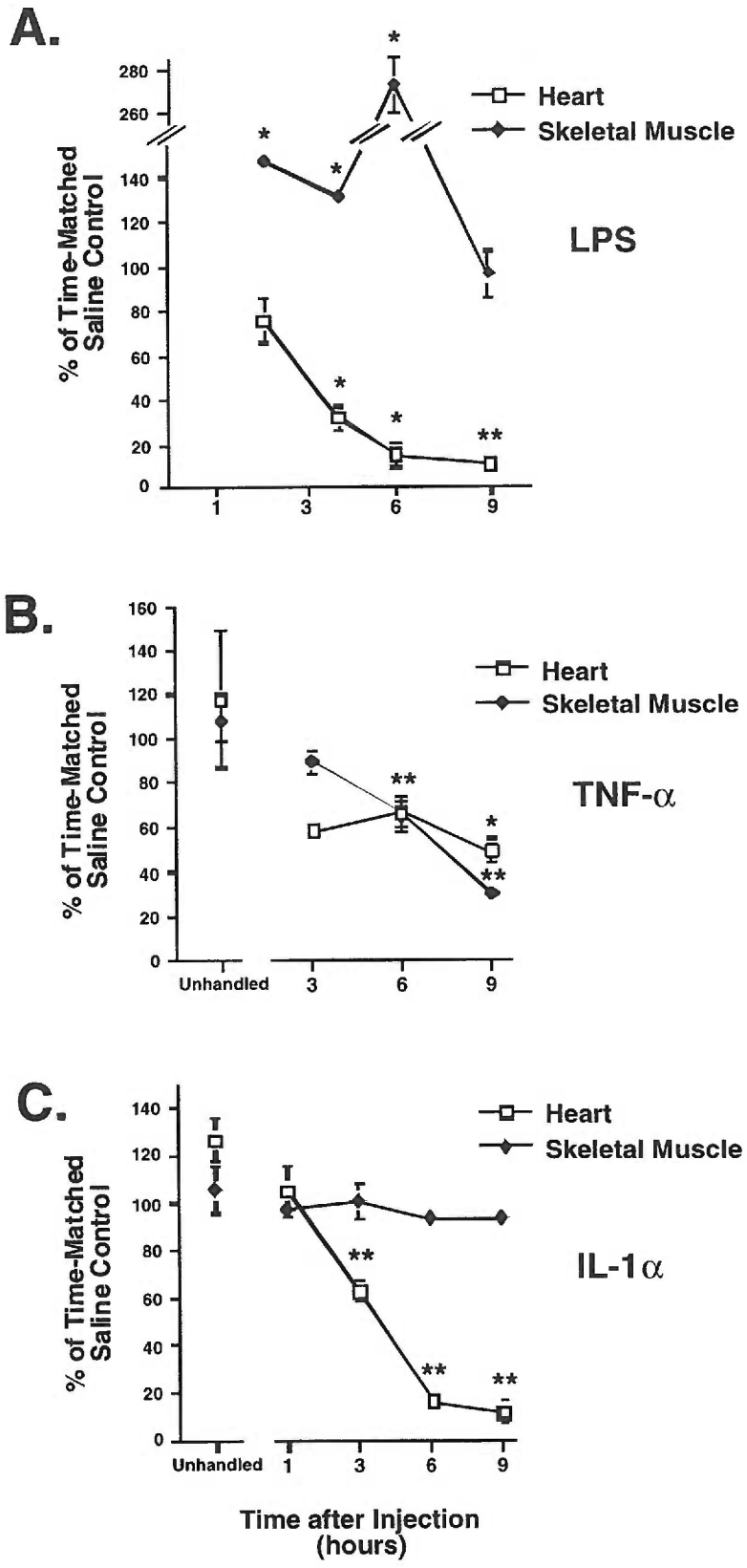
A.
% of Time-Matched Saline Control
Heart
Skeletal Muscle
LPS
B.
% of Time-Matched Saline Control
Heart
Skeletal Muscle
TNF-α
Unhandled
C.
% of Time-Matched Saline Control
Heart
Skeletal Muscle
IL-1α
Unhandled
Time after Injection (hours)

**Figure 5.3.** CRH-R2 expression and coupling to elevations in cAMP in adult mouse ventricular cardiac myocytes. A) RNase protection analysis of CRH receptor expression in cultures of adult mouse ventricular cardiomyocytes. CRH-R2 mRNA is highly expressed in adult mouse cardiomyocytes and whole heart, while CRH-R1 mRNA is undetectable. B) Harvesting of individual cardiomyocytes with a 6 μm-bore glass pipette. C) RT-PCR analysis of CRH receptor expression from four ventricular cardiomyocytes that were individually isolated and pooled for RT-PCR. CRH-R2 (68 bp) is evident following two rounds of PCR amplification. +, positive control; M, myocytes. D) Ucn and CRH stimulate increases in cAMP accumulation in adult mouse ventricular cardiomyocytes from wild-type mice, but not Crhr2$^{-/-}$ mice. Points are the mean ±SEM of triplicate wells/experiment and representative of duplicate experiments.

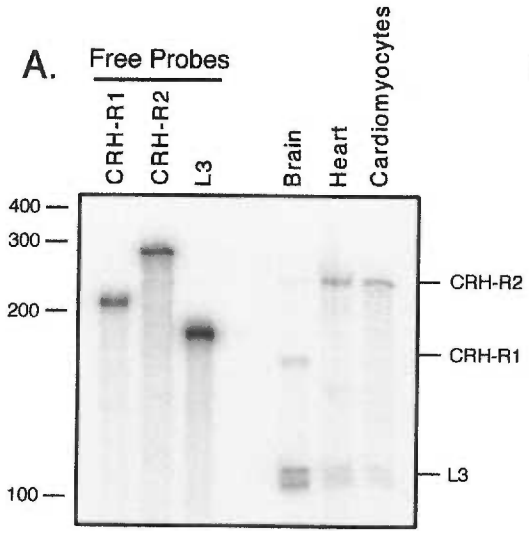
A.
Free Probes
CRH-R1
CRH-R2
L3
Brain
Heart
Cardiomyocytes
400
300
200
100
CRH-R2
CRH-R1
L3

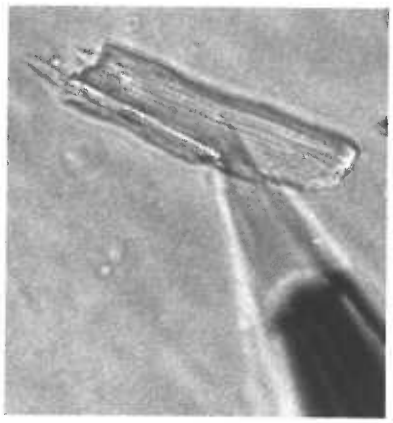
B.

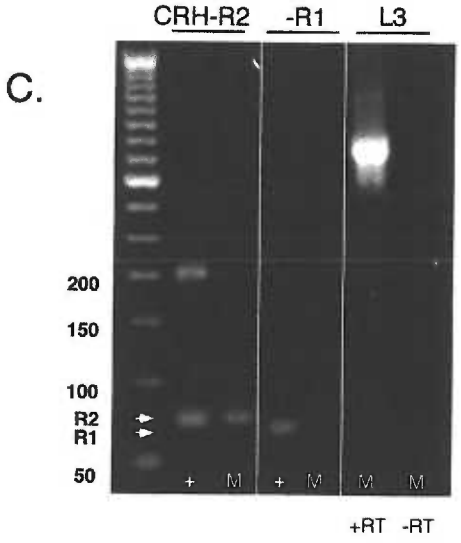
C.
CRH-R2
-R1
L3
200
150
100
R2
R1
50
+
M
+
M
M
M
+RT
-RT

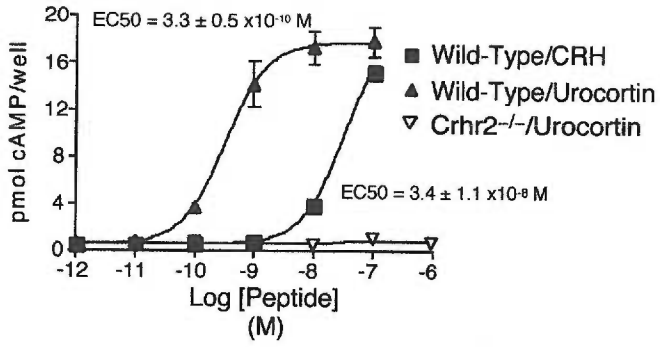
D.
EC50 = 3.3 ± 0.5 x10-10 M
EC50 = 3.4 ± 1.1 x10-8 M
Wild-Type/CRH
Wild-Type/Urocortin
Crhr2-/-/Urocortin
pmol cAMP/well
20
16
12
8
4
0
-12
-11
-10
-9
-8
-7
-6
Log [Peptide]
(M)

**Figure 5.4.** Cytokines and corticosterone do not regulate CRH-R2 in adult mouse ventricular cardiomyocytes. Myocytes were treated with the indicated concentrations of recombinant mouse TNF-α, IL-1α, IL-6, corticosterone or medium alone for nine hours. CRH-R2 mRNA was quantitated by RNase protection and normalized to L3 mRNA, a ribosomal gene used to control for RNA loading. Bars represent the mean of duplicate samples +STDEV and are expressed as the percent of CRH-R2 mRNA in medium (control) treated cells. The experiment was performed twice yielding similar results. One-way ANOVA with Newman-Keuls post-hoc analysis and Student's t-test revealed no significant differences in the means of control vs. treatment samples.

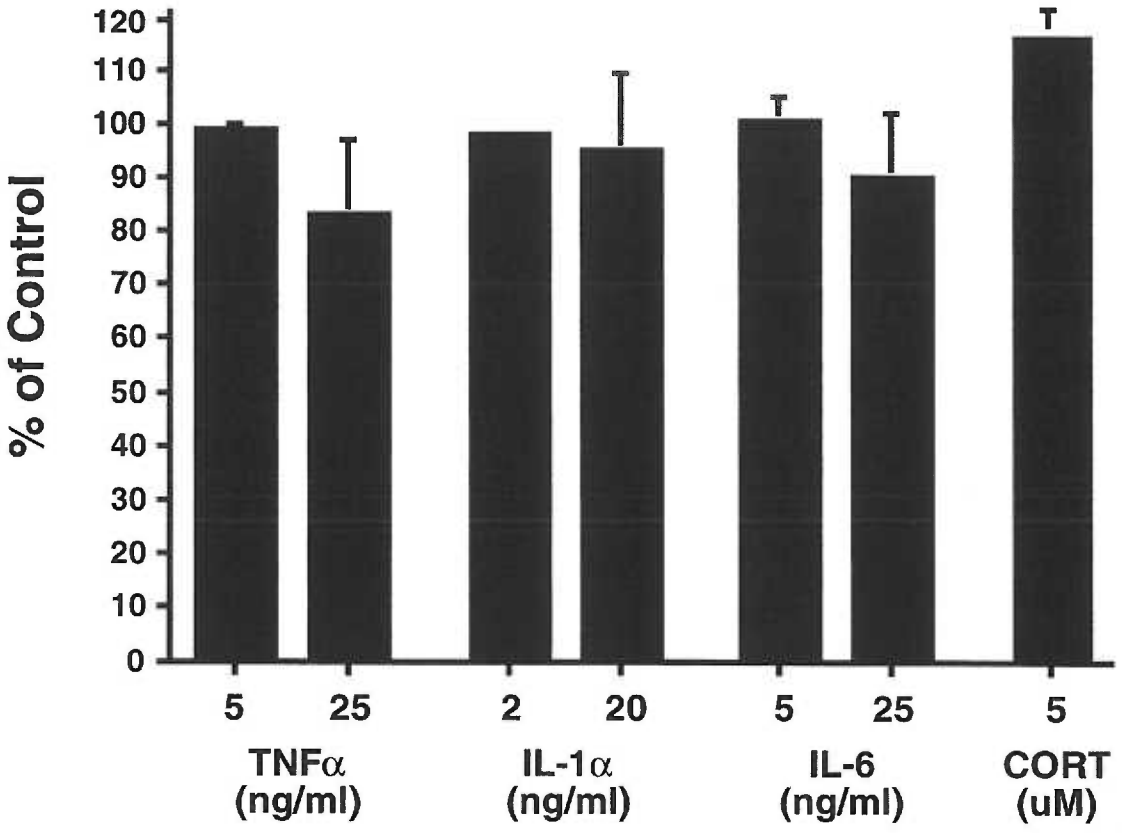
% of Control
120
110
100
90
80
70
60
50
40
30
20
10
0
5
25
2
20
5
25
5
TNFα (ng/ml)
IL-1α (ng/ml)
IL-6 (ng/ml)
CORT (uM)

**Figure 5.5.** Ucn regulation of CRH-R2 mRNA in adult mouse ventricular cardiomyocytes. Myocytes were treated with the indicated concentrations of Ucn or medium alone for nine hours. CRH-R2 mRNA was quantitated by RNase protection and normalized to L3 mRNA, a ribosomal gene used to control for RNA loading. Bars represent the mean of duplicate samples +STDEV (except for the 1nM dose of Ucn) and are expressed as the percent of CRH-R2 mRNA in medium (control) treated cells. The experiment was performed three times yielding similar results. *$p<0.05$ by one-way ANOVA with Newman-Keuls post-hoc analysis in medium vs. Ucn treated cardiomyocytes.

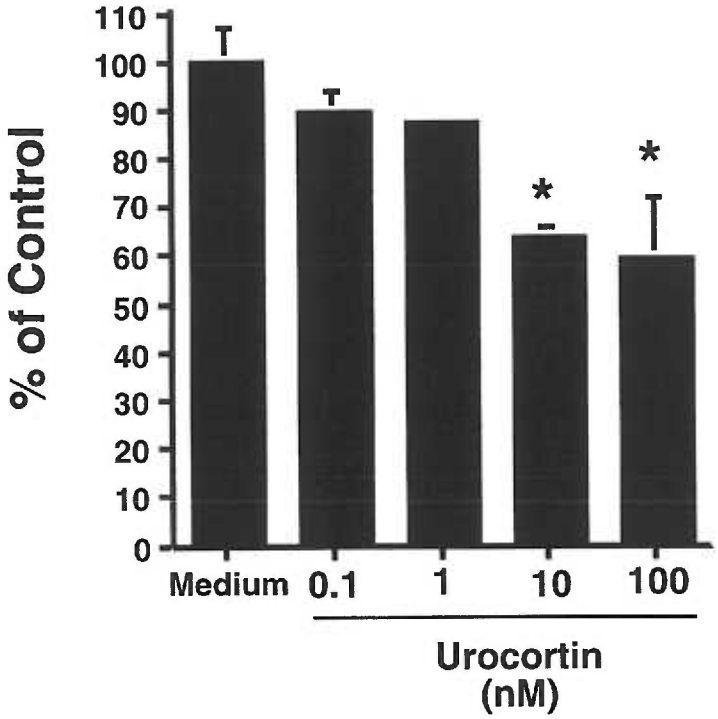
% of Control
110
100
90
80
70
60
50
40
30
20
10
0
*
*
Medium
0.1
1
10
100
Urocortin
(nM)

# Appendix

The results presented in this section concern aspects of CRH-R2 that do not have a strong thematic relationship, but add vital information to our understanding of CRH-R2. Thus, the findings should be considered as independent pieces yet to be fit into a larger picture of CRH-R2 and cardiac biology. This appendix provides evidence supporting the following:

1) that intrinsic cardiac cells may be a source of ligands for CRH receptors in the heart,
2) that CRH receptors may regulate cardiomyocyte growth and cardiac adaptation to hypertension,
3) that adrenergic agents regulate CRH receptor expression and function in cardiomyocytes, and
4) that CRH-R1 expression is inducible in cardiac myocytes.

We believe these results support the hypothesis that cardiac CRH receptors mediate direct CRH and Ucn stimulation of the heart. Discussions of our findings appear in the Summary and Conclusions section of this dissertation.

## Introduction

We have demonstrated that adult mouse ventricular cardiomyocytes express CRH-R2, which is coupled to cAMP production in these cells and mediates Ucn-induced increases in cardiac function in vivo. Furthermore, we have shown that CRH-R2 expression is downregulated in the mouse heart by inflammation, a potent stressor of the cardiovascular system. However, glucocorticoids and cognitive stress do not appear to regulate cardiac CRH-R2 expression. Thus, CRH-R2 may be an important modulator of cardiac function specifically during cardiovascular stress. However, currently the sources of ligand for CRH-R2, namely Ucn or CRH, in the heart are unclear.

Hypertension is a form of cardiovascular stress that induces adaptive responses in the heart (323). Pulmonary hypertension, induced by chronic hypoxia, results in increased afterload specifically on the right ventricle (324). The increase in afterload requires the right ventricle to generate a greater amount of force during systole to sustain perfusion of the lungs (194). Elevations in adrenergic stimulation increase the force generated during each cycle of myocyte contraction, but prolonged stimulation induces cardiomyocyte hypertrophy.

The hypertrophic growth of adult ventricular cardiomyocytes involves re-expression of embryonic genes such as atrial natriuretic peptide (ANP), skeletal α-actin and β-myosin heavy chain (325). In addition, the expression of genes involved in the contractile apparatus, including α-myosin heavy chain, troponin C and ventricular-specific myosin light chain-2, is upregulated, resulting in enhancement of the force-generating capacity of cardiomyocytes (325). However, chronic stimulation-induced hypertrophy of adult cardiomyocytes eventually leads to disorganization of myofibrils, decreased peak force of contraction, apoptosis and a fall in cardiac output. The end result of chronic pulmonary hypertension is failure of the right ventricle (326).

Hyperplastic and hypertrophic growth of immature cardiomyocytes is a normal ontogenic process that allows the neonatal heart to adapt to the increasing demands of the

developing vascular system (325). In the rat, neonatal cardiac myocytes are initially small, mononuclear cells with incomplete transverse tubule systems. During the first three weeks after birth myocytes continue to proliferate, but become binucleated with increasing frequencey. Proliferation and DNA synthesis cease by 3 weeks after birth, and the pattern of gene expression is altered. The myocytes enter a phase of hypertrophic growth, increasing their sarcomere and myofibril content. In addition, cardiac myocytes undergo changes in their adrenergic response pathways. The density of β-adrenergic receptors on the surface of cardiac myocytes increases more than 4-fold, with the proportion of $\beta_1$- to $\beta_2$-adrenergic remaining constant (327). However, while both $\beta_1$- and $\beta_2$-adrenergic receptors contribute to the inotropic response of neonatal rat cardiac myocytes to isoproterenol, only $\beta_1$-adrenergic receptors mediate the inotropic effect of isoproterenol on adult rat cardiac myocytes (327). Thus, neonatal and adult cardiac myocytes differ at the levels of gene expression, cellular structure and coupling of receptors to intracellular signaling pathways.

## Materials and Methods.

**Dissection of mouse hearts.** Mice were euthanized, and hearts were removed and placed in ice-cold phosphate-buffered saline containing heparin (10 U/ml). Connective and fatty tissue was dissected away first. Pulmonary vessels, vena cava and aorta were then removed. Ventricles were separated from atria by a single cut ventral of the aortic and atrio-ventricular valves. Atria and ventricles were flash frozen in liquid nitrogen and stored at -80°C until use.

**Regulation of CRH-R2 mRNA in mouse heart by hypoxia.** Litters from timed-pregnant CD-1 mice were randomized into groups and placed with mothers within 1 day of birth. Control (normoxic) groups were housed in normal atmospheric conditions (~21% $O_2$). Hypoxic groups were housed in cages within plexiglass chambers that were continuously perfused with a nitrogen/carbon dioxide/oxygen gas mixture containing 11% $O_2$. After 16 days, remaining hypoxic groups were returned to normal atmospheric conditions. Groups of mice were sacrificed on their day of birth, or 4, 16, and 32 days of age. Hearts were quickly removed, ventricles were dissected away from atria, and the posterior wall of right ventricles were separated from the septum and posterior wall of left ventricles. Hearts were weighed to quantitate hypertrophy and then flash frozen in liquid nitrogen.

**Isolation of adult rat ventricular cardiac myocytes.** Cardiomyocytes were isolated from hearts of adult wild-type (C57Bl/6) or CRH-R2 KO mice as described (279, 328). Briefly, mice were injected with heparin (200 units) and anesthetized with a mixture of ketamine (8 mg/mouse) and xylazine (2 mg/mouse). Hearts were removed with the aorta intact and connective tissue was removed. Hearts were mounted onto modified Langerdorf apparatus and perfused with a 95% $O_2$/5% $CO_2$ saturated $Ca^{2+}$ free Joklik's

medium. Hearts were then perfused with Joklik's medium containing 2 mg/ml collagenase type II (CLS2, Worthington Biochemicals, Freehold, NJ) until soft. Ventricles were removed, teased apart and incubated in collagenase solution. Cardiomyocytes were allowed to pellet under gravity for 20 min., and the supernantant (non-myocytes) was removed. Isolated cells were passed through a 70 μm mesh filter and plated onto laminin-coated Primaria (Falcon) tissue culture surfaces in DMEM containing 10% FBS, NaPyruvate, NEAA, holo-transferrin (5 μg/ml), insulin (10 μg/ml), 3 μg/ml ARA-C, 2X MEM vitamins and penicillin/streptomycin.

**Isolation of neonatal rat ventricular cardiac myocytes.**

Myocytes were isolated from neonatal rat hearts (Sprague-Dawley, 1-day old) as previously described (231). Briefly, hearts were dissected and placed in $Ca^{2+}$/bicarbonate-free HEPES buffered Hank's solution (CBFHH, pH 7.5) with heparin (Sigma) and cut into 1-2 $mm^3$ portions. Pieces were washed and cells liberated by 10-16 digestions in CBFHH containing trypsin (0.15%) and DNase (20 ug/ml) at room temperature. Cells were pelleted through calf serum and washed in MEM containing 5% calf serum. Cells were pre-plated on Primaria 100 mm plates (Falcon) for 30-45 minutes to allow non-myocytes to adhere to the surface. Non-adherent cells (enriched for myocytes) were removed, counted, and plated overnight in MEM containing vitamin $B_{12}$ (20 ug/ml), 5% calf serum and BrdU (0.1 mM) to inhibit cell proliferation. The following day, cells were washed and placed in serum-free culture medium.

**RNase Protection for Ucn, CRH, CRH-R1 and CRH-R2.** Quantitation of CRH-R2 mRNA was perfomed as previously described (260). Briefly, total RNA was isolated from tissues or isolated ventricular cardiomyocytes using RNA STAT-60 according to manufacturer's protocol (Tel-Test, Inc., Friendswood, TX). Mouse CRH-R2 was detected with a 239 nt probe spanning TM3 and TM4. Mouse Ucn was detected with a 238 nt probe and CRH detected with a 142 nt probe, both of which span the precursor and

mature peptide coding regions. Rat CRH-R1 was detected with a 260 nt probe, and rat CRH-R2 was detected with a 352 nt probe. A 146 nt probe corresponding to rat GAPDH was used as a control for RNA loading. A 216 nt Rsa I fragment or 110 nt Dde I fragment of L3 cDNA, encoding a mouse ribosomal protein, was also used as a control for loading of RNA. 32P-UTP probes for CRH-R2 and mouse L3 were synthesized in vitro and hybridized to total RNA overnight. Reactions were digested with RNase A (1 mg/ml) and $T_1$ RNase (600 U/ml) and resolved on a 6% polyacrylamide gel. Gels were exposed to phosphorimage screens, developed and mRNAs were quantitated using the IP Lab Gel software package (Signal Analytics, Vienna, VA). All CRH-R2 band intensities were normalized to L3 band intensities from the same RNA sample.

**Stimulation of cAMP production in adult mouse ventricular cardiac myocytes.** Cardiomyocytes were plated into laminin coated 24-well Primaria tissue culture plates and cultured overnight at 37°C (5% $CO_2$). Cells were washed and incubated in serum-free DMEM for 90 min followed by 30 min incubation in serum-free DMEM containing 1mM IBMX (Sigma, St. Louis, MO). Myocytes were stimulated with graded concentrations of Ucn or CRH for 25 minutes in DMEM (1 mM IBMX). Medium was removed and cAMP was extracted in 95% EtOH/20 mM HCl overnight at -20°C. cAMP was quantitated using a commercially available cAMP RIA kit (Biomed Tech, Inc, Stoughton, MA)

**Hypertrophy of neonatal rat ventricular cardiac myocytes.** Cultured neonatal rat ventricular cardiomyocytes were transfected for 4 hours with pCMVb plasmid that contain a β-galactosidase gene under the control of a cytomegalovirus (CMV) promoter (Clonetech). Cells were washed and incubated for 48 hours in medium alone or medium containing Ucn or phenylephrine. Subsequently, cells were washed, lightly fixed and

stained overnight with β-galactosidase substrate (X-gal, Sigma). 2-dimensional area of cells was quantitated using video microscopy.

**Statistical analysis.** The differences in means of CRH-R2 mRNA in normal and hypertrophied ventricles was analyzed by Student's t-test.

**Results.**

We examined the expression of Ucn and CRH mRNA in adult mouse heart. Both Ucn and CRH mRNA are expressed in whole mouse heart (atria, ventricles, some aorta and pulmonary vessels) at levels comparable to those in whole mouse brain (**Figure Appendix 1A**). Removal of vena cava and aorta, and dissection of atria from ventricles demonstrates that CRH and Ucn mRNA are localized to the ventricles. The lower level of Ucn mRNA, relative to CRH mRNA, in the ventricles (**Figure Appendix 1B**) compared to that seen in whole heart (**Figure Appendix 1A**) may indicate that Ucn mRNA is also expressed in the vena cava and/or aorta, which were removed prior to dissection of the atria and ventricle, while CRH is predominantly localized to the ventricles. Alternatively, there could have been a greater difference in the specific activities of the Ucn and CRH probes. Additionally, the absence of Ucn and CRH mRNA in atria may be due to the lower amount of total RNA used as shown by the lighter L3 signal, a control for RNA loading.

We examined the regulation of CRH-R2 in the left and right ventricles of mice raised under normal atmospheric or hypoxic (11% $O_2$) conditions. Mice raised from birth under hypoxic conditions develop larger right ventricles compared to control mice (**Figure Appendix 2A**), whereas the wet weight of the left ventricle is not significantly effected by hypoxia (**Figure 2B**). It was not determined whether the increase in mass of the right ventricles of hypoxic mice was due more to hyperplastic myocyte expansion or cardiomyocyte hypertrophy. The levels of CRH-R2 mRNA in the enlarged right ventricles of mice raised for 16 days in a hypoxic environment was decreased (50% reduction) compared to normal controls (**Figure Appendix 3**). However, after hypoxic mice were housed in a normal atmospheric environment (21% $O_2$) for another 16 days (recovery), CRH-R2 mRNA levels in the enlarged right ventricle was similar to those in control right ventricles. In contrast, CRH-R2 levels in the left ventricle of normal and hypoxic mice, which do not display left ventricular hypertrophy, were similar. Downregulation of CRH-R2 mRNA in the hypertrophied right ventricle of mice exposed to hypoxic conditions

suggests that CRH-R2 may be a link between Ucn/CRH and the adaptive, hypertrophic response of the heart to increased afterload. Therefore, we examined the effect of Ucn on cardiomyocyte growth *in vitro*. We find that Ucn dose-dependently induces hypertrophy of isolated neonatal rat cardiomyocytes (**Figure Appendix 4**). Thus, it is possible that CRH-R2 mediates a hypertrophic effect of Ucn or CRH on the heart, and this contributes to the hypertrophy of the right ventricle during chronic hypoxia.

We have shown that adult mouse heart and ventricular cardiomyocytes express CRH-R2 mRNA, but we have found no molecular or functional evidence for expression of CRH-R1 in the mouse heart and cardiomyocytes. We examined the cardiac expression of CRH receptors in the rat, and we have found that CRH-R2 mRNA is also highly expressed in adult rat hearts and ventricular cardiomyocytes (**Figure Appendix 5**). However, we also detect a low level of CRH-R1 mRNA in adult rat ventricular cardiomyocytes and, to a lesser extent, adult rat heart. In addition, both CRH-R2 and CRH-R1 mRNAs are detectable in neonatal rat ventricular cardiomyocytes, but again the levels of CRH-R2 mRNA (in unstimulated myocytes) are greater than those of CRH-R1 (**Figure Appendix 6**). Thus, mice and rats display species differences in the expression of cardiac CRH receptors.

Because the function of the cardiac myocytes is tightly regulated by adrenergic agents produced by the adrenal glands and the sympathetic nervous system *in vivo*, we examined the effect of adrenergic stimulation on CRH receptor expression and function in isolated cardiac myocytes. We find that CRH-R1 and CRH-R2 expression in neonatal rat ventricular cardiomyocytes is induced by phenylephrine, an $\alpha_1$-adrenergic receptor agonist (**Figure Appendix 6**). Induction of CRH-R1 mRNA is rapid, peaking after 2 hours of phenylephrine stimulation, but decreasing despite continued (48 hrs) exposure of cells to the $\alpha_1$-adrenergic receptor agonist. In contrast, phenylephrine-induction of CRH-R2 mRNA levels is comparatively delayed, only being apparent after 48 hours of $\alpha_1$-adrenergic receptor stimulation. In addition, CRH receptors and $\alpha_1$-adrenergic receptors

synergistically mediate increases in intracellular cAMP in neonatal rat ventricular cardiomyocytes (**Figure Appendix 7**). Thus, adrenergic stimulation may enhance the response of the neonatal rat heart to Ucn or CRH; acute adrenergic stimulation may amplify the cAMP response of cardiac myocytes to CRH receptor stimulation, while chronic adrenergic stimulation may increase the expression of CRH receptors within the heart. Adult mouse cardiomyocytes may also display induction of CRH-R1 expression by phenylephrine and enhancement of the cAMP response to Ucn/CRH by co-stimulation with phenylephrine, but this remains to be tested. If adult mouse and neonatal rat cardiomyocytes are similar in this respect, this could indicate that the effect(s) of Ucn/CRH on the mouse heart is enhance by simultaneous, or even prior elevations in sympathetic catecholamine (e.g. norepinephrine, epinephrine) release.

**Figure Appendix 1.** Ucn and CRH are expressed in mouse heart. A) RNA from whole mouse brains and hearts were probed for Ucn and CRH mRNA by RNase protection. B) Mouse atria and ventricle were probed separately for Ucn and CRH mRNA by RNase protection. Atria and ventricles from two mice were examined (mouse #1 and mouse #2). Molecular weight markers are indicated on the left. Location of protected probes is indicated on the right. L3 was used as a control for RNA loading.

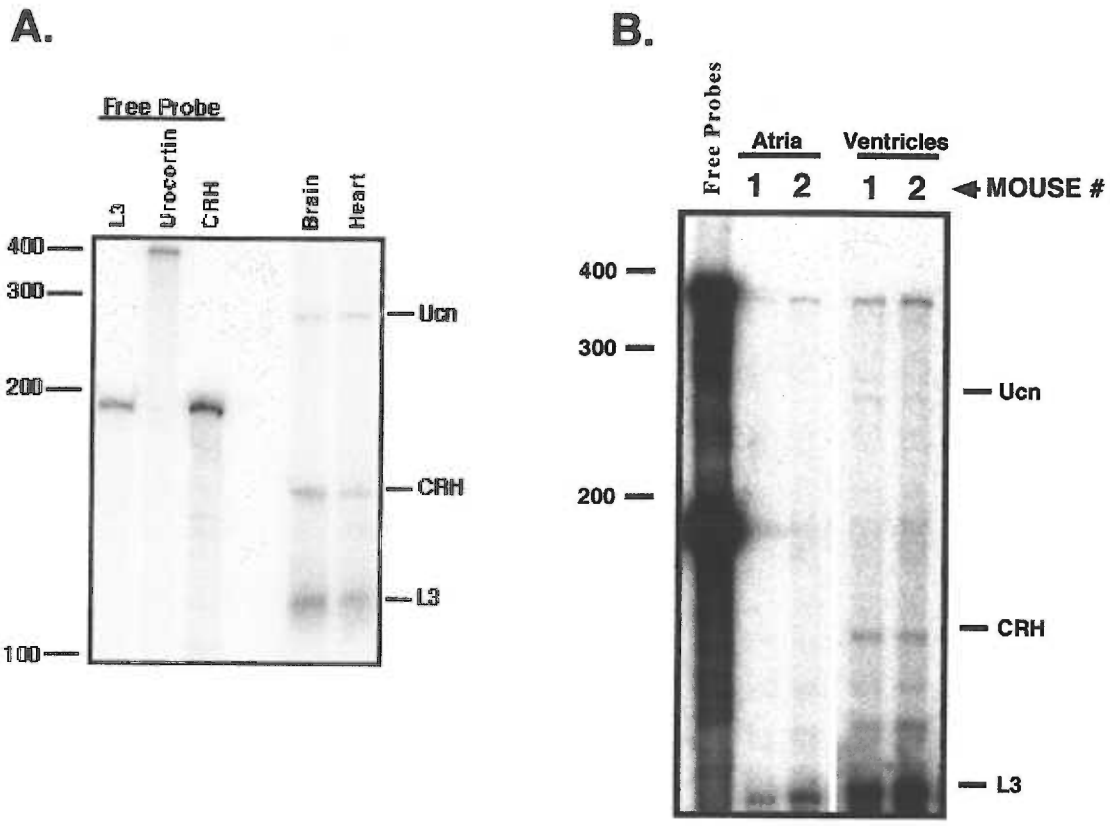
A.
Free Probe
L3
Urocortin
CRH
Brain
Heart
400
300
200
100
Ucn
CRH
L3
B.
Free Probes
Atria
Ventricles
1 2 1 2
MOUSE #
400
300
200
Ucn
CRH
L3

**Figure Appendix 2.** Hypoxia induces enlargement of the right ventricle in mice. LV+S, left ventricle plus septum; RV, right ventricle. A) Wet weights of dissected mouse right ventricles. Mice were allowed to develop in normoxic atmosphere (~21% $O_2$) or hypoxic (11% $O_2$) conditions for the first 16 days. All mice were raised under normal atmospheric conditions from days 17-32 (normoxic recovery). *$p<0.005$. B) Wet weights of dissected mouse left ventricles plus septum. All points represent the mean ±STDEV.

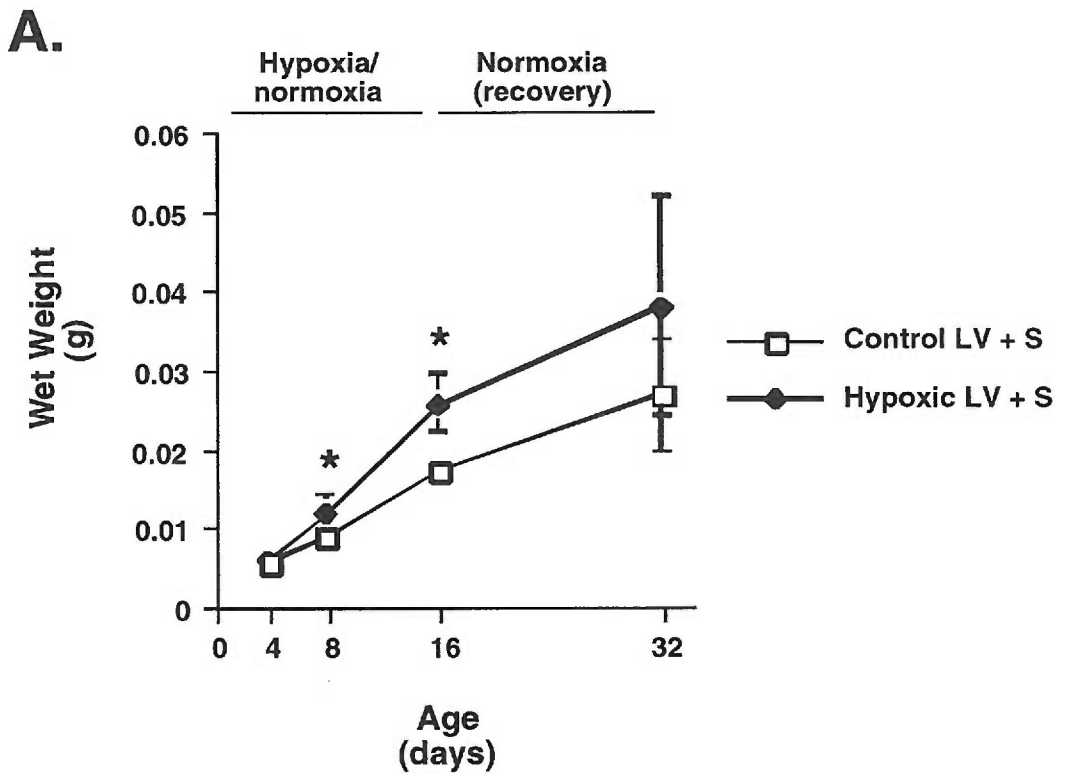
A.
Hypoxia/
normoxia
Normoxia
(recovery)
0.06
0.05
0.04
0.03
0.02
0.01
0
Wet Weight
(g)
*
*
0
4
8
16
32
Age
(days)
Control LV + S
Hypoxic LV + S

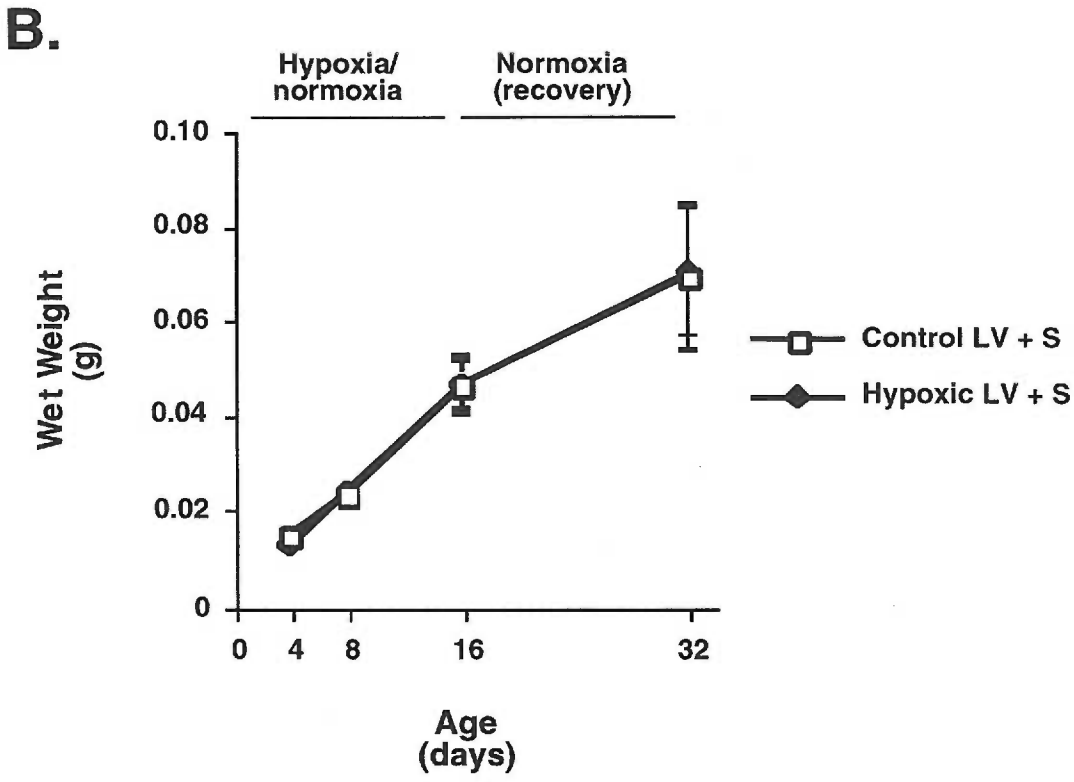
B.
Hypoxia/
normoxia
Normoxia
(recovery)
0.10
0.08
0.06
0.04
0.02
0
Wet Weight
(g)
0
4
8
16
32
Age
(days)
Control LV + S
Hypoxic LV + S

**Figure Appendix 3.** Hypoxia downregulates CRH-R2 mRNA in the right ventricle. LV+S, left ventricle plus septum; RV, right ventricle. A) CRH-R2 mRNA levels in whole mouse heart (day of birth) or left ventricle plus septum and right ventricle. Mice were allowed to develop in normal atmosphere (~21% $O_2$) or hypoxic (11% $O_2$) conditions for the first 16 days. All mice were raised under normal atmospheric conditions from days 17-32. CRH-R2 mRNA was quantitated by RNase protection and normalized to GAPDH, a control for RNA loading. *$p<0.001$ by Student's t-test. B) CRH-R2 mRNA levels in left ventricle plus septum or right ventricle of hypoxic mice, expressed as a percentage of normoxic controls.

A.

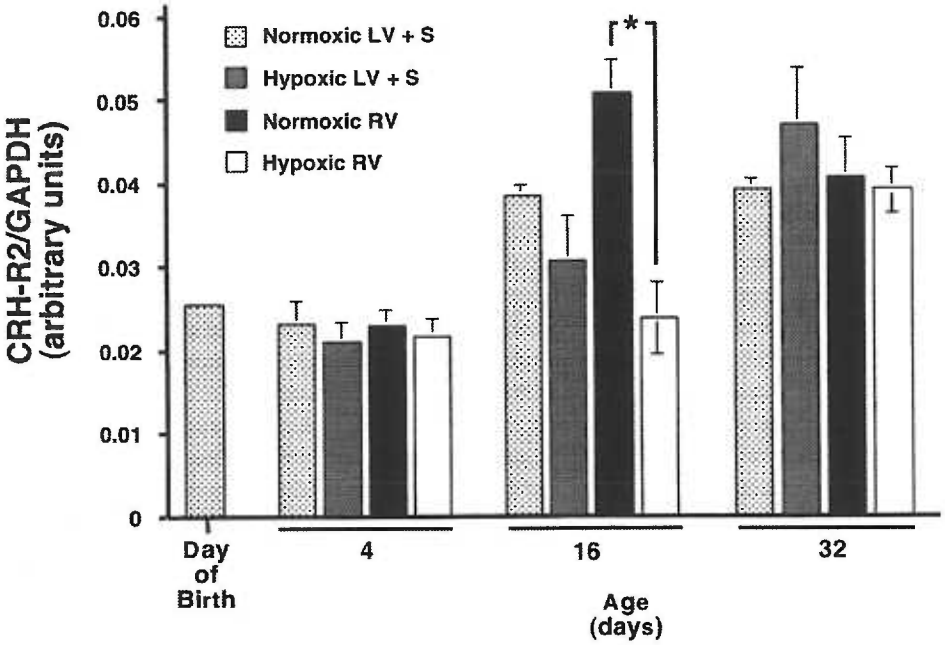
CRH-R2/GAPDH
(arbitrary units)
0.06
0.05
0.04
0.03
0.02
0.01
0
Normoxic LV + S
Hypoxic LV + S
Normoxic RV
Hypoxic RV
*
Day
of
Birth
4
16
32
Age
(days)

B.

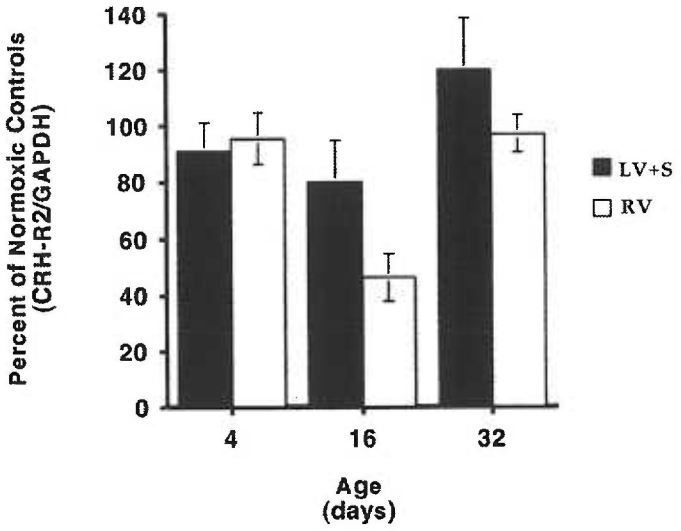
Percent of Normoxic Controls
(CRH-R2/GAPDH)
140
120
100
80
60
40
20
0
LV+S
RV
4
16
32
Age
(days)

**Figure Appendix 4.** Ucn induces hypertrophy of cultured neonatal rat cardiac mycoytes. Myocytes were cultured for 2 days in medium alone or medium containing $10^{-12}$ to $10^{-9}$ nM Ucn or $10^{-6}$ phenylephrine as a positive control. The 2-dimensional area of the myocytes was quantitated and expressed as the percent increase in area above medium-treated controls. *$p<0.001$ one-way ANOVA (Neuman-Keuls post-hoc) media control vs Ucn treated.

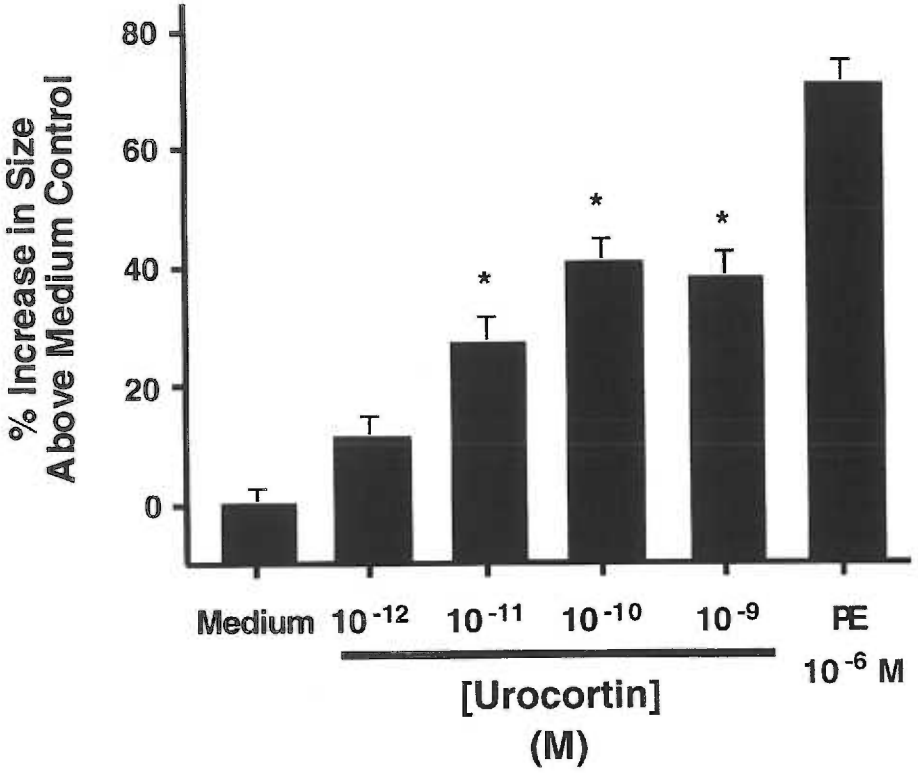
% Increase in Size
Above Medium Control
80
60
40
20
0
*
*
*
Medium
10-12
10-11
10-10
10-9
PE
10-6 M
[Urocortin]
(M)

**Figure Appendix 5.** CRH-R2 mRNA is highly expressed in adult rat ventricular cardiac myocytes. CRH-R2 and CRH-R1 mRNA levels were measured in whole rat heart and brain by RNase protection. L3 was used as a control for RNA loading.

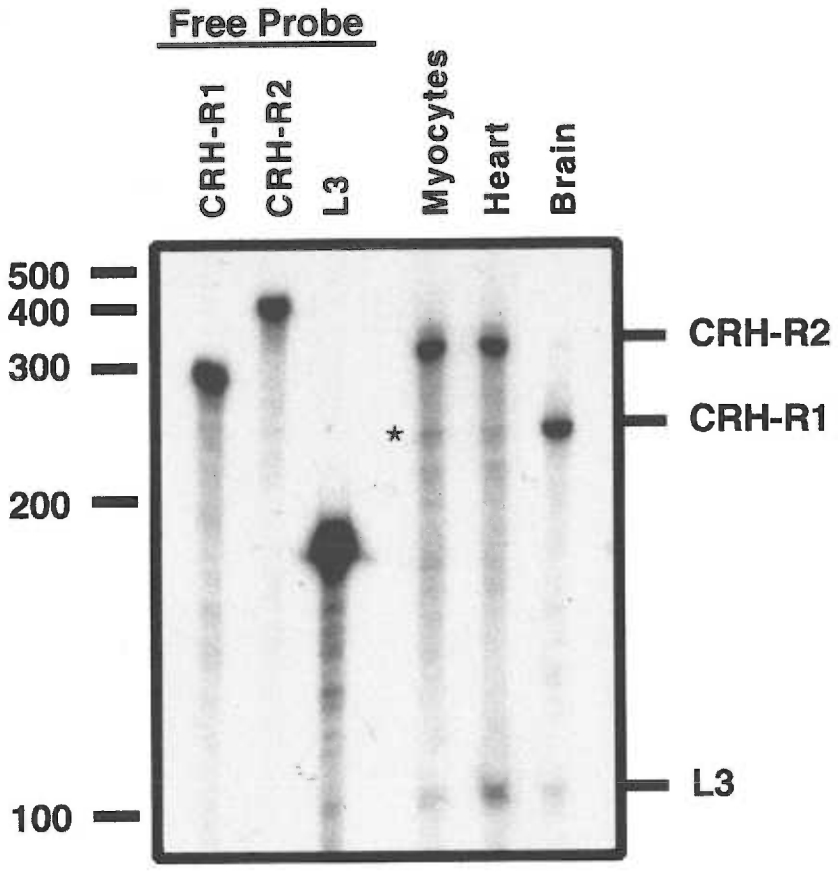


***Note detectable expression of CRH-R1 mRNA in cardiac myocytes and, to a lesser extent, whole heart**

**Figure Appendix 6.** Expression of CRH-R1 and CRH-R2 in neonatal rat cardiac myocytes, and their differential regulation by $\alpha_1$-adrenergic stimulation. RNase protection of CRH-R1 and CRH-R2 in adult rat brain, heart, untreated neonatal rat cardiomyocytes, and cardiomyocytes incubated with phenylephrine, an $\alpha_1$-adrenergic agonist, for 2, 24 or 48 hours. L3 was used as a control for RNA loading.

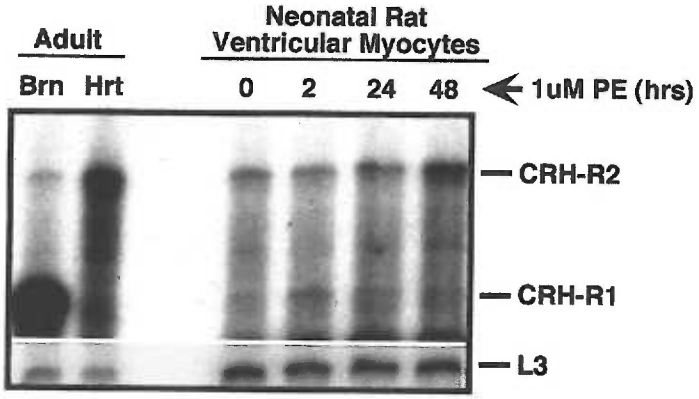
Adult
Neonatal Rat
Ventricular Myocytes
Brn Hrt
0 2 24 48
1uM PE (hrs)
CRH-R2
CRH-R1
L3

**Figure Appendix 7.** Phenylephrine enhances Ucn-stimulated increases in cAMP in neonatal rat cardiac myocytes. Myocytes were incubated with increasing doses of Ucn in the presence or absence of phenylephrine, an $\alpha_1$-adrenergic receptor agonist. A) Dose-dependent effect of Ucn on intracellular cAMP. B) Alternate presentation of the synergistic effect of Ucn and phenylephrine on intracellular cAMP levels in neonatal rat cardiac myocytes.

A.

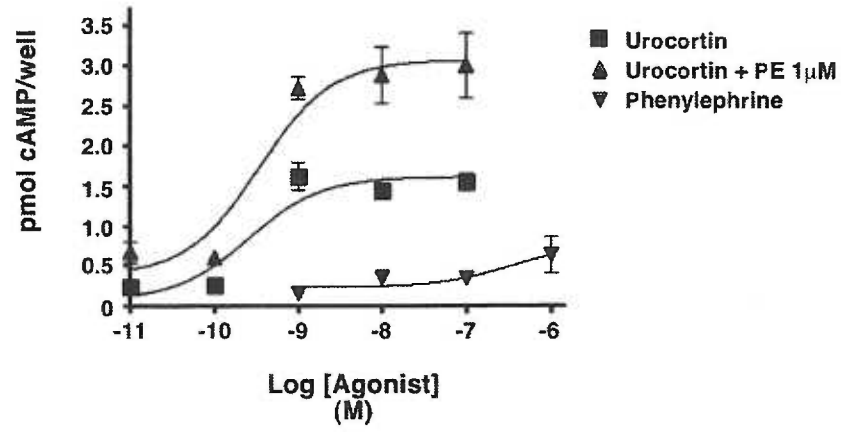
pmol cAMP/well
3.5
3.0
2.5
2.0
1.5
1.0
0.5
0
-11
-10
-9
-8
-7
-6
Log [Agonist]
(M)
Urocortin
Urocortin + PE 1μM
Phenylephrine

B.

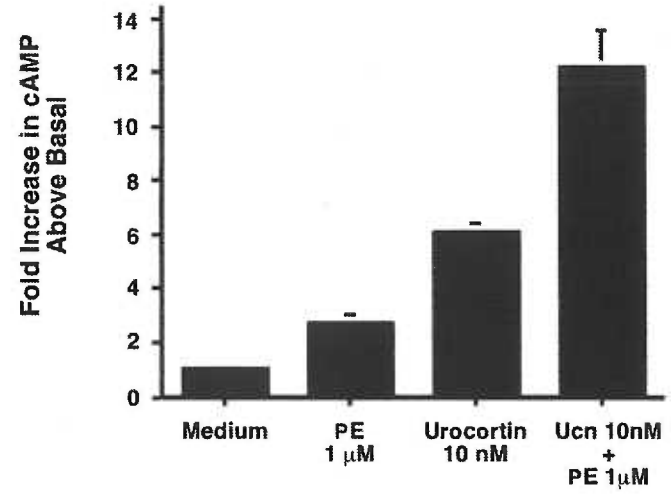
Fold Increase in cAMP
Above Basal
14
12
10
8
6
4
2
0
Medium
PE
1 μM
Urocortin
10 nM
Ucn 10nM
+
PE 1μM

# Chapter 6

# Summary and Conclusions

## Summary and Conclusions

We have shown that primary adult mouse ventricular cardiac myocytes express CRH-R2. We detected CRH-R2 mRNA in cardiomyocyte-enriched cultures by RNase protection and in individually isolated mouse cardiac myocytes by RT-PCR. So far, we have only detected CRH-R2 in adult mouse ventricular cardiomyocytes; CRH-R1 mRNA is undetectable in neonatal mouse hearts, adult mouse hearts, and adult mouse cardiomyocytes by RNase protection. We have shown that CRH-R2 in mouse cardiomyocytes mediates Ucn and CRH-induced increases in intracellular cAMP. Cardiomyocytes isolated from the hearts of adult *Crh2*$^{-/-}$ mice do not show elevated intracellular cAMP levels in response to Ucn or CRH stimulation. Thus, cardiomyocyte expression of CRH-R2 provides a mechanism for the direct influence of Ucn or CRH on the function of the heart.

Our findings in adult mouse ventricular cardiomyocytes are complemented by our findings using rat (neonatal and adult) cardiac myocytes and the atrial myocyte tumor cell lineage, AT-1, all of which express CRH-R2. It is important, however, that although cardiomyocytes express functional CRH-R2 in rodent myocardium, we cannot rule out expression of CRH-R2 by other cell types within the heart. The vasodilatory actions of Ucn and CRH in mammals *in vivo* and in isolated rat hearts *ex vivo* strongly implicates vascular endothelial cells and/or smooth muscle cells as targets of Ucn/CRH actions. Furthermore, *in situ* hybridization studies done by others have shown a perivascular pattern of CRH-R2 mRNA in arterioles in the heart and the brain. Changes in blood flow through the coronary vasculature are intimately linked to changes in cardiac contractile function. Thus, a clear understanding of the role of Ucn, CRH, and CRH-R2 in the heart requires the identification of other cardiac cell types that express CRH-R2 and mediate the vascular effects of Ucn and CRH.

Neonatal rat cardiac myocytes currently represent a unique system of CRH receptor expression and function in mammals. Specifically, we have shown that neonatal rat ventricular cardiomyocytes express both CRH-R1 and CRH-R2 mRNAs. Neonatal rat cardiomyocytes also do not show the pharmacological profile characteristic of CRH-R2 (Ucn >> CRH). In addition, we have found that CRH-R1 and CRH-R2 are differentially regulated by $\alpha_1$-adrenergic receptor stimulation. Incubation of cultured neonatal rat cardiomyocytes with phenylephrine causes a rapid upregulation of CRH-R1 mRNA (2 hours), but CRH-R1 expression progressively decreases to basal levels by 48 hours despite continuous stimulation. In contrast, phenylephrine stimulated upregulation of CRH-R2 mRNA levels only after 48 hours of incubation of neonatal cardiomyocytes with phenylephrine. Intriguingly, we found that phenylephrine and Ucn act in synergy to stimulate cAMP production in neonatal rat cardiomyocytes. It is possible that our findings in the neonatal rat may be representative of CRH receptor expression and function in cardiomyocytes from mouse, and possibly other species.

The induction of CRH receptor expression and enhancement of CRH receptor signaling by $\alpha_1$-adrenergic receptors has several implications. First, adrenergic stimulation may also induce CRH-R1 expression in other types of cardiac myocytes, including those from mice, adult rats and possibly humans. Second, CRH-R1 and CRH-R2 may not have redundant functions in neonatal rat cardiomyocytes, and CRH-R1 may play an important role in early function or development of the neonatal heart as compared to adult hearts. It is possible that CRH-R1 and -R2 are linked to different signaling pathways in neonatal cardiac myocytes, or they may heterodimerize in these cells to produce a mode of receptor binding, signaling, and regulation different from CRH-R1 or -R2 alone. Third, $\alpha_1$-adrenergic receptors are known to be coupled to $G\alpha_i$, a negative regulator of adenylyl cyclase and cAMP production. However, we found that high levels of phenylephrine alone caused elevations of intracellular cAMP, and phenylephrine and Ucn synergized to increase intracellular cAMP levels. Thus, $\alpha_1$-adrenergic receptors may also couple to $G\alpha_s$ in

neonatal rat cardiomyocytes, and they may interact with CRH receptors to enhance their coupling to adenylyl cyclase signaling. Finally, the positive interaction between CRH and adrenergic pathways that we have observed in neonatal cardiomyocytes contrasts with the antagonistic effect of urotensin I, likely through CRH-R2, on $\alpha_1$-adrenergic receptor-induced vasoconstriction of rat mesenteric vessels demonstrated by others (130). Thus, adrenergic and CRH receptor interactions may be cell-type specific, and this specificity may be the molecular basis for the ability of Ucn or CRH to enhance cardiac function while effectively dilating mesenteric arteries.

We have been able to detect Ucn and CRH mRNA expression in the mouse heart, raising the intriguing possibility that Ucn or CRH act in an autocrine/paracrine manner within the heart to stimulate cardiomyocytes. Specifically, using RNase protection we detected Ucn and CRH mRNA in mouse ventricles but not atria. In the rat, intracardiac ganglion cells are in the S-A node, which is located where the right atrium borders the wall of the superior vena cava, and the A-V node, which is in the wall of the right atrium just dorsal of the atrioventricular valve. Thus, our findings suggest that intracardiac ganglia do not express Ucn or CRH. Instead, ventricular cardiomyocytes, fibroblasts, endothelial, or smooth muscle cells may express Ucn or CRH. However, the cellular origin of Ucn and CRH peptides within the entire mouse heart should be examined using specific antibodies to verify the identity of Ucn- or CRH-positive cardiac cells. In addition, because CRH-like immunoreactivity has been found in sympathetic ganglia, including the stellate, the presence of Ucn or CRH mRNA and peptides in sympathetic chain ganglia supplying the heart should be investigated.

We have shown that CRH-R2 in mice mediates the systemic effects of Ucn on the cardiovascular system. Ucn reduces mean arterial pressure in wild-type but not *Crh2*$^{-/-}$ mice. Furthermore, Ucn increases the velocity of left ventricular contraction ($Vcf_c$) in wild-type but not *Crh2*$^{-/-}$ mice. It is known that increased intracellular levels of cAMP cause an increase in cardiomyocyte contractility, or force of contraction, and that CRH-R2 mediates

the stimulation of intracellular cAMP in mouse cardiomyocytes by Ucn *in vitro*. Thus, we hypothesize that the increase in velocity of left ventricular contraction is a direct effect of Ucn on the myocardium. This hypothesis is further supported by the work of others, which shows that CRH increased the contractile function of perfused rat hearts and isolated myocardial tissue from guinea pigs. In addition, Ucn (i.v.) increases maximal aortic flow, the peak rate of increase in aortic flow (dF/dt), and cardiac output in the conscious sheep (273). Importantly, in the sheep model, Ucn is not a potent vasodilator because mean arterial pressure was increased with the increase in aortic flow. Thus, in sheep, increased contractile function is not due to changes in afterload. Yet in mice, Ucn causes marked hypotension, and the index of cardiac function that we quantitated, $Vcf_c$, is not independent of changes in blood pressure. Thus, in our experiments, we cannot separate a direct action of Ucn on the mouse heart from the effect of Ucn on arterial pressure. Future experiments to quantitate cardiac function in the mouse would need to employ a method that is independent of changes in preload and afterload, such as pressure-volume relationships. Because such studies are difficult to perform, the effect of Ucn on contractile function of the heart may be more easily investigated using an *in vitro* system of isolated, beating cardiomyocytes.

To address whether CRH-R2 may participate in regulating cardiac function during stress, we studied the regulation of CRH-R2 expression in the heart by inflammation and hypoxia. We found that bacterial endotoxin-induced inflammation significantly decreases CRH-R2 mRNA levels in the mouse heart, and this effect partially depends on TNFα. Exogenous TNFα or IL-1α also significantly downregulate CRH-R2 mRNA levels in the heart. In addition, chronic hypoxia, which brings about pulmonary hypertension and increased afterload on the right ventricle, caused a decrease in steady state CRH-R2 mRNA levels in the right but not left ventricle. Importantly, decreased expression of CRH-R2 mRNA in the heart is reversible. Between 9 and 24 hours after injection of endotoxin, CRH-R2 mRNA levels in the heart return to near baseline levels. Furthermore, CRH-R2

mRNA in the right ventricles of mice exposed to 16 days of hypoxia returns to control levels after 16 days of recovery in normoxic conditions. Thus, expression of CRH-R2 in the mouse heart is reversibly downregulated by cardiovascular stressors, including inflammation and pulmonary hypertension.

We investigated the regulation of CRH-R2 mRNA in mouse skeletal muscle by endotoxin to determine whether downregulation of CRH-R2 expression in peripheral tissues is a general effect of inflammation. The variable regulation of CRH-R2 mRNA in the skeletal muscle by inflammation and inflammatory mediators indicates that regulation of CRH-R2 expression is tissue specific. Importantly, the downregulation of CRH-R2 in skeletal muscle by TNFα but not IL-1α parallels the differential effects of these cytokines on skeletal muscle catabolism. TNFα is an effective inducer of protein degradation in skeletal muscle while, in most studies, IL-1α is not. The upregulation of CRH-R2 in skeletal muscle by endotoxin indicates that control of CRH-R2 expression in skeletal muscle is likely dependent on the relative abundance of many factors induced during inflammation.

In addition to directly inducing vasodilation and depressing cardiomyocyte contractile function, endotoxin, TNFα, and IL-1α are potent activators of the HPA axis. However, we do not detect significant effects of dexamethasone, a glucocorticoid receptor type I and II agonist, on CRH-R2 expression in the heart. Furthermore, we did not find significant downregulation of cardiac CRH-R2 mRNA at various time points following a 90-minute restraint stress. Therefore, we hypothesize that CRH-R2 mRNA in the mouse heart is specifically downregulated by cardiovascular stressors, including inflammation and changes in afterload, but not simply by cognitive stressors or activators of the HPA axis. However, it is possible that CRH-R2 mRNA levels were significantly altered during the restraint stress, and returned to near pre-stress levels after 90 minutes. In addition, systemic ACTH has effects on the cardiovascular system, including decreasing blood

pressure and increasing heart rate, and we cannot rule out a role for ACTH in the regulation of CRH-R2 in the heart.

To identify direct mediators of CRH-R2 downregulation in cardiac cells, we studied the regulation of CRH-R2 mRNA in isolated cardiac myocytes. The peak decrease of CRH-R2 mRNA in mouse heart *in vivo* was observed 9 hours following injection of endotoxin or cytokines. Our studies failed to demonstrate downregulation of CRH-R2 mRNA in cardiac myocytes following a 9-hour incubation with low or high levels of TNFα, IL-1α, or IL-6. However, we do find that incubation of cardiomyocytes with Ucn results in a dose-dependent downregulation of CRH-R2 mRNA levels. Thus, similar to pituitary CRH-R1 and several other GPCRs, CRH-R2 expressed by cardiomyocytes is subject to ligand-induced, homologous downregulation at the level of mRNA accumulation. More importantly, our *in vitro* findings suggest that Ucn instead of cytokines may directly downregulate CRH-R2 expression in cardiac myocytes *in vivo*.

A model of how CRH-R2 may be regulated in the heart emerges from the findings described above (**Fig. 6.1**). Cytokines such as TNFα or IL-1 increase Ucn or CRH release into the heart, and Ucn/CRH increases the contractile function (positive inotropism) of the heart via CRH-R2-mediated effects on cardiac myocytes. This CRH-R2 mediated stimulation opposes the direct depressive effects (negative inotropism) of cytokines on the myocardium. However, prolonged exposure to agonist leads to downregulation of CRH-R2 in cardiac myocytes at the level of mRNA accumulation. As a result, the mouse heart is less able to respond to further Ucn or CRH stimulation, and this contributes to depressed cardiac function observed late in sepsis syndrome.

The vasodilatory effects of cytokines leads to hypotension and eventually decreased perfusion of peripheral organs. Cytokines and hypotension also activate the central nervous system via vagal afferents, resulting in increased autonomic outflow to the heart to accommodate the increased demand caused by hypotension. Since CRH-like peptides are found throughout the sympathetic nervous system, we propose that Ucn or CRH are a

component of the increased autonomic outflow to the heart during sepsis. Furthermore, because Ucn and CRH mRNA are detectable in the heart itself, cytokines or hypotension may stimulate intracardiac cells to release CRH peptides, which stimulate cardiac myocytes in an autocrine/paracrine manner.

Hypoxia and pulmonary hypertension also increase the demand on the heart, particularly the right ventricle. We propose that downregulation of CRH-R2 in the right ventricle of hypoxic mice also reflects increased Ucn or CRH stimulation of the right ventricle and eventual agonist-induced downregulation of CRH-R2 at the level of mRNA accumulation. Moreover, based on our finding that Ucn induces hypertrophy of cultured neonatal cardiac myocytes, it is possible that Ucn or CRH acting through CRH receptors contribute to hypertrophy of the right ventricle in the aforementioned model of hypoxia. Recovery of CRH-R2 expression in the right ventricle after 16 days of normoxia may then result from decreased release of Ucn or CRH into the right ventricle.

Our findings implicate CRH-R2 in the control of the heart during stress. Further experiments are required to strengthen the physiological connection between CRH-R2 and regulation of heart function proposed here. The contribution of CRH-R2 to changes in heart function *in vivo*, the location(s) of Ucn/CRH production in the heart, and how Ucn/CRH release is regulated during stress remain to be elucidated. Our *in vitro* model of CRH-R2 in ventricular cardiac myocytes will enable future studies investigating the molecular and cellular effects of CRH-R2 on the myocardium, the functional interaction(s) of CRH-R2 and adrenergic receptor-mediated signaling pathways, and the mechanism(s) of CRH receptor regulation in cardiac myocytes. Our characterization of the function of CRH-R2 in the mouse heart contributes to the rapidly growing research focus on mechanisms of heart disease, which are being facilitated by the adaptation of sensitive methods for measuring cardiac function in the mouse and creation of genetic models of cardiovascular dysfunction, including *Crh2*$^{-/-}$ mice. Ultimately, the clinical relevance of our findings in the mouse model needs to be tested by comparing CRH-R2 expression in hearts of normal,

septic, and hypertensive humans. Such studies will add to our understanding of the roles of Ucn and CRH in normal cardiac physiology and the pathogenesis of cardiovascular disease.

## Coda.

Our discovery and characterization of CRH-R2 expression and function in mouse cardiac myocytes defines a direct pathway for actions of the stress-responsive neurohormones, Ucn and CRH on the mammalian myocardium. CRH, Ucn, and their cognate receptors, CRH-R1 and CRH-R2, in the central nervous system have been implicated in regulating stress in mammals; they have been shown to regulate adaptive neuroendocrine, autonomic and behavioral responses to adverse stimuli. Our findings suggest that CRH-R2 and its ligands also play a direct role in the adaptive responses of the heart to unfavorable conditions. Furthermore, regulation of CRH-R2 mRNA in the heart is an important molecular link between two forms of cardiovascular stress: inflammation and hypoxia-induced pulmonary hypertension. Therefore, clarification of the roles of CRH-R2, Ucn and CRH in the regulation of the mammalian heart will contribute significantly to our understanding of how heart function is regulated during stress, and thereby lead to new strategies for the treatment of cardiovascular dysfunction.

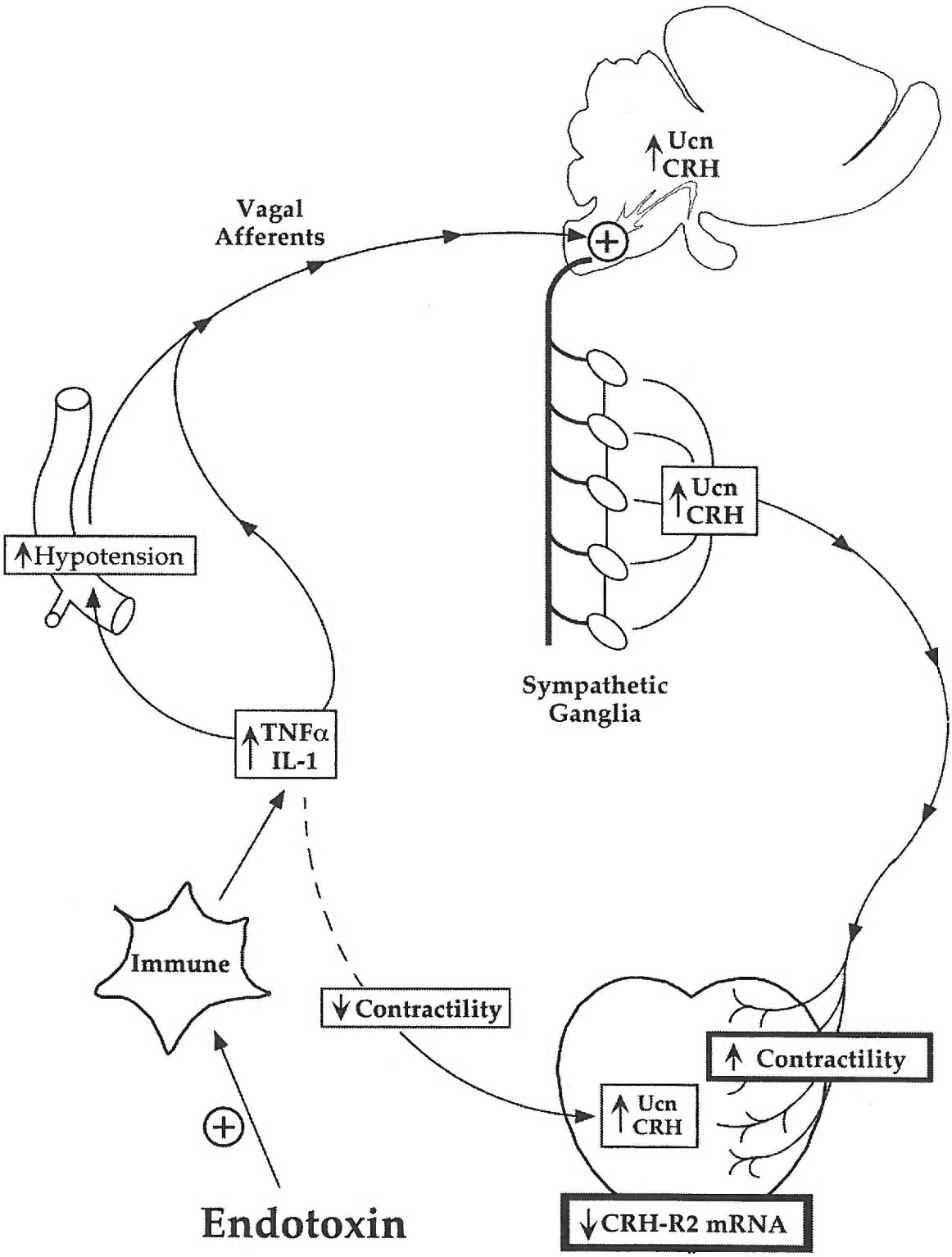


**Figure 6.1.** Model of CRH-R2 regulation in the heart *in vivo*.

## Literature cited


1. **Vale, W., J. Speiss, C. Rivier, and J. Rivier.** 1981. Characterization of a 41-residue ovine hypothalamic peptide that stimulates secretion of corticotropin and β-endorphin. *Science 213:1394-1397.*

2. **Oddis, C., and M. Finkel.** 1997. Cytokines and nitric oxide synthase inhibitor as mediator of adrenergic refractoriness in cardiac myocytes. *Eur J Pharmacol 320:167-174.*

3. **Morley, S. D., C. Schonrock, D. Richter, Y. Okawara, and K. Lederis.** 1991. Corticotropin-releasing factor (CRF) gene family in the brain of the teleost fish Catastomus commersoni (white sucker): molecular analysis predicts distinct precursors for two CRFs and one urotensin I peptide. *Molecular Marine Biology and Biotechnology 1:48-57.*

4. **Stenzel-Poore, M. P., K. A. Heldwein, P. Stenzel, S. Lee, and W. W. Vale.** 1992. Characterization of the genomic corticotropin-releasing factor (CRF) gene from *Xenopus laevis*: two members of the CRF family exist in amphibians. *Mol. Endocrinol. 6:1716-1724.*

5. **Rivier, C., J. Rivier, and W. Vale.** 1982. Inhibition of adrenocorticotropic hormone secretion in the rat by immunoneutralization of corticotropin-releasing factor. *Science 218:377-379.*

6. **Rivier, J., C. Rivier, and W. Vale.** 1984. Synthetic competitive antagonists of corticotropin-releasing factor: effect on ACTH secretion in the rat. *Science 224:889-891.*

7. **Venihaki, M., and J. Majzoub.** 1999. Animal models of CRH deficiency. *Front Neuroendocrinol 20:122-145.*

8. **Timpl, P., R. Spanagel, I. Sillaber, A. Kresse, J. M. Reul, G. K. Stalla, V. Blanquet, T. Steckler, F. Holsboer, and W. Wurst.** 1998. Impaired stress response and reduced anxiety in mice lacking a functional corticotropin-releasing hormone receptor. *Nature Genetics 19:162-6.*

9. **Smith, G. W., J. M. Aubry, F. Dellu, A. Contarino, L. M. Bilezikjian, L. H. Gold, R. Chen, Y. Marchuk, C. Hauser, C. A. Bentley, P. E. Sawchenko, G. F. Koob, W. Vale, and K. F. Lee.** 1998. Corticotropin releasing factor receptor 1-deficient mice display decreased anxiety, impaired stress response, and aberrant neuroendocrine development. *Neuron 20:1093-102.*

10. **Montecucchi, P., A. Henschen, and V. Erspamer.** 1979. Structure of sauvagine, a vasoactive peptide from the skin of a frog. *Gesellsch Biol Chem 360:1178.*

11. **MacCannell, K., and K. Lederis.** 1977. Dilation of the mesenteric vascular bed of the dog produced by a peptide, urotensin I. *J Phar and Exp Ther 203:38-46.*

12. **Lederis, K., and M. Medakovic.** 1974. Pharmacological observations on the hypotensive action of extracts of teleost fish urophyses (urotensin I) in the rat. *Brit J Pharmacol 51:315-324.*

13. **Lederis, K., A. Letter, D. McMaster, T. Ichikawa, K. MacCannell, Y. Kobayashi, J. Rivier, W. Vale, and J. Fryer.** 1983. Isolation, analysis of structure, synthesis, and biological actions of urotensin I neuropeptides. *Can J Biochem Cell Biol 61:602-614.*

14. **Donaldson, C., S. Sutton, M. Perrin, A. Corrigan, K. Lewis, J. Rivier, J. Vaughan, and W. Vale.** 1996. Cloning and characterization of human urocortin. *Endocrinology 137:2167-2170.*

15. **Vaughan, J., C. Donaldson, K. Lewis, S. Sutton, R. Chan, A. V. Turnbull, D. Lovejoy, C. Rivier, J. Rivier, P. E. Sawchenko, and W. Vale.** 1995. Urocortin, a mammalian neuropeptide related to fish urotensin I and to corticotropin-releasing factor. *Nature 378:287-292.*

16. **Thompson, R. C., A. F. Seasholtz, and E. Herbert.** 1987. Rat corticotropin-releasing hormone gene: sequence and tissue-specific expression. *Molecular Endocrinology 1:363-370.*

17. **Zhao, L., C. J. Donaldson, G. W. Smith, and W. W. Vale.** 1998. The structures of the mouse and human urocortin genes (Ucn and UCN). *Genomics 50:23-33.*

18. **Brar, B., T. Sanderson, N. Wang, and P. Lowry.** 1997. Post-translational processing of human procorticotropin-releasing factor in transfected mouse neuroblastoma and chinese hamster ovary cell lines. *J Endocrinol 154:431-440.*

19. **Dong, W., B. Seidel, M. Marcinkiewicz, M. Chretien, N. Seidah, and R. Day.** 1997. Cellular localization of the prohormone convertases in the hypothalamic paraventricular and supraoptic nuclei: selective regulation of PC1 in corticotrophin-releasing hormone parvocellular neurons mediated by glucocorticoids. *J Neurosci 17:563-575.*

20. **Fricker, L., and S. Snyder.** 1982. Enkephalin convertase: purification and characterization of a specific enkephalin-synthesizing carboxypeptidase localized to adrenal chromaffin granules. *Proc Natl Acad Sci USA 79:3886-3890.*

21. **Eipper, B. A., B. T. Bloomquist, E. J. Husten, S. L. Milgram, and R. E. Mains.** 1993. Peptidylglycine alpha-amidating monooxygenase and other processing enzymes in the neurointermediate pituitary. *Annals of the New York Academy of Sciences 1993 May 31;680:147-60.*

22. **Giraud, P., J. Maltese, F. Boudouresque, P. Salers, L. Ouafik, M. Renard, F. Pelen, and C. Oliver.** 1992. Peptidylglycine alpha-amidating monooxygenase activity and TRH and CRF biosynthesis: role of copper. *32.*

23. **Palkovits, M., M. Brownstein, and W. Vale.** 1985. Distribution of corticotropin-releasing factor in rat brain. *Fed Proc 44:215-219.*

24. **Morin, S., N. Ling, X. Liu, S. Kahl, and D. Gehlert.** 1999. Differential distribution of urocortin- and corticotropin-releasing factor-like immunoreactivities in the rat brain. *Neuroscience 92:281-291.*

25. **Muglia, L. J., N. A. Jenkins, D. J. Gilbert, N. G. Copeland, and J. A. Majzoub.** 1994. Expression of the mouse corticotropin-releasing hormone gene in vivo and targeted inactivation in embryonic stem cells. *J. Clin. Invest. 93:2066-2072.*

26. **Brouxhon, S., A. Prasad, S. Joseph, D. Felten, and D. Bellinger.** 1998. Localization of corticotropin-releasing factor in primary and secondary lymphoid organs of the rat. *Brain Behav Immun 12:107-122.*

27. **Crofford, L. J., H. Sano, K. Karalis, E. L. Webster, E. A. Goldmuntz, G. P. Chrousos, and R. L. Wilder.** 1992. Local secretion of corticotropin-releasing hormone in the joints of Lewis rats with inflammatory arthritis. *Journal of Clinical Investigation 90:2555 - 2564.*

28. **Bittencourt, J. C., J. Vaughan, C. Arias, R. A. Rissman, W. W. Vale, and P. E. Sawchenko.** 1999. Urocortin expression in rat brain: evidence against a pervasive relationship of urocortin-containing projections with targets bearing type 2 CRF receptors. *J. Comp. Neurol. 415:285-312.*

29. **Tunrbull, A., J. Vaughan, J. Rivier, W. Vale, and C. Rivier.** 1999. Urocortin is not a significant regulator of intermittent electrofootshock-induced adrenocorticotropin secretion in the intact male rat. *Endocrinology 140:71-78.*

30. **Aguilera, G.** 1994. Regulation of pituitary ACTH secretion during chronic stress. *Front Neuroendocrinol 15:321-350.*

31. **Li, Y., and R. Dampney.** 1994. Expression of fos-like protein in brain following sustained hypertension and hypotension in conscious rabbits. *Neuroscience 61:613-634.*

32. **Potts, P., J. Ludbrook, T. Gillman-Gaspari, J. Horiuchi, and R. Dampney.** 2000. Activation of brain neurons following central hypervolaemia and hypovolaemia: contribution of baroreceptor and non-baroreceptor inputs. *Neuroscience 95:499-511.*

33. **Kageyama, K., M. Bradbury, L. Zhao, A. Blount, and W. Vale.** 1999. Urocortin messenger ribonucleic acid: tissue distribution in the rat and regulation in thymus by lipopolysaccharide and glucocorticoids. *Endocrinology 140:5651-5658.*

34. **Weninger, S., L. Peters, and J. Majzoub.** 2000. Urocortin expression in the Edinger-Westphal nucleus is up-regulated by stress and corticotropin-releasing hormone deficiency. *Endocrinology 141:256-263.*

35. **Karalis, K., H. Sano, J. Redwine, S. Listwak, R. wilder, and G. Chrousos.** 1991. Autocrine or paracrine inflammatory actions of corticotropin-releasing hormone in vivo. *Science 254:421-423.*

36. **Kavelaars, A., R. E. Ballieux, and C. J. Heijnen.** 1989. The role of IL-1 in the corticotropin-releasing factor and arginine-vasopressin-induced secretion of immunoreactive β-endorphin by human peripheral blood mononuclear cells. *J. Immunol. 142:2338-2342.*

37. **Angioni, S., F. Petraglia, A. Gallinelli, A. Cossarizza, C. Franceschi, M. Muscettola, A. genazzani, N. Surico, and A. Genazzani.** 1993. Corticotropin-releasing hormone modulates cytokine release in cultured human peripheral blood mononuclear cells. *Life Sci 53:1735-1742.*

38. **Genedani, S., M. Bernardi, M. Baldini, and A. Bertolini.** 1992. Influence of CRH and a-MSH on the migration of human monocytes in vitro. *Neuropeptides 23:99-102.*

39. **Singh, V. K., and S. C. Leu.** 1990. Enhancing effect of corticotropin-releasing factor on the production of interleukin-1 and interleukin-2. *Neurosci. Lett. 120:151-154.*

40. **Theoharides, T., L. Singh, W. Boucher, X. Pang, R. Letourneau, E. Webster, and G. Chrousos.** 1998. Corticotropin-releasing hromone induces skin mast cell degranulation and increased vascular permeability, a possible explanation for its proinflammatory effects. *Endocrinology 139:403-413.*

41. **Webster, E., D. Lewis, D. Torpy, E. Zachman, K. Rice, and G. Chrousos.** 1996. In vivo characterization of antalarmin, a nonpeptide corticotropin-releasing hromone (CRH) receptor antagonist: suppression of pituitary ACTH release and peripheral inflammation. *Endocrinology 137:5747-5750.*

42. **Wei, E. T., S. Serda, and J. Q. Tian.** 1988. Protective actions of corticotrophin-releasing factor on thermal injury to rat pawskin. *Journal of Pharmacology and Experimental Therapeutics 247:1082-1085.*

43. **Karalis, K., H. Sano, J. Redwine, S. Listwak, R. L. Wilder, and G. P. Chrousos.** 1991. Autocrine or paracrine inflammatory actions of corticotrophin-releasing hormone in vivo. *Science 254:421-423.*

44. **Torpy, D., E. Webster, E. Zachman, G. Aguilera, and G. Chrousos.** 1999. Urocortin and inflammation: confounding effects of hypotension on measures of inflammation. *Neuroimmunomodulation 6:182-186.*

45. **Stenzel, P., R. Kesterson, W. Yeung, R. D. Cone, M. B. Rittenberg, and M. P. Stenzel-Poore.** 1995. Identification of a novel murine receptor for corticotropin-releasing hormone expressed in the heart. *Molecular Endocrinology 9:637-645.*

46. **Perrin, M. H., C. J. Donaldson, R. Chen, K. A. Lewis, and W. W. Vale.** 1993. Cloning and expression of a rat brain corticotropin releasing factor (CRF) receptor. *Endocrinology 133:3058-3061.*

47. **Perrin, M., C. Donaldson, R. Chen, A. Blount, T. Berggren, L. Bilezikjian, P. Sawchenko, and W. Vale.** 1995. Identification of a second corticotropin-releasing factor receptor gene and characterization of a cDNA expressed in heart. *Proc. Natl. Acad. Sci. USA 92:2969-2973.*

48. **Lovenberg, T. W., C. W. Liaw, D. E. Grigoriadis, W. Clevenger, D. T. Chalmers, E. B. DeSouza, and T. Oltersdorf.** 1995. Cloning and

characterization of a functionally distinct corticotropin-releasing factor receptor subtype from rat brain. *Proc. Natl. Acad. Sci. USA 92:836-840.*

49. **Chen, R., K. Lewis, M. Perrin, and W. W. Vale.** 1993. Expression cloning of a human corticotropin-releasing-factor receptor. *Proc. Natl. Acad. Sci. USA 90:8967-8971.*

50. **Scheer, A., F. fanelli, T. costa, P. DeBenedetti, and S. cotechhia.** 1997. The activation process of the a1b-adrenergic receptor: potential role of protonation and hydrophobicity of a highly conserved aspartate. *Proc Natl Acad Sci USA 94:808-813.*

51. **Tsai-Morris, C., E. Buczko, Y. Geng, A. Gamboa-Pinto, and M. Dufau.** 1886. The genomic structures of the rat corticotropin-releasing factor receptor. *J Biol Chem 271:14519-14525.*

52. **Shetzline, M., R. Premont, J. Walker, S. Vigna, and M. Caron.** 1998. A role for receptor kinases in the regulatino of class II G protein-coupled receptors. *J Biol Chem 273:6756-6762.*

53. **Ulrich, C., M. Holtamann, and L. Miller.** 1998. Secretin and vasoactive intestinal peptide receptors: members of a unique family of G protein-coupled receptors. *Gastroenterology 114:382-397.*

54. **Nozu, T., V. Martinez, J. Rivier, and Y. Tache.** 1999. Peripheral urocortin delays gastric emptying: role of CRF receptor 2. *Am J Physiol 276:G867-G874.*

55. **Chalmers, D. T., T. W. Lovenberg, and E. B. DeSouza.** 1995. Localization of novel corticotropin-releasing factor receptor (CRF2) mRNA expression to specific subcortical nuclei in rat brain: comparison with CRF1 receptor mRNA expression. *J. Neurosci. 15:6340-6350.*

56. **Mansi, J., S. Rivest, and G. Drolet.** 1996. Regulation of corticotropin-releasing factor type 1 (CRF1) receptor messenger ribonucleic acid in the paraventricular nucleus of rat hypothalamus by exogenous CRF. *Endocrinology 137:4619-4629.*

57. **Rivest, S., N. Laflamme, and R. Nappi.** 1995b. Immune challenge and immobilization stress induce transcription of the gene endcoding CRF receptor in selective nuclei of the rat hypothalamus. *J Neurosci 15:2680-2695.*

58. **Kostich, W. A., A. Chen, K. Sperle, and B. L. Largent.** 1998. Molecular identification and analysis of a novel human corticotropin-releasing factor (CRF) receptor: the CRH2γ receptor. *Molecular Endocrinology 12:1077-1085.*

59. **Ardati, A., V. Goetschy, J. Gottowick, S. Henriot, O. Valdenaire, U. Deuschle, and G. Kilpatrick.** 1999. Human CRF2a and b splice variants: pharmacological characterization using radioligand binding and a luciferase gene expression assay. *Neuropharmacology 38:441-448.*

60. **Vita, N., P. Laurent, S. Lefort, P. Chalon, J.-M. Lelias, M. Kaghad, G. L. Fur, D. Caput, and P. Ferrara.** 1993. Primary structure and functional expression of mouse pituitary and human brain corticotrophin- releasing factor receptors. *FEBS 335:1-5.*

61. **Gottowik, J., V. Goetschy, S. Henriot, E. Kitas, B. Fluhman, R. G. Clerc, J. L. Moreau, F. J. Monsma, and G. J. Kilpatrick.** 1997. Labelling of CRH1 and CRH2 receptors using the novel radioligand, [3H]-urocortin. *Neuropharmacology 36:1439-1446.*

62. **Deak, T., K. Nguyen, A. Ehrlich, L. Watkins, R. Spencer, S. Maier, J. Licinio, M. Wong, G. CHrousos, E. Webster, and P. Gold.** 1999. The impact of the nonpeptide corticotropin-releasing hormone antagonist antalarmin on behavioral endocrine responses to stress. *Endocrinology 140:79-86.*

63. **Heinrichs, S. C., H. Min, S. Tamraz, M. Carmouche, S. A. Boehme, and W. W. Vale.** 1997. Anti-sexual and anxiogenic behavioral consequences of corticotropin-releasing factor overexpression are centrally mediated. *Psychoneuroendocrinology 22:215-24.*

64. **Coste, S. C., R. A. Kesterson, K. A. Heldwein, S. L. Stevens, J. K. Hill, A. D. Heard, J. H. Hollis, S. E. Murray, G. A. Pantely, A. R. Hohimer, D. C. Hatton, T. J. Phillips, D. A. Finn, M. J. Low, M. B. Rittenberg, P. Stenzel, and M. P. Stenzel-Poore.** 2000. Abnormal adaptations to stress and impaired cardiovascular function in mice lacking corticotropin-releasing hormone receptor-2. *Nat. Gen. 24:403-409.*

65. **Bale, T. L., A. Contarino, G. W. Smith, R. Chan, L. H. Gold, P. E. Sawchenko, G. F. Koob, W. W. Vale, and K. Lee.** 2000. Mice deficient for corticotropin-releasing hormone receptor-2 display anxiety-like behavior and are hypersensitive to stress. *Nature Genetics 24:410-414.*

66. **Kishimoto, T., J. Radulovic, M. Radulovic, C. R. Lin, C. Schrick, F. Hooshmand, O. Hermanson, M. G. Rosenfeld, and J. Spiess.** 2000. Deletion of Crhr2 reveals an anxiolytic role for corticotropin-releasing hormone receptor-2. *Nature Genetics 24:415-419.*

67. **Valdenaire, O., T. Giller, V. Breu, J. Gottowik, and G. Kilpatrick.** 1997. A new functional isoform of the human CRF2 receptor for corticotropin-releasing factor. *Biochemi Biophys Acta 1352:128-132.*

68. **Saitoh, M., J. Hasegawa, and H. Mashiba.** 1990. Effect of corticotropin-releasing factor on the electrical and mechanical activities of the guinea-pig ventricular myocardium. *Gen. Pharmacol. 21:337-342.*

69. **Haug, C., M. Grunt, S. Schmid, G. Steinbach, A. Metzele, V. Maier, F. S. Keck, and A. Grunert.** 1994. Effect of corticotropin releasing factor on atrial natriuretic peptide release from the isolated perfused rat heart. *Drug Res. 44:579-582.*

70. **Grunt, M., C. Huag, L. Duntas, P. Pauschinger, V. Maier, and E. F. Pfeiffer.** 1992. Dilatory and inotropic effects of corticotropin-releasing factor (CRF) on the isolated heart. *Horm. Metab. Res. 24:56-59.*

71. **Grammatopoulos, D., and E. Hillhouse.** 1999. Activation of protein kinase C by oxytocin inhibits the biological activity of the human myometrial corticotropin-releasing hormone receptor at term. *Endocrinology 140:585-594.*

72. **Grammatopoulos, D., and E. Hillhouse.** 1999. Basal and interleukin-1b-stimulated prostaglandin production from cultured human myometrial cells: differential regulation by corticotropin-releasing hormone. *J Clin Endocrinol Metab 84:2204-2211.*

73. **Chang, C.-P., R. V. Pearse, S. O'Connell, and M. G. Rosenfeld.** 1993. Identification of a seven transmembrane helix receptor for corticotropin-releasing factor and sauvagine in mammalian brain. *Neuron 11:1187-1195.*

74. **Kishimoto, T., R. V. P. II, C. R. Lin, and M. G. Rosenfeld.** 1995. A sauvagine/corticotropin-releasing factor receptor expressed in heart and skeletal muscle. *Proc. Natl. Acad. Sci. USA 92:1108-1112.*

75. **Liaw, C. W., T. W. Lovenberg, G. Barry, T. Oltersdorf, D. E. Grigoriadis, and E. B. DeSouza.** 1996. Cloning and characterization of the human corticotropin-releasing factor-2 receptor complementary deoxyribonucleic acid. *Endocrinology 137:72-77.*

76. **Liaw, C., T. Lovenberg, G. Barry, T. Oltersdor, D. Grigoriadis, and E. DeSouza.** 1996. Cloning and characterization of the human corticotropin-releasing factor-2 receptor complementary deoxyribonucleic acid. *Endocrinology 137:72-77.*

77. **Dautzenberg, F., G. Kilpatrick, S. Wille, and R. Hauger.** 1999. The ligand-selective domains of corticotropin-releasing factor type1 and type 2 receptor reside in different extracellular domains: generation of chimeric receptors with a novel ligand-selective profile. *J Neurochem 73:821-829.*

78. **Myers, D., J. Trinh, and T. Myers.** 1998. Structure and function of the ovine type 1 corticotropin-releasing factor receptor (CRF1) and a corboxyl-terminal variant. *Mol Cell Endocrinol 144:21-35.*

79. **Gonzalez, G., and K. Lederis.** 1988. Sauvagine-like and corticotropin-releasing factor-like immunoreactivity in the brain of the bullfrog (Rana catesbeiana). *Cell Tissue Res 253:29-37.*

80. **Cervini, L., P. Theobald, A. Corrigan, A. Craig, C. Rivier, W. Vale, and J. Rivier.** 1999. Corticotropin-releasing factor (CRF) agonists with reduced amide bonds and Ser7 substititutions. *J Med Chem 42:761-768.*

81. **Kornreich, W. D., R. Galyean, Jean-Francois Hernandez, A. G. Craig, C. J. Donaldson, G. Yamamoto, C. Rivier, W. Vale, and J. Rivier.** 1992. Alanine series of ovine corticotropin releasing factor (oCRF): a structure-activity relationship study. *J. Med. Chem. 35:1870-1876.*

82. **Ruhmann, A., I. Bonk, C. Lin, M. Rosenfeld, and J. Spiess.** 1998. Structural requirements for peptidic antagonists of the corticotropin-releasing factor receptor (CRFR): development of CRFR2b-selective antisauvagine-30. *Proc Natl Acad Sci USA 95:15264-15269.*

83. **Beyermann, M., S. Rothemund, N. Heinrich, K. Fechner, J. Furkert, M. Dathe, R. Winter, E. Krause, and M. Bienert.** 2000. A role for a helical connector between two receptor binding sites of a long-chain peptide hormone. *J Biol Chem 275:5702-5709.*

84. **Rivier, J., S. L. Lahrichi, J. Gulyas, J. Erchegyi, S. C. Koerber, A. G. Craig, A. Corrigan, C. Rivier, and W. Vale.** 1998. Minimal-size, constrained corticotropin-releasing factor agonists with i-(i+3) Glu-Lys and Lys-Glu bridges. *Journal of Medicinal Chemistry 41:2614-20.*

85. **Pallai, P., M. Mabilia, M. Goodman, W. Vale, and J. Rivier.** 1983. Structural homology of corticotropin-releasing factor, sauvagine, and urotensin I: circular dichroism and prediction studies. *Proc. natl. Acad. Sci. USA 80:6770-6774.*

86. **Gulyas, J., C. Rivier, M. Perrin, S. C. Koerber, S. Sutton, A. Corrigan, S. L. Lahrichi, A. G. Craig, W. Vale, and J. Rivier.** 1995. Potent,

structurally constrained agonists and competitive antagonists of corticotropin-releasing factor. *Proc. Natl. Acad. Sci. 92:10575-10579.*

87. **Koerber, S., J. Gulyas, S. Lahrichi, A. Corrigan, A. Craig, C. Rivier, WVale, and J. Rivier.** 1998. Constrained corticotropin-releasing factor (CRF) agonists and antagonists with i-(i+30 Glu-Xaa-DXbb-Lys bridges. *J Med Chem 41:5002-5011.*

88. **Wille, S., S. Sydow, M. Palchaudhuri, J. Spiess, and F. Dautzenberg.** 1999. Identification of amino acids in the N-terminal domain of corticotropin-releasing factor receptor 1 that are important determinants of high affinity ligand binding. *J Neurochem 72:388-395.*

89. **Qi, L., A. Leung, Y. Xiong, K. Marx, and A. Abou-Samra.** 1997. Extracellular cysteines of the corticotropin-releasing factor receptor are critical for ligand interaction. *Biochemistry 36:12442-12448.*

90. **Liaw, C., D. Grigoriadis, M. Lorang, E. DeSouza, and R. Maki.** 1997. Localization of agonist- and antagonist-binding domains of human corticotropin-releasing factor receptors. *Mol. Endocrinol 11:2048-2053.*

91. **Jones, S., and F. Romano.** 1990. Myocardial beta adrenergic receptor coupling to adenylate cyclase during developing septic shock. *Circ Shock 30:51-61.*

92. **Kozicz, T., H. Yanaihara, and A. Arimura.** 1999. Distribution of urocortin-like immunoreactivity in the central nervous system of the rat. *J Comp Neurol 391:1-10.*

93. **Bittencourt, J., and P. Sawchenko.** 2000. Do centrally administered neuropeptides access cognate receptor?: an analysis in the central corticotropin-releasing factor system. *J Neurosci 20:1142-1156.*

94. **Rossant, C., R. Pinnock, J. Hughes, M. Hall, and S. McNulty.** 1999. Corticotropin-releasing factor type1 and type 2a receptors regulate phosphorylation of

calcium/cyclic adenosine 3',5'-monophosphate response element-binding protein and activation of p42/p44 mitogen-activated protein kinase. *Endocrinology 140:1525-1536.*

95. **Tojo, K., and A. Abou-Samra.** 1993. Corticotropin-releasing factor (CRF) stimulates 45Ca2+ uptake in the mouse corticotroph cell line AtT-20. *Life Sci 52:621-630.*

96. **Kiang, J.** 1997. Corticotropin-Releasing Factor-Like Peptides Increase Cytosolic [Ca2+] In Human Epidermoid a-431 Cells. *European Journal of Pharmacology 329:237-244.*

97. **Kuryshev, Y. A., G. V. Childs, and A. K. Ritchie.** 1996. Corticotropin-releasing hormone stimulates Ca2+ entry through L- and P-type Ca2+ channels in rat corticotropes. *Endocrinol. 137:2269-2277.*

98. **Fazal, N., A. Slominski, M. Choudhry, E. Wei, and M. Sayeed.** 1998. Effect of CRF and related peptides on calcium signaling in human and rodent melanoma cells. *FEBS lett 435:187-790.*

99. **Bundey, R., and D. Kendall.** 1999. Inhibition of receptor-mediated calcium responses by corticotrophin-releasing hormone in the CATH.a cell line. *Neuropharmacology 38:39-47.*

100. **Grammatopoulos, D., N. G. N. Milton, and E. W. Hillhouse.** 1994. The human myometrial CRH receptor: G proteins and second messengers. *Mol. Cell Endocrinol. 99:245-250.*

101. **Grammatopoulis, D., S. Thompson, and E. Hillhouse.** 1995. The human myometrium expresses multiple isoforms of the corticotropin-releasing hormone receptor. *J Clin Endocrinol Metab 80:2388-2393.*

102. **Grammatopoulos, D., and E. Hillhouse.** 1998. Solubilization and biochemical characterization of the human myometrial corticotropin-releasing hormone receptor. *Mol Cell Endocrinol 138:185-198.*

103. **Hauger, R., F. Dautzenberg, A. Flaccus, T. Liepold, and J. Spiess.** 1997. Regulation of corticotropin-releasing factor receptor function in human Y-79

retinoblastoma cells: rapid and reversible homologous desensitization but prolonged recovery. *J Neurochem 68:2308-2316.*

104. **Dieterich, K., D. Grigoriadis, and E. DeSouza.** 1996. Homologous desensitization of human corticotropin-releasing factor1 receptor in stable transfected mouse fibroblast cells. *Brain Res 710:287-292.*

105. **Hauger, R., R. Smith, S. Braun, F. Dautzenberg, and K. Catt.** 2000. Rapid agonist-induced phosphorylation of the human CRF Receptor, type1: A potential mechanism for homologous desensitization. *Biochem Biophys Res Comm 268:572-576.*

106. **Smart, D., A. Coppell, C. Rossant, M. Hall, and A. McKnight.** 1999. Characterisation using microphysiometry of CRF receptor pharmacology. *Eur J Pharmacol 379:229-235.*

107. **Clark, R., B. Knoll, and R. Barber.** 1999. Partial agonists and G protein-coupled receptor desensitization. *Trends Pharmacol Sci 20:279-286.*

108. **Pozzoli, G., L. M. Bilezikjian, M. H. Perrin, A. L. Blount, and W. W. Vale.** 1996. Corticotropin-releasing factor (CRF) and glucocorticoids modulate the expression of type 1 CRF receptor messenger ribonucleic acid in rat anterior pituitary cell cultures. *Endocrinol. 137:65-71.*

109. **Sakai, K., N. Horiba, Y. Sakai, F. Tozawa, H. Demura, and T. Suda.** 1996. Regulation of corticotropin-releasing factor receptor messenger ribonucleic acid in rat anterior pituitary. *Endocrinology 137:1758-1763.*

110. **Smit, M., E. Roovers, H. Timmerman, Y. v. d. Vrede, A. Alewijnse, and R. Leurs.** 1996. Two distinct pathways for histamine H2 receptor down-regulation. *J Biol Chem 271:7574-7582.*

111. **Nickenig, G., and T. Murphy.** 1996. Enhanced angiotensin receptor type1 mRNA degradation and induction of polyrobosomal mRNA binding proteins by angiotensin II in vascular smooth muscle cells. *Mol Parmacol 50:743-751.*

112. **Mitchusson, K., B. Blaxall, A. Pende, and J. Port.** 1998. Agonist-mediated destabilization of human b1-adrenergic receptor mRNA: role of the 3' untranslated region. *Biochem Biophys Res Comm 252:357-362.*

113. **Izzo, N., T. Tulenko, and W. Colucci.** 1994. Phorbol esters and norepinephrine destabilize a1b-adrenergic receptor mRNA in vascular smooth muscle cells. *J Biol Chem 269:1705-1710.*

114. **Hadock, J. R.** 1989. Agonist-induced destabilization of β-adrenergic receptor mRNA. *J. Biol. Chem. 264:19928-19933.*

115. **Barrett, P., A. MacLean, G. Davidson, and P. Morgan.** 1996. Regulation of the Mel 1a melatonin receptor mRNA and protein levels in the ovine pars tuberalis: evidence for a cyclic adenosine 3',5'-monophosphate-independent Mel 1a receptor coupling and an autoregulatory mechanism of expression. *Mol Endocrinol 10:892-902.*

116. **Francis, D., CCaldji, F. Champagne, P. Plotsky, and M. Meaney.** 1999. The role of corticotropin-releasing factor-norepinephrine systems in mediating the effects of early experience on the development of behavioral and endocrine responses to stress. *Biol Psychiatry 46:1153-1166.*

117. **Lee, N., J. Earle-Hughes, and C. Faser.** 1994. Agonist-mediated destabilization of m1 muscarinic acetylcholine receptor mRNA. *J Biol Chem 269:4291-4298.*

118. **Aubry, J. M., A. V. Turnbull, G. Pozzoli, C. Rivier, and W. Vale.** 1997. Endotoxin decreases corticotropin-releasing factor receptor 1 messenger ribonucleic acid levels in the rat pituitary. *Endocrinology 138:1621-6.*

119. **Merchenthaler, I., M. Hynes, S. Vingh, A. Schally, and P. Petrusz.** 1983. Immunocytochemical localization of corticotropin-releasing factor (CRF) in the rat spinal cord. *Brain Res 275:373-377.*

120. **Li, C., and T. McDonald.** 1997. Source of corticotropin-releasing hromone-like innervation of the adrenal glands of fetal and postnatal sheep. *Brain Res 767:87-91.*

121. **Aguilera, G., M. Millan, R. Hauger, and K. Catt.** 1991. Corticotropin-releasing factor receptors: distribution and regulation in brain, pituitary and peripheral tissues. *Ann NY Acad Sci 512:48-62.*

122. **Udelsman, R., J. Harwood, M. Millan, G. Chrousos, D. Goldstein, R. Zimlichman, K. Catt, and G. Aguilera.** 1986. Functional corticotropin releasing factors in the primate peripheral sympathetic nervous system. *Nature 319:147-150.*

123. **Keegan, C., J. Herman, I. Karolyi, K. O'Shea, S. Camper, and A. Seacholtz.** 1994. Differential expression of corticotropin-releasing hormone in developing mouse embryos and adult brain. *Endocrinology 134:2547-2555.*

124. **Shafton, A., R. Fernley, and R. McAllen.** 1994. Is CRF a ganglionic transmitter or modulator in the cat sudomotor pathway? *Brain Res 652:129-136.*

125. **Bileviciute, I., M. Ahmed, J. Bergstrom, A. Ericsson-Dahlstrand, A. Kreicbergs, and T. Lundeberg.** 1997. Expression of corticotropin-releasing factor in the peripheral nervous system of the rat. *Neuroreport 8:3127-3130.*

126. **Udelsman, R., W. Gallucci, J. Bacher, D. Loriaux, and G. Chrousos.** 1986. Hemodynamic effects of corticotropin releasing hormone in the anesthetized cynomolgus monkey. *Peptides 7:465-471.*

127. **MacCannell, K. L., P. Hamilton, K. Lederis, C. A. Newton, and J. Rivier.** 1984. Corticotropin releasing factor-like peptides produce selective dilatation of the dog mesenteric circulation. *Gastroenterol. 87:94-102.*

128. **Gardiner, S., A. Compton, and T. Bennett.** 1988. Regional haemodynamic effects of depressor neuropeptides in conscious, unrestrained , Lon Evans and Brattleboro rats. *Br J Pharmacol 95:197-208.*

129. **Brown, M., L. Fisher, J. Spiess, J. Rivier, C. Rivier, and W. Vale.** 1982. Comparison of the biologic actions of corticotropin-releasing factor and sauvagine. *Regul Pept 4:107-114.*

130. **Bolt, G. R., H. Itoh, K. Lederis, and K. L. MacCannell.** 1989. Differential antagonism of Alpha-1 and Alpha-2 adrenoceptor-mediated vasoconstrictor responses by a vasodilator peptide, Urotensin I: Comparison with Nifedipine. *J. Pharmacol. Exp. Therap. 251:1147-1154.*

131. **Kobayashi, Y., Y. Suzuki, K. Lederis, and J. Rivier.** 1983. Vasodilatory activity of urotensin I on isolated rat arteries. *Proc. West. Pharmacol. Soc. 26:235-238.*

132. **Overton, J., and L. Fisher.** 1991. Differential hemodynamic responses to central versus peripheral administration of corticotropin-releasing factor in conscious rats. *J Auto Nerv Sys 35:43-52.*

133. **Fisher, L.** 1989a. Central autonomic modulation of cardiac baroreflex by corticotropin-releasing factor. *Am J Physiol 256:H949-H955.*

134. **Fisher, L.** 1989b. Corticotropin-releasing factor: endocrine and autonomic integration of responses to stress. *Trends Pharmacol Sci 10:189-193.*

135. **Lei, S., R. Richter, M. Bienert, and M. Mulvany.** 1993. Relaxing actions of corticotropin-releasing factor on rat resistance arteries. *British J. Pharmacol. 108:941-947.*

136. **Saitoh, M., J. Hasegawa, and H. Mashiba.** 1990. Effect of corticotropin-releasing factor on the electrical and mechanical activites of the guinea-pig ventricular myocardium. *Gen Pharmacol 21:337-342.*

137. **Grunt, M., J. Glaser, H. Schmidhuber, P. Pauschinger, and J. Born.** 1993. Effects of corticotropin-releasing factor on isolated rat heart activity. *Am. J. Physiol. 264:H1124-H1129.*

138. **Haug, C., M. Grunt, S. Schmid, G. Steinbach, A. Metzele, V. Maier, F. S. Keck, and A. Grunert.** 1994. Effect of corticotropin-releasing factor on atrial natriuretic peptide release from the isolated perfused heart. *Arzneimittel-Forschung 44:579-582.*

139. **Janeway, C., and P. Travers.** 1997. *Immunobiology*. Current Biology/Garland, New York.

140. **Ceconi, C., S. curello, T. Bachetti, A. Corti, and R. Ferrari.** 1998. Tumor Necrosis Factor in Congestive Heart Failure: a mechanism of disease for the new millennium. *Prog Cardio Disease 41 (Suppl):25-30.*

141. **Feldman, A., A. Combes, D. Wagner, T. Kadakomi, T. Kubota, Y. Li, and C. McTiernan.** 2000. The role of tumor necrosis factor in the pathophysiology of heart failure. *J Am Coll Cardiol 35:537-544.*

142. **Tracey, K.** 1994. Tumor Necrosis Factor-Alpha. In *The Cytokine Handbook*. A. Thomson, ed. Harcourt Brace, New York, p. 289-318.

143. **Kapadia, S., J. Lee, G. Torre-Amione, H. Birdsall, T. Ma, and D. Mann.** 1995. Tumor necrosis factor-a gene and protein expression in adult feline myocardium after endotoxin administration. *J Clin Invest 96:1042-1052.*

144. **Kapadia, S., H. Oral, J. Lee, M. Nakano, G. Taffet, and D. Mann.** 1997. Hemodynamic regulation of tumor necrosis factor-a gene and protein expression in adult feline myocardium. *Circ Res 81:187-195.*

145. **Giroir, B., J. Hohnson, T. Brown, G. Allen, and B. Beutler.** 1992. The tissue distribution of tumor necrosis factor biosynthesis durin endotoxemi. *J Clin Invest 90:693-698.*

146. **Peschon, J., D. Torrance, K. Stocking, M. Glaccum, C. Otten, C. Willis, K. Charrier, P. Morrissey, C. Ware, and K. Mohler.** 1998. TNF receptor-deficient mice reveal divergent roles for p55 and p75 in several models of inflammation. *J Immunol 160:943-952.*

147. **Matsumoto, M., Y. Fu, H. Molina, and D. Chaplin.** 1997. Lymphotoxin-a-deficient and TNF receptor-I-deficient mice define developmental and functional characteristics of germinal centers. *Immunological Rev 156:137-144.*

148. **Ramshaw, I., A. Ramsay, G. Karupiah, M. Rolph, S. Mahalingam, and J. Ruby.** 1997. Cytokines and immunity to viral infections. *Immunological Rev 159:119-135.*

149. **Beutler, B., I. Milsark, and A. Cerami.** 1985. Passive immunization against cachectin/tumor necrosis factor protects mice from lethal effects of endotoxin. *Science 229.*

150. **Kollias, G., E. douni, G. Kassiotis, and D. Kontoyiannis.** 1999. On the role of tumor necrosis factor and receptors in models of multiorgan failure, rheumatoid arthritis, multiple sclerosis and inflammatory bowel disease. *Immunological Rev 169:175-194.*

151. **Rosenbaum, J., Y. Han, J. Park, M. Kennedy, and S. Planck.** 1998. Tumor necrosis factor-a is not essential in endotoxin induced eye inflammation: studies in cytokine receptor deficient mice. *J Rheumatol 25.*

152. **Dinarello, C.** 1994. Interleukin-1. In *The Cytokine Handbook.* A. Thomson, ed. Harcourt Brace, New York, p. 31-56.

153. **Alheim, K., and T. Bartfai.** 1998. The interleukin-1 system: receptors, ligands and ICE in the brain and their involvment in the fever response. *Ann NY Acad Sci 840:51-59.*

154. **Fantuzzi, G., and C. Dinarello.** 1996. The inflammatory response in interleukin-1b-deficient mice: comparison with other cytokine-related knock-out mice. *J Leuko Biol 59:489-493.*

155. **Li, P., H. Allen, S. Banerjee, S. Franklin, L. Herzog, C. Johnston, J. McDowell, M. Paskind, L. Rodman, J. Salfeld, E. Towne, D. Tracey, S. Wardwell, F. Wei, W. Wong, R. Kamen, and T. Seshadri.** 1995. Mice

deficient in IL-1b-converting enzyme are defective in production of mature IL-1b and resistant to endotoxic shock. *Cell 80:401-411.*

156. **Arend, W., M. Malyak, C. Guthridge, and C. Gabay.** 1998. Interleukin-1 receptor antagonist: role in biology. *Annu Rev Immunol 16:27-55.*

157. **Kopf, M., A. Ramsay, F. Brombacher, H. Baumann, G. Freer, C. Galanos, J. Gutierrez-Ramos, and G. Kohler.** 1995. Pleiotropic defects of IL-6-deficient mice including early hematopoiesis, T and B cel function, and acute phase responses. *Ann NY Acad Sci 762:308-318.*

158. **Kopf, M., G. LeGros, A. Coyle, and M. Kosco-Vilbois.** 1995. Immune responses of IL-4, IL-5 and IL-6 deficient mice. *Immunol Rev 148:45-69.*

159. **Heinrich, P., I. Behrmann, G. Muller-Newen, F. Schaper, and L. Graeve.** 1998. Interleukin-6-type cytokine signalling through the gp130/Jak/STAT pathway. *Biochem J 334:297-314.*

160. **Kovalovich, K., R. DeAngelis, W. Li, E. Furth, G. Ciliberto, and R. Taub.** 2000. Increased toxin-induced liver injury and fibrosis in interleukin-6-deficient mice. *31.*

161. **Qureshi, S., P. Gros, and D. Malo.** 1999. The LPS locus: genetic regulation of host responses to bacterial lipopolysaccharide. *Inflam Res 48:613-620.*

162. **Ulevitch, R., and P. Tobias.** 1995. Receptor-dependent mechanisms of cell stimulation by bacterial endotoxin. *Ann Rev Immunol 13:437-457.*

163. **Fenton, M., and D. golenbock.** 1998. LPS-binding proteins and receptors. *J Leuko Biol 64:25-32.*

164. **Wurfel, M., B. Monks, R. Ingalls, R. Dedrick, R. Delude, D. Zhou, N. Lamping, R. Schumann, R. Thieringer, M. Fenton, S. Wright, and D. Golenbock.** 1997. Targeted deletion of the lipopolysaccharide (LPS)-binding protein gene leads to profound suppression of LPS responses ex vivo, wheras in vivo responses remain intact. *J Exp Med 186:2051-2056.*

165. **Bone, R.** 1991. The pathogenesis of sepsis. *Ann Intern Med 115:457-469.*

166. **Smith, S., C. Terminelli, L. Kenworthy-Bott, A. Calzetta, and J. Donkin.** 1994. The cooperative effects of TNF-alpha and IFN-gamma are determining factors in the ability of IL-10 to protect mice from lethal endotoxemia. *J Leuko Biol 55:711-718.*

167. **Tracey, K., H. Vlassara, and A. Cerami.** 1989. Cachectin/tumor necrosis factor. *Lancet 1:1122-1126.*

168. **Michalek, S., R. Moore, J. McGhee, D. Rosenstreich, and S. Mergenhagen.** 1980. The primary role of lymphoreticular cells in the mediation of host responses to bacterial endotoxin. *J Infect Dis 141:55-63.*

169. **Johnston, R.** 1988. Monocytes and macrophages. *N Engl J Med 318:747-752.*

170. **Parratt, J., and A. Vegh.** 1999. Coronary vascular endothelium-myocyte interactions in protection of the heart by ischaemic preconditioning. *J Phys Pharm 50:509-524.*

171. **Sugishita, K., K. Kinugawa, T. Shimizu, K. Harada, H. Matsui, T. Takahashi, T. Serizawa, and O. Kohmoto.** 1999. Cellular basis for the acute inhibitory effects of IL-6 and TNFa on excitation-contraction coupling. *J Mol Cell Cardiol 31:1457-1467.*

172. **Kumar, A., R. Brar, P. Wang, L. Dee, G. Skorupa, F. Khadour, R. Schulz, and J. Parrillo.** 1999. Role of nitric oxide and cGMP in human septic serum-induced depressio of cardiac myocyte contractility. *Am J Physiol 276:R265-R276.*

173. **Hattori, Y., N. Nakanishi, and K. Kasai.** 1997. Role of nuclear factor kB in cytokine-induced nitric oxide and tetrahydrobiopterin synthesis in rat neonatal cardiac myocytes. *J Mol Cell Cardiol 29:1585-1592.*

174. **Bick, R., J. Liao, T. King, A. LeMaistre, J. McMillin, and L. Buja.** 1997. Temporal effects of cytokines on neonatal cardiac myocyte Ca2+ transients and adenylate cyclase activity. *Am J Physiol 272:H1937-H1944.*

175. **Kinugawa, K., O. Kohmoto, A. Yao, T. Serizawa, and T. Takahashi.** 1997. Cardiac inducible nitric oxide synthase negatively modulates myocardial function in cultured rat myocytes. *Am J Physiol 272:H35-H47.*

176. **Flesch, M., H. Kilter, B. Cremers, U. Laufs, M. Sudkamp, M. Ortmann, F. Muller, and M. Bohm.** 1999. Effects of endotoxin on human myocardial contractility, involvement of nitric oxide and peroxynitrite. *J Amer Coll Cardiol 33:1062-1070.*

177. **Yamamoto, K., U. Ikeda, K. Okada, T. Saito, Y. kawahara, M. Okuda, M. Yokoyama, and K. Shimada.** 1997a. Arginine vasopressin increases nitric oxide synthesis in cytokine-stimulated rat cardiac myocytes. *Hypertension 30:1112-1120.*

178. **Yamamoto, K., U. Ikeda, and K. shimada.** 1997b. Natriuretic peptides modulate nitric oxide synthesis in cytokine-stimulated cardiac myocytes. *J Mol Cell Cardiol 29:2375-2382.*

179. **Raymond, R.** 1990. When does the heart fail during shock? *Circ Shock 30:27-41.*

180. **Raymond, R., and J. Gordey.** 1989. The effect of hypodynamic endotoxin shock on myocardial high energy phosphates in the rat. *Cardiovasc Res 23:200-204.*

181. **McDonough, K., C. Lang, and J. Spitzer.** 1984. Depressed function of isolated hearts from hyperdynamic septic rats. *Circ Shock 12:241-251.*

182. **Kettelhut, I., and A. Goldberg.** 1988. Tumor necrosis factor can induce fever in rats without activating protein breakdown in muscle of lipolysis in adipose tissue. *J Clin Invest 81:1384-1389.*

183. **Goodman, M.** 1991. Tumor necrosis factor induces skeletal muscle protein breakdown in rats. *Am J Physiol 260:E727-E730.*

184. **Chang, H., and B. Bistrian.** 1998. The role of cytokines in the catabolic consequences of infection. *J Parent Enter Nutrition 22:156-166.*

185. **Goldberg, A., I. Kettelhut, K. Furuno, J. Fagan, and V. Baracos.** 1988. Activation of protein breakdown and prostaglandin E2 production in rat skeletal muscle in fever is signaled by a macrophage product distinct from interleukin 1 or other known monokines. *J Clin Invest 81:1378-1383.*

186. **Ling, P., B. Bistrian, B. Mendez, and N. Istfan.** 1994. Effects of systemic infusions of endotoxin, tumor necrosis factor, and interleukin-1 on glucose metabolism in the rat: relationship to endogenous glucose production and peripheral tissue glucose uptake. *Metabolism 43:279-284.*

187. **DelAguila, L., K. Claffey, and J. Kirwan.** 1999. TNF-a impairs insulin signaling and insulin stimulation of glucose uptake in C2C12 muscle cells. *Am J Physiol 276:E849-E855.*

188. **Lang, C., and C. Dobrescu.** 1989. Interleukin-1 induced increases in glucose utilization are insulin mediated. *Life Sci 45:2127-2134.*

189. **Baker, S., and E. Reddy.** 1998. Modulation of life and death by the TNF receptor superfamily. *Oncogene 17:3261-3270.*

190. **Kopp, E., R. MEdzhitov, J. Carothers, C. Xiao, I. Douglas, C. Janeway, and S. Ghosh.** 1999. ECSIT is an evolutionarily conserved intermediate in the Toll/IL-1 signal transduction pathway. *Genes Dev 13:2059-2071.*

191. **Maier, S., L. Goehler, M. Fleshner, and L. Watkins.** 1998. The role of the vagus nerve in cytokine-to-brain communication. *Ann NY Acad Sci 840:289-300.*

192. **Ericsson, A., K. Kovacs, and P. Sawchenko.** 1994. A functional anatomical analysis of central pathways subserving the effects of interleukin-1 on stress-related neuroendocrine neurons. *J Neurosci 14:897-913.*

193. **Goehler, L., J. Relton, S. Maier, and L. Watkins.** 1994. Biotinylated interleukin-1 receptor antagonist (IL-1ra) labels paraganglia in the rat liver hilus and hepatic vagus. *Proc Soc Neurosci 20:956-.*

194. **Guyton, A., and J. Hall.** 1997. *Textbook of medical physiology.* W.B. Saunders Co., Philadelphia, PA.

195. **Elmquist, J., T. Scammell, and C. Saper.** 1997. Mechanisms of CNS response to systemic immune challenge: the febrile response. *Trends Neurosi 20:565-570.*

196. **Banks, W., and A. Kastin.** 1991. Blood to brain trasnport of interleukin links the immune and central nervous systems. *Life Sci 48:PL117-121.*

197. **Saper, C., and C. Breder.** 1994. The neurologic basis of fever. *N Engl J Med 330:1880-1886.*

198. **VanDam, A., M. Brouns, W. Man-a-hing, and F. Berkenbosch.** 1993. Immunocytochemical detection of prostaglandin E2 in microvasculature and in neurons of rat brain after administration of bacterial endotoxin. *Brain Res 613:331-336.*

199. **Elmquist, J., T. Scammell, C. Jacobson, and C. Saper.** 1996a. Distribution of Fos-like immunoreactivity in the rat brain following intravenous lipopolysaccharide administration. *J Comp Neurol 371:85-103.*

200. **Elmquist, J., and C. Saper.** 1996b. Activation of the neurons projecting to the paraventricular hypothalamic nucleus by intravenous lipopolysaccharide. *J Comp Neurol 374:315-331.*

201. **Farkas, E., A. Jansen, and A. Lowey.** 1998. Periaqueductal gray matter input to cardiac-related sympathetic premotor neurons. *Brain Res 792:179-192.*

202. **Bittencourt, J. C., J. Vaughan, C. Arias, R. A. Rissman, W. W. Vale, and P. E. Sawchenko.** 1999. Urocortin expression in rat brain: Evidence against a pervasive relationship of urocortin-containing projections with targets bearing type 2 CRF receptors. *J Comp Neurol 415:285-312.*

203. **Ranson, R., K. Motawei, S. Pyner, and J. Coote.** 1998. The paraventricular nucleus of the hypothalamus sends efferents to the spinal cord of the rat that closely appose sympathetic preganglionic neurones projecting to the stellate ganglion. *Exp Brain Res 120:164-172.*

204. **Jansen, A., M. Wessendorf, and A. Loewy.** 1995a. Transneuronal labeling of CNS neuropeptide and monoamine neurons after pseudorabies virus injections into the stellate ganglion. *Brain Res 683:1-24.*

205. **Jansen, A., X. Nguyen, V. Karpitskiy, T. Mettenleiter, and A. Lowey.** 1995b. Central command neurons of the sympathetic nervous system: basis of the fight-or-flight response. *Science 270:644-646.*

206. **VandeKar, L., and M. Blair.** 1999. Forebrain pathways mediating stress-induced hormone secretion. *Front Neuroendocrinol 20:1-48.*

207. **Turnbull, A., S. Lee, and C. Rivier.** 1998. Mechanisms of hypothalamic-pituitary-adrenal axis stimulation by immune signals in the adult rat. *Ann NY Acad Sci 840:434-443.*

208. **Gatti, S., and T. Bartfai.** 1993. Induction of tumor necrosis factor-a mRNA in the brain after peripheral endotoxin treatment: comparison with interleukin-1 family and interleukin-6. *Brain Res 624:291-294.*

209. **Bateman, A., A. Singh, T. Kral, and S. Solomon.** 1989. The immune-hypothalamic-pituitary-adrenal azis. *Endo Rev 10:92-112.*

210. **Rivest, S., and N. Laflamme.** 1995a. Neuronal activity and neuropeptide gene transcription in the brains of immune-challenged rats. *J Neuroendocrinol 7:501-525.*

211. **Aguilera, G., D. Jessop, M. Harbuz, A. Kiss, and S. Lightman.** 1997. Differential regulation of hypothalamic pituitary corticotropin releasing hormone receptors during development of adjuvant-induced arthritis in the rat. *J Endocrinology 153:185-191.*

212. **Stenzel-Poore, M., W. Vale, and C. Rivier.** 1993. Relationship between antigen-induced immune stimulation and activation of the hypothalamic-pituitary-adrenal axis in the rat. *Endocrinology 132:1313-1318.*

213. **Pozzoli, G., L. Bilezikjian, M. Perrin, A. Blount, and W. Vale.** 1996. Corticotropin-releasing factor (CRF) and glucocorticoids modulate the expression of

type 1 CRF receptor messenger ribonucleic acid in rat anterior pituitary cell cultures. *Endocrinology 137:65-71.*

214. **Irwin, M.** 1993. Brain corticotropin-releasing hormone- and interleukin-Iβ-induced suppression of specific antibody production. *Endocrinology 133:1352-1360.*

215. **Ekman, R., B. Servenius, M. G. Castro, P. J. Lowry, A.-S. Cederlund, O. Bergman, and H. O. Sjorgren.** 1993. Biosynthesis of corticotropin-releasing hormone in human T-lymphocytes. *J Neuroimmuno 44:7-14.*

216. **Audhya, T., R. Jain, and C. S. Hollander.** 1991. Receptor-mediated immunomodulation by corticotropin-releasing factor. *Cell Immunol 134:77-84.*

217. **Leu, S., and V. Singh.** 1993. Suppression of in vitro antibody production by corticotropin-releasing factor neurohormone. *J Neuroimmunol 45:23-30.*

218. **Rivier, C., J. Rivier, K. Lederis, and W. Vale.** 1983. In vitro and in vivo ACTH-releasing activity of ovine CRF, sauvagine and urotensin-I. *Regul. Pept. 5:139-143.*

219. **Lederis, K., J. Fryer, J. Rivier, K. L. MacCannell, Y. Kobayashi, N. Woo, and K. L. Wong.** 1985. Neurohormones from fish tails. II: Actions of urotensin I in mammals and fishes. *Rec. Prog. Horm. Res. 41:553-576.*

220. **Potter, E., S. Sutton, C. Donaldson, R. Chen, M. Perrin, K. Lewis, P. E. Sawchenko, and W. Vale.** 1994. Distribution of corticotropin-releasing factor receptor mRNA expression in the rat brain pituitary. *Proc. Natl. Acad. Sci. USA 91:8777-8781.*

221. **Lovenberg, T. W., D. T. Chalmers, C. Liu, and E. B. DeSouza.** 1995. CRF2α and CRF2β receptor mRNAs are differentially distributed between the rat central nervous system and the peripheral tissues. *Endocrinology 136:4139-4142.*

222. **Field, L. J.** 1988. Atrial natriuretic factor-SV40 T antigen transgenes produce tumors and cardiac arrhythmias. *Science 239:1029-1033.*

223. **Delcarpio, J. B., N. A. Lanson, L. J. Field, and W. C. Claycomb.** 1991. Morphological characterization of cardiomyocytes isolated from a transplantable tumor derived from transgenic mouse atria (AT-1 cells). *Circ. Res. 69:1591-1600.*

224. **Steinhelper, M. E., N. A. Lanson, K. P. Dresdner, J. B. Delcarpio, A. L. Wit, W. C. Claycomb, and L. J. Field.** 1990. Proliferation in vivo and in culture of differentiated adult atrial cardiomyocytes from transgenic mice. *Am. J. Physiol. 259:H1826-H1834.*

225. **Cook, J. L., S. Bhandaru, J. F. Giardina, W. C. Claycomb, and R. N. Re.** 1995. Identification and antisense inhibition of a renin-angiotensin system in transgenic cardiomyocytes. *Am. J. Physiol. 268:H1471-H1482.*

226. **Drvota, V., H. Wei, J. Haggblad, B. Carlsson, and C. Sylven.** 1995. β-Adrenergic receptor function in cultured AT-1 cardiomyocytes. *Biochem. Biophys. Res. Commun. 207:13-19.*

227. **Yang, T., D. J. Snyders, and D. M. Roden.** 1995. Ibutilide, a methanesulfonanilide antiarrhythmic, is a potent blocker of the rapidly activating delayed rectifier K+ current (IKr) in AT-1 cells. *Circulation 91:1799-1806.*

228. **Delcarpio, J. B., and W. C. Claycomb.** 1995. Cardiomyocyte transfer into the mammalian heart. *Ann NY Acad Sci 752:267-285.*

229. **Yang, T., M. S. Wathen, A. Felipe, M. M. Tamkun, D. J. Snyders, and D. M. Roden.** 1994. K+ currents and K+ channel mRNA in cultured atrial cardiac myocytes (AT-1 cells). *Circ. Res. 75:870-878.*

230. **Lanson, N. A., C. C. Glembotski, M. E. Steinhelper, L. J. Field, and W. C. Claycomb.** 1992. Gene expression and atrial natriuretic factor processing and secretion in cultured AT-1 cardiac myocytes. *Circulation 85:1835-1841.*

231. **Simpson, P., and S. Savion.** 1982. Differentiation of rat myocytes in single cell cultures with and without proliferating nonmyocardial cells. *Circ Res 50:101-116.*

232. **Bader, D., T. Masaki, and D. A. Fischman.** 1982. Immunochemical analysis of myosin heavy during avian myogenesis in vivo and in vitro. *J. Cell Biol. 95:763-770.*

233. **Hansen, M., L. Jelinek, R. Jones, J. Stegeman-Olsen, and E. Barklis.** 1993. Assembly and composition of intracellular particles formed by moloney murine leukemia virus. *J. Virol. 67:5163-5174.*

234. **Beavo, J. A., N. L. Rogers, O. B. Crofford, J. G. Hardman, E. W. Sutherland, and E. V. Newman.** 1970. Effects of xanthine derivatives on lipolysis and on adenosine 3', 5' -monophosphate phosphodiesterase activity. *Mol Pharmacol 6:597-603.*

235. **Baldwin, H. A., S. Rassnick, J. Rivier, G. F. Koob, and K. T. Britton.** 1991. CRH antagonist reverses the "anxiogenic" response to ethanol withdrawal in the rat. *Psychopharmacology 103:227-232.*

236. **Fisher, R. A., S. M. Robertson, and M. S. Olson.** 1988. Stimulation and homologous desensitization of calcitonin gene-related peptide receptors in cultured beating rat heart cells. *Endocrinology 123:106-112.*

237. **Wynn, P. C., J. P. Harwood, K. J. Catt, and G. Aguilera.** 1988. Corticotropin-releasing factor (CRF) induces desensitization of the rat pituitary CRF receptor-adenylate cyclase. *Endocrinology 122:351-358.*

238. **Kapcala, L. P., and C.-F. Weng.** 1992. In vitro regulation of immunoreactive β-endorphin secretion from adult and fetal hypothalamus by sequential stimulation with corticotropin-releasing hormone. *Brain Res 588:13-20.*

239. **Hauger, R. L., M. R. Irwin, M. Lorang, G. Aguilera, and M. R. Brown.** 1993. High intracerebral levels of CRH result in CRH receptor downregulation in the amygdala and neuroimmune desensitization. *Brain Res 616:283-292.*

240. **Kobilka, B.** 1992. Adrenergic receptors as models for G protein-coupled receptors. *Annu. Rev. Neurosci. 15:87-114.*

241. **Westphal, R. S., J. R. Backstrom, and E. Sanders-Bush.** 1995. Increased basal phosphorylation of the constitutively active serotonin 2C receptor accompanies agonist-mediated desensitization. *Mol Pharmacol 48:200-205.*

242. **Kuznetsov, V., E. Pak, R. B. Robinson, and S. F. Steinberg.** 1995. $\beta_2$-Adrenergic receptor actions in neonatal and adult rat ventricular myocytes. *Circ. Res. 76:40-52.*

243. **Rybin, V. O., and S. F. Steinberg.** 1994. Protein kinase C isoform expression and regulation in the developing rat heart. *Circ. Res. 74:299-309.*

244. **Woodcock, E. A., M. Fullerton, S. Land, and I. J. Kuraja.** 1991. Culturing rat neonatal myocytes causes changes in the phophatidylinositol turnover pathway. *Clin Exp Pharmacol Physiol 18:331-335.*

245. **Lederis, K., A. Letter, D. McMaster, and G. Moore.** 1982. Complete amino acid sequence of Urotensin-I, a hypotensive and corticotropin-releasing neuropeptide from Catostomus. *Science 218:162-164.*

246. **Church, D. J., V. v. d. Bent, M. B. Vallotton, and U. Lang.** 1994. Role of prostaglandin-mediated cyclic AMP formation in protein kinase C-dependent secretion of atrial natriuretic peptide in rat cardiomyocytes. *Biochem. J. 303:217-225.*

247. **Schiebinger, R. J., and A. C. Santora.** 1989. Stimulation by calcitonin gene-related peptide of atrial natriuretic peptide secretion in vitro and its mechanism of action. *Endocrinology 124:2473-2479.*

248. **Ruskoaho, H.** 1992. Atrial natriuretic peptide: synthesis, release, and metabolism. *Pharmacol. Rev. 44:479-602.*

249. **Ambler, S. K., and M. F. Leite.** 1994. Regulation of atrial natriuretic peptide secretion by $\alpha$1-adrenergic receptors: the role of different second messenger pathways. *J. Mol. Cell. Cardiol. 26:391-402.*

250. **Xiong, Y., L. Xie, and A.-B. Abou-Samra.** 1995. Signaling properties of mouse and human corticotropin-releasing factor (CRF) receptors: decreased coupling efficiency of human type II CRF receptor. *Endocrinol. 136:1828-1834.*

251. **Endoh, M.** 1995. The effects of various drugs on the myocardial inotropic response. *Gen Pharmacol 26:1-31.*

252. **Hescheler, J., M. Kameyama, W. Trautwein, G. Mieskes, and H. D. Soling.** 1987. Regulation of cardiac calcium channels by protein phosphatases. *Eur. J. Biochem. 165:261-266.*

253. **Takasago, T., T. Imagawa, and M. Shigekawa.** 1989. Phosphorylation of the cardiac ryanodine receptor by cyclic AMP-dependent protein kinase. *J. Biochem. 106:872-877.*

254. **Takasago, T., T. Imagawa, K. Furukawa, T. Ogurusu, and M. Shigekawa.** 1991. Regulation of the cardiac ryanodine receptor by protein kinase-dependent phophorylation. *J. Biochem. 109:163-170.*

255. **Bell, D., and J. McDermott.** 1994. Use of the cyclic AMP antagonist, Rp-cAMPS, to distinguish between cyclic AMP-dependent and cyclic AMP-independent contractile responses in rat ventricular cardiomyocytes. *J. Mol. Cell. Cardiol. 26:1439-1448.*

256. **Vamvakopoulos, N. C., and G. P. Chrousos.** 1994. Hormonal regulation of human corticotropin-releasing hormone gene expression: implications for the stress response and immune/inflammatory reaction. *Endocr Rev 15:409-417.*

257. **Shibahara, S., Y. Morimoto, Y. Furutani, M. Notake, H. Takahashi, S. Shimizu, S. Horikawa, and S. Numa.** 1983. Isolation and sequence analysis of the human corticotropin-releasing factor precursor gene. *EMBO J. 2:775-779.*

258. **Montecucchi, P. C., and A. Henshen.** 1981. Amino acid composition and sequence analysis of sauvagine, a new active peptide from the skin of *Phyllomedusa sauvagei. Int. J. Pept. Prot. Res. 18:113-120.*

259. **Sutton, R. E., G. F. Koob, M. L. Moal, J. Rivier, and W. Vale.** 1982. Corticotropin-releasing factor produces fear-enhancing behavioral activation in rats. *J. Neurosci. 10:176-183.*

260. **Heldwein, K. A., D. L. Redick, M. B. Rittenberg, W. C. Claycomb, and M. P. Stenzel-Poore.** 1996. Corticotropin-releasing hormone receptor expression and functional coupling in neonatal cardiac myocytes and AT-1 cells. *Endocrinol. 137:3631-3639.*

261. **Bale, T. L., K.-F. Lee, and W. W. Vale.** 1999. CRF2 deficient mice have altered peripheral vascularization. *Soc. Neurosci. Abstr. 25:156.*

262. **Parkes, D., S. Rivest, S. Lee, C. Rivier, and W. Vale.** 1993. Corticotropin-releasing factor activates c-fos, NGFI-B, and corticotropin-releasing factor gene expression within the paraventricular nucleus of the rat hypothalamus. *Molecular Endocrinology 7:1357-1367.*

263. **Ono, N., D. E. Bedran, J. C. Castro, and S. M. McCann.** 1985. Ultrashort-loop positive feedback of corticotropin (ACTH)-releasing factor to enhance ACTH release in stress. *Proc. Natl. Acad. Sci. USA 82:3528-3531.*

264. **Liebsch, G., R. Landgraf, M. Engelmann, P. Lorscher, and F. Holsboer.** 1999. Differential behavioral effects of chronic infusion of CRH 1 and CRH 2 receptor antisense oligonucleotides into the rat brain. *J. Psychiatr. Res. 33:153-163.*

265. **Spruijt, B. M., J. A. van Hooff, and W. H. Gispen.** 1992. Ethology and neurobiology of grooming behavior. *Physiol. Rev. 72:825-852.*

266. **McEwen, B. S.** 1998. Stress, adaptation and disease: allostasis and allostatic load. *Ann. N. Y. York Acad. Sci. 840:33-44.*

267. **Spina M, Merlo-Pich E, Chan Rk, Basso Am, Rivier J, Vale W, and Koob Gf.** 1996. Appetite-suppressing effects of urocortin, a CRF-related neuropeptide. *Science 273:1561-4.*

268. **Arase, K., D. A. York, H. Shimizu, N. Shargill, and G. A. Bray.** 1988. Effects of corticotropin-releasing factor on food intake and brown adipose tissue thermogenesis in rats. *Am. J. Physiol. 255:E255-9.*

269. **Woods, S. C., R. J. Seeley, D. Porte, Jr., and M. W. Schwartz.** 1998. Signals that regulate food intake and energy homeostasis. *Science 280:1378-83.*

270. **Bradbury, M. J., M. McBurnie, D. Denton, K.-F. Lee, and W. W. Vale.** 1999. Divergent effects of CRF receptors on food intake and weight gain: acute vs. chronic urocortin administration in WT and CRFR1-/- mice. *Endocrine Soc. Abstr. 81:224.*

271. **Overton, J. M., and L. A. Fisher.** 1991. Differentiated hemodynamic responses to central versus peripheral administration of corticotropin-releasing factor in conscious rats. *Journal of the Autonomic Nervous System 35:43-52.*

272. **Okosi, A., B. K. Brar, M. Chan, L. D'Souza, E. Smith, A. Stephanou, D. S. Latchman, H. S. Chowdrey, and R. A. Knight.** 1998. Expression and protective effects of urocortin in cardiac myocytes. *Neuropeptides 32:167-71.*

273. **Parkes, D. G., J. Vaughan, J. Rivier, W. Vale, and C. N. May.** 1997. Cardiac inotropic actions of urocortin in conscious sheep. *Am. J. Physiol. 272:H2115-22.*

274. **Fentzke, R. C., C. E. Korcarz, S. G. Shroff, H. Lin, J. Sandelski, J. M. Leiden, and R. M. Lang.** 1997. Evalulation of ventricular and arterial hemodynamics in anesthetized closed-chest mice. *J. Am. Soc. Echocard. 10:915-925.*

275. **Warltier, D. C., and P. S. Pagel.** 1992. Cardiovascular and respiratory actions of desflurane: is desflurane different from isoflurane? *Anesth. Analg. 75:S17-29; discussion S29-31.*

276. **Miyakoda, G., A. Yoshida, H. Takisawa, and T. Nakamura.** 1987. β-Adrenergic regulation of contractility and protein phosphorylation in spontaneously beating isolated rat myocardial cells. *J. Biochem. 102:211-224.*

277. **Franklin, K., and G. Paxinos.** 1997. *The mouse brain in stereotaxic coordinates*. Academic Press, San Diego, CA.

278. **Gu, G., F. Varoqueaux, and R. B. Simerly.** 1999. Hormonal regulation of glutamate receptor gene expression in the anteroventral periventricular nucleus of the hypothalamus. *J. Neurosci. 19:3213-3222.*

279. **Wagoner, L. E., L. Zhao, D. K. Bishop, S. Chan, S. Xu, and W. H. Barry.** 1996. Lysis of adult ventricular myocytes by cells infiltrating rejecting murine cardiac allografts. *Circulation 93:111-119.*

280. **Fukamizu, A., K. Sugimura, E. Takimoto, F. Sugiyama, M. S. Seo, S. Takahashi, T. Hatae, N. Kajiwara, K. Yagami, and K. Murakami.** 1993. Chimeric renin-angiotensin system demonstrates sustained increase in blood pressure of transgenic mice carrying both human renin and human angiotensinogen genes. *J. Biol. Chem. 268:11617-21.*

281. **Lenz, H. J., L. A. Fisher, W. W. Vale, and M. R. Brown.** 1985. Corticotropin-releasing factor, sauvagine and urotensin I: effects on blood flow. *Am. J. Physiol. 249:R85-R90.*

282. **Wong, M., J. Licinio, K. Pasternak, and P. Gold.** 1994. Localization of corticotropin-releasing hormone (CRH) receptor mRNA in adult rat brain in situ hybridization histochemistry. *Endocrinol. 135:2275-2278.*

283. **Schurmeyer, T. H., P. W. Gold, W. T. Gallucci, T. P. Tomai, G. G. Cutler, D. L. Loriaux, and G. P. Chrousous.** 1985. Effects and pharmacokinetic properties of the rat/human corticotropin-releasing factor in rhesus monkeys. *Endocrinology 117:300-306.*

284. **Parrillo, J. H.** 1993. Pathogenic mechanisms of septic shock. *N. Engl. J. Med. 328:1471-1477.*

285. **Alexander, H. R., G. M. Doherty, C. M. Buresh, D. J. Venzon, and J. A. Norton.** 1991. A recombinant human receptor antagonist to interleukin-1 improves survival after lethal endotoxemia in mice. *J. Exp. Med. 1991:1029-1032.*

286. **Dinarello, C. A.** 1991. The proinflammatory cytokines interleukin-1 and tumor necrosis factor and treatment of the septic shock syndrome. *J. Infect. Dis. 163:1177-1184.*

287. **Ohlsson, K., P. Bjork, M. Bergenfeldt, R. Hageman, and R. C. Thompson.** 1990. Interleukin-1 receptor antagonist reduces mortality from endotoxin shock. *Nature 348:550-552.*

288. **Tracey, K. J., Y. Fong, S. G. Hesse, K. R. Manogue, A. T. Lee, G. C. Kuo, S. F. Lowry, and A. Cerami.** 1987. Anti-cachectin/TNF monoclonal antibodies prevent septic shock during lethal bacteraemia. *Nature 330:662-664.*

289. **Baydoun, A. R., R. D. Foale, and G. E. Mann.** 1993. Bacterial endotoxin rapidly stimulates prolonged endothelium-dependent vasodilatation in the rat isolated perfused heart. *Br. J. Pharmacol. 109:987-991.*

290. **Rivier, C., R. Chizzonite, and W. Vale.** 1989. In the mouse, the activation of the hypothalamic-pituitary-adrenal axis by a lipopolysaccharide (endotoxin) is mediated through interleukin-1. *Endocrinology 125:2800-2805.*

291. **Rivest, S., N. Laflamme, and R. E. Nappi.** 1995. Immune challenge and immobilization stress induce transcription of the gene encoding the CRF receptor in selective nuclei of the rat hypothalamus. *J. Neurosci. 15:2680-2695.*

292. **Finkel, M. S., C. V. Oddis, T. D. Jacob, S. C. Watkins, B. G. Hattler, and R. L. Simmons.** 1992. Negative inotropic effects of cytokines on the heart mediated by nitric oxide. *Science 257:387-389.*

293. **Makino, S., J. Schulkin, M. A. Smith, K. Pacak, M. Palkovits, and P. W. Gold.** 1995. Regulation of corticotropin-releasing hormone receptor messenger

ribonucleic acid in the rat brain and pituitary by glucocorticoids and stress. *Endocrinol. 136:4517-4525.*

294. **Luo, X., A. Kiss, C. Rabadan-Diehl, and G. Aguilera.** 1995. Regulation of hypothalamic and pituitary corticotropin-releasing hormone receptor messenger ribonucleic acid by adrenalectomy and glucocorticoids. *Endocrinol. 136:3877-3883.*

295. **Owens, M., and C. Nemeroff.** 1991. Physiology and pharmacology of corticotropin-releasing factor. *Pharmacol. Rev. 43:425-471.*

296. **Heldwein, K. A., J. E. Duncan, P. Stenzel, M. B. Rittenberg, and M. P. Stenzel-Poore.** 1997. Endotoxin regulates corticotropin-releasing hormone receptor 2 (CRH-R2) in heart and skeletal muscle. *Mol. Cell. Endocrinol. 31:167-172.*

297. **Beutler, B., I. W. Milsark, and A. C. Cerami.** 1985. Passive immunization against cachectin/tumor necrosis factor protects mice from lethal effects of endotoxin. *Science 229:869-871.*

298. **Kumar, A., V. Thota, L. Dee, J. Olson, E. Uretz, and J. Parrillo.** 1996. Tumor necrosis factor-alpha and interleukin-1 beta are responsible for depression of in vitro myocardial cell contractility induced by serum from humans with septic shock. *J. Exp. Med. 183:949-958.*

299. **Vary, T. C., L. Voisin, and R. N. Cooney.** 1996. Regulation of peptide-chain initiation in muscle during sepsis by interleukin-1 receptor antagonist. *Am. J. Physiol. 271:E513-E520.*

300. **Ling, P. R., J. H. Schwartz, and B. R. Bistrian.** 1997. Mechanisms of host wasting induced by administration of cytokines in rats. *Am. J. Physiol. 272:E333-339.*

301. **Vary, T. C.** 1998. Regulation of skeletal muscle protein turnover during sepsis. *Curr. Opin. Nutr. Metab. Care. 1:217-224.*

302. **Perlstein, R. S., M. H. Whitnall, J. S. Abrams, E. H. Mougey, and R. Neta.** 1993. Synergistic roles of interleukin-6, interleukin-1 and tumor necrosis factor in the adrenocorticotropin response to bacterial lipopolysaccharide in vivo. *Endocrinology 132:946-952.*

303. **Peckham, I., S. Sobel, R. Jaenisch, and E. Barklis.** 1991. Retrovirus activation in embryonal carcinoma cells by cellular promoters. *Genes Develop. 3:2062-2071.*

304. **Claycomb, W. C., and J. N. Lanson.** 1984. Isolation and culture of the terminally differentiated adult mammalian ventricular cardiac muscle cell. *In Vitro 20:647-651.*

305. **de Kloet, E.** 1991. Brain corticosteroid receptor balance and homeostatic control. *Front. Neuroendocrinol. 12:95-164.*

306. **Nishimori, T., M. Tsujino, K. Sato, T. imai, F. Marumo, and Y. Hirata.** 1997. Dexamethasone-induced up-regulation of adrenomedullin and atrial natriuretic peptide genes in cultured rat ventricular myocytes. *J Mol Cell Cardiol 29:2125-2130.*

307. **Orlowski, J., and J. Lingrel.** 1990. Thyroid and glucocorticoid hormones regulate the expression of multiple Na,K-ATPase genes in cultured neonatal rat cardiac myocytes. *J Biol Cehm 265:3462-3470.*

308. **Singh, K., J. Balligand, T. Fischer, T. Smith, and R. Kelly.** 1995. Glucocorticoids increase osteopontin expression in cardiac myocytes and microvascular endothelial cells. *J Biol Chem 270:28471-28478.*

309. **Kageyama, K., M. Bradbury, L. Zhao, A. L. Blount, and W. W. Vale.** 1999. Urocortin messenger ribonucleic acid: Tissue distribution in the rat and regulation in thymus by lipopolysaccharide and glucocorticoids. *Endocrinology 140:5651-5658.*

310. **Bone, R. C.** 1991. The pathogenesis of sepsis. *Ann. Intern. Med. 115:457-469.*

311. **Abel, F.** 1989. Myocardial function in sepsis and endotoxin shock. *Am J Physiol 257:R1265-R1281.*

312. **Frantz, S., L. Kobzik, K. Young-Dae, R. Fukazawa, R. Medzhitov, R. T. Lee, and R. A. Kelly.** 1999. Toll4 (TLR4) expression in cardiac myocytes in normal and failing myocardium. *Journal of Clinical Investigation 104:271-280.*

313. **Chang, H. R., and B. Bistrian.** 1998. The role of cytokines in the catabolic consequences of infection and injury. *Journal of Parenteral and Enteral Nutrition 22:156-166.*

314. **Zamir, O., P. Hasselgren, D. von Allmen, and J. E. Fischer.** 1991. The effect of interleukin-1a and the glucocorticoid receptor blocker RU 38486 on total and myofibrillar protein breakdown in skeletal muscle. *Journal of Surgical Research 50:579-583.*

315. **Zamir, O., P. Hasselgren, H. James, T. Higashiguchi, and J. E. Fischer.** 1993. Effect of tumor necrosis factor or interleukin-1 on muscle amino acid uptake and the role of glucocorticoids. *Surg Gynecol Obstet 177:27-32.*

316. **Mealy, K., J. J. B. van Lanschot, B. G. Robinson, J. Rounds, and D. W. Wilmore.** 1990. Are the catabolic effects of tumor necrosis factor mediated by glucocorticoids? *Arch Surg 125:42-48.*

317. **Bateman, A., A. Singh, T. Kral, and S. Solomon.** 1989. The immune-hypothalamic-pituitary-adrenal axis. *Endocrine Rev. 10:92-112.*

318. **Hadcock, J., H. Wang, and C. Malbon.** 1989. Agonist-induced destabilization of b-adrenergic receptor mRNA. *J Biol Chem 264:19928-19933.*

319. **Hara, Y., Y. Ueta, I. Isse, N. Kabashima, I. Shibuya, Y. Hattori, and K. Yamashita.** 1997. Increase of urocortin-like immunoreactivity in the rat supraoptic nucleus after dehydration but not food deprivation. *Neurosci Lett 229:65-68.*

320. **Dampney, R. A. L.** 1994. Functional organization of central pathways regulating the cardiovascular system. *Physiological Reviews 74:323-364.*

321. **Tiaho, F., and J. M. Nerbonne.** 1996. VIP and secretin augment cardiac L-type calcium channel currents in isolated adult rat ventricular myocytes. *Pflugers Arch - Eur J Physiol 432:821-830.*

322. **Huang, M.-H., P. R. K. III, and J. L. I. Jr.** 1999. Ca2+-induced Ca2+ release involved in positive inotropic effect mediated by CGRP in ventricular myocytes. *Am J Physiol 276:R259-R264.*

323. **Eichhorn, E., and M. Bristow.** 1996. Medical therapy can improve the biological properties of the chronically failing heart. A new era in the treatment of heart failure. *Circulation 94:2285-2286.*

324. **Klinger, J., R. Betit, L. Curtin, R. Warburton, D. Wrenn, M. Steinhelper, L. Field, and N. Hill.** 1993. Cardiopulmonary responses to chronic hypoxia in transgenic mice that overexpress ANP. *J App Physiol 75:198-205.*

325. **Zhu, H.** 1997. Myocardial cellular development and morphogenesis. In *The Myocardium*. G. Langer, ed. Academic Press, New York, p. 33-80.

326. **Rockman, H., S. Ono, R. Ross, L. Jones, M. Karimi, V. Bhargava, J. Ross, and K. Chien.** 1994. Molecular and physiological alterations in murine ventricular dysfunction. *Proc Natl Acad Sci USA 91:2694-2698.*

327. **Kuznetsov, V., E. Pak, R. Robinson, and S. Steinberg.** 1995. b2-adrenergic receptor actions in neonatal and adult rat ventricular myocytes. *Circ Res 76:40-52.*

328. **Claycomb, W., and N. Lanson.** 1984. Isolation and culture of the terminally differentiated adult mammalian ventricular cardiac muscle cell. *In Vitro 20:647-651.*